University of Dundee

University of Dundee

DOCTOR OF PHILOSOPHY

Investigating the organisation and function of the membrane proteins of the Type VII secretion system in Staphylococcus aureus

Jäger, Franziska

Award date:
2017

Link to publication

General rights
Copyright and moral rights for the publications made accessible in the public portal are retained by the authors and/or other copyright owners and it is a condition of accessing publications that users recognise and abide by the legal requirements associated with these rights.

- Users may download and print one copy of any publication from the public portal for the purpose of private study or research.
- You may not further distribute the material or use it for any profit-making activity or commercial gain
- You may freely distribute the URL identifying the publication in the public portal

Take down policy
If you believe that this document breaches copyright please contact us providing details, and we will remove access to the work immediately and investigate your claim.

Download date: 05. May. 2023

Investigating the organisation and function of the membrane proteins of the Type VII secretion system in *Staphylococcus aureus*

by

Franziska Jäger

School of Life Sciences, University of Dundee

August 2017

Thesis submitted to the University of Dundee in partial fulfilment of the requirements for the degree of Doctor of Philosophy

Copyright © Franziska Jäger, August 2017.

All rights reserved. This copy of the thesis has been supplied on condition that anyone, who consults it, is understood to recognise that its copyright rests with the author and that no quotation from the thesis, nor any information derived therefrom, may be published without the author's prior, written consent.

Declaration

I declare that I am the author of this thesis and that, unless otherwise stated, all references cited have been consulted; that the work of which this thesis is a record of has been performed by me, and that it has not been previously accepted for a higher degree: where the thesis is based upon joint research, the nature and extent of my individual contribution is defined.

Franziska Jäger

Abstract

The Type VII/Ess protein secretion system (T7SS) is found in many Gram positive bacteria, including the opportunistic human and animal pathogen *Staphylococcus aureus*. Previous work has shown that the *S. aureus* T7SS machinery comprises six core components of which four, EsaA, EssA, EssB and EssC are integral membrane proteins. EssC, the largest T7 component, is a member of the FtsK/SpoIIIE family of membrane-bound ATPases that harness the energy of ATP hydrolysis with the movement of macromolecules. The aim of this thesis was to probe the organisation of the membrane-embedded components of the secretion system and to determine whether EssC plays a role in substrate recognition.

A range of detergents was tested for their ability to solubilise EsaA, EssB and EssC from the *S. aureus* inner membrane. The zwitterionic detergent Foscholine-12 was subsequently used for further study as it was the only detergent identified that was able to extract reasonable levels of each protein from the membrane. Blue-native PAGE analysis identified homomeric complexes of Foscholine-solubilised EsaA and EssB proteins. Crosslinking analysis in native membranes provided further evidence for EsaA and EssB homo-dimerisation, and also revealed the presence of high molecular weight multimers of EssC. Surprisingly, there was no evidence from crosslinking that any of the components interacted with each other, or with the EssA protein. Furthermore, EssC multimers detected in whole cells were not dependent upon the presence of any other Ess component or substrate protein for their assembly.

The EssC protein from *S. aureus* strains can be grouped into four variants (EssC1-EssC4) that have sequence variability in their C-terminal domains. These variants are associated with unique clusters of candidate substrate-encoding genes. Here it was shown that each EssC variant can interact with the remaining Ess components from strain RN6390 to facilitate secretion of EsxA but not the substrate protein EsxC. Thus, EssC appears to be a specificity determinant for T7 substrate secretion in *S. aureus.*

Table of Contents

Table of Figures

Table of Tables

List of Abbreviations

aa	amino acid	**MFP**	membrane fusion protein
ABC	ATP-binding cassette	**MOPS**	3-(N-morpholino)propanesulfonic acid
Amp	Ampicillin	**MRSA**	Methicillin resistant *S. aureus*
APS	Ammoniumpersulfate	**MSCRAMM**	microbial surface component recognising adhesive matrix molecules
ATc	Anhydrotetracycline	**NBD**	nucleotide binding domain
ATP	adenosine triphosphate	**nm**	Nanometer
BAM	barrel assembly machinery	**NHS**	N-hydroxysuccinimide
BCG	bacillus Calmette-Guérin	**N-terminal**	amino terminal
BN	blue native	**OD_{600}**	optical density at a wavelength of 600 nm
BS^3	bis(sulfosuccinimidyl)suberate	**ORF**	open reading frame
BSA	Bovine Serum Albumin	**PAGE**	Polyacrylamide gel electrophoresis
CA-MRSA	community-associated MRSA	**PBS**	phosphate-buffered saline
CL	cardiolipin	**PCR**	polymerase chain reaction
CMC	critical micellar concentration	**PG**	phosphatidylglycerol
Cml	Chloramphenicol	**pmf**	proton motive force
C-terminal	carboxy terminal	**PMSF**	Phenylmethylsulfonylfluoride
ddH_2O	double-destilled water	**PVDF**	Polyvinylidene difluoride
DDM	n-Dodecyl-β-D-maltoside	**PVL**	Panton-Valentine leukicidin
DMSO	Dimethylsulfoxide	**RD1**	region of difference 1
DSP	dithiobis(succinimidyl propionate)	**RFU**	relative fluorescence unit
DSS	Disuccinimidyl suberate	**rpm**	revolutions per minute
DUF	domain of unknown function	**RT**	room temperature
ECL	enhanced chemiluminescence	**SCC**	staphylococcal cassette chromosome
EDTA	Ethylendiamintetraacetate	**SDS**	Sodiumdodecylsulfate
FHA	fork-head associated domain	**sec**	seconds
x *g*	relative centrifugal force in multiples of standard gravity	**sn**	Supernatant
HEPES	2-[4-(2-hydroxyethyl)piperazin-1-yl]ethanesulfonic acid	**spA**	staphylococcal protein A
hr	hours	**T7SS**	Type VII Secretion System
HSP	high speed pellet	**Tat**	twin arginine translocation
kb	kilo base	**TAE**	Tris-Acetat-EDTA-buffer
kDa	kilo Dalton	**TEMED**	Tetramethylethylendiamine
LB	Lysogeny broth (medium)	**TEV**	Tobacco etch virus
LDAO	Lauryldimethylamine oxide	**TMD**	Transmembrane domain
Lys-PG	lysyl-phospatidylglycerol	**Tris**	Tris(hydroxymethyl)aminomethane
mDa	mega Dalton	**TSB**	Tryptic Soy Broth (medium)
min	minutes	**WT**	wild type

Acknowledgements

First, I would like to thank my supervisor Professor Tracy Palmer for offering me the opportunity to work on this project. Thanks for all your patience, the constructive ideas and discussions, the endless proofreading and for always encouraging me not to give up when my experiments didn't work.

I would also like to thank the TP/FS group and the entire MMB division for creating such an enjoyable workplace, especially to all the people who shared an office and work bay with me in the past four years. Thanks for putting up with my OCD, I'm sure it wasn't easy sometimes. Special thanks go to Dr. Holger Kneuper for his supervision in the lab, his help in getting me started with my project and for sharing his knowledge throughout the years, Magali Roger, Sergio Galán Bartual, Sofia Ferreira and Jon Cherry for their friendship in the lab and beyond and especially to Karim Rafie for all the fun evenings in Mennie's where we slowly made our way through the Whisky list.

Outside the lab it's Jennifer McDowall I would like to thank in particular. Thanks for our unique friendship, all the emotional support and all the fun trips we've taken, I hope we keep up this tradition. More thanks go to the guys from TNT Dundee who were always able to cheer me up after a hard day in the lab. So far away from home they soon became my Scottish family. Thank you also to Steven Wuttge not only for being an amazing supervisor in the lab but also a good friend over all these years and Stephanie Gathmann for being by my side since the first day at Uni.

I would like to say an extra special thank you to my parents without whom I wouldn't be where I am today. Thank you for the encouragement when I decided to quit my job with the wish to study, for always believing in me and for all the support and love not only in the last ten years.

And at last, of course, Thilo. Thanks for being such an amazing boyfriend. Thank you for all your love and support even when it meant living in a long-distance relationship for such a long time so I could follow my dreams. Thanks also for putting up with my moods, especially during the last six months while I was writing this thesis. I love you.

1
Introduction

1.1 *Staphylococcus aureus*

Staphylococcus aureus, a Gram-positive bacterium, is almost omnipresent in the environment and is commonly found in the human respiratory tract and on the skin. Three patterns of human carriage have been identified. Approximately 20 % of the human population are persistent carriers who are permanently colonised and almost always carry one type of strain. Around 60 % of people are intermittent carriers, harbouring *S. aureus* periodically with the colonising strain changing with varying frequency. A minority of around 20 % of people almost never carry *S. aureus* and are therefore called non-carriers (Kluytmans *et al.*, 1997).

While *S. aureus* is mainly found on mucosal surfaces, the organism is also able to colonise other moist and soft regions of the human body. Although *S. aureus* is not always pathogenic, minor injuries such as a skin cut can provide a route for the bacterium to reach the underlying tissue where it can cause a wide range of suppurative infections or more serious diseases such as pneumonia, mastitis, toxic shock syndrome or even meningitis (Sibbald *et al.*, 2006). Most staphylococcal infections are nosocomial and the cause of postsurgical wound infections. However, more recently an increase in numbers of cases of community-acquired, antibiotic resistant *S. aureus* infections have been observed world wide (Grundmann *et al.*, 2002; Vandenesch *et al.*, 2003; Harbarth *et al.*, 2005).

1.1.1 *S. aureus* virulence factors

As a successful pathogen, *S. aureus* critically relies on the production and secretion of a number of virulence factors that allow the bacterium to adhere to surfaces, invade the host and evade the immune system (Kong *et al.*, 2016). Colonisation is initiated with the help of adhesins. The major class of these virulence factors are the so-called MSCRAMMs (microbial surface component recognising adhesive matrix molecules), proteins which are covalently anchored to the cell wall peptidoglycan and can specifically attach to plasma or extracellular matrix

components (Foster *et al.*, 2014). Additionally *S. aureus* secretes a wide range of exoproteins such as exotoxins and enzymes like nucleases, proteases and lipases (Dinges *et al.*, 2000). The main function of these exoproteins is thought to be the conversion of host tissue into nutrients required for growth but some also have cytolytic activity, for example haemolytic α-toxin, which is able to form β-barrel pores in the plasma membrane leading to leakage and lysis of the target cell (Foster, 2005).

Virulence of *S. aureus* is generally considered to be multifactorial. Necrotizing pneumonia for instance is associated with the activity of the MSCRAMM family member spA (staphylococcal protein A), α- and β-toxin which together cause cell damage, inflammation and necrosis of the respiratory epithelium (Gomez *et al.*, 2004; Bartlett *et al.*, 2008; Hayashida *et al.*, 2009). Exceptions are so-called toxinoses such as toxic shock syndrome and staphylococcal food poisoning which are caused by the toxic shock syndrome toxin and different staphylococcal enterotoxins, respectively (Lowy, 1998).

1.1.2 Antibiotic resistance of *S. aureus*

S. aureus is known to be an astonishingly adaptable pathogen and infamous for its ability to become resistant to antibiotics. Infections caused by antibiotic-resistant strains often occur in epidemic waves. To date three waves have been described, with the first one starting shortly after the introduction of penicillin into clinical practice in the 1940s (Kirby, 1944). Introduction of methicillin marks the onset of the second wave with the first reports of *S. aureus* resistant to this antibiotic published in 1961, only one year after its introduction (Barber, 1961; Jevons *et al*, 1961). This early report might be due to the fact, that *S. aureus* had already developed methicillin-resistance long before its use, back in the 1940, at the time where penicillin was still the main antibiotic in use (Harkins *et al.*, 2017). While penicillin-resistance is narrow in its spectrum, methicillin-resistance is broad; conferring resistance to the entire class of β-lactam

antibiotics and the third wave began in the mid to late 1990s with the emergence of a new MRSA (methicillin resistant *S. aureus*) strain. This community-associated MRSA (CA-MRSA) contains two particular genetic elements: a type IV staphylococcal cassette chromosome (SCC) *mec* element and a virulence gene encoding a leukocyte-killing toxin called Panton-Valentine leukicidin (PVL), which is not found in hospital-acquired MRSA (Vandenesch *et al.*, 2003). Vancomycin has long been a last-resort antibiotic for multiple drug resistant *S. aureus* strains. However, the first strain showed reduced sensitivity to this antibiotic in 1996 and in 2002 the first highly-vancomycin resistant strain was isolated (Hiramatsu *et al.*, 1997; Weigel *et al.*, 2003).

1.2 Protein secretion in bacteria

The cell membrane represents a permeability barrier between the cell and its environment and forms a permanently closed system. However, approximately 20 % of polypeptides synthesized by bacteria are located partially or completely outside the cytoplasm (Pugsley, 1993). Therefore, specialised transport systems are necessary to allow direct exchange of substrates and proteins between the cell cytoplasm and the external medium. While some secretion systems are found in almost all bacteria, secreting a wide variety of substrates, some are only identified in a small number of bacteria. Most of the secreted proteins play essential roles in nutrient acquisition, respiration and competition with other organisms but are also important virulence factors (Sandkvist *et al.*, 1997; Ochsner *et al.*, 2002; Cao *et al.*, 2016).

1.2.1 General protein secretion via the Sec- or Tat-pathways

The general secretory pathway (Sec-pathway) and twin arginine translocation pathway (Tat-pathway) are the two major pathways that secrete proteins across the cytoplasmic membrane (Natale *et al.*, 2008). They have been identified in all domains of life and are the most highly conserved mechanisms of protein secretion (Robinson and Bolhuis, 2004; Papanikou *et al.*,

2007). While the Sec pathway primarily translocates proteins in their unfolded state, the Tat pathway mediates translocation of secretory proteins in their folded state.

Secretion by the Sec-pathway relies on a cleavable signal sequence at the N-terminus of the secreted protein. Signal sequences are 20 – 30 amino acids (aa) in length containing a positively charged amino terminus, a hydrophobic core and a polar carboxyl-terminus (Papanikou *et al.*, 2007). Targeting and translocation through the Sec machinery has three major components: a piloting factor such as signal recognition particle or the chaperone SecB, that recognise N-terminal signal sequences, the ATPase protein SecA that functions as a molecular motor to drive the translocation across the membrane and the membrane integrated protein conducting channel SecYEG (Natale *et al.*, 2008).

Genomes of Mycobacteria and some Gram-positive bacteria encode two homologues of the SecA protein: SecA1 and SecA2, where SecA1 is responsible for 'housekeeping' export while SecA2 exports a specific subset of proteins and is implicated in virulence (Braunstein *et al.*, 2003; Lenz *et al.*, 2003). Currently two types of SecA2 systems are known. Some bacteria which harbour a SecA2 also encode an accessory SecY protein, known as SecY2, and these function together as a SecA2-SecY2 system, while other bacteria contain SecA2-only systems lacking a SecY2. While proteins secreted via the SecA2-only systems probably use the SecYEG channel, proteins of the SecA2-SecY2 system are highly glycosylated and incompatible with the canonical SecA1-SecYEG pathway (Sharma *et al.*, 2003; Rigel *et al.*, 2009; Sardis and Economou, 2010; Fagan and Fairweather, 2011). Proteins secreted by the Sec apparatus can serve many roles, and a number of proteins that promote virulence of bacterial pathogens are transported through this pathway for example in the Gram-positive pathogens *Listeria monocytogenes, Streptococcus gordonii* and *Staphylococcus aureus,* the Gram-negative bacteria *Vibrio cholerae, Klebsiella pneumoniae* and *Yersinia enterocolitica*, as well as in Mycobacteria (Bensing and Sullam, 2002; Braunstein *et al.*, 2003; Lenz *et al.*, 2003; Korotkov *et al.*, 2012).

Translocation of substrates by the Tat-pathway is dependent on a signal peptide containing a pair of arginine residues close to the amino terminus (Palmer *et al.*, 2010). In Gram-negative bacteria and in actinobacteria the Tat machinery consists of the three membrane proteins TatA, TatB and TatC, whereas in Gram-positive firmicutes and archaea the Tat systems only contain TatA and TatC (Palmer and Berks, 2012). In *Escherichia coli* TatB and TatC form a complex that binds the signal peptide of the substrate leading to the recruitment and polymerisation of TatA. This polymerisation not only forms the transport channel but also initiates the translocation of the substrate protein. Finally, once the substrate is translocated the signal peptide is cleaved off and TatA depolymerises (Palmer and Berks, 2012). Proteins transported via the Tat-pathway include redox enzymes, membrane proteins but also virulence factors like the Phospholipase C enzyme as described for *P. aeruginosa* (Ochsner *et al.*, 2002; Lee *et al.*, 2006).

1.2.2 Protein secretion systems in Gram-negative bacteria

In Gram-negative bacteria the cell envelope consists of an inner and an outer membrane through which synthesised proteins need to be translocated in order to reach the extracellular milieu or, in some cases, be directly transported into the cytoplasm of a target cell. To achieve this, eight dedicated secretion systems are used by Gram-negative bacteria, numbered Type I – Type IX (excluding the Type VII secretion system), which all have their own characteristics depending on the nature of the secreted protein (e.g. folded or unfolded, with or without signal peptides) and their function (e.g. translocation of the protein into the extracellular milieu or direct injection into a host cell) (Tseng *et al.*, 2009; Costa *et al.*, 2015). Generally, all eight secretion systems can be divided into two groups: those using a two-step mechanism, and those which secrete proteins in a single step (Figure 1.1). When using a two-step mechanism (e.g. the Type II, Type V, Type VIII and Type IX secretion systems), proteins are first translocated across the inner membrane via the Sec- or Tat-pathways, before being secreted across the outer membrane in a separate step. Of the remaining four secretion systems (Type I, Type III, Type IV

and Type VI) only the Type I secretion system recognises substrate proteins via a C-terminal signal sequence, translocating the protein into the extracellular milieu. The remaining three secretion systems however, secrete proteins without using a recognisable signal sequence by directly injecting them into the host cell through their needle-like apparatus.

The Type I secretion system closely resembles ATP-binding cassette (ABC) transport systems and consists of three essential structural components. The ABC transporter protein participates in recognition of the substrate, catalyses ATP hydrolysis to provide energy for transport, and interacts with the membrane fusion protein (MFP) in the inner membrane. The MFP spans the periplasm to associate with the outer membrane factor (OMF), which generates a pore in the outer membrane, through which the substrate is translocated in an unfolded state (Thomas *et al.*, 2014). Substrates of the Type I secretion system rely on an uncleaved C-terminal signal sequence and vary widely in size from small proteins of 20 kDa up to a molecular weight of 900 kDa (Thomas *et al.*, 2014). They contribute to virulence in a variety of bacterial pathogens, for example the metalloproteases secreted by *Serratia marcescens* and the hemolysins secreted by *E. coli* (Delepelaire, 2004).

The Type II secretion system is one of the two-step secretion systems and translocates substrates across the outer membrane that are first delivered to the periplasm via the Sec or Tat pathway. The Type II secretion machinery consists of four subassemblies: the outer-membrane complex, the inner-membrane platform, the secretion ATPase and the pseudopilus (Korotkov *et al.*, 2012). The outer-membrane complex resides in the outer membrane and serves as the channel through which folded substrates are translocated (Korotkov *et al.*, 2011). While being embedded in the inner membrane, the inner-membrane platform extends into the periplasm and contacts the outer-membrane complex, the ATPase, and the pseudopilus to coordinate export of substrates (Korotkov *et al.*, 2012). A number of bacterial pathogens use the Type II secretion system to transport virulence factors such as *Vibrio cholerae, Yersinia pestis* and *Pseudomonas aeruginosa* (Sandkvist, 2001*).*

The Type III secretion system consists of a complex structure also called the injectisome, which can be divided into three main components: the base complex, the needle component and the translocon (Abrusci *et al.*, 2014). The base complex can be separated into three parts: The cytoplasmic components, two inner and two outer rings. While the inner rings interact with the cytoplasmic membrane the outer rings interact with the peptidoglycan layer and the outer membrane. Together they form a socket-like structure with a centre shaft (Kubori *et al.*, 1998). The needle component originates from this centre shaft, and it is a filament which is known to extend into the extracellular space (Kubori *et al.*, 1998; Worrall *et al.*, 2016). The translocon is assembled upon contact with host cells and forms a pore that is essential for secretion of effector proteins into the host cell, a step which is essential for virulence of many pathogens, including *Yersinia, Salmonella,* and *Shigella* (Büttner, 2012).

Similar to the Type III secretion system the Type IV secretion systems allows for direct transfer of substrates into the host cell. The Type IV secretion system is ancestrally related to bacterial DNA conjugation systems and is therefore able to secrete a variety of substrates such as individual proteins as well as protein-protein and protein-DNA complexes (Cascales and Christie, 2003). This feature supports a variety of functions, including conjugative transfer of DNA, translocation of effector proteins or DNA/protein complexes and DNA uptake and release directly into the host cell. This secretion system plays crucial roles in the pathogenesis in a wide range of bacteria such as *Neisseria gonorrhoeae, Legionella pneumophila* and *Helicobacter pylori* (Backert and Meyer, 2006).

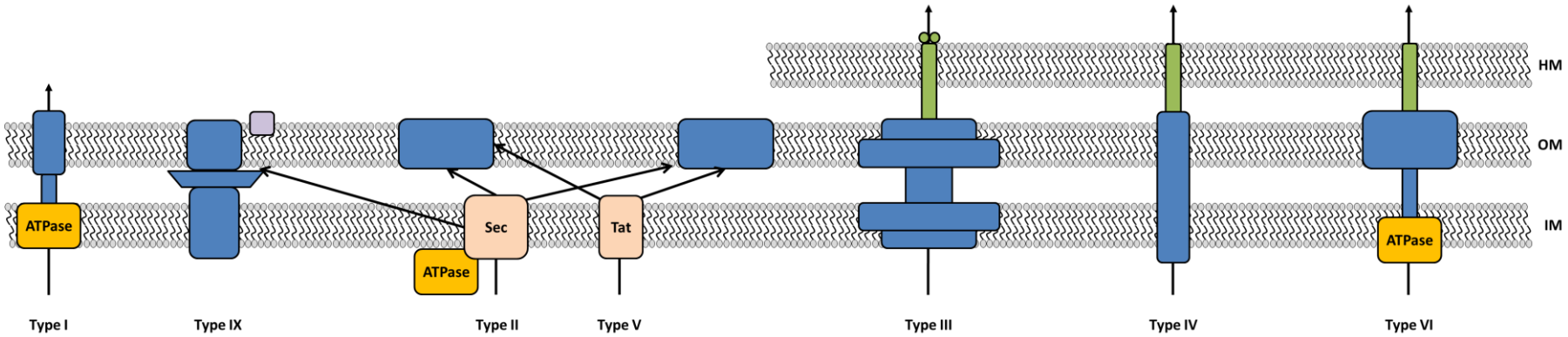

Figure 1.1: Overview of the major protein secretion systems in Gram-negative bacteria. Some proteins are secreted across both membranes in a single step (Type I, III, IV, and VI secretion systems). Other proteins are first transported via the Sec or Tat pathway into the periplasm before being translocated across the outer membrane via the Type II, Type V or Type IX secretion system. **IM:** inner membrane; **OM:** outer membrane; **HM:** host membrane; **Blue:** membrane components; **Green:** secretion needle; **Purple:** PoV shuttle protein. Adapted from Tseng *et al.* (2009) and Veith *et al.* (2017).

The Type V secretion system is the second general secretion system which transports proteins using a two-step mechanism where secreted substrates rely on a cleavable N-terminal signal sequence to be translocated into the periplasm by the Sec-pathway (Van Ulsen *et al.*, 2014). Type V secretion systems can be divided into five types and consist of an N-terminal extracellular domain ('passenger domain') and a C-terminal β-barrel domain in the outer membrane (Henderson *et al.*, 2004). Four types have the passenger domain and pore-forming domain encoded as a single gene whereas in the two-partner system the pore-forming domain and the passenger domain are encoded by two separate genes (Leo *et al.*, 2012). Although it was originally proposed that the passenger domain is translocated across the outer membrane through a channel formed exclusively by the β-barrel domain, recent experiments suggest that translocation of the passenger domain and membrane integration of the β-barrel domain are facilitated by the barrel assembly machinery (BAM) complex and therefore that the β-barrel is completely assembled before the translocation begins (Bernstein, 2015). Proteins secreted by the Type V secretion machinery are mainly virulence factors used by *Haemophilus influenzae, Vibrio cholerae and Neisseria meningitidis,* to name a few (Van Ulsen *et al.,* 2014).

The Type VI secretion system is composed of 13 conserved proteins together with a variable complement of accessory elements and is able to deliver proteins directly into bacterial and eukaryotic cell targets (Russell *et al.*, 2014). These effectors have numerous functions, with many directed against the bacterial cell wall and membrane, supporting the proposal that this secretion machinery has a key role in bacterial competition. It may also play a role in bacterial communication due to its ability to transport effector proteins from one bacterium to another in a contact-dependent manner (Russell *et al.*, 2014). The Type VI secretion system shares structural homology to the tail tubes of some bacteriophages and because of that it has been hypothesized that this secretion machinery may have arisen from inverted phage tails that eject proteins outside of the bacterial cell rather than injecting them inside the cell (Cianfanelli *et al.*, 2016). It could be shown that the Type VI secretion system increases the fitness of *Vibrio*

cholerae, Serratia marcescens and *Vibrio parahaemolyticus* when these bacteria were grown in competition with other bacteria under laboratory conditions (Russell *et al.*, 2014).

The most recently discovered secretion system in Gram-negative bacteria is the Type IX secretion system, a novel secretion system which emerged in the *Fibrobacteres-Chlorobi-Bacteroidetes* superphylum. It is composed of up to 29 proteins with 18 identified so far spreading over 13 distinct loci (Heath *et al.*, 2016; Veith *et al.*, 2017). Substrates secreted by the Type IX secretion system rely on an N-terminal signal peptide for the translocation across the inner membrane via the Sec-pathway. Additionally, these substrates also contain a C-terminal signal which mediates not only the secretion across the outer membrane via the Type IX secretion system but also their attachment to the cell surface (Seers *et al.*, 2006; Chen *et al.*, 2011). For some of the identified proteins a function could be assigned, for example three proteins are involved in regulation and four other proteins interact to form the secretion apparatus who spans both membranes (Sato *et al.*, 2010; Shrivastava *et al.*, 2013; Veith *et al.*, 2017). In addition to the secretion apparatus an attachment complex has been identified consisting of four proteins. One of these proteins was identified as a sortase which catalyses a transpeptidation reaction, anchoring the substrates to the cell wall (Veith *et al.*, 2017).

1.2.3 Protein secretion systems in Gram-positive bacteria

In contrast to Gram-negative bacteria, which possess two phospholipid membranes separated by a periplasmic compartment, Gram-positive bacteria contain only a single lipid bilayer and a surrounding cell wall which is mainly composed of peptidoglycan. Covalently attached to the peptidoglycan are several macromolecules such as wall teichoic acids, surface proteins and the polysaccharide capsule (Navarre and Schneewind, 1999). Despite these differences in their architectures, Gram-positive bacteria also use the general Sec- and Tat-pathways. However, Gram-positive bacteria also harbour specialised secretion systems for the translocation of

proteins into and across the cell wall. Two different kinds of mechanisms can be found in Gram-positive bacteria: one by which proteins are covalently attached to the cell wall, and one for the translocation of proteins into the extracellular milieu (Schneewind and Missiakas, 2012).

For the attachment of proteins to the cell wall, Gram-positive bacteria encode a variety of enzymes, called sortases. In total there are 6 different classes of sortases (class A – F), of which class A and class C are the best studied (Spirig *et al.*, 2011; Bradshaw *et al.*, 2015). Enzymes of the class A sortases have a general 'housekeeping' function and are able to attach more than 40 different proteins to the cell wall. Most surface proteins attached by class A enzymes contain an N-terminal signal peptide, as well as a C-terminal cell wall sorting signal, which is composed of a pentapeptide amino acid cleavage site, LPXTG, and a hydrophobic domain. They are first targeted to the Sec pathway for translocation across the membrane where subsequently the signal peptide is cleaved, while sortase A scans translocated proteins for the LPXTG motif sequence. Following cleavage of the translocated protein by sortase A between the threonine and glycine of the LPXTG motif, the enzyme catalyses the formation of an amide bond between the carboxyl group of threonine and the amino group of a cell wall cross-bridge. Transglycosylation and transpeptidation reactions result in the covalent attachment of surface proteins to the cell wall (Kline *et al.*, 2009). Class C enzymes are used for the assembly of pili, another example of cell surface proteins. Both pili and proteins attached to the surface by class A enzymes are found in many bacteria including pathogens such as *Staphylococcus aureus* and *Streptococcus pneumoniae* and play important roles in virulence, making them potential candidates for drug targets (Spirig *et al.*, 2011).

For the secretion of proteins into the extracellular milieu, Gram-positive bacteria elaborate a specialised secretion system, called the Type VII secretion system (T7SS). It was first discovered in the Actinobacterial pathogens *Mycobacterium tuberculosis* and *Mycobacterium bovis*, where it was shown to be essential for virulence and to secrete two small proteins, ESAT-6 (early secreted antigenic target – 6 kDa) and CFP-10 (culture filtrate protein – 10 kDa) (Hsu *et al.*, 2003;

Pym *et al.*, 2003; Stanley *et al.*, 2003). Since then it was identified in other bacteria such as *Staphylococcus aureus, Bacillus subtilis* and *Listeria monocytogenes* (Pallen, 2002; Way and Wilson, 2005; Burts *et al.*, 2005; Baptista *et al.*, 2013). The T7SS is defined by two characteristics: the presence of one or more substrates belonging to the WXG100 family and an ATPase protein which belongs to the FtsK/SpoIIIE family (Ates *et al.*, 2016). While the T7SS plays various roles in virulence in some bacteria it can also be involved in growth and iron acquisition (Abdallah *et al.*, 2007).

1.3 The Type VII protein secretion system (T7SS)

As mentioned above, secretory proteins of Gram-positive bacteria only need to pass through the cytoplasmic membrane and peptidoglycan layer to enter the extracellular environment. However, members of the *Mycobacteriaceae* and *Corynebacteriaceae* contain a plasma membrane and a Gram-negative-like outer membrane containing mycolic acids which is covalently linked to other (glyco)lipids (Jankute *et al.*, 2015). Additionally, it could be shown that both, pathogenic and non-pathogenic mycobacterial species consist of a capsular layer of approximately 30 nm thickness present in the cell envelopes (Sani *et al.*, 2010; Ates *et al.*, 2016).

Staphylococcus aureus, Bacillus subtilis and *Listeria monocytogenes* belong to the Firmicutes (low G+C Gram-positive bacteria) whereas *Mycobacterium tuberculosis* and *Corynebacterium diphtheriae* belong to the Actinobacteria (high G+C Gram-positive bacteria) and the T7SS has been classified into two sub-types: the T7SSa or ESX for Actinobacteria and the T7SSb or ESS for Firmicutes (Figure 1.2).

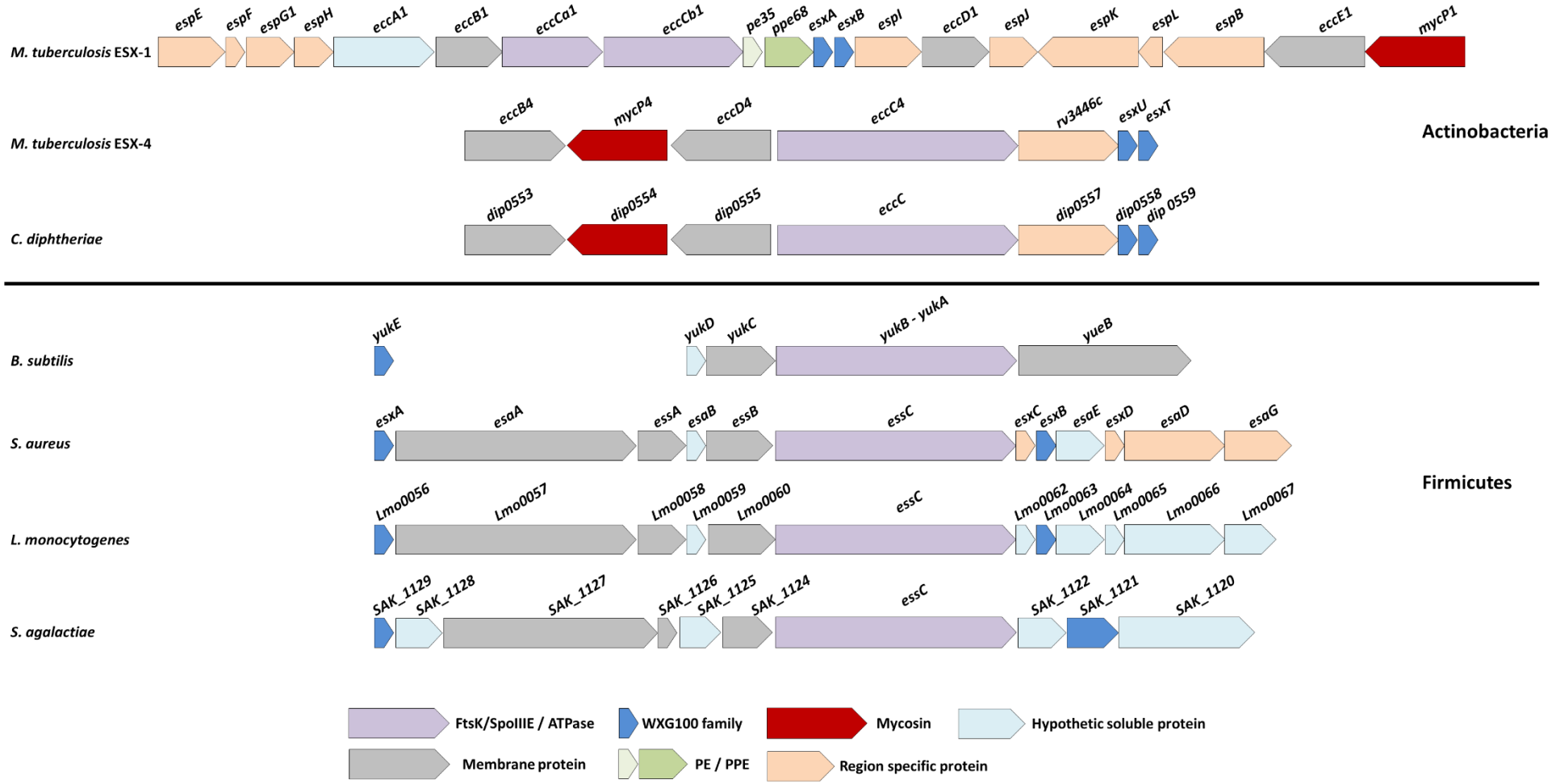

Figure 1.2: Comparison of gene clusters encoding T7SSa or T7SSb secretion systems.

1.3.1 The Type VII protein secretion system in Actinobacteria

The archetypal substrates of the T7SSa / ESX secretion system in Actinobacteria are ESAT-6 and CFP-10, which have subsequently been renamed EsxA and EsxB (Sørensen *et al.*, 1995; Bitter *et al.*, 2009). These proteins belong to the WXG100 protein family (Pallen, 2002), which structurally have been shown to form helical hairpins, with the hairpin bend containing the conserved Trp-X-Gly (WXG) motif. They each have a size of approximately 100 amino acids (Renshaw *et al.*, 2005; Figure 1.3 A). EsxA and EsxB are encoded at the *esx-1* locus and are absent in the attenuated vaccine strains *Mycobacterium bovis* bacilli Calmette-Guérin (BCG) and *Mycobacterium microti*, due to spontaneous deletions of different sizes of the *esx-1* locus, each of which is known as region of difference 1 (RD1) (Mahairas *et al.*, 1996; Pym *et al.*, 2002; Brodin *et al.*, 2002; Pym *et al.*, 2003). EsxA and EsxB form a heterodimer and the complex is an antiparallel four-helix bundle, with strong evidence that they are transported as such (Renshaw *et al.*, 2005; Sysoeva *et al.*, 2014). Structural analyses of EsxB revealed an elongated C-terminus, containing a conserved YxxxD/E secretion motif which is not only crucial for secretion of EsxA and EsxB but could also be shown to interact with the membrane component EccC (Renshaw *et al.*, 2005; Champion *et al.*, 2006; Daleke *et al.*, 2012a; Figure 1.3 A). EsxA and EsxB play a key role in bacterial virulence and they are critical for Mycobacteria to replicate in macrophages and suppress the immune response of host cell (Pym *et al.*, 2002; Pym *et al.*, 2003).

Another major class of T7SS secreted substrates are the so called PE/PPE proteins which to date have only been described in members of the Actinobacteria and are most widespread in the slow-growing species of Mycobacteria (Gey van Pittius *et al.*, 2006). PE/PPE proteins are named after a conserved Pro-Glu and Pro-Pro-Glu motif at the N-terminus and have several characteristics in common with the Esx proteins (Ates *et al.*, 2016). For instance PE/PPE proteins are transported as heterodimers in an antiparallel four-helix bundle, similar to EsxA and EsxB (Strong *et al.*, 2006; Figure 1.3 B). Another conserved characteristic is the flexible tail at the C-terminus of the PE protein which also harbours the YxxxD/E secretion motif (Daleke *et al.*,

2012a). However, contrary to the Esx substrate proteins, secretion of PE/PPE proteins relies on an additional soluble protein, called EspG, which was shown to recognise a binding motif localised in the extended domain of the PPE proteins (Daleke *et al.*, 2012b; Ekiert and Cox, 2014; Korotkova *et al.*, 2014; Phan *et al.*, 2017). Some PE/PPE proteins could be identified as virulence factors where they are not only required for survival in macrophages and granulomas but also modulate the host immune response by mediating apoptosis and cytokine secretion (Ramakrishnan, 2000; Basu *et al.*, 2007).

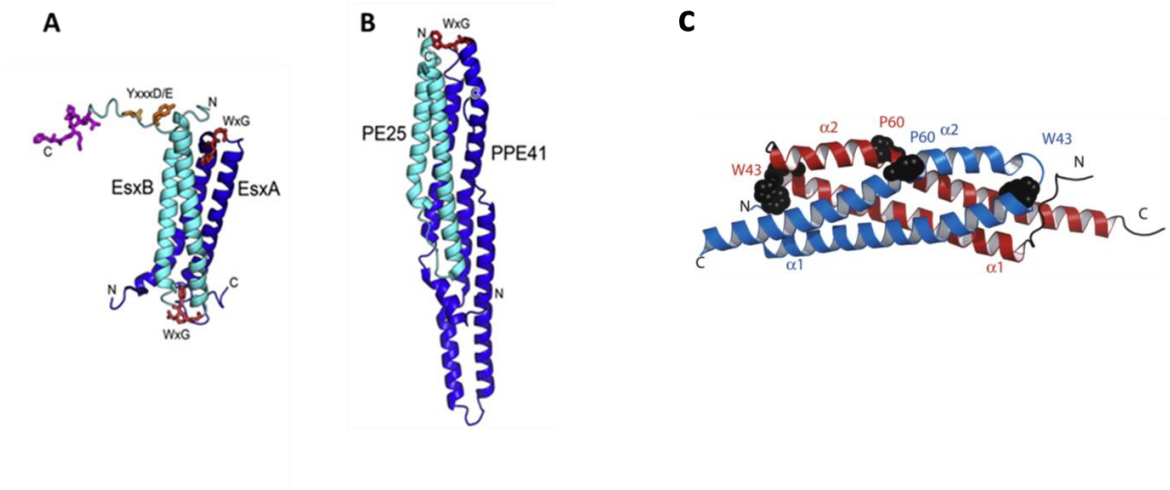

Figure 1.3: Structures of Type VII substrates. A: EsxA-EsxB (Renshaw *et al.*, 2005); **B:** PE25-PPE41 (Strong *et al.*, 2006). WxG motifs are shown in red; secretion signal motifs YxxxD/E are shown in orange; The C-terminal region of EsxB for interaction with EccC is shown in magenta; it should be noted, that the secretion signal is also present in the PE25 sequence but is disordered in the structure. **C:** EsxA-EsxA dimer of *S. aureus* (Sundaramoorthy *et al.*, 2008). A ribbon diagram with subunit A in blue and subunit B in red and labelled helices.

In addition to the two major classes of T7SS substrates, other substrates have also been identified, including members of the DUF2563 and DUF2580 protein families. Both, DUF2563 and DUF2580 family are restricted to Mycobacteria. Little is known about the DUF2563 family, while EspC and EspF have been identified as DUF2580 family members which are secreted by ESX-1 (Ates *et al.*, 2016). The best studied protein among the Esp substrates is EspB. Structural

analyses revealed that this protein not only contains an N-terminal helix-turn-helix motif followed by a T7 secretion signal motif, it also shows a very similar fold to PE/PPE dimers, indicating that EspB is probably secreted as a monomer (Daleke *et al.*, 2012a; Solomonson *et al.*, 2015). A lack of EspB secretion is linked to delays in extrapulmonary dissemination of *M. tuberculosis* in mice (Ohol *et al.*, 2010).

T7SSs are highly versatile secretion systems with up to five different T7SS encoded by pathogenic Mycobacteria, termed ESX-1 to ESX-5 with ESX-1, ESX-3 and ESX-5 being essential for full virulence (Cole *et al.*, 1998; Bitter *et al.*, 2009; Gröschel *et al.*, 2016; Figure 1.4). The different T7SSs each have specific characteristics such as the presence of accessory components and different roles in physiology and virulence. However there are conserved core components required by all the T7SSs, such as an EsxAB pair, EccC, EccD and mycosin (Abdallah *et al.*, 2009). Mycosins belong to the subtilisin protein family and comprise a signal sequence, a protease domain and a C-terminal transmembrane region (Brown *et al.*, 2000; Dave *et al.*, 2002). The defined role of these proteases in the secretion process remains unclear but they seem to have a functional role in various ESX systems, being involved in substrate processing as well as negative regulation of the secretion process (Ohol *et al.*, 2010). Moreover, each T7SS also has a unique set of substrates. For example, while ESX-1 could be shown to secrete EspA/C and EsxA/B, ESX-5 was identified as a major pathway for the translocation of PE/PPE proteins (Champion *et al.*, 2006; Abdallah *et al.*, 2009; Champion *et al.*, 2009; Daleke *et al.*, 2011).

The first T7SS system to be identified was the ESX-1 secretion system and it is therefore the best studied. As already mentioned it not only secretes EsxA and EsxB but also some PE/PPE proteins and numerous Esp proteins (Champion *et al.*, 2006; Champion *et al.*, 2009; Sani *et al.*, 2010). The ESX-1 secretion system plays a major role in virulence. Several cellular events could be shown to be related to the activity of a functional ESX-1 system such as disruption of the host cell membrane as well as induced apoptosis in macrophages to establish and spread mycobacterial infection (Smith *et al.*, 2008; Aguilo *et al.*, 2013; Aguiló *et al.*, 2013). However, in addition to

roles in virulence in *M. tuberculosis* it could also be shown that ESX-1 is essential for DNA transfer in *M. smegmatis* (Coros *et al.*, 2008).

Immediately next to the ESX-1 locus is the ESX-2 region which harbours genes encoding for the complete set of core secretion components, a PE/PPE protein couple as well as two Esp proteins (Stoop *et al.*, 2012). However, mutagenesis studies have shown that this system is not required for virulence or growth (Sassetti *et al.*, 2003; Sassetti and Rubin, 2003). In fact, genomic analyses recently revealed a non-functional ESX-2 system in *M. leprae* and *M. lepromatosis*, suggesting that this system may not be essential and host-orientated (Singh *et al.*, 2015).

The genes encoding the ESX-3 system are conserved among pathogenic and non-pathogenic Mycobacteria, and the locus encodes a full set of core components, an Esx and a PE/PPE pair as well as the Esp protein EspG (Sassetti *et al.*, 2003; Sassetti and Rubin, 2003; Siegrist *et al.*, 2009). It is regulated by the iron-dependent transcriptional repressor (IdeR) and the zinc uptake repressor (Zur) with the system being involved in zinc and iron homeostasis (Rodriguez *et al.*, 2002; Maciag *et al.*, 2007; Serafini *et al.*, 2009; Siegrist *et al.*, 2009). Additionally, ESX-3 is essential for the growth of *M. tuberculosis* by secreting soluble factors which are probably essential for optimal iron and zinc uptake (Sassetti *et al.*, 2003; Serafini *et al.*, 2009). The Esx protein pair EsxG and EsxH play a key role in bacterial virulence by impairing phagosome maturation (Tinaztepe *et al.*, 2016). Moreover, a role of the ESX-3 system in host-pathogen interactions was suggested as EsxH strongly induces interferon-γ (IFNγ) secretion in T cells (Tufariello *et al.*, 2016; Portal-Celhay *et al.*, 2016).

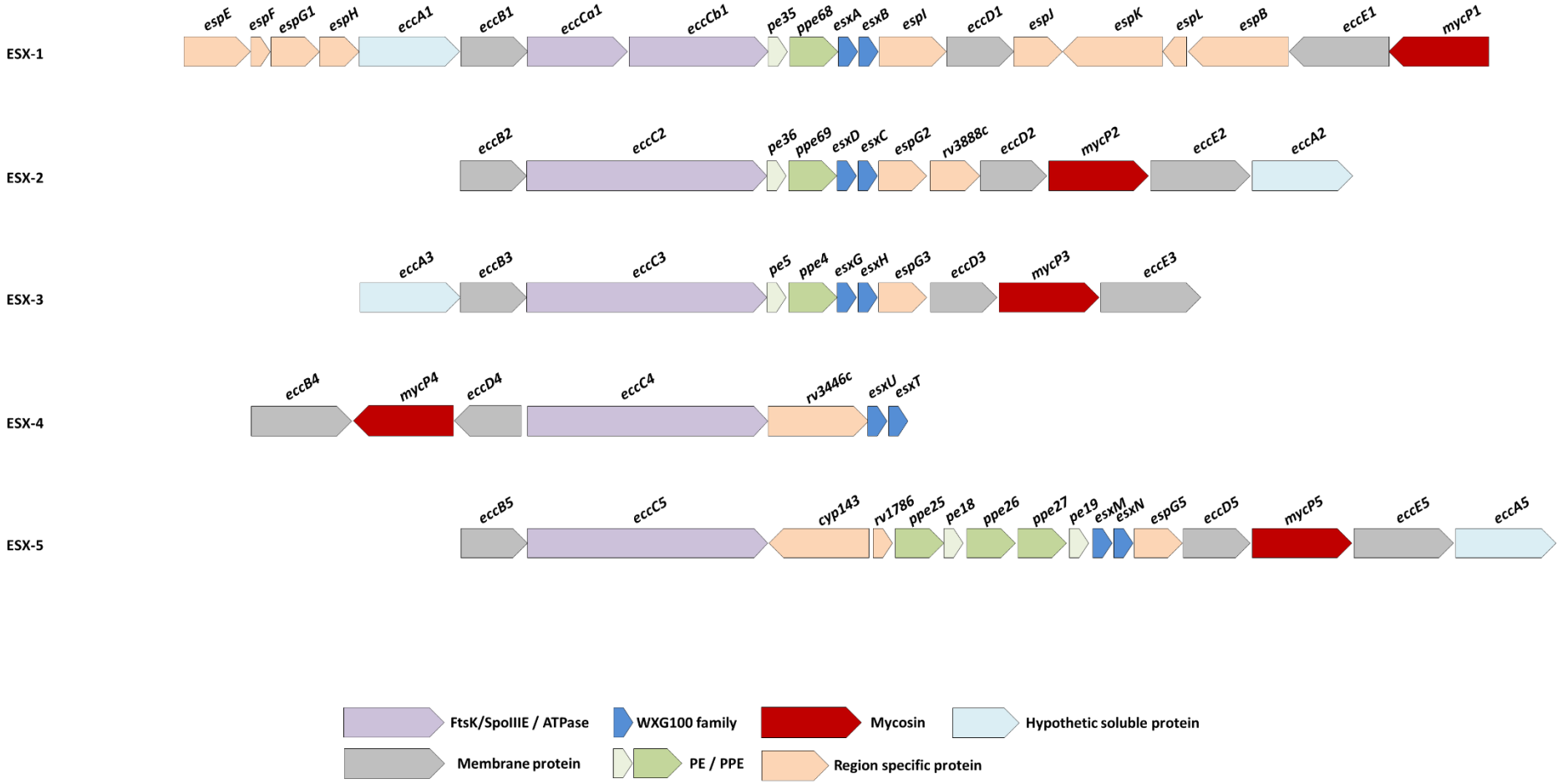

Figure 1.4: Genetic organisation of the five ESX secretion systems in *M. tuberculosis*. Adapted from Bitter *et al.* (2009).

ESX-4 is the most archaic T7 secretion system in Mycobacteria with homologues found in other Actinobacteria such as *Corynebacterium diphtheriae* (Gey van Pittius *et al.*, 2006). It is the smallest ESX-locus with a minimal set of T7S genes (Figure 1.4). However, genomic analyses revealed that *M. leprae* and *M. lepromatosis* have lost the *esx-4* locus, suggesting that Esx-4, similar to ESX-2, is not host-orientated and non-essential (Singh *et al.*, 2015). In fact, secretion of the Esx protein pair EsxT and EsxU could not be detected under laboratory conditions in *M. tuberculosis*, supporting this hypothesis (Målen *et al.*, 2007).

Probably the most recently evolved T7SS in Mycobacteria is the ESX-5 system which is only present in slow-growing species (Gey van Pittius *et al.*, 2006). It is one of the most important modulators of host-pathogen interaction and crucial for cell wall stability (Di Luca *et al.*, 2012). ESX-5 is also essential for mycobacterial growth by exporting cell envelope proteins that are essential to acquire nutrients (Ates *et al.*, 2015; Elliott and Tischler, 2016). Additionally it was shown to be a major pathway for the secretion of PE and PPE proteins, exporting a large number of these proteins of diverse subtypes, many of which are not encoded by the *esx-5* locus (Abdallah *et al.*, 2006; Abdallah *et al.*, 2009; Daleke *et al.*, 2011; Bottai *et al.*, 2012). In the same study Bottai *et al.* (2012) also demonstrated that *M. tuberculosis* deletion mutants of *esx5* show loss of secretion of the *esx5*-encoded EsxN and PPE41, reduction of cell wall integrity and attenuation in macrophages in a mouse infection model.

1.3.1.1 Structural organisation of the Type VII secretion system in M. tuberculosis

The actinobacterial Type VII secretion system comprises five conserved membrane components, EccB, EccC, EccD, EccE and MycP, that are essential for substrate secretion (Stanley *et al.*, 2003; Brodin *et al.*, 2006). EccB is a 51 kDa protein with a 40 amino acid (aa) N-terminal domain followed by a single membrane spanning helix and a C-terminal fold of ~400 amino acids (Wagner *et al.*, 2016). EccE is 44 kDa and has two transmembrane domains and one globular

domain (Houben *et al.*, 2012). While EccB and EccE are relatively hydrophilic, EccD is a highly hydrophobic protein of 54 kDa with a ubiquitin-like N-terminal domain of ~110 amino acids followed by a 30 amino acid linker and 11 TMDs (Wagner *et al.*, 2016). While little is known about the function of EccB and EccE, EccD has been proposed to form the membrane pore through which substrates are transported, although no evidence for channel activity has yet been provided (Stanley *et al.*, 2003). So far only EccC has a predicted function, since this membrane protein has three conserved nucleotide binding domains (NBDs) located at the cytoplasmic side of the membrane and shows homology to members of the FtsK/SpoIIIE family of ATPases. One characteristic for members of this protein family is that they form ring-like hexamers which has now also been shown for EccC (Massey *et al.*, 2006; Rosenberg *et al.*, 2015; Beckham *et al.*, 2017). The fifth membrane protein, MycP, belongs to the subtilisin protein family and is anchored to the membrane with the protease domain facing the extracellular side (Brown *et al.*, 2000; Dave *et al.*, 2002).

Complex formation between the membrane proteins EccB, EccC, EccD and EccE has been shown for the mycobacterial ESX-1 and ESX-5 secretion systems. For the ESX-5 secretion system a complex of ~1.5 mDa could be isolated with $EccB_5$, $EccC_5$, $EccD_5$ and $EccE_5$ in a ratio of 2:2:2:1 (Houben *et al.*, 2012). EccE is underrepresented in this complex relative to the other three membrane components. EccE is not present in the most archaic ESX-4 secretion system in Mycobacteria and was shown to be located on the periphery of the ESX-5 complex suggesting that this protein may not be an absolute mechanistic requirement for the function of T7a secretion systems (Beckham *et al.*, 2017). The remaining three proteins form the core of the ESX-5 secretion machinery and are found as a hexameric arrangement. EccC located at the centre, forming the central pore, with EccB forming a collar-like structure around this pore (Beckham *et al.*, 2017; Figure 1.5 A). For the ESX-1 secretion system a complex of $EccB_1$, $EccC_{1a}$, $EccC_{1b}$, $EccD_1$ and $EccE_1$, could be isolated in the ratio 4:9:7:1:4. The only protein that has not

been isolated as part of the membrane complex is mycosin MycP, although it was recently discovered to be essential for complex stability (Van Winden *et al.*, 2016).

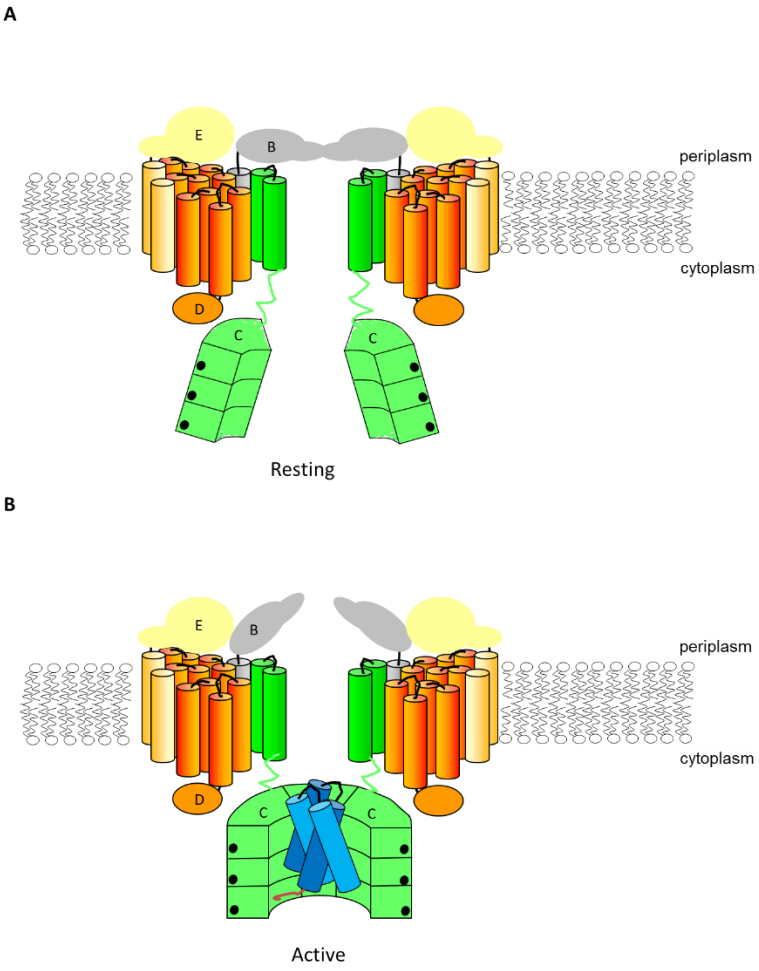

Figure 1.5: Possible model for ESX-5 organisation under resting and active conditions. A: In the resting state the ATPase protein EccC is in a monomeric state with EccB sealing the translocation channel at the periplasmic side. **B:** Interaction with the C-terminal signal sequence of a heterodimeric substrate protein initiates hexamerisation of EccC followed by the translocation of the substrate across the cytoplasmic membrane in a folded state. The three P-loop ATPase domains of EccC are each shown with a generic bound nucleotide (black circle). Taken from Palmer (2017), with permission.

Assembly of the Type VII secretion system is thought to be driven by interaction of EsxB with EccC, the only two components conserved across all T7a and T7b subtypes. Binding of EsxB to the C-terminal ATPase domain has been reported to promote the hexamerisation of EccC followed by a 'just-in-time' post-translational control mechanism in which energy is only used

upon the recognition of key substrates by EccC (Rosenberg *et al.*, 2015; Figure 1.5 B). In their study, Rosenberg *et al.* (2015) showed that an EsxB monomer bound to EccC and existed as homodimer in isolation, suggesting that EsxB stabilises EccC-multimers by forming EccC:EccB:EccB:EccC complexes. However, while EsxB seems to promote assembly and activation of EccC, binding of EsxA, another substrate that forms a tight 1:1 complex with EsxB but does not directly interact with EccC, leads to disassembly and inhibition of the multimeric ATPase. This result suggests that EsxA inactivates EccC by removing the stabilising effect of the EsxB:EsxB interaction, presumably by forming EccC:EsxB:EsxA trimers instead of EccC:EccB:EccB:EccC tetramers. However, it should be noted that these experiments were carried out *in vitro* using the purified cytosolic part of EccC together with purified EsxB and EsxA and more recently substrate-independent hexamerisation of EccC was observed from detergent solubilised membranes (Beckham *et al.*, 2017).

1.3.2 The Type VII protein secretion system in Firmicutes

As discussed above, proteins of the WXG100 family are conserved components that help to characterise Type VII secretion systems. Bioinformatic studies comparing the different homologues of this family revealed that these proteins were not restricted to the Actinobacteria, but were also found in members of the Firmicutes such as *Staphylococcus aureus* and *Bacillus subtilis* (Pallen, 2002; Baptista *et al.*, 2013). Moreover, Firmicutes also harbour homologues of the EccC proteins of Actinobacteria. However, other genes coding for T7a components such as EccB and EccD proteins are lacking in the T7b loci, while a variable number of other genes are found (Figure 1.2).

The T7b cluster in *B. subtilis* is known as the *yuk/yue* locus, containing the six genes *yukAB, yukC, yukD, yukE, yueB* and *yueC*. Interestingly, YukE seems to be the only WXG100 family protein associated with the *Bacillus* system (Baptista *et al.*, 2013; Sysoeva *et al.*, 2014; Huppert *et al.*,

2014) Its secretion is dependent on YukBA, a FtsK/SpoIIIE family ATPase of which only one of the three ATPase domains is required for secretion (Ramsdell *et al.*, 2015). *YukD* encodes a small ubiquitin-like protein with a very short C-terminal tail (Van Den Ent and Löwe, 2005). Another interesting finding is that one protein encoded by the *yuk/yue* regulon of *B. subtilis,* YueB, is a surface-exposed phage receptor that was recently also implicated in conjugative DNA transfer (São-José *et al.*, 2004; São-José *et al.*, 2006; Rösch *et al.*, 2014).

1.4 The Type VII protein secretion system in *S. aureus*

The ESAT-6 secretion system (Ess) in *S. aureus* is probably the best characterised Type VII protein secretion system outside Mycobacteria, where it is required for virulence in murine abscess, pneumonia and skin-infection models (Burts *et al.*, 2005; Kneuper *et al.*, 2014; Wang *et al.*, 2016). Mutational and bioinformatic analyses have revealed that the Ess machinery consists of six core components, of which four are predicted to be membrane-bound proteins, one cytoplasmic protein and one extracellular protein (Burts *et al.*, 2005; Kneuper *et al.*, 2014; Warne *et al.*, 2016; Figure 1.6). The function of these core components together with the additional proteins encoded at the *ess* locus are described in further detail below.

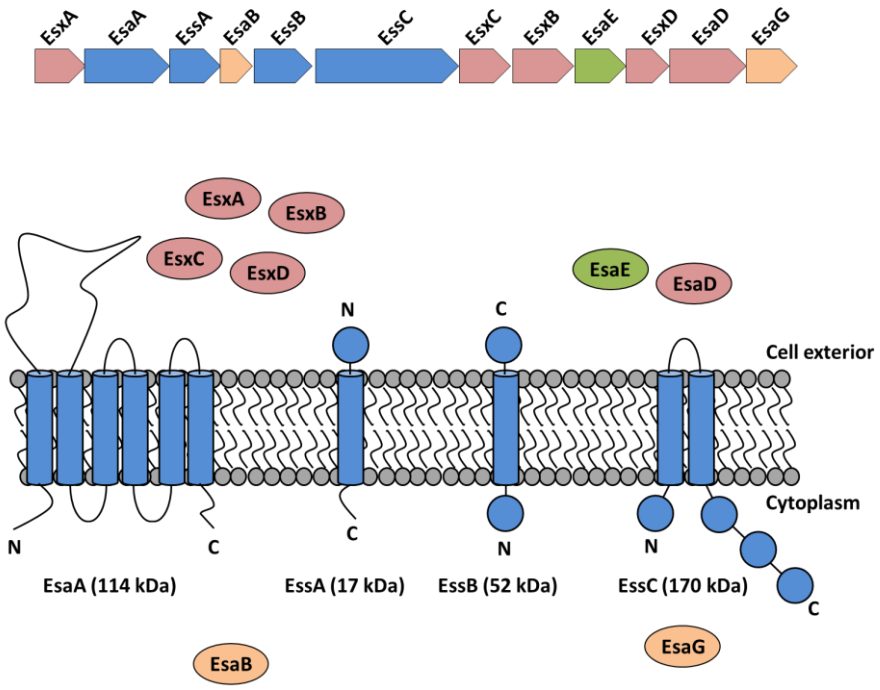

Figure 1.6: The Staphylococcal T7b secretion system. Cartoon showing the membrane components **(blue)**; secreted proteins **(red)**; cytoplasmic proteins **(orange)** and the chaperone EsaE **(green)**.

1.4.1 Substrate proteins of the T7SS in *S. aureus*

The first two T7 substrates characterised in *S. aureus* were EsxA and EsxB, which both belong to the WXG100 family and share 21 % and 18 % sequence identity with EsxA and EsxB in *M. tuberculosis*, respectively (Burts *et al.*, 2005). EsxA is proposed to be a core component of the Ess machinery in *S. aureus*. EsxA is required for bacterial virulence and was recently shown to suppress host cell apoptosis during intracellular infection (Burts *et al.*, 2005; Kneuper *et al.*, 2014; Korea *et al.*, 2014). In contrast to the mycobacterial EsxA and EsxB, the *S. aureus* proteins are not secreted as heterodimers in *S. aureus*; instead x-ray crystallography of EsxA revealed the formation of a homodimer (Sundaramoorthy *et al.*, 2008, Figure 1.3 C). However, both EsxA and EsxB reportedly play an important role in the pathogenesis of staphylococcal abscesses in mice and it was demonstrated that EsxA mediates the release of *S. aureus* from host cells with the help of EsxB (Burts *et al.*, 2005; Korea *et al.*, 2014).

EsxC (formerly EsaC) and EsxD (formerly EsaF) are two further proteins identified as T7SS substrates (Burts *et al.*, 2008; Anderson *et al.*, 2013). EsxD contains a similar C-terminal YxxxD/E secretion signal which is conserved among substrates of the T7SSa secretion system in Mycobacteria (Daleke *et al.*, 2012a; Anderson *et al.*, 2013). However, both EsxC and EsxD lack the WXG100 motif, nor do they share any sequence features of PE/PPE or Esp protein families. EsxC is described as a small protein of ~130 amino acids which is, similar to EsxA and EsxB, produced during murine infection by *S. aureus* and is required for persistence (Burts *et al.*, 2008). Genetic and biochemical analyses suggested that EsxA and EsxB form homodimers but do not interact with one another. In contrast, EsxC can form a homodimer or heterodimerise with EsxA, while EsxD is able to interact with EsxB (Anderson *et al.*, 2013).

The only secreted protein for which a function has been assigned is EsaD. Initially it was described as a membrane protein being displayed on the staphylococcal surface that was required for the secretion of EsxA. It was reported to play a role in pathogenesis of the *S. aureus* Newman strain in a mouse abscess model (Anderson *et al.*, 2011). However, a recent study revealed EsaD to be a secreted anti-bacterial toxin with a C-terminal nuclease domain which targets the DNA of sensitive strains of *S. aureus* (Cao *et al.*, 2016). Moreover, bioinformatics analyses revealed EsaD to be absent from many strains of *S. aureus* including ST398 and MRSA252, making it unlikely to be an essential core component of the T7SS (Warne *et al.*, 2016).

Two further proteins, EsaE and EsaG, are involved in the biogenesis of EsaD. EsaE, which was shown to act as a chaperone, binds to the non-nuclease part of EsaD, and probably targets the complex to the membrane bound secretion apparatus, similar to the EspG-chaperone which interacts with large PE/PPE proteins in pathogenic Mycobacteria (Daleke *et al.*, 2012b; Ekiert and Cox, 2014; Korotkova *et al.*, 2014; Cao *et al.*, 2016; Ohr *et al.*, 2017; Anderson *et al.*, 2017). However, in contrast to EspG in Mycobacteria, EsaE was shown not only to interact with the ATPase protein, EssC, but also to be secreted together with EsaD (Cao *et al.*, 2016). EsaG was initially identified as a protein of unknown function belonging to the DUF600 family. However,

in recent studies EsaG was shown to bind to the nuclease domain of EsaD, acting as an anti-toxin which prevents the EsaD-producing cell from self-intoxication. Additionally, introduction of EsaG into sensitive *S. aureus* strains showed a significant protection against EsaD-mediated killing (Cao *et al.*, 2016; Ohr *et al.*, 2017).

Very recently, other T7 secreted antibacterial toxins mediating contact-dependent interspecies antagonism were identified in *Streptococcus intermedius* (Whitney *et al.*, 2017). These proteins belong to the WXG superfamily harbouring a conserved N-terminal LXG domain, a central domain of variable length, and a C-terminal variable toxin domain. These LXG proteins were shown to transit the Ess secretion system by interacting with a WXG protein. Interestingly, secretion of the WXG interaction partners could not be detected, suggesting that the WXG proteins possibly act as analogues to the mycobacterial chaperone EspG, delivering the LXG proteins to the secretion apparatus. A further protein carrying the LXG motif was recently identified in *S. aureus* ST398, named EsxX. This protein was shown to be secreted by the Ess machinery and deletion analysis indicated that it plays an important role in immune evasion and virulence (Dai *et al.*, 2017).

1.4.2 The EsaB protien

The last remaining soluble protein encoded in the *ess* cluster is EsaB. EsaB is described as a small soluble protein of 80 amino acids, conserved in firmicutes producing the T7SS (Van Den Ent and Löwe, 2005; Burts *et al.*, 2005). Studies with the *S. aureus* Newman strain suggested that EsaB was a negative transcriptional regulator of *esxC* (Burts *et al.*, 2008). By contrast, in the *S. aureus* strain RN6390, EsaB does not regulate *esxC* or any other genes encoded at the *ess* locus but rather has been shown to be essential for the activity of the Ess secretion system. Deletion of *esaB* resulted in a loss of secretion of EsxA and EsxC but did not have an effect on the production of these proteins (Kneuper *et al.*, 2014; Casabona *et al.*, 2017a). Similar results were obtained

for the *B. subtilis* homologue where deletion of *yukD* abolished the activity of the T7SS and it was therefore suggested that EsaB regulates the activity of the secretion machinery post-translationally (Baptista *et al.*, 2013; Huppert *et al.*, 2014). Moreover, it could be shown that *esaB*-deletion is associated with upregulation of genes involved in iron acquisition. Upregulation of the same iron-acquisition genes was also observed in an *essC* mutant, suggesting that EsaB, like EssC, is a core component of the T7SS (Casabona *et al.*, 2017a; Casabona *et al.*, 2017b).

Structural analyses of EsaB and YukD revealed that the proteins have a ubiquitin-like fold (Van Den Ent and Löwe, 2005). However, EsaB lacks the C-terminal tail essential for the activity of ubiquitin. It is interesting to note, that a ubiquitin-like domain is also associated with the cytoplasmic N-terminus of the mycobacterial T7SS component EccD, suggesting that EsaB-like components are essential features of all T7SS (Wagner *et al.*, 2016).

1.4.3 Membrane-bound components of the T7SS in *S. aureus*

The T7SS in *S. aureus* is composed of four membrane proteins: EsaA, EssA, EssB and EssC. EsaA is a large protein with six predicted transmembrane domains (TMDs) and a large extracellular loop that is known to reach the surface of the cell (Dreisbach *et al.*, 2010). It shows structural homology to YueB, a phage receptor in *B. subtilis* and its requirement in substrate secretion appears to be strain-dependent. In fact, it could be shown to be an essential component of the Ess machinery in *B. subtilis* and the *S. aureus* strain RN6390 but has also been reported to be non-essential for the *S. aureus* Newman strain (Burts *et al.*, 2005; Baptista *et al.*, 2013; Kneuper *et al.*, 2014).

EssA is the smallest of the membrane proteins with a single TMD and a globular domain at the extracellular side. It is critical for the secretion of EsxA. However, secretion studies using the *essA* deletion mutant suggested that it may not be completely essential for the secretion of EsxC, since low level of EsxC could still be detected in the supernatant (Kneuper *et al.*, 2014).

EssB is another small protein with globular domains on both sides of the membrane. EssB-C has been predicted to be localised at the trans-side of the membrane and EssB-N in the cytoplasm (Chen *et al.*, 2012; Zoltner *et al.*, 2013a; Zoltner *et al.*, 2013b). The cytoplasmic domain harbours a pseudokinase fold but lacks the ATP-binding signature motifs and is therefore unable to bind ATP-analogues (Zoltner *et al.*, 2013b). Like EssA, EssB is also essential for T7SS activity and was shown to be required for the pathogenesis of *S. aureus* (Burts *et al.*, 2005; Chen *et al.*, 2012; Kneuper *et al.*, 2014). Structural analyses of EssB suggest that it dimerises, but at the outset of this project no additional interaction partners were identified (Zoltner *et al.*, 2013a).

The best characterised membrane protein is the FtsK/SpoIIIE family ATPase EssC, the largest of all proteins encoded by the *ess* locus in *S. aureus*. It has a globular domain at the N-terminus that contains two repeats of a fork-head associated domain (FHA) and this is directly followed by two TMDs (Zoltner *et al.*, 2016). The FHA domain is a small protein domain identified in a number of proteins in different species with a wide range of functions like transcription, translation, recognition of phosphothreonine epitopes, DNA repair and protein degradation (Tanaka *et al.*, 2007; Li *et al.*, 2013; Xu *et al.*, 2014; Liang *et al.*, 2015). The FHA domain in EssC may therefore play a role in interacting with the other proteins in the T7SS. However, so far no function could be assigned to the FHA domains in EssC, except for contributing to overall protein stability. Since deletion of these domains leads to loss of detectable EssC (Zoltner *et al.*, 2016). At its C-terminus EssC possesses three iterations of a P-loop domain, named D1, D2 and D3, which are all essential for secretion. Interestingly module D3 does not bind ATP whereas D2 binds ATP with high affinity. However, deletion of D3 suggests that this module is essential for T7SS activity since secretion of EsxA and EsxB could not be detected in this mutant. Similar to the FHA domain module D2 is also required for the production of a stable and functional protein, since deletion of this module also results in loss of detectable EssC or EsxA and EsxB in the supernatant (Zoltner *et al.*, 2016). Structural analyses of EssC suggest that this protein forms hexamers with an internal pore of ~30 Å, wide enough to accommodate substrate dimers

(Zoltner *et al.*, 2016). A recent study revealed that the 5' portion of *essC* is conserved among all *S. aureus* strains, but there are four variants of the 3'-region, which largely covers the final ATPase domain (Warne *et al.*, 2016). Together with the observation that the C-terminal domain of the mycobacterial EccC is essential for substrate recognition, these data suggest that the variable EssC-domains from different *S. aureus* species might be involved in the recognition of different secreted substrates (Rosenberg *et al.*, 2015; Warne *et al.*, 2016).

1.4.4 Genomic analysis of *S. aureus* strains

An analysis of 153 *S. aureus* genome sequences revealed that the *ess* locus can be grouped into four distinct clusters. While the first five *ess*-encoded genes from *esxA* to *essB* are highly conserved with a similarity of up to 100 %, three of the four clusters do not encode the described substrates EsxB, EsxC, EsxD or EsaD, which are encoded downstream of *essC* in the *S. aureus* strains RN6390 and Newman (Warne *et al.*, 2016). Instead, each of these groups has a distinct set of genes downstream of the core *ess* genes, indicating discrete repertoires of substrates (Figure 1.7). Additionally, the *essC* genes from these isolates showed high sequence conservation in their 5'-regions but variability in their 3'-region, encoding the C-terminal ATPase domain. The sequence variability in EssC encoded by the different groupings is thought to be responsible for substrate recognition, interaction and secretion (Warne *et al.*, 2016). A possible link between this variability and the unique genes encoded downstream of EssC will be discussed in Chapter 5.

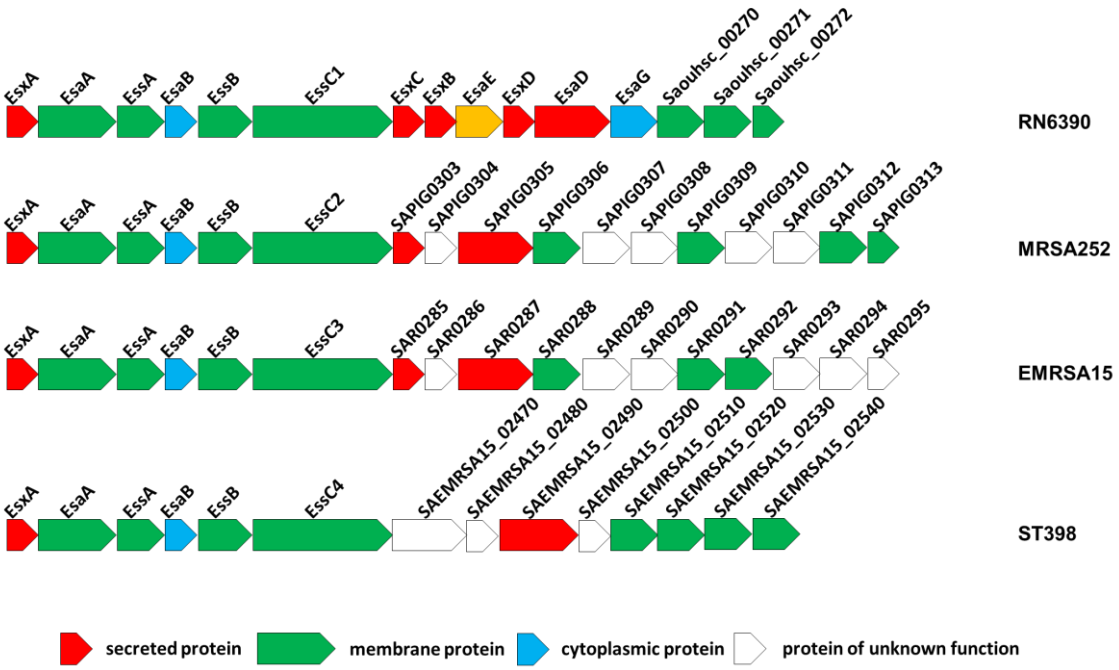

Figure 1.7: Genetic variants of the *ess* locus found across *S. aureus* strains. Adapted from Warne *et al.* (2016).

1.6 Aims of this study

In contrast to the mycobacterial Type VII secretion system little is known about how the core Ess machinery is organised or how protein secretion is mediated in *S. aureus*. Therefore, the aim of this thesis was to derive fundamental knowledge about the organisation of the core membrane components of the Ess machinery. A further aspect of the thesis work was to shed light on the linkage between the different variants of the ATPase protein EssC and the unique set of substrates encoded immediately downstream among different *S. aureus* strains.

2
Materials and Methods

Materials

All of the appliances, chemicals, bacterial strains and plasmids used in this study are given below.

2.1 Chemicals

Table 2.1: Chemicals used in this study

Chemicals	Source of supply
Acrylamide/Bis-Acrylamide (ProtoFLOWGel)	Flowgen Bioscience (Nottingham)
Agarose	Melford Laboratories Ltd. (Suffolk)
Ammoniumpersulfate (APS)	Melford Laboratories Ltd. (Suffolk)
Anhydrotetracycline	Sigma-Aldrich (Suffolk)
Ampicillin (Amp)	Formedium Ltd. (Norfolk)
2-[Bisamino]-2--1,3-propanediol (bis-TRIS)	Melford Laboratories Ltd. (Suffolk)
Chloramphenicol (Cam)	Sigma-Aldrich (Suffolk)
Coomassie Blue	Sigma-Aldrich (Suffolk)
1,4-Dithiothreitol (DTT)	Formedium Ltd. (Norfolk)
Deoxyribonuclease I from bovine	Sigma-Aldrich (Suffolk)
Digitonin	Sigma-Aldrich (Suffolk)
Dimethyl sulfoxide (DMSO)	VWR (Leuven)
Disuccinimidyl suberate (DSS)	Thermo Scientific (Rockford)
n-Dodecyl-β-D-maltoside	Sigma-Aldrich (Suffolk)
Foscholin-12	Anatrace (Maumee)
Gel-Red Nucleic Acid Stain	Biotium (Hayward)
HiMark™ Pre-stained HMW Protein standard	Thermo Scientific (Rockford)
Imidazole	Sigma-Aldrich (Suffolk)
Lauryldimethylamine oxide	Sigma-Aldrich (Suffolk)
Lysostaphin	Ambi (Lawrence)
MOPS-SDS Running Buffer (20x)	Formedium Ltd. (Norfolk)
NativeMark™ Unstained Protein standard	Thermo Scientific (Rockford)
NuPAGE® Transfer Buffer	Thermo Scientific (Rockford)
NuPAGE® Loading Buffer	Thermo Scientific (Rockford)
Phenylmethanesulfonyl fluoride	Sigma-Aldrich (Suffolk)
Polyethylene Glycol 6000 (PEG 6000)	Duchefa Biochemie (Haarlem)
Precision Plus Protein™ Standards (all Blue)	Bio-Rad (Hertfordshire)
Skimmed milk powder (Marvel Original)	Chivers Ireland Ltd (Dublin)
Sodiumdodecylsulfate (SDS)	Melford Laboratories Ltd. (Suffolk)
Sodium Deoxycholate	Sigma-Aldrich (Suffolk)
N,N,N',N'–Tetramethylethylendiamine (TEMED)	VWR (Leuven)
Trichloracetic acid (TCA)	Sigma-Aldrich (Suffolk)
Tricine	Sigma-Aldrich (Suffolk)
Triton – X- 100	Sigma-Aldrich (Suffolk)
Tween 20	VWR (Leuven)

2.2 Appliances

Table 2.2: Appliances used in this study

Appliance	Model, Producer
Äkta:	Äkta pure (GE Healthcare)
	Äkta start (GE Healthcare)
Cell disruptor:	Digital Sonifier (Branson)
	Thermo electron corporation French Press cell disruptor
	Aminco Pressure Cell 30 000 psi
Centrifuges:	accuSpin™ 1R (Thermo Scientific)
	Avanti® J-26 XP (Beckman)
	Biofuge pico (Heraeus)
	J6-MI Centrifuge (Beckman)
	Optima™ L-100 XP Ultracentrifuge (Beckman)
	Optima™ TLX Ultracentrifuge (Beckman)
Electroporator	GenePulser XCell (Bio-Rad)
Incubator:	Genlab incubator
	Infors Multitron (Infors)
	Innova 2100 platform shaker (New Brunswick Scientific)
	TC-7 (New Brunswick Scientific)
Medical Film Processor	Model SRX-101A (Konica Minolta)
Native PAGE gel chamber	Mini Gel Tank (Thermo Scientific)
SDS gel chamber	Mini-PROTEAN® Tetra (Bio-Rad)
Transfer cell:	iBlot Dry Blotting System (Thermo Scientific)
	iBlot 2 Dry Blotting System (Thermo Scientific)
	Transblot SD Semi-dry transfer cell (Bio-Rad)
Platereader	BioTek ELx808 (Thermo Scientific)

2.3 Columns, Equipment and Kits

Table 2.3: Columns, Equipment and Kits used in this study

Material	Source of supply
Chromatography paper 3mm Chr	Whatman
DC™ Protein assay Reagent A + B	Bio-Rad
DNA Clean & Concentrator™-5	Epigenetics company
HisTrap™ HP 1 ml	GE Healthcare
Hybond™-ECL Nitrocellulose membrane 0.2 µm	GE Healthcare
iBlot® Transfer Stacks PVDF	Thermo Scientific
iBlot® 2 Transfer Stacks nitrocellulose	Thermo Scientific
Immobilon Western Chemiluminescent HRP substrate	Millipore
Immobilon-P Membrane, PVDF, 0.45 µm	Millipore
Medical Film	Konica Minolta
Minisart® Syringe filter, hydrophilic (0.2 µm / 0.45 µm)	Sartorius stedim
NativePAGE™ Novex® 4-16% Bis-Tris Protein Gels, 1.0 mm, 10 well	Thermo Scientific
QIA®prep Spin Miniprep Kit	Qiagen
QIA®quick PCR Purification Kit	Qiagen
rAPid Alkaline Phosphatase	Roche
Superdex 200 10/300 GL	GE Healthcare
T4 DNA Ligase	Roche
Vivaspin 20 (10 kDa / 50 kDa)	GE Healthcare

2.4 Bacterial Strains

Table 2.4: Bacterial Strains used in this study

Strain	Resistance	Genotype	Reference
***E. coli* DC10B**	None	*dam*$^{+}$ *dcm*$^{-}$ *hsdRMS endA1 recA1*	(Monk *et al.*, 2012)
***E. coli* JM110**	None	*rpsL* (Str^{r}) *thr leu thi-1 lacY galK galT ara tonA tsx dam dcm supE44 Δ(lac-proAB)* [F' *traΔ36 proAB lacI*^{q} *ΔM15*]	Stratagene
***E. coli* DH5α**	None	Φ80d *Δ(lacZ)M15 recA1 endA1 gyrA96 thi-1 hsdR*17 ($r_k^-m_k^+$) *supE44 relA1 deoR* Δ(*lacZYA-argF*)U169	Promega
***E. coli* BL21 DE3**	None	*E. coli* B: F^{-}, *dcm*, *ompT*, *hsdS*(rB-, mB-), *gal*, λDE3	(Studier and Moffatt, 1986)
***S. aureus* RN6390**	None	NCTC8325 derivative, *rbsU*, *tcaR*, cured of ϕ11, ϕ12, ϕ13	(Novick *et al.*, 1993)
***S. aureus* RN6390 ΔesaA**	None	*esaA* deletion	(Kneuper *et al.*, 2014)
***S. aureus* RN6390 ΔessA**	None	*essA* deletion	(Kneuper *et al.*, 2014)
***S. aureus* RN6390 ΔessB**	None	*essB* deletion	(Kneuper *et al.*, 2014)
***S. aureus* RN6390 ΔessC**	None	*essC* deletion	(Kneuper *et al.*, 2014)
***S. aureus* RN6390 ΔesxA**	None	*esxA* deletion	(Kneuper *et al.*, 2014)
***S. aureus* RN6390 ΔesxB**	None	*esxB* deletion	(Kneuper *et al.*, 2014)
***S. aureus* RN6390 Δess**	None	complete deletion from *esxA* - *esaG*	(Kneuper *et al.*, 2014)
***S. aureus* RN6390 ΔesaD**	None	*esaD* deletion	(Cao *et al.*, 2016)
***S. aureus* RN6390 ΔesaDG**	None	*esaDG* deletion	(Cao *et al.*, 2016)
***S. aureus* RN6390 ΔesaE**	None	*esaE* deletion	(Cao *et al.*, 2016)
***S. aureus* RN6390 Δstp1**	None	*stp1* deletion	this study
***S. aureus* RN6390 Δstp1_ΔpknB**	None	*stp1* and *pknB* deletion	this study
***S. aureus* MRSA252**	None	*S. aureus* clinical MRSA isolate	(Holden *et al.*, 2004)
***S. aureus* MRSA252 ΔessC**	None	*essC* deletion	lab stock
***S. aureus* EMRSA 15**	None	From Sanger Institute stocks	Prof. Sharon Peacock
***S. aureus* EMRSA 15 ΔessC**	None	*essC* deletion	lab stock
***S. aureus* 10.1252.X**	None	Human ST398 isolate	Roslin Institute, Edinburgh, original strain from Scottish MRSA Reference Lab
***S. aureus* 10.1252.X ΔessC**	None	*essC* deletion	lab stock

2.5 Plasmids

Table 2.5: Plasmids used in this study

Plasmid	Vector	Resistance	Characteristics	Reference
pET15bTEV		Amp	Protein overexpression plasmid. Protein expressed under the control of the T7 promoter. Permits fusion of a (His)6- tag followed by a TEV protease cleavage site to the N-terminus of the overexpressed protein, ApR	Prof. Bill Hunter
pIMAY		Cml, Amp	Temperature-sensitive plasmid for gene knockouts	(Monk *et al.*, 2012)
pRAB11		Cml, Amp	*E. coli/S. aureus* shuttle vector, inducible protein expression, amp^r, cml^r	(Helle, Kull *et al.* 2011)
pRMC2		Cml, Amp	*E. coli/S. aureus* shuttle vector, inducible protein expression, amp^r, cml^r	(Corrigan and Foster, 2009)
pRMC2 h	pRMC2	Cml, Amp	pRMC2 variant coding for N-terminal hexahistidine tag	(Kneuper *et al.*, 2014)
pRMC2 ch	pRMC2	Cml, Amp	pRMC2 variant coding for C-terminal hexahistidine tag	(Jäger *et al.*, 2016)
pRMC2-yfp	pRMC2	Cml, Amp	pRMC2 with yfp fragment from pKM3a cloned *Bgl*II/*Eco*RI for transcriptional and translational yfp fusions, no start codon, AGATCT in frame	(Casabona *et al.*, 2017)
pEsxA	pRMC2	Cml, Amp	*esxA* gene from *S. aureus* RN6390 cloned *Kpn*I/*Eco*RI into pRMC2	lab stock
ppEsxA-yfp	pRMC2-yfp	Cml, Amp	*esxA* gene from *S aureus* RN6390 with own promoter region cloned *Kpn*I/*Bgl*II into pRMC2-yfp for expression from own promoter	(Casabona *et al.*, 2017)
pEsxA-his	pET15bTEV	Amp	pET15bTEV with esxA gene from *S. aureus*	Prof. Bill Hunter
EsaA – nhis	pRMC2 h	Cml, Amp	pRMC2h expressing His_6-EsaA	(Kneuper *et al.*, 2014)
EssA – chis	pRMC2 ch	Cml, Amp	pRMC2ch expressing His_6-EssA	(Jäger *et al.*, 2016)
EssB – nhis	pRMC2 h	Cml, Amp	pRMC2h expressing His_6-EssB	(Jäger *et al.*, 2016)
EssC 11	pRAB 11	Cml, Amp	pRAB11 with *essC* fragment from *S aureus* RN6390 cloned *Bgl*II/*Eco*RI for inducible EssC expression	lab stock
EssC	pRMC2	Cml, Amp	pRMC2 with *essC* fragment from *S aureus* RN6390 cloned *Bgl*II/*Eco*RI for inducible *essC* expression	lab stock
EssC / dFHA	pRMC2	Cml, Amp	pRMC2 with *essC* fragment coding for aa M190-F1479 from *S aureus* RN6390 cloned *Bgl*II/*Eco*RI for inducible *essC* expression	lab stock
EssC / dATP2	pRMC2	Cml, Amp	pRMC2 with *essC* fragment coding for aa M1-P958 from *S aureus* RN6390 cloned *Bgl*II/*Eco*RI for inducible *essC* expression	lab stock
EssC / dCTD	pRMC2	Cml, Amp	pRMC2 with essC fragment coding for aa M1-P1248 from *S aureus* RN6390 cloned *Bgl*II/*Eco*RI for inducible *essC* expression	lab stock
EssC - chis	pRMC2	Cml, Amp	pRMC2 with *essC* fragment from *S aureus* RN6390 with added C-terminal	(Jäger *et al.*, 2016)

			His6-tag cloned *Bgl*II/*Eco*RI for inducible EssChis expression	
EssC$_{MRSA252}$	pRAB11	Cml, Amp	pRAB11 with *essC* fragment from *S. aureus* MRSA252 cloned *Sac*I for inducible EssC expression	lab stock
EssC$_{EMRSA15}$	pRAB11	Cml, Amp	pRAB11 with *essC* fragment from *S. aureus* EMRSA15 cloned *Sac*I for inducible EssC expression	this study
EssC$_{10.1252.X\ ST398}$	pRAB11	Cml, Amp	pRAB11 with *essC* fragment from *S. aureus* 10.1252.X ST 398 cloned *Sac*I for inducible EssC expression	this study
EssCATP2-his	pET15bTEV	Amp	pET15bTEV with *essC* fragment coding for the last two ATPase domains from *S. aureus* cloned *Xho*I / *Bam*HI for inducible EssC expression	this study
pEsxC-his	pET15bTEV	Amp	pET15bTEV with *esxC* gene from *S. aureus*	Prof. Bill Hunter
pEsaE-his	pET15b	Amp	pET15b with *esaE* gene from *S. aureus* cloned *Nde*I / *Xho*I for inducible EsaE expression	lab stock
EsaD	pRAB 11	Cml, Amp	pRAB11 with *esaD* fragment from *S. aureus* RN6390 cloned *Kpn*I / *Bgl*II for inducible EsaD expression	this study
EsaD-yfp	pRMC2	Cml, Amp	*esaD*(H528A) from *S. aureus* RN6390 cloned into pRMC2-yfp for inducible EsaD-yfp expression	lab stock
pIMAY stp1	pIMAY	Cml	*stp1* (serine/threonine phosphatase) gene flanking regions in pIMAY for single gene knockout	lab stock
pIMAY stp1-pknB	pIMAY	Cml	*stp1/pknB* genes flanking regions in pIMAY for double gene knockout	lab stock

2.6 Synthetic oligonucleotides

Table 2.6: synthetic oligonucleotides used in this study

Label	Sequence (5‘ - 3‘)	Restriction site
esaA nhis fw	GGAAGATCTAAAAAGAAAAATTGGATTTATG	*Bgl*II
esaA nhis rev	GGTGAGCTCATTAGATTAATCTCTCTTTCTTAAAG	*Sac*I
essA chis fw	GATGGTACCGAAAGAGAGATTAATCTAATGTTG	*Kpn*I
essA chis rev	CTAGATCTAATGTTACTTTTACGTGCTGATTCA	*Bgl*II
essB nhis fw	GATAGATCTGTTAAAAATCATAACCCTAAAAATG	*Bgl*II
essB nhis rev	CGAGAATTCACTATTTTTTTCTTTCAGCTTCTTGGCGT	*Eco*RI
essC ATP2 fw	GGACTCGAGTGGTCAGATGATGCAAAAGAAG	*Xho*I
essC ATPase rev	GGTGGATCCTTTAAACCATCTAATTTTTTG	*Bam*HI
esaD rev bgl II	GCGCAGATCTCTACTTATTTAATATTCTTCTAATATTTCT	*Bgl*II
pRMC2 seq I	GACAGGTACCAGGAGGTTTCTACTTATGACAAAAGATATTGAATATCTAAC	*Kpn*I
essCfwdSacI	AAAGAGCTCTAGGACTGAGGCAAAGACAATGC	*Sac*I
essCr2EMRSA15	CAAATCTCATAGAGCTCTCGTTTTATTCAAATAA	*Sac*I
essCr2ST398	CATAATTGAGCTCCCTATTGAATTAATTTTATTTT	*Sac*I

All synthetic oligonucleotides were obtained from Sigma-Aldrich (Suffolk). Restriction sites are marked in red. Ribosome binding sites shaded in grey.

Methods

All growth media used in this study contained the appropriate antibiotics with the final concentration as follows:

Chloramphenicol	10 µg/ml
Ampicillin	125 µg/ml

Components of growth media used in this study:

LB-Medium:	1.0 % Bacto-Tryptone (w/v) 0.5 % yeast extract (w/v) 1.0 % NaCl (w/v)	TSB-Medium:	1.7 % casein peptone (w/v) 0.3 % soya peptone (w/v) 0.25 % glucose (w/w) 0.5 % NaCl (w/v) 0.25 % K_2HPO_4 (w/v)

2.7 cell biology methods

2.7.1 Cell cultivation

2.7.1.1 for expression tests

For expression tests the respective plasmids were introduced into *S. aureus* and transformants were incubated on solid TSB-medium with appropriate antibiotics overnight at 37 °C. A single colony was used for inoculation of an overnight culture. The following day 10 ml of fresh TSB medium was inoculated with an aliquot of the overnight culture to give an OD_{600} of 0.1. For induction of expression of plasmid-encoded proteins, the appropriate concentration of Anhydrotetracycline (ATc) was added when the OD_{600} of the culture reached 0.5 and incubated at 37 °C with vigorous shaking until an OD_{600} of 2.0 was reached. 0.5 ml of the culture was used for the preparation of a whole cell sample by centrifuging at 17 000 x *g* for 2 min and retaining the pellet. For the supernatant samples, 5ml of the culture was harvested by centrifugation for

15 min at 2 770 x *g*. To remove cell debris the supernatant was filtered through a 0.45 µm syringe filter and stored at -20 °C prior to Trichloracetic acid (TCA) precipitation.

2.7.1.2 for DSS crosslinking

For *in vitro* crosslinking experiments, the respective plasmids were introduced into *S. aureus* RN6390 and transformants were incubated on solid TSB medium with appropriate antibiotics overnight at 37 °C. A single colony was used for the inoculation of a 5 ml overnight culture. The following day 50 ml of fresh TSB-medium was inoculated with an aliquot of the overnight culture to give an OD_{600} of 0.1. For induction of expression of plasmid-encoded proteins, the appropriate concentration of ATc was added when the OD_{600} of the culture reached 0.5, and the culture was incubated at 37 °C with vigorous shaking until an OD_{600} of 2.0 was reached. The culture was harvested by centrifugation for 10 min at 2 770 x *g*.

2.7.1.3 for PFA crosslinking

For *in vivo* crosslinking experiments the respective plasmids were introduced into *S. aureus* RN6390 and transformants were incubated on solid TSB medium with appropriate antibiotics overnight at 37 °C. A single colony was used for the inoculation of a 5 ml overnight culture. The following day 50 ml of fresh TSB-medium was inoculated with overnight culture to give an OD_{600} of 0.1. For induction of expression of plasmid-encoded proteins, the appropriate concentration of ATc was added when the OD_{600} of the culture reached 0.5, and the culture was incubated at 37 °C with vigorous shaking until an OD_{600} of 1.0 was reached. The culture was harvested by centrifugation for 10 min at 2 770 x *g*.

2.7.1.4 for protein purification

For protein purification the respective plasmids were introduced into *E. coli* and transformants were incubated on solid LB-medium with appropriate antibiotics overnight at 37 °C. A single

colony was used for the inoculation of a culture that was grown for eight hours. 150 µl of this was then used for inoculation of a 100 ml of fresh medium and incubated overnight. The following day 2 x 500 ml of fresh LB-medium was inoculated with the overnight culture to give an OD_{600} of 0.1 and incubated at 37 °C with vigorous shaking. For induction of expression of plasmid-encoded proteins, 1 mM IPTG was added when the OD_{600} of the culture was between 0.6 – 0.8 and the culture was then incubated at 25 °C with vigorous shaking overnight. Cells were harvested the next day by centrifugation for 30 min at 4 °C at 3 600 x *g*.

2.7.1.5 for growth curve experiments

In preparation for growth curve experiments the respective plasmids were introduced into *S. aureus* and transformants were incubated on solid TSB-medium with appropriate antibiotics overnight at 37 °C. A single colony was used for inoculation of an overnight culture. The following day 10 ml of fresh TSB medium was inoculated with an aliquot of the overnight culture to give an OD_{600} of 0.1. After reaching an OD_{600} of 0.5, 1 ml of culture was taken to continue the experiment. For induction of expression of plasmid-encoded proteins, Anhydrotetracycline (ATc) was added to a final concentration of 500 ng/ml. Three times 150 µl of culture was then added into a 96 well plate and cell growth and fluorescence monitored over a time 18 hours by 37 °C. Optical density was measured in 20 min intervals with a shaking step 20 second before every read.

2.7.2 Preparation of competent cells

2.7.2.1 **E. coli** *competent cells prepared with transformation buffer*

To prepare *E. coli* competent cells 10 ml LB medium was inoculated from a stationary-phase culture of the strain of interest at 1:100 dilution. The culture was grown at 37 °C with vigorous shaking at 200 rpm until an OD_{600} 0.4 – 0.5 was reached. After chilling on ice for 10 min the cells were harvested by centrifugation for 10 min at 2 770 x *g*. The supernatant was removed and the

cell pellet was resuspended in ice-cold transformation buffer (to 1/10th of the original culture volume) and chilled on ice for further 20 min before use, or snap frozen and stored at – 80 °C.

Transformation Buffer: 10 g PEG 6000
5 ml 1 M $MgSO_4$
5 ml DMSO
→ fill up to 100 ml with fresh LB broth

2.7.2.2 S. aureus *electro-competent cells*

To prepare electro-competent *S. aureus* cells, 50 ml of fresh prewarmed TSB-medium was inoculated with the host strain to an OD_{600} = 0.5 and incubated for 30 min at 37 °C with vigorous shaking. After chilling on ice for 10 min the cells were harvested by centrifugation for 10 min at 2 770 x *g*. The supernatant was removed and the cell pellet was washed in 25 ml sterile, ice cold MilliQ water before pelleting again by centrifugation for 10 min at 2 770 x *g*. This washing step was repeated once more. Finally, the cell pellet was resuspended in 5 ml sterile, ice cold 10 % (w/v) glycerol and re-pelleted by centrifugation for 10 min at 2 770 x *g*. After this washing step was repeated once more, the cell pellet was resuspended in 1ml sterile, ice cold 10 % (w/v) glycerol and centrifuged for 10 min at 2 770 x *g*. The supernatant was removed again and the cell pellet resuspended in 250 µl sterile, ice-cold 10 % (w/v) glycerol before storage at -80 °C in 50 µl aliquots.

2.7.3 Transformation of competent cells

2.7.3.1 E. coli *competent cells prepared with transformation buffer*

For transformation, 150 µl of *E. coli* competent cells were mixed with 1 µl of plasmid DNA solution and chilled on ice for 30 min. Subsequently the cells were heat-shocked at 42 °C for 1 min and immediately placed on ice for further 2 min. 800 µl LB-medium without antibiotics were added and the cells were incubated at 37 °C for 1 h with vigorous shaking. Afterwards the

cells were pelleted at 1 000 x *g* for 5 min, resuspended in 100 µl LB and plated on LB medium containing appropriate antibiotics. The plates were incubated overnight at 37 °C.

2.7.3.2 S. aureus *electro-competent cells*

For transformation, a 50 µl aliquot of *S. aureus* electro-competent cells was used. The cells were chilled on ice for 5 min and left at room temperature for a further 5 min. The cells were then incubated for 2 min at 56 °C followed by a centrifugation step for 1 min at 5000 x *g*. The cell pellet was resuspended in 50 µl of 10 % glucose / 500 mM sucrose, and up to 5 µg of plasmid-DNA were added. The sample was transferred to a 0.1 cm electroporation cuvette and treated with Pulse 21kV/cm, 100 Ω and 25 µF. 1 ml of 500 mM sucrose / TSB was added immediately and the culture incubated at 37 °C for 1.5 h with vigorous shaking. Afterwards the cells were centrifuged at 1 000 x *g* for 5 min, resuspended in 100 µl 500 mM sucrose / TSB and plated onto TSB medium containing appropriate antibiotics. The plates were incubated overnight at 37 °C.

2.8 Molecular biology methods

2.8.1 Polymerase chain reaction

Each sample contained 50 µl with the following components:

Table 2.7: Chemical composition of typical PCR samples

Component	volume [µl]
double-distilled H_2O	32.5 - 34.5
5 x buffer (Rxn Herculase)	10.0
dNTP-Mix (per 10 mM dATP, dCTP, dGTP, dTTP)	1.0
Primer 1 [100 µM]	0.5
Primer 2 [100 µM]	0.5
DNA-Template [~300 - 500 ng]	3.0 – 5.0
DNA Polymerase Herculase II	0.5

The PCR machine was programmed as follows:

Table 2.8: PCR programme

Reaction step	parameter:
Preheating	2 min at 95 °C
Denaturation	30 sec at 95 °C
Annealing	30 sec at 50 °C - 53 °C
Elongation	45 sec to 4 min at 72 °C
Final step	3 – 7 min at 72 °C
Cycles	29

The time for elongation was varied depending on the size of the template, allowing for 1 kb per minute. The final step was 2 – 3 x the elongation time.

2.8.2 Purification of DNA products

After performing PCR reactions, PCR products were cleaned by following the protocol of the QIA®quick PCR Purification Kit (Qiagen). Depending on the amount of DNA, 30 to 50 µl ddH_20 was used for the elution step.

2.8.3 DNA digestion by restriction and preparing for cloning

1.0 µg of DNA was digested using 15 U of the appropriate restriction enzymes in a buffer provided by Agilent in a final volume of 50 µl. For *Kpn*I digestion 0.01 % BSA (v/v) was also included. The samples were incubated for 1.5 h at 37 °C.

Following digestion DNA samples were purified (see 2.8.2) and the vectors for cloning were dephosphorylated using shrimp alkaline phosphatase (Roche). 3.7 µl 10 x alkaline phosphatase buffer and 1.5 µl of alkaline phosphatase were added to each reaction. The samples were incubated for 1 h at 37 °C. To stop the reaction the samples were subsequently incubated for 2 min at 72 °C.

2.8.4 DNA ligation

T4 DNA ligase (Roche) was used to clone inserts into the appropriate vector. Insert DNA was mixed with vector DNA in a ratio of 3:1 in 1 x T4 ligase buffer with a final volume of 10 µl. The samples were incubated for 2.5 h at room temperature and transformed into the appropriate *E. coli* strain.

2.8.5 Colony PCR

To check if colonies contained clones of interest, colony PCR was carried out. A single colony was resuspended in 60 µl ddH_20 and 2 µl was used as template for the PCR reaction. Each sample contained 25 µl with the following components:

Table 2.9: Chemical composition of the colony PCR samples

Component	volume [µl]
5 x Go *Taq* Buffer	5.0
Colony	2.0
Primer (colony PCR pRMC2 primer)	0.5
dNTPs	0.5
DMSO	0.5
$MgCl_2$ [25 mM]	3.0
Go *Taq*-Polymerase	0.5
double-distilled H_2O	13.0

The PCR machine was programmed as follows:

Table 2.10: PCR programme

Reaction step	parameter:
Preheating	2 min at 95 °C
Denaturation	30 sec at 95 °C
Annealing	30 sec at 50 °C / 53 °C
Elongation	45 sec to 4 min at 72 °C
Final step	3 – 7 min at 72 °C
Cycles	29

The time for elongation was varied depending on the size of the template, allowing for 1 kb per minute. The final step was 2 – 3 x the elongation time.

2.8.6 Agarose gel electrophoresis

DNA samples were analysed using 1 % (w/v) agarose gels prepared in 1 x TAE buffer containing Gel red (Biutium) in a ratio 1:20 000. The samples were mixed with 10 x DNA loading dye and loaded on the gel together with DNA size markers (Roche). Gels were run in 1 x TAE buffer for 30 min at 100 V. After separation all bands were visualised under UV light.

TAE Buffer, pH 8.0:	40 mM Tris
	1.14 % (v/v) acetic acid
	1 mM EDTA

2.8.7 Plasmid DNA preparation

E. coli cells were incubated overnight in 10 ml LB-medium containing the appropriate antibiotics at 37 °C with vigorous shaking. The following day cells were harvested by centrifugation for 10 min at 2 770 x *g*. Plasmid DNA was isolated by following the protocol of the QIA®prep Spin Miniprep Kit (Qiagen) using 50 µl ddH_20 for plasmid DNA elution.

2.8.8 DNA Sequencing

DNA sequencing was performed using the Sanger Sequencing technique based on selective incorporation of chain-terminating dideoxynucleotides by DNA polymerase during *in vitro* DNA replication. Sequencing was undertaken by the Sequencing Service at the University of Dundee, Dundee, UK and the results analysed using the BioEdit software.

2.9 Biochemical methods

2.9.1 Cell fractionation

2.9.1.1 for expression tests

A cell pellet obtained from 0.5 ml of a *S. aureus* culture grown to an OD_{600} of 2.0 (as described in Section 2.7.1.1.) was washed with 500 µl of 1 x PBS and re-pelleted. The pellet was resuspended in 500 µl 1 x PBS and 50 µg/ml Lysostaphin was added. The samples were incubated at 37 °C for 30 min before boiling for 5 min at 95 °C and were then stored at -20 °C until further use.

For preparing membrane fractions, the cell pellet obtained from the 5 ml aliquot used for the preparation of supernatant samples was used, and was resuspended in 1 ml Buffer 1. After adding 50 µg Lysostaphin, the sample was incubated for 30 min at 37 °C followed by a centrifugation step for 10 min at 10 000 x *g*. The pellet was then resuspended in 1 ml 1 x PBS and disrupted by sonication (three times for 15s with a pulse on an off for 1 second, an amplitude of 20 % and a 20 second pause between each step). Subsequently the sonicated sample was centrifuged for 30 min at 227 000 x *g* to pellet the membranes. Membranes were resuspended in 100 µl Buffer 2 and stored at - 20 °C for further use.

Buffer 1:	50 mM Tris/HCl, pH 7.5 500 mM sucrose	Buffer 2:	1 x PBS 0.5 % Triton

2.9.1.2 for DSS crosslinking experiments

For *in vitro* crosslinking experiments, cell pellets were washed in 1 ml M1 buffer followed by centrifugation for 10 min at 2 770 x *g*. The pellet was then resuspended in 1 ml M2 buffer containing 100 µg Lysostaphin and was supplemented with 0.1 mM PMSF and a few crystals DNAse I. After an incubation time of 30 min at 37 °C, the sample was lysed by sonication (as described in Section 2.9.1.1) and centrifuged for 5 min at 17 000 x *g* to obtain the low speed

pellet. The supernatant was centrifuged again for 30 min at 227 000 x *g*. The high speed pellet (containing the membranes) was resuspended in 100 µl M1 Buffer.

M1 Buffer:	20 mM MOPS/NaOH, pH 7.2 200 mM NaCl	M2 Buffer:	20 mM MOPS/NaOH, pH 7.2 200 mM NaCl 2.5 mM EDTA

2.9.1.3 for PFA crosslinking experiments

After incubation with paraformaldehyde (PFA), cell suspensions were pelleted by centrifugation for 10 min at 2 770 x *g*. The pellet was resuspended in 1 ml T2 buffer containing 100 µg Lysostaphin, 0.1 mM PMSF and a few crystals of DNAse I. After an incubation time of 30 min at 37 °C, the sample was lysed by sonication (as described in Section 2.9.1.1) and centrifuged for 5 min at 17 000 x *g* to obtain the low speed pellet. The supernatant was centrifuged again for 30 min at 227 000 x *g*. The high speed pellet was resuspended in 100 µl T1 buffer.

T1 Buffer:	50 mM Tris/HCl, pH 7.5 200 mM NaCl	T2 Buffer:	50 mM Tris/HCl, pH 7.5 200 mM NaCl 2.5 mM EDTA

2.9.1.4 Solubilisation of the membrane extracts

Membrane fractions were prepared as described above (see Section 2.9.1.2). 400 µg of total protein was then used for solubilisation. Firstly, the membrane fraction was centrifuged for 30 min at 227 000 x *g* at 4 °C and subsequently resuspended in 40 µl of solubilisation buffer containing 1 mM DTT and 0.1 mM PMSF. After adding 2 % (final concentration) of the appropriate detergent, the samples were incubated at 25 °C for 2 h with vigorous shaking at 1000 rpm. To separate the solubilised proteins from remaining membrane fractions the samples were subsequently centrifuged for 20 min at 89 000 x *g*.

Solubilisation Buffer: 50 mM Na-PO_4, pH 8.0
300 mM NaCl
10 % Glycerol (v/v)
2 % appropriate detergent

2.9.1.5 for protein purification

Cell pellets were washed in 20 ml Buffer A containing 1 mM DTT and a Mini protease Inhibitor tablet (Roche). Samples were lysed by passing through a French press with a pressure of 12 000 psi. The cytosol was separated from the membrane and unbroken cells by centrifugation for 1 h at 160 000 x g at 4 °C. The cytosol was subsequently filtered using a 0.45 µm syringe filter and supplemented with 25 mM imidazole prior to protein purification.

Buffer A: 50 mM Na-PO_4, pH 7.8
300 mM NaCl
10 % glycerol (v/v)

2.9.2 Lowry protein concentration determination

To determine the concentration of protein present in membrane fractions, a 1:10 dilution of the membrane samples was prepared. 5 µl of this dilution were added, in triplicate, to a microtiter plate. 25 µl of Solution A of the DC™ Protein assay from Bio-Rad were added to the samples, filled up with 200 µl of Solution B from the Kit and chilled at RT for 15 min. Subsequently the Protein concentration was measured at OD_{750} nm using the BioTek ELx808 plate reader. Bovine serum albumin (BSA, Sigma) was used as standard.

2.9.3 TCA precipitation

1 ml of culture supernatant was mixed with 50 µg of Sodium deoxycholate and 10 % TCA. The samples were chilled on ice overnight followed by a centrifugation step for 5 min at 10 000 x *g* at 4 °C. The supernatant was removed and 500 µl ice-cold 80 % ethanol was added to the cell

pellet. The samples were centrifuged again for 5 min at 10 000 x *g* at 4 °C. After removing the ethanol, the pellet was allowed to air-dry for 30 min at 37 °C before being resuspended in 30 µl 50 mM Tris/HCl, pH 8.0 containing 4 % SDS.

2.9.4 bis-Tris polyacrylamide gel electrophoresis

The gels used in this study contained 6 % acrylamide in the stacking gel. The resolving gel contained between 8 % and 15 % acrylamide depending on the size of the protein of interest. Supernatant samples were mixed with 4 x NuPAGE® loading buffer, whereas cell samples were mixed with 2 x NuPAGE® loading buffer. Before loading into the wells, the samples were incubated for 10 min at 95 °C. To determine the relative molecular mass of the protein of interest, 5 µl of a Protein ladder (Precision plus Protein™ All Blue Standards, Bio-Rad) were loaded alongside the sample. Proteins were separated in MOPS-SDS running buffer (Formedium) at 110 V. Subsequently the gels were incubated in NuPAGE® transfer buffer containing 20 % methanol for electroblotting.

MOPS-SDS-Running Buffer:	50.00 mM MOPS	NuPAGE® Transfer Buffer:	25 mM Bicine
	50.00 mM Tris base		25 mM Bis-Tris base
	3.47 mM SDS		1 mM EDTA
	1.00 mM EDTA		

2.9.5 SDS polyacrylamide gel electrophoresis

Gels used in this study contained 4 % acrylamide in the stacking gel. The resolving gel contained between 5 % and 12.5 % acrylamide depending on the size of the protein. Samples were mixed with 6x SDS loading buffer prior loading. To determine the relative molecular mass of the protein of interest, 7.5 µl of a Protein ladder (HiMark™ Pre-stained protein standard, Thermo Scientific) were loaded alongside the sample. Proteins were separated in Tris-SDS running buffer at 100 V. Subsequently gels were incubated in Tris-glycine transfer buffer for electroblotting.

Tris-SDS-Running Buffer: 25 mM Tris base
192 mM glycine
0.1 % SDS (w/v)

Tris-glycine-Transfer Buffer: 25 mM Tris/HCl, pH 7.5
192 mM glycine
20 % methanol (v/v)

2.9.6 Blue Native polyacrylamide gel electrophoresis

Blue Native polyacrylamide gel electrophoresis (BN PAGE) was carried out as described by Wittig *et al.* (2006) using precast 4 – 16 % gradient bis-Tris gels (Thermo Scientific). Solubilised membrane protein samples were prepared as described above (Section 2.9.1.4) and supplemented with a final concentration of 5 % glycerol and 0.2 % Coomassie Blue. To determine the relative molecular mass of the protein of interest, 8 µl of a Protein ladder (NativeMark™ Unstained Protein standard, Thermo Scientific) were loaded alongside the sample. Proteins were separated at 4 °C and 150 V using an electrophoresis Bolt Mini-gel tank (Novex, Life Technologies) containing 25 mM imidazole (Anode Buffer) in the front chamber and Cathode Buffer B in the front chamber. Once the solubilised protein samples migrated approximately one quarter of the way through the gel, the run was paused to replace Cathode Buffer B with Cathode Buffer B/10. The run was then continued at 250 V until the migration front reached the bottom of the gel. Gels were immediately used for Western Blotting using a semi-dry transfer system (see 2.9.6.2).

Cathode Buffer B: 50.0 mM Tricine
7.5 mM imidazole
0.2 mM Coomassie Blue

Cathode Buffer B/10: 50.0 mM Tricine
7.5 mM imidazole
0.02 mM Coomassie Blue

2.9.6 Western blotting and immunological detection of proteins

Following bis-Tris-PAGE (see 2.9.4) or SDS PAGE (see 2.9.5) proteins were transferred to nitrocellulose (GE Healthcare) or PVDF (Immobilon) membrane by use of the semi-dry method. PVDF membranes were pre-activated in 100 % methanol for 15 sec followed by a 2 min washing

step in ddH_20. The gel, membrane and filter paper were soaked in NuPAGE Transfer buffer (see 2.9.4). The transfer was performed at 20 V for 60 min.

For dry transfer the iBlot and iBlot2 devices (Thermo Scientific) were used. Following SDS PAGE nitrocellulose membranes were used with customer setting of 20 V for 1 min, 23 V for 4 min and 25 V for 2.5 min. PVDF membranes were used following BN PAGE with the transfer programme P0 (20 V for 7 min).

PVDF membranes after dry transfer from BN PAGE were destained in 25 % methanol / 10 % acetic acid solution for 2 h at room temperature with gentle agitation. After a washing step in ddH_20 membranes were dried, the protein ladder marked and the membrane completely destained in 100 % methanol before being washed in TBS/Tween three times for 10 min.

Subsequently membranes were blocked in 5 % skimmed milk suspended in TBS/Tween for 1h at room temperature or overnight at 4 °C with shaking. After discarding the blocking buffer the membrane was incubated with the primary antibody in 5 % skimmed milk for 1 h at room temperature. If the first antibody was not conjugated to horseradish peroxidase (HRP-conjugated), incubation with a secondary antibody was necessary. In this case the membrane was washed three times for 10 min with TBS/Tween at room temperature and incubated for further 45 min with the secondary antibody in 5 % skimmed milk at room temperature, followed by three washing steps with TBS/Tween each for 10 min.

Finally, the membrane was incubated in 2 ml chemiluminescent HRP substrate. The chemiluminescent bands were exposed on medical Film and developed in Medical film Processor (Model SRX-101A Konica Minolta).

Table 2.11: Antibodies used in this study.

primary antibody	dilution	reference
rabbit anti EssB	1: 5 000	(Kneuper *et al.*, 2014)
rabbit anti EssA	1:10 000	lab stock
rabbit anti EssC	1:10 000	(Kneuper *et al.*, 2014)
rabbit anti EsxC	1: 2 000	(Kneuper *et al.*, 2014)
rabbit anti EsxA	1: 2 500	(Kneuper *et al.*, 2014)
rabbit anti EsaA	1:10 000	(Kneuper *et al.*, 2014)
mouse anti His	1: 2 000	lab stock
mouse anti His IgG HRP conjugate	1:10 000	Abcam
rabbit anti TrxA	1:20 000	(Miller *et al.*, 2010)
secondary antibody	**dilution**	**reference**
goat anti rabbit IgG HRP conjugate	1:10 000	Bio-Rad
goat anti mouse IgG HRP conjugate	1:10 000	Bio-Rad

TBS/Tween: 10 mM Tris/HCl, pH 7.5
250 mM NaCl
0.1 % Tween 20

2.9.7 crosslinking experiments

2.9.7.1 in vitro *crosslinking*

Disuccinimidyl suberate (DSS) crosslinking experiments were carried out with membrane fractions containing 30 µg of total protein. The samples were mixed with a final concentration of 2 mM DSS or with DMSO only (control sample) and made up to 50 µl with crosslinking buffer. After an incubation time of 30 min at room temperature the reaction was quenched by adding 100 mM Tris/HCl, pH 8.0. Finally all samples were made up to 73.3 µl with 4 x NuPAGE Loading Buffer and 1 µg of total protein loaded on a bis-Tris-Gel.

Buffer X1: 20 mM HEPES/NaOH, pH 7.4
20 mM KCl
250 mM sucrose
1 mM EDTA

When crosslinking purified proteins, paraformaldehyde (PFA) was used as a crosslinker. 20 µg of the largest protein, EssC, was used for each crosslinking reaction, what resembles a molar concentration of 6.7 µmol/L. All other proteins were mixed in a molar ratio of 1:1 and one

sample, containing the ATPase protein EssC, treated with 2 mM ATP / 2 mM $MgCl_2$ in addition to the crosslinker. PFA was added to a final concentration of 0.6 % and the sample was filled up to 50 µl with buffer X2. The reaction was incubated at room temperature for 30 min after which it was quenched by adding 100 mM Tris/HCl, pH 7.8. Finally, all samples were made up to 73.3. µl with 4 x NuPAGE loading buffer and 5 µl loaded on a bis-Tris-gel.

Buffer X2: 50 mM HEPES/NaOH, pH 7.8
100 mM NaCl
10 % glycerol (v/v)

2.9.7.2 in vivo crosslinking

Paraformaldehyde (PFA) crosslinking experiments were carried out in whole cells suspended in 1 x PBS. Paraformaldehyde was added to the cell suspension to a final concentration of 0.6 % and samples incubated for 30 min at room temperature. The reaction was quenched by adding 100 mM Tris/HCl, pH 8.0. Subsequently membrane fractions were obtained as described in Section 2.9.1.3

2.9.8 Protein purification

Protein purification was carried out using an Äkta start (GE Healthcare). A 1 ml His-Trap HP column (GE Healthcare) charged with Ni^{2+} was calibrated with five column volumes (CV) of buffer B1. After the sample was loaded, the column was washed with buffer B1 for 10 CV after which fractions were collected over a linear imidazole concentration gradient from 25 mM to 250 mM over 18 CV. Fractions containing the protein of interest were pooled and concentrated in a spin concentrator (GE Healthcare) exchanging buffer B with buffer A to remove the imidazole.

Buffer B1: 50 mM Na-PO_4, pH 7.8
300 mM NaCl
10 % glycerol (v/v)
25 mM imidazole

Buffer B2: 50 mM Na-PO_4, pH 7.8
300 mM NaCl
10 % glycerol (v/v)
250 mM imidazole

2.9.9 Size exclusion chromatography

Size exclusion chromatography (SEC) was performed on EssCATP2-his to check for hexameric formation of the protein. SEC was conducted using a Superdex 200 10/300 column (GE Healthcare) using an Äkta pure (GE Healthcare). The purified protein (see Section 2.9.8) was concentrated to 500 µl using a spin concentrator (GE Healthcare) followed by centrifugation for 30 min at 4 °C at 10 000 x *g* to remove any aggregates. Prior to injection of the sample, the column was washed with buffer C for 3 CV and equilibrated with the same buffer over 5 CV. A 500 µl loop was used to load the sample followed by elution of protein in 500 µl aliquots into a 96 well tray. Samples containing the protein of interest were analysed by SDS PAGE prior to pooling and concentrating while changing buffer C against buffer A for future crosslinking experiments.

Buffer C: 50 mM Tris/HCl, pH 7.8
100 mM NaCl

3
Detergent extraction and BN PAGE analysis of the essential membrane proteins of the T7SS

3.1 Introduction

Prior studies of the ESX-1 and ESX-5 T7SSs from Mycobacteria have shown that the EccB, EccC, EccD and EccE components form a complex of ~1.5 mDa, with a likely 6:6:6:6 stoichiometry (Houben *et al.*, 2012; van Winden *et al.*, 2016; Beckham *et al.*, 2017). Recent negative stain structural analysis of ESX-5 has indicated that the ATPase EccC lies at the centre of this complex and probably forms the protein transport channel (Beckham *et al.*, 2017). By analogy it is likely that in firmicutes, the homologous protein EssC also acts as the transport channel, in agreement with structural and modelling studies on domains of this protein (Rosenberg *et al.*, 2015; Zoltner *et al.*, 2016). However, apart from EccC/EssC, none of the other essential membrane components of the T7SS are conserved between the two types of T7SS, raising the possibility that they may have different architectures.

As outlined in Chapter 1, the *S. aureus* T7SS has four critical membrane components: EsaA, EssA, EssB and EssC (Burts *et al.*, 2005; Kneuper *et al.*, 2014). The predicted topologies and domain structures of these proteins are shown in Fig 3.1.

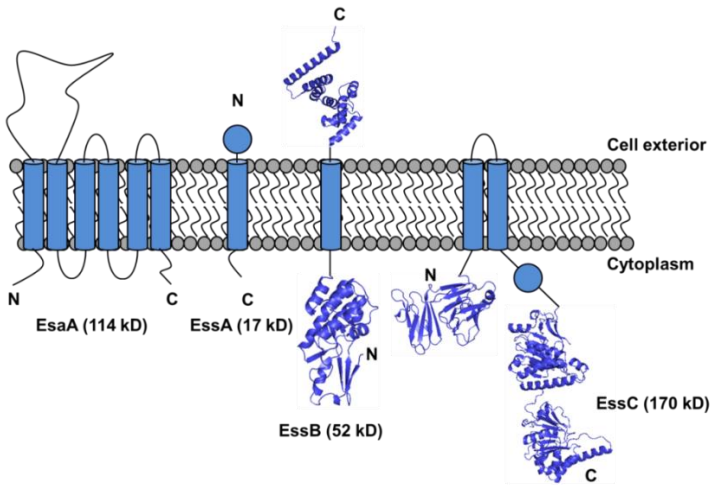

Figure 3.1: Membrane components of the *S. aureus* T7SS. The sizes and predicted topologies of EsaA, EssA, EssB and EssC are shown. Also included is existing structural information for EssB and EssC. The co-ordinates and structure factor data for EssB-C and EssB-N are deposited in the PDB under code 2YNQ and 4ANO, respectively. Co-ordinates and structure factor data for EssC-N and EssC-C are deposited in the PDB under code 5FWH and 5FV0, respectively.

EsaA is a 114 kDa protein with six predicted TMDs and a large extracellular loop that is known to reach the surface of the cell (Dreisbach *et al.*, 2010). EssA is a small protein of 17 kDa with a single TM and a globular domain at the extracellular side. EssB is another monotopic membrane protein with globular domains on both sides of the membrane and a size of 52 kDa (Chen *et al.*, 2012; Zoltner *et al.*, 2013a). Currently the functions of any of these three proteins are unknown. EssC, at 170 kDa, is the largest of the four membrane proteins and consists of a globular domain at the N-terminus with two repeats of a fork-head associated domain (FHA), followed by two TMDs and three P-loop ATPase domains at the C-terminus (Tanaka *et al.*, 2007; Rosenberg *et al.*, 2015; Zoltner *et al.*, 2016).

So far all of the structural analysis of *S. aureus* T7SS membrane components was undertaken following heterologous production of domains of these proteins in *E. coli* (Chen *et al.*, 2012; Zoltner *et al.*, 2013a; Zoltner *et al.*, 2013b; Zoltner *et al.*, 2016). To date there is very little published methodology for extraction of membrane proteins directly from the *S. aureus* membrane, and there are likely to be differences in the cytoplasmic membrane lipid composition between *S. aureus* and *E. coli*. Bacteria are able to adapt to stresses such as changes in temperatures and osmolarity or exposure to membrane-damaging compounds by either changing the type of fatty acid or the type of polar head group, leading to a different set of phospholipids (Zhang and Rock, 2008). While *E. coli* and *S. aureus* ensure survival in stationary growth phase by increasing the cardiolipin (CL) concentration (Short and White, 1971; Hiraoka *et al.*, 1993) it could be shown that *S. aureus* also uses the same mechanism to adapt to osmotic stress (Hayami *et al.*, 1979; Tsai *et al.*, 2011). CL, also called di-phosphatidylglycerol, together with phosphatidylglycerol (PG) are the most common bacterial phospholipids. They consist of a negatively charged head group giving the membrane anionic properties. However, *S. aureus* is able to modify PG by attaching L-lysine to the PG-head group, resulting in a positive charge of the lipid (Gould and Lennarz, 1967). This modification partially neutralises the charge on the *S. aureus* membrane, which increases resistance against cationic antimicrobial peptides but also

has an influence on the synthesis of membrane proteins (Peschel *et al.*, 2001; Sievers *et al.*, 2010; Staubitz *et al.*, 2004).

Before being able to investigate the architecture of the T7SS membrane components from *S. aureus* it was therefore necessary to first find a detergent which was able to extract these membrane proteins. Detergents can be separated into three main groups with different characteristics: ionic, non-ionic, and zwitterionic. Ionic detergents consist of a head group which is positively or negatively charged followed by a hydrophobic hydrocarbon chain or steroidal backbone. Non-ionic detergents in contrast have an uncharged hydrophilic head group, whereas zwitterionic detergents combine the properties of the ionic and non-ionic detergents. Also belonging to the ionic detergents are the so called bile acid salts. Bile acid salts have a different backbone comprising of rigid steroidal groups. As a result they form small kidney-shaped aggregates compared to the spherical micelles formed by ionic linear-chain detergents (Seddon *et al.*, 2004; Figure 3.2).

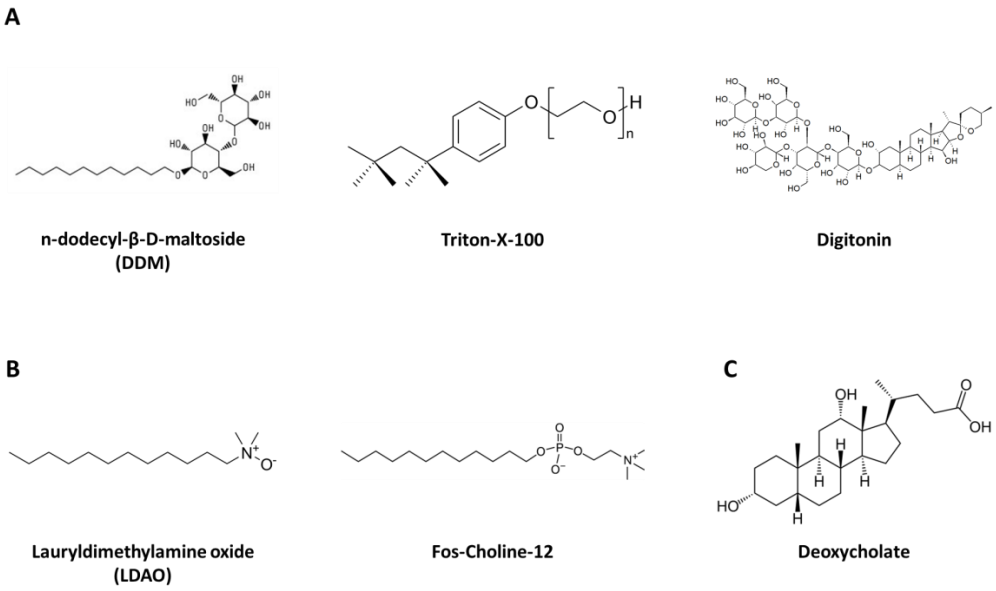

Figure 3.2: Structures of the detergents used in this study. Detergents shown in **A** are non-ionic; **B** zwitterionic; and **C** ionic bile acid salt.

3.2 Aim

The aim of this Chapter was to develop expression systems and membrane extraction protocols to facilitate the isolation of complexes containing the Ess membrane components from the native organism.

Results

3.3. Genetic manipulation of the Ess membrane protein-encoding genes

To facilitate purification of Ess complexes, His-tagged variants of each of the Ess membrane proteins, EsaA, EssA, EssB and EssC needed to be constructed to allow inducible production in the native host, *S. aureus*. To achieve this, the backbone vector pRMC2 was used (Corrigan and Foster, 2009; Figure 3.3). This vector encodes the TetR repressor protein and the TetR-controlled $P_{xyl/tetO}$ promoter, which is used to induce protein production upon addition of Anhydrotetracycline (ATc).

As *S. aureus* is known to produce many extracellular proteases, His-tags were introduced onto the cytoplasmic-facing termini of each protein. For EsaA and EssB the N-terminus was chosen, and for EssA the C-terminus (Figure 3.1). A plasmid-encoded C-terminal His-tagged variant of EssC had already been constructed by Dr. Holger Kneuper (Jäger *et al.*, 2016). For construction of the N-terminal His-tagged variants of EsaA and EssB a modified pRMC2 vector, pRMC2 h, was used, where DNA coding for an N-terminal His-tag had been introduced (Kneuper *et al.*, 2014). The gene coding for *esaA* was introduced using the restriction sites *Bgl*II and *Sac*I while the gene coding for *essB* was inserted via the restriction sites *Bgl*II and *Eco*RI. The C-terminal His-tagged variant of EssA was produced from a modified pRMC2 vector (pRMC2 ch; Jäger *et al.*, 2016), that already contained DNA coding for a C-terminal His-tag, introducing the *essA* gene using the restriction sites *Kpn*I and *Bgl*II (see Table 2.6 for the sequence of the primers used in this work).

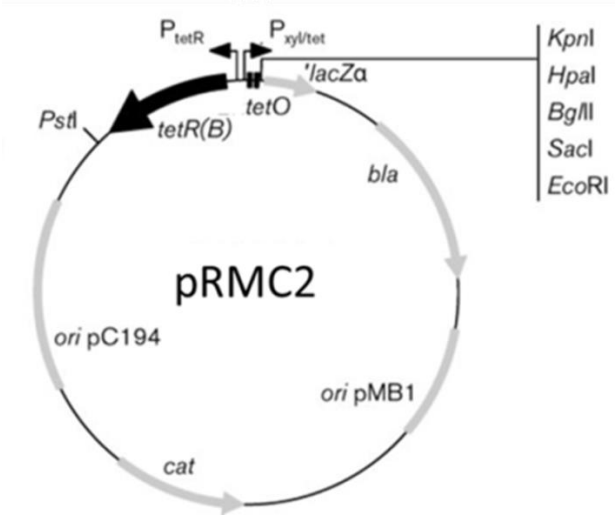

Figure 3.3: Vector used for the genetic manipulation of *ess* encoding genes. The *tetR(B)* region regulates the protein expression by induction with Anhydrotetracycline (ATc).

3.3.1 Testing expression of the His-tagged proteins

Before further study of the recombinant His-tagged membrane proteins, it was first important to determine whether the added His-tag interfered with the stability and/or functionality of each protein. Therefore it was necessary to check for stable production of each membrane protein by western blotting, and to find induction levels for each which ensured protein production comparable to the native level produced by the *S. aureus* RN6390 wild type strain. The *S. aureus* RN6390 wild type strain was therefore included as a control, alongside the single deletion strains lacking *esaA*, *essA*, *essB* or *essC* each producing the cognate plasmid-encoded protein. Each single deletion strain harbouring the empty pRMC2 vector was used as a negative control.

In the first step, different induction levels were tested by adding between 25 ng/ml and 200 ng/ml ATc to cultures of these strains. After an OD_{600} of 2.0 was reached, cells were harvested, lysed with Lysostaphin and immunoblotted using polyclonal antisera raised to the appropriate protein. In Figure 3.4 it can be seen that while 50 ng/ml ATc was required to give

approximately native level expression of EsaA, 25 ng/ml ATc was sufficient to produce native levels of the EssB and EssC variants. Detection of the EssA protein via immunoblot was not possible due to the poor quality of the antiserum (Data not shown).

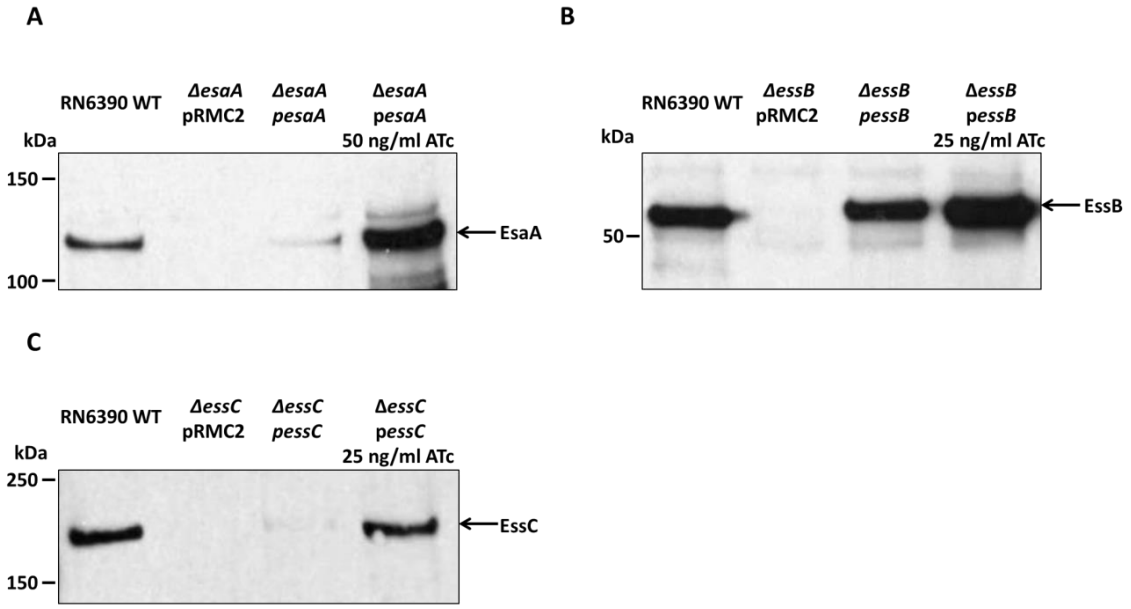

Figure 3.4: Immunological detection of the plasmid-encoded His-tagged proteins EsaA-His, EssB-His and EssC-His. 10 µl of whole cell samples were loaded on a bis-Tris gel containing either 8 % (for EsaA and EssC) or 10 % (for EssB) acrylamide. For immunological detection polyclonal antibodies raised against the purified proteins were used.

3.3.2 Testing the activity of the ESS machinery after complementation with the His-tagged proteins

Once an induction level restoring approximately wild type production of EsaA, EssB and EssC was found, it was next tested if the His-tagged proteins retained activity. It should be noted that these experiments were also carried out using the *essA* mutant strain, even though production of a stable EssA protein could not be verified by western blotting, as it was reasoned that if the plasmid-encoded variant of EssA is able to rescue the activity of the system it would prove that the protein is functionally produced. Cells of each of the *esaA, essA*, *essB* and *essC* mutant strains, producing the cognate plasmid-encoded His-tagged protein, were grown to an OD_{600} of

2.0 in the presence of ATc and separated into culture supernatant (sn) and cellular fractions (c). Samples were then immunoblotted against the T7SS secreted proteins EsxA and EsxC.

Neither EsxA nor EsxC was detectable in the supernatant of each of the individual deletion strains harbouring the empty pRMC2 vector (Figure 3.5). However, reintroducing the plasmid-encoded His-tagged protein could rescue T7 secretion activity in each case, as the secreted proteins EsxA and EsxC could be identified by immunoblot in the supernatants of the complemented strains (Figure 3.5). While for EsaA and EssB re-introduction of the plasmid-encoded protein was sufficient to restore secretion activity (Figure 3.5 A and C), WT levels of secretion activity could only be restored for EssC after induction with 25 ng/ml ATc, the same amount needed for approximately WT production of the protein (Figure 3.5 D). The secretion activity of the system could also be restored after re-introduction of the plasmid-encoded variant of EssA although only after induction of the protein production with a final concentration of 100 ng/ml ATc (Figure 3.5 B). In each of these experiments the cytosolic protein TrxA was used as a negative control and its detection only in the cell samples indicates that there is no lysis of the cells and the detection of the proteins EsxA and EsxC in the supernatant is due to secretion (Figure 3.5).

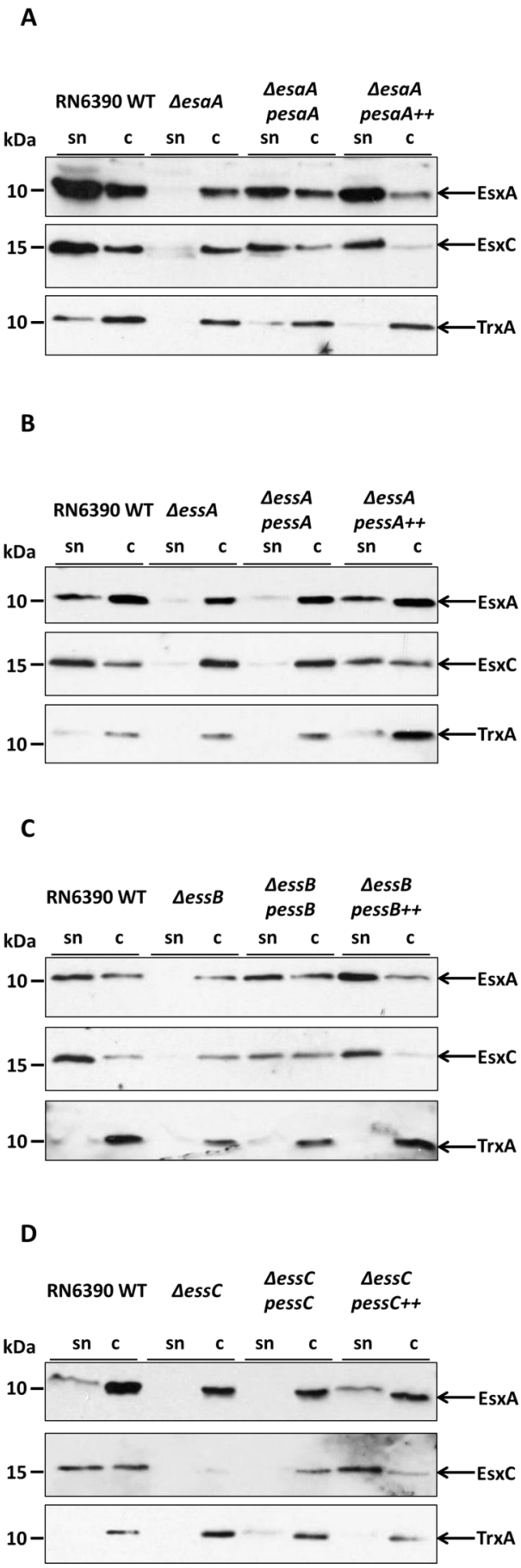

Figure 3.5: Plasmid-encoded EsaA-His, EssA-His EssB-His and EssC-His support secretion of EsxA and EsxC. The RN6390 WT strain together with the isogenic deletion strains *esaA*, *essA*, *essB* or *essC* harbouring the empty pRMC2 vector (Δ*esaA,* Δ*essA,* Δ*essB,* Δ*essC*, respectively) or pRMC2 encoding a His-tagged variant of the indicated gene (Δ*esaA pesaA*, Δ*essA pessA*, Δ*essB pessB*, Δ*essC pessC*) were grown in TSB medium. After reaching an OD_{600} = 0.5 cultures harbouring the pRMC2 vector encoding a His-tagged variant were supplemented with ATc to a final concentration of 25 ng/ml for EssB and EssC(Δ*essB pessB*$^{++}$, Δ*essC pessC*$^{++}$), 50 ng/ml for EsaA (Δ*esaA pesaA*$^{++}$) and 100 ng/ml for EssA (Δ*essA pessA*$^{++}$) to induce plasmid-encoded protein production. An equivalent of 200 µl of culture supernatant (sn) and 10 µl of resuspended cell sample (c) adjusted to an OD_{600} = 1.0 were separated on a bis-Tris gel containing 15 % acrylamide and immunoblotted using the Anti-EsxA or Anti-EsxC antisera or a control antiserum raised against TrxA.

3.3.3 Detection of recombinant proteins using anti-His-tag antibodies

Since the complementation of the *essA* mutant with the His-tagged EssA protein could restore T7 secretion activity, attempts were made to detect the protein using anti-His-tag antisera. Cells of the RN6390 WT strain together with *essA* deletion strain either producing the plasmid-encoded protein or harbouring the empty pRMC2 vector were grown to an OD_{600} = 2.0 in the presence of 100 ng/ml ATc, harvested and treated with Lysostaphin as described earlier. To also confirm the presence of the His-tag for the other membrane components *esaA, essB* and *essC* deletion strains carrying the plasmid-encoded His-tagged variants were also used, together with *esaA, essB* or *essC* strains harbouring the empty pRMC2 vector. Cells of these strains were grown under the same conditions as described for EssA using the same concentration of ATc required to restore protein production to an approximately WT level (Section 3.3.1). Cells were separated on bis-Tris gels followed by immunoblotting with anti His-tag antibodies.

Unfortunately none of the whole cell fractions gave obvious cross-reacting bands with the anti His-tag antiserum (data not shown). Therefore membrane fractions of each strain were prepared, separated on bis-Tris gels and immunoblotted. As seen in Figure 3.6 the presence of the His-tag could only be confirmed on the EssB protein (Figure 3.6 C). However, the signal was not as strong as that detected using the native EssB antiserum (compare upper and lower panels). For EssC only a faint band could be detected when blotting against the His-tag, barely visible above the background (Figure 3.6 D). For EsaA detection of the His-tag was not possible while for EssA neither the protein itself nor the His-tag could be detected by immunoblot (Figure 3.6 A and B).

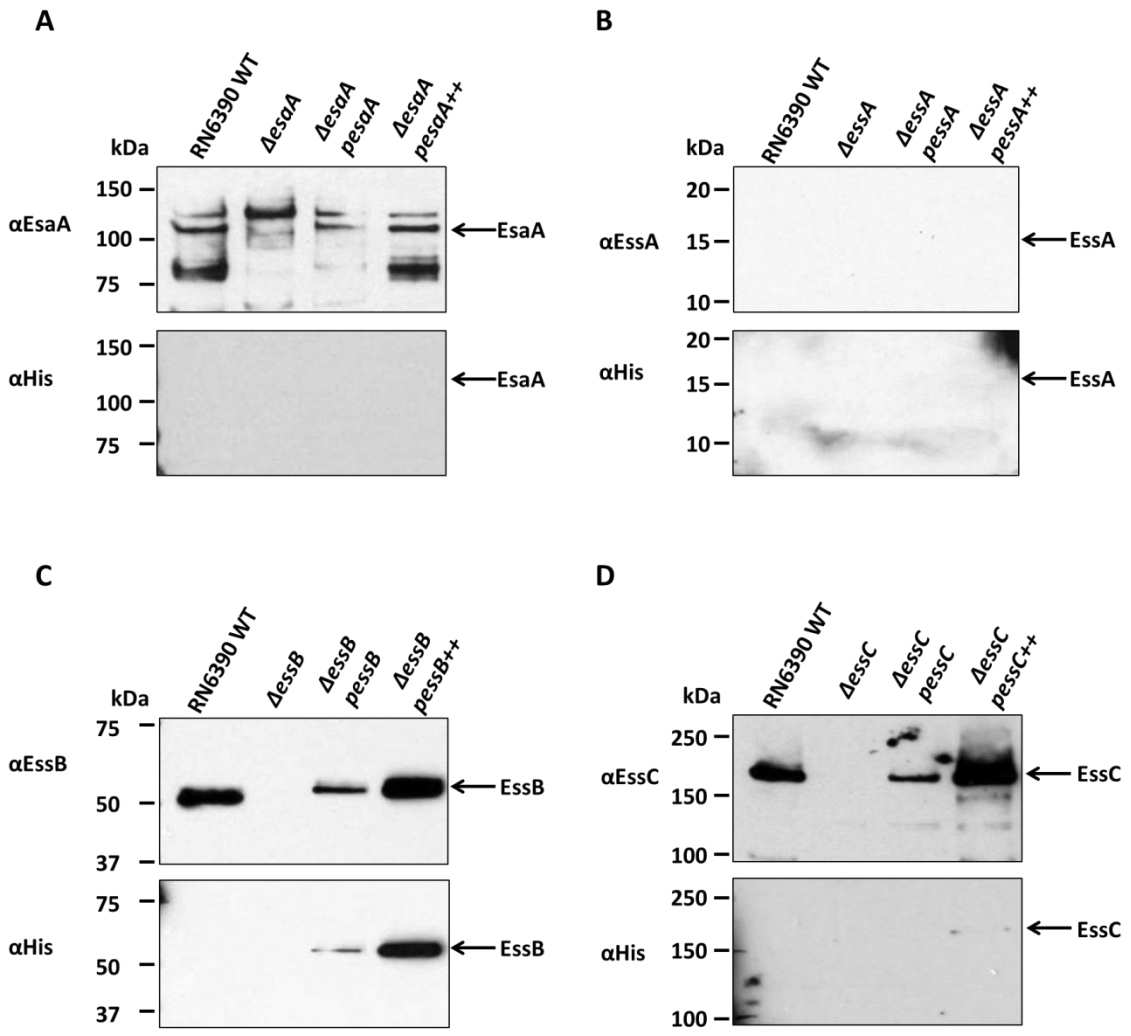

Figure 3.6: Immunological detection of the His-tagged Ess proteins. Membrane fractions were prepared from strain RN6390 WT or the isogenic *esaA*, *essA*, *essB* or *essC* deletion strains, either harbouring the empty pRMC2 vector (lanes labelled Δ*esaA,* Δ*essA,* Δ*essB,* Δ*essC*, respectively) or pRMC2 overproducing a His-tagged variant of the indicated gene (Δ*esaA pesaA*$^{++}$, Δ*essA pessA*$^{++}$, Δ*essB pessB*$^{++}$, Δ*essC pessC*$^{++}$). 10 µg of total membrane protein was loaded on a bis-Tris gel containing 8 %, 10 % or 15 % acrylamide for the detection of EsaA and EssC, EssB or EssA, respectively. The upper panels are Western blots using polyclonal antisera raised against the specific protein. The lower panels are Western Blots using a monoclonal anti His antibody (Abcam).

3.4 solubilisation of the Ess membrane proteins

3.4.1 Identification of detergents able to extract Ess proteins from the membrane of *S. aureus*

Initial analysis of the ESX-5 secretion system membrane complex used BN PAGE analysis of membrane fractions of *M. marinum* and *M. bovis* BCG (Houben *et al.*, 2012). BN PAGE analysis

is widely used when studying membrane complexes as it is possible to maintain the native protein conformation. In standard SDS gels SDS denatures and binds to the proteins, conferring a negative charge which allows the proteins to migrate towards the positively charged electrode. In BN PAGE coomassie blue dye is used instead of SDS. This also binds to the proteins, resulting in a negative charge, but contrary to SDS keeps the proteins in their native state. The absence of SDS in the gels and running buffer makes it necessary to solubilise the bacterial membrane in advance. The first step was therefore to identify a detergent that would effectively solubilise the ESS membrane proteins. To this end, membrane fractions of the RN6390 WT strain were prepared and solubilised using six different detergents. The results are shown in Figure 3.7.

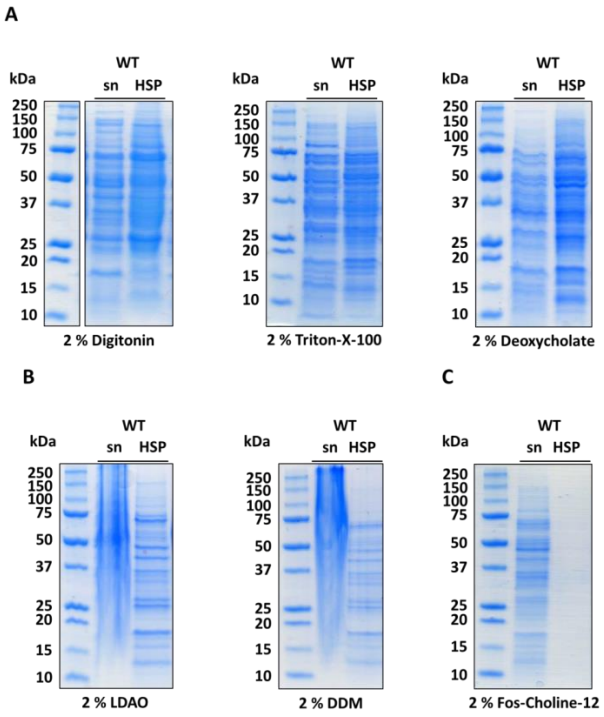

Figure 3.7: Detergent solubilisation of *S. aureus* membrane proteins. The six indicated detergents were tested for the efficiency to solubilise total membrane protein. 400 µg of total protein were solubilised using 2 % of the indicated detergent by incubation for 2 h at RT with vigorous stirring. To remove insoluble material the samples were centrifuged at 89 000 x *g* for 20 min at 4 °C. 10 µl of the supernatant (sn) together with 10 µl of the resuspended high-speed-pellet (HSP) were then separated on bis-Tris gels containing 12 % acrylamide. **LDAO:** Lauryldimethylamine oxide; **DDM:** n-dodecyl-β-D-maltoside.

Deoxycholate and Triton-X-100 are detergents that have already been used in other experiments when working with *S. aureus* (Burts *et al.*, 2008). As shown in Figure 3.7 A, these detergents, together with Digitonin, were partly successful at solubilising proteins from the *S. aureus* membrane. Approximately half of the total membrane proteins could be extracted by these detergents as the amount of protein in the detergent extracted supernatant was roughly the same as in the unextracted membrane (high-speed pellet). Comparing these three detergents showed that Triton-X-100 was most successful in solubilisation of the membrane proteins as more proteins could be found in the supernatant than when solubilising with Deoxycholate or Digitonin. N-Dodecyl β-D-maltoside (DDM) and Lauryldimethylamine oxide (LDAO) apparently failed to efficiently extract any protein from the membrane, since almost no distinguishable protein bands were found in the supernatant following detergent treatment (Figure 3.7 B), instead large smears were observed. However, comparing these two detergents with Digitonin, Triton-X-100 and Deoxycholate it was noticeable that the amount of protein found in the high-speed pellet was lower after solubilisation with LDAO or DDM than after the partial solubilisation with Digitonin, Triton-X-100 or Deoxycholate (Figure 3.7 A and B). Usually smeary gels are an indicator for overloading or degradation of the protein. Since the samples were not boiled prior loading it is possible that a problem in handling the samples resulted in the smearing observed with these detergents. The sixth detergent, Fos-Choline 12, appeared to be the most successful detergent since no protein was found in the high-speed pellet after the solubilisation and all of the protein appeared in the supernatant (Figure 3.7 C).

3.4.2 Identification of detergents able to solubilise the target proteins EsaA, EssB and EssC

Since Digitonin, Triton-X-100, Deoxycholate and Fos-Choline-12 were able to cleanly solubilise proteins from the *S. aureus* RN6390 membrane, it was next tested whether these detergents were able to extract the target proteins EsaA, EssB and EssC. DDM was also included in these

experiments even though it had resulted in smearing previously. 5 µg of solubilised protein (sn) and an equal amount of insoluble fraction (HSP) were separated on bis-Tris gels followed by immunoblotting against antisera raised against EsaA, EssB and EssC. Figure 3.8 shows the results for the solubilisation of EsaA.

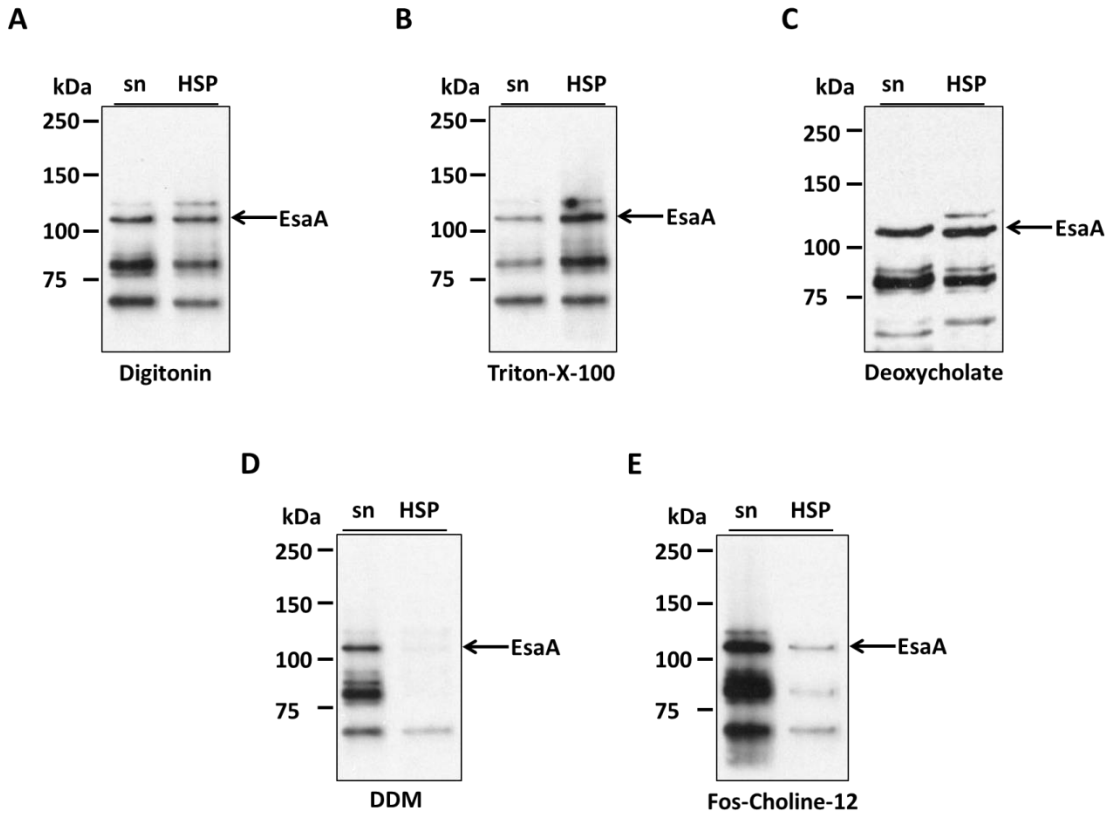

Figure 3.8: Detergent extraction of EsaA. Membrane fractions were treated with 2 % of the indicated detergent followed by centrifugation for 20 min at 89 000 x *g* to remove solubilised (sn) and insoluble material (HSP). 5 µg of total protein were loaded on a bis-Tris gel containing 8 % acrylamide and subsequently transferred on a nitrocellulose membrane followed by immunological detection of EsaA.

Given that Digitonin, Triton-X-100 and Deoxycholate were able to successfully solubilise a range of *S. aureus* membrane proteins (Figure 3.7), it is perhaps not surprising that each of these detergents could also solubilise EsaA, since the antigen could be detected in the supernatant as well as in the high-speed pellet after treatment with each of these (Figure 3.8 A – C). The coomassie-stained gels in Fig 3.7 suggested that Triton-X-100 was the most successful detergent among these three as more proteins could be detected in the supernatant than in the high-

speed pellet. However, looking at the Western blots for EsaA, Triton-X-100 seems to be the least successful detergent as less EsaA could be detected in the soluble fraction after treatment of the membrane with this detergent compared to the amount of EsaA in the supernatant when treated with Digitonin or Deoxycholate. Surprisingly DDM was able to extract all of EsaA from the membrane (Figure 3.8 D) even though the coomassie stained gel in Fig 3.7 did not show any discrete protein bands in the soluble fraction. Fos-Choline-12 was deemed to be the most promising detergent following coomassie staining for total extracted protein (Figure 3.7), and it was clearly able to extract most of the EsaA protein from the membrane (Figure 3.8 E).

Similar results were also seen when immunoblotting for detection of EssB. Digitonin, Triton-X-100 and Deoxycholate were partially successful in solubilising this protein as approximately half of the EssB was detected in the soluble fraction (Figure 3.9 A – C). Contrary to EsaA, Triton-X-100 seemed to be the most successful among these three detergents as more EssB protein could be detected in the supernatant than in the high-speed pellet (Figure 3.9 B). Fos-Choline-12 proved even better at extracting EssB, and most of the protein was found in the soluble fraction with almost no EssB left in the unextracted membrane (Figure 3.9 E). Again, however, the best result was observed for using the detergent DDM, which was able to extract all of EssB (Figure 3.9 D).

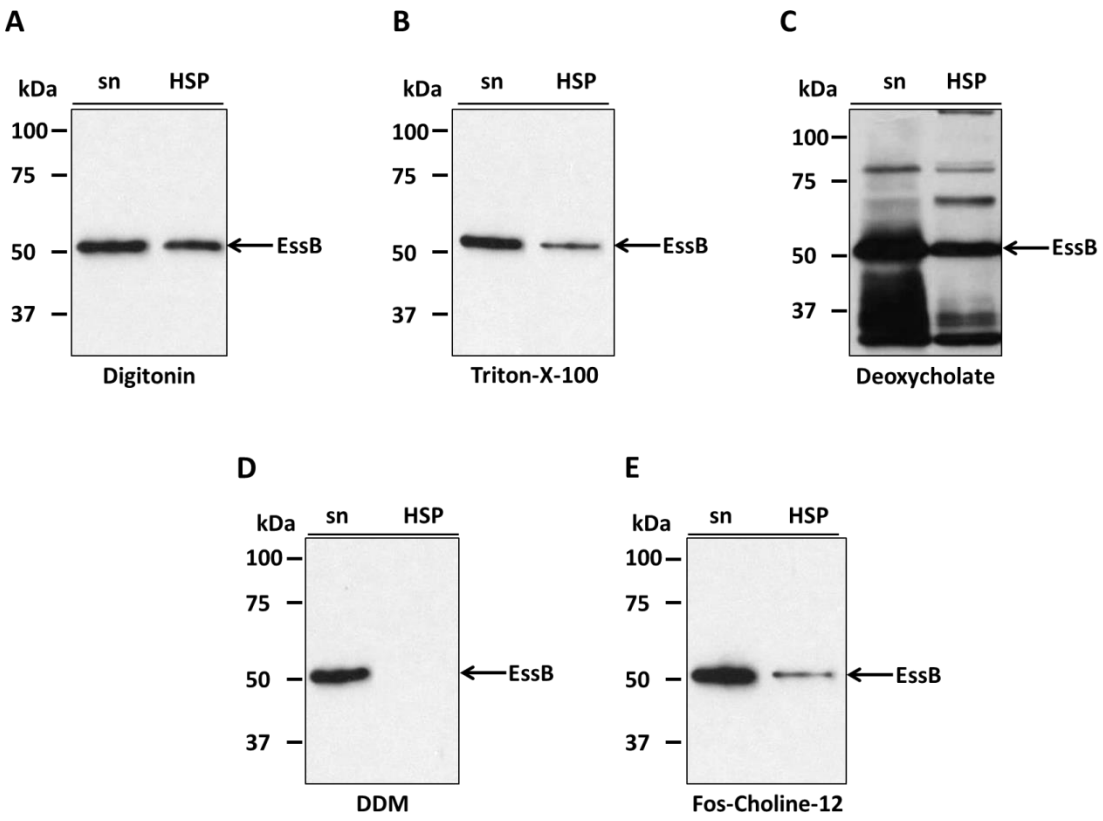

Figure 3.9: Detergent extraction of EssB. Membrane fractions were treated with 2 % of the indicated detergent followed by centrifugation for 20 min at 89 000 x *g* to remove solubilised (sn) and insoluble material (HSP). 5 µg of total protein were loaded on a bis-Tris gel containing 10 % acrylamide and subsequently transferred on a nitrocellulose membrane followed by immunological detection of EssB.

Different behaviour of these detergents was seen, however, when immunoblotting for EssC. While Digitonin, Triton-X-100 and Deoxycholate were able to solubilise at least 50 % of EsaA and EssB, none of the detergents were able to solubilise comparable amounts of EssC (Figure 3.10 A – C). In fact, EssC could only be detected in the soluble fraction when the membrane was treated with Digitonin while none of the protein could be extracted from the membrane by using either Triton-X-100 or Deoxycholate. Also in contrast to EsaA and EssB, are the results obtained using DDM. While DDM was able to solubilise 100 % of EsaA and EssB, all of EssC remained in the membrane (Figure 3.10 D). The best result for EssC extraction was achieved when using Fos-Choline-12 as it was able to extract between 50 and 100 % of the EssC present in the membrane (Figure 3.10 E).

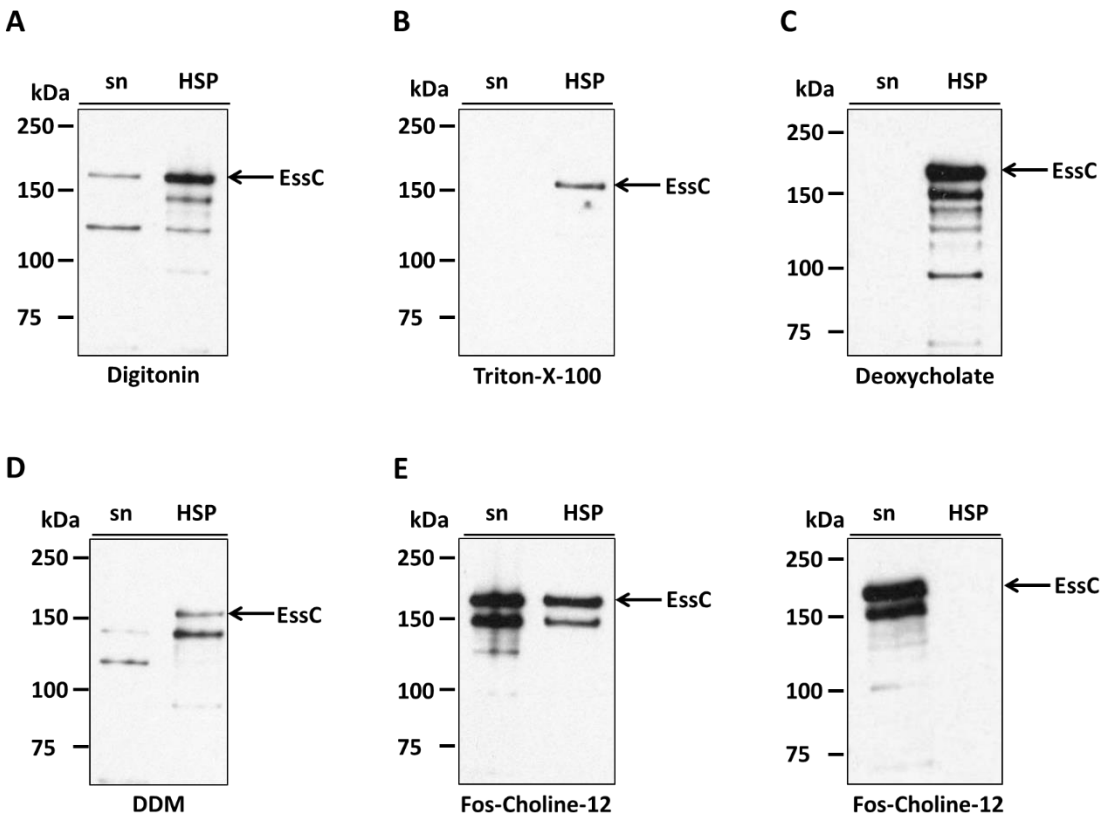

Figure 3.10: Detergent extraction of EssC. Membrane fractions were treated with 2 % of the indicated detergent followed by centrifugation for 20 min at 89 000 x *g* to remove solubilised (sn) and insoluble material (HSP). 5 µg of total protein were loaded on a bis-Tris gel containing 8 % acrylamide and subsequently transferred on a nitrocellulose membrane followed by immunological detection of EssC. In **E.** two separate experimental extractions with Fos-Choline-12 are shown.

3.5 complex formation under native conditions

With Fos-Choline-12 being the only detergent able to extract reasonable levels of all three proteins from the membrane, the next step was to test whether they are part of the same complex by carrying out BN PAGE. Samples were solubilised with 2 % Fos-Choline-12 followed by a centrifugation step to separate the soluble from the insoluble material. Extracted protein was then separated on gels containing a gradient of 4 – 16 % acrylamide and blotted using antibodies raised against EsaA, EssB and EssC.

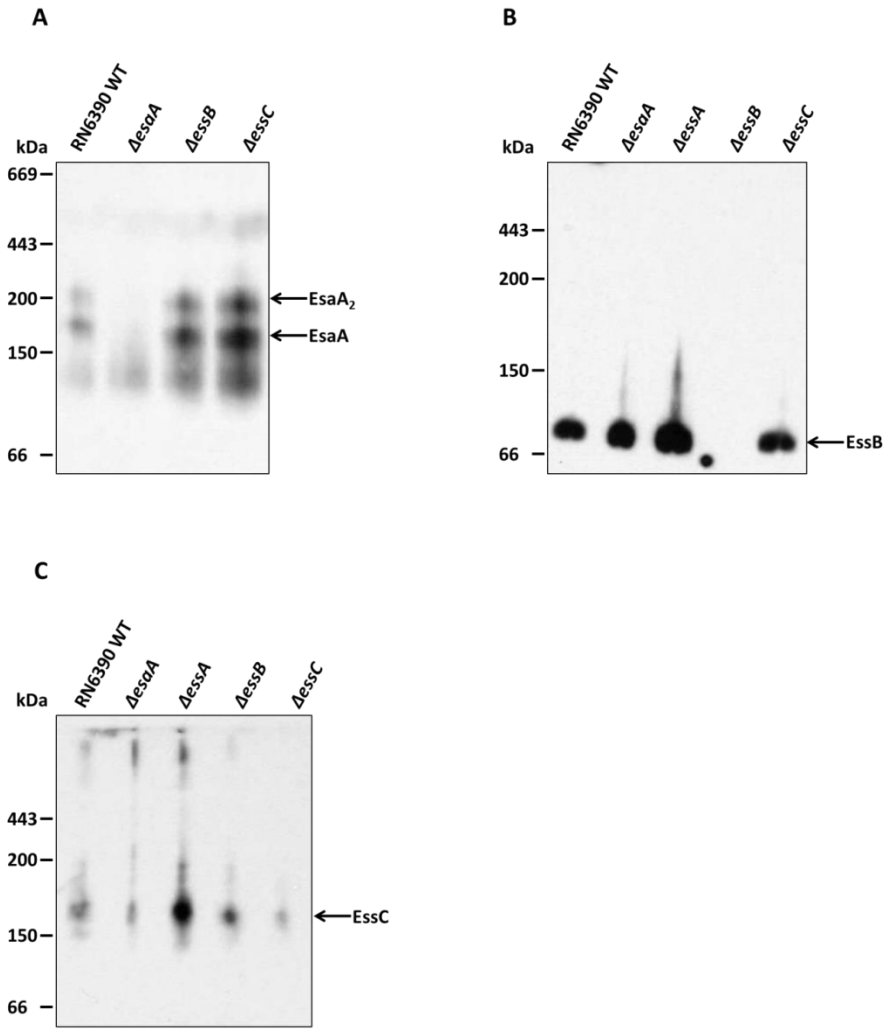

Figure 3.11: Blue native PAGE analysis of EsaA-, EssB- and EssC-containing complexes. Membrane fractions from the RN6390 WT strain or the indicated deletion mutant were prepared and solubilised using 2 % Fos-Choline-12. An equivalent of 5 µg of total membrane protein of the solubilised material was loaded on a BN gel containing a gradient of 4 – 16 % acrylamide. Subsequently the proteins were transferred on a PVDF membrane followed by immunological detection of the membrane proteins EsaA, EssB and EssC.

Figure 3.11 A shows that two separate complexes could be detected that contained EsaA. One of these migrates close to the 150 kDa marker and one just above the 200 kDa marker. These same complexes are still detected when any of *essA*, *essB* or *essC* are deleted and therefore most likely do not contain any of the other ESS membrane proteins. Since the size of EsaA is 114 kDa, these two bands could potentially correspond to monomers and dimers of EsaA.

Contrary to analysis of EsaA, only a single band was detected for EssB that migrated between the 66 kDa and 150 kDa marker (Figure 3.11 B). This band did not migrate at the same position as the complexes containing EsaA and it therefore seems unlikely that the two proteins are in the same complex following Fos-Choline-12 extraction. Moreover the same EssB-containing complex could be identified from strains lacking *esaA*, *essA* or *essC* indicating that none of the encoded proteins are found within this EssB complex. With a calculated size of 52 kDa for an EssB monomer, this band could correspond to an EssB dimer which would be consistent with the literature, where EssB from *Geobacillus thermodenitrificans* is able to form homo-dimers (Zoltner *et al.*, 2013a; Zoltner *et al.*, 2013b).

For EssC only one band could be detected, running just above the 150 kDa marker (Figure 3.11 C). The same complex could be detected when analysed from cells lacking EsaA, EssA or EssB. EssC has a size of 170 kDa so this band could correspond to an EssC monomer. However, a fainter band of similar size was also detectable in membranes extracted from the *essC* deletion strain which leads to the conclusion that the signal may not correspond to EssC.

3.6 Discussion

3.6.1 EsaA, EssA, EssB and EssC are essential for T7SS activity.

In this Chapter, His-tagged variants of the core T7SS membrane proteins EsaA, EssA, EssB and EssC have been constructed. To prevent potential proteolysis by extracellular proteases, the tag was introduced onto a cytoplasmic facing terminus of each protein. It was shown that the plasmid-encoded tagged variants retained activity because they restored T7 secretion to a strain lacking the native copy of each protein. The findings presented here are in accordance with the prior literature where it was shown that EssA, EssB and EssC are essential for secretion in the *S. aureus* Newman strain and EsaA additionally also for the secretion in the RN6390 strain of *S. aureus* (Burts *et al.*, 2005; Kneuper *et al.*, 2014).

Surprisingly, despite confirming by DNA sequencing of the constructed plasmids that the tag sequence should be present on each protein, it was only possible to confirm the presence of the His-tag on EssB by Western blot (Figure 3.6). The reason for this is not clear. One explanation could be that the tags are cleaved off after protein production by cytoplasmic proteases. Previous work from Dr Holger Kneuper involved adding different tags at different positions of EssC, including His-, and also single or double Strep-tags onto the N-terminus as well as the C-terminus of the protein. In agreement with the work presented here, none of those tags could be detected immunologically, again for reasons that are unclear.

3.6.2 EsaA, EssA, EssB and EssC are not part of the same complex following Fos-Choline-12 membrane extraction

As a pre-requisite to purifying ESS membrane complexes, it was necessary to solubilise the *S. aureus* membrane. Six detergents were tested for this purpose, of which three were non-ionic (DDM, Triton-X-100 and Digitonin), two zwitterionic (LDAO and Fos-Choline-12) and one was ionic (Deoxycholate). EsaA and EssB could be partially membrane extracted with Deoxycholate, whereas this detergent did not solubilise EssC. From the three non-ionic detergents used, Triton-X-100 and Digitonin were able to extract approximately 50 % of the total EsaA and EssB protein while there was 100 % extraction of each of these using DDM. All three of these detergents failed to solubilise the third membrane protein, EssC. This is particularly striking since DDM was used to isolate the 1.5 mDa complex of the distantly related ESX-5 secretion system of *M. marinum* which consists of four membrane proteins, including the EssC homologue EccC (Houben *et al.*, 2012; Beckham *et al.*, 2017). The zwitterionic detergents LDAO and Fos-Choline-12 showed very different abilities to extract the Ess proteins although sharing a high similarity in their structure (Figure 3.2). While LDAO failed to solubilise any proteins from the *S. aureus* membrane, Fos-Choline-12 was the only detergent able to successfully solubilise 50 % - 100 % of each of the target membrane proteins. In contrast to LDAO Fos-Choline-12 contains a

phosphate group (Figure 3.12) which could have a more stabilising effect on the protein during the solubilisation process making this detergent more successful compared to LDAO. The ability of S. aureus to produce lysyl-phosphatidylglycerol (Lys-PG) could also have an effect on the efficiency of detergents. Properties of membrane proteins are usually modulated by interactions with the head groups of membrane lipids. Lys-PG partially neutralises the membrane surface charge with an impact on the protein-lipid head group interaction (Sievers *et al.*, 2010) which could also explain why only the zwitterionic Fos-Choline-12 is able to extract all target membrane proteins while DDM was sufficient to solubilise proteins from *M. marinum*.

That no interaction could be seen in between the different proteins may potentially lie in the detergent used. Fos-Choline-12 is a zwitterionic detergent and these detergents are known to be more deactivating than non-ionic detergents. It should be noted that demonstration of complex formation for the ESX-5 secretion system in *M. marinum* employed DDM for solubilisation of the membrane proteins (Houben *et al.*, 2012; Beckham *et al.*, 2017).

4
Probing interactions between the Ess membrane components by chemical crosslinking

4.1 Introduction

As discussed in Chapter 3, no heteromeric interactions between the Ess membrane proteins could be detected following their extraction from the membrane with detergent. One possible explanation for this could be that Fos-Choline-12, the only detergent identified that was able to solubilise the EsaA, EssB and EssC membrane components, may disrupt interactions between the proteins. Chemical crosslinking has long been used as a tool for studying protein complexes. Chemical crosslinkers induce the formation of a covalent bond between two nearby residues within one or more polypeptide chains (Back *et al.*, 2003; Leavell *et al.*, 2004). The covalent bond is formed as the result of the attachment of a functional group onto the target protein by the reactive group of the crosslinking reagent.

Several features have to be considered when choosing a suitable crosslinking reagent. Most important are the spacer arm length, water-solubility, and cell membrane permeability. The spacer arm length may provide some information about the proximity between conjugated proteins. For example, if the conjugation of two proteins is successful with the use of a crosslinking reagent having a long spacer arm but not with a shorter crosslinking reagent the proteins might be located in the same part of the membrane but not directly interacting. Only a successful conjugation of two proteins with a crosslinking reagent containing a short spacer arm provides evidence about intimate contact between the proteins. The spacer arm length also gives information about water-solubility and consequently about the cell membrane permeability. The spacer region is often comprised of alkyl chains which means the longer the spacer the more hydrophobic and therefore water-insoluble and membrane permeable the crosslinking reagent (Leitner *et al.*, 2010). For the investigation of integral membrane proteins a water-insoluble crosslinker is therefore more suitable as it is able to penetrate the cell membrane. Another important aspect in the choice of a suitable crosslinking reagent is the reactive group of the targeted proteins, as only a small number contains selectable targets for

chemical crosslinking. Table 4.1 gives an overview over protein targets which are suitable for the majority of crosslinking reagents.

Table 4.1: Reactive groups for protein conjugation.

Group	target functional group	occurrence
Primary amines	-NH_2	at the N-terminus of each polypeptide chain; in the side chain of lysine residues
Carboxyls	-COOH	at the C-terminus of each polypeptide chain; in the side chain of aspartic acid and glutamic acid
Sulfhydryls	-SH	in the side chain of cysteine
Carbonyls	-CHO	created by oxidising carbohydrate groups in glycoproteins

Crosslinking reagents targeting sulfhydryls are very specific with the need for two cysteines located within close proximity on the protein surface. Therefore disulphide crosslinkers are mainly used for detailed studies of protein interaction in complexes that have already been identified by other methods (Kneuper *et al.*, 2012; Rollauer *et al.*, 2012; Cléon *et al.*, 2015; Huang *et al.*, 2017).

More suitable for the investigation of a possible interaction between less well studied proteins are crosslinking reagents targeting primary amines. Primary amines are present in each polypeptide chain and are often outward facing which makes them more accessible for conjugation (Back *et al.*, 2003). Candidates for crosslinking reagents targeting primary amines are bis(sulfosuccinimidyl)suberate (BS^3), dithiobis(succinimidyl propionate) (DSP) and disuccinimidyl suberate (DSS). All three products belong to the so called NHS esters and have a spacer arm length of 11.4 – 12 Å. BS^3 contains a hydrophilic sulfonyl component, whereas DSP and DSS are water-insoluble and therefore cell membrane permeable. The covalent bond is generated as the N-hydroxysuccinimide (NHS) group of the crosslinking reagent reacts with primary amines of the target protein. The reaction is shown in Figure 4.1.

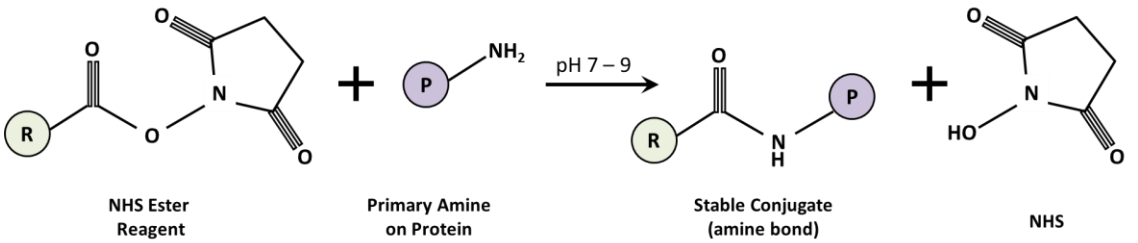

Figure 4.1: Reaction Scheme for chemical conjugation of a NHS ester to a primary amine. (R): crosslinking reagent having the NHS ester reactive group; **(P):** Protein containing the primary amine group.

Another crosslinking reagent targeting primary amines is formaldehyde. It is the smallest aldehyde which reacts with proteins in a two-step mechanism. In the first step the nucleophilic group of an amino acid forms a covalent bond with formaldehyde which results in a methylol adduct converting into a Schiffs base. In the second step this Schiffs base stabilises crosslink formation by binding another functional group of an additional protein through a methylene bridge (Hoffman *et al.*, 2015). The small size and its ability to permeate biological membranes without the use of chemical solvents makes formaldehyde a preferred crosslinking reagent for investigating interaction between proteins *in vivo* (Sutherland *et al.*, 2008). Additionally formaldehyde is known to 'freeze' protein complexes in a native state which makes it possible to crosslink dynamic complexes (Vasilescu *et al.*, 2004; Sutherland *et al.*, 2008)

4.1.1 Dynamic complex formation in protein secretion systems

Protein secretion systems are often dynamic and only adopt their active configuration upon interaction with a substrate. A good example of this can be seen with the twin-arginine translocation (Tat) protein export system. In *E. coli* the Tat machinery consists of three main components: TatA, TatB and TatC (Bogsch *et al.*, 1998; Sargent *et al.*, 1998; Weiner *et al.*, 1998; Sargent *et al.*, 1999). TatB and TatC are known to form a hetero-oligomeric membrane-bound complex that acts as the receptor for substrate proteins, which are targeted to the pathway with the aid of specific N-terminal signal peptides. Tat signal peptides contain a conserved 'S-R-R-x-

F-L-K twin-arginine' motif, giving the transport system its name, that is specifically recognised by TatC (Alami *et al.*, 2003). The translocation pore is formed by the third protein, TatA. It could be shown that substrate binding to the TatBC complex results in the association of TatA with the complex, where it subsequently multimerises to form channel-like structures (Mori and Cline, 2002; Alami *et al.*, 2002; Alcock *et al.*, 2013). Crosslinking of TatA to the TatBC complex is dependent on the pmf and the presence of a bound substrate, and only persists until the substrate is translocated across the membrane (Mori and Cline, 2002; Alami *et al.*, 2003; Dabney-Smith and Cline, 2009). Following substrate translocation TatA disassembles and the Tat system returns to the resting state. A full model of the Tat transport cycle is shown in Figure 4.2.

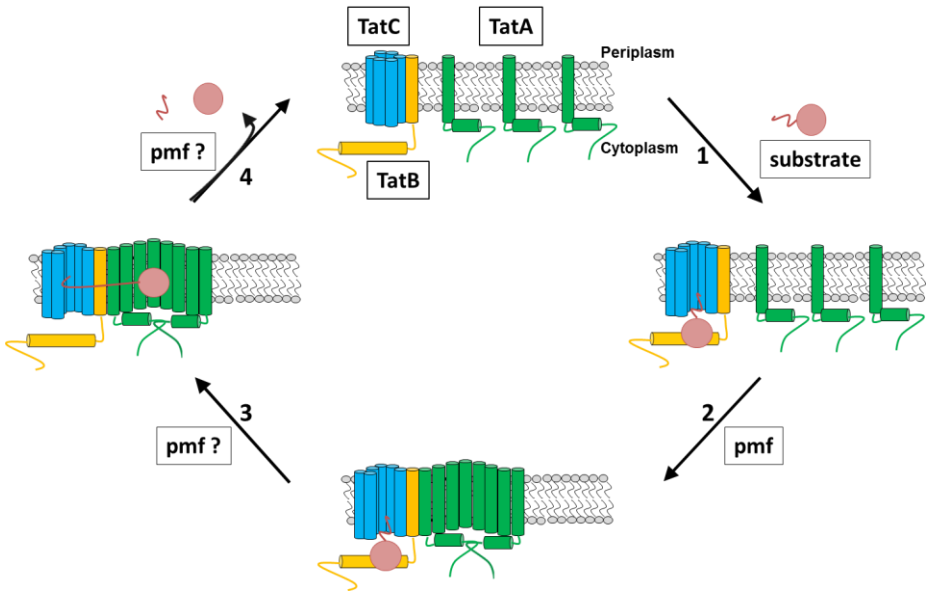

Figure 4.2: The Tat protein transport cycle. Top: The TatBC complex and dispersed protomers of TatA form separated assemblies under resting conditions. **1:** Binding of a substrate to the TatBC complex via its twin arginine signal peptide. **2:** pmf-dependent interaction of the TatA protomers with the substrate-bound TatBC complex to form a transport channel. **3:** Translocation of the substrate across the membrane through the transport channel formed by TatA. It is not clear whether the pmf is also required at this step. **4:** The transported substrate is released and the signal peptide cleaved off. The TatBC complex and TatA multimers dissociate back into the resting state. Adapted from Palmer *et al.* (2010) and Palmer and Berks (2012).

4.2 Aim

The results presented in Chapter 3 indicate that EsaA and EssB form homomeric complexes following detergent extraction but interactions with other components of the Ess machinery could not be shown. The aim of this chapter was to investigate interactions between the Ess membrane components in the native environment, both *in vitro* and *in vivo*, using chemical crosslinking.

Results

4.3 *In vitro* crosslinking studies using DSS

Firstly, experiments were carried out *in vitro* using isolated membranes, and crosslinking was carried out using DSS, which crosslinks exposed primary amine-containing residues with a preference for lysine. Membrane fractions were prepared from the RN6390 WT strain, from the *esaA, essA, essB* and *essC* isogenic deletion strains and from the isogenic deletion strains that had been complemented with a plasmid-encoded copy of the missing gene (see Section 2.9.7.1). For each sample, 30 µg of total membrane protein were incubated with a final concentration of 2 mM DSS for 30 min after which the reactions were quenched with Tris-HCl and then analysed by immunoblot using antibodies raised against the membrane proteins EsaA, EssB and EssC. An untreated membrane sample from each strain/plasmid combination was also loaded as a negative control (Figure 4.3).

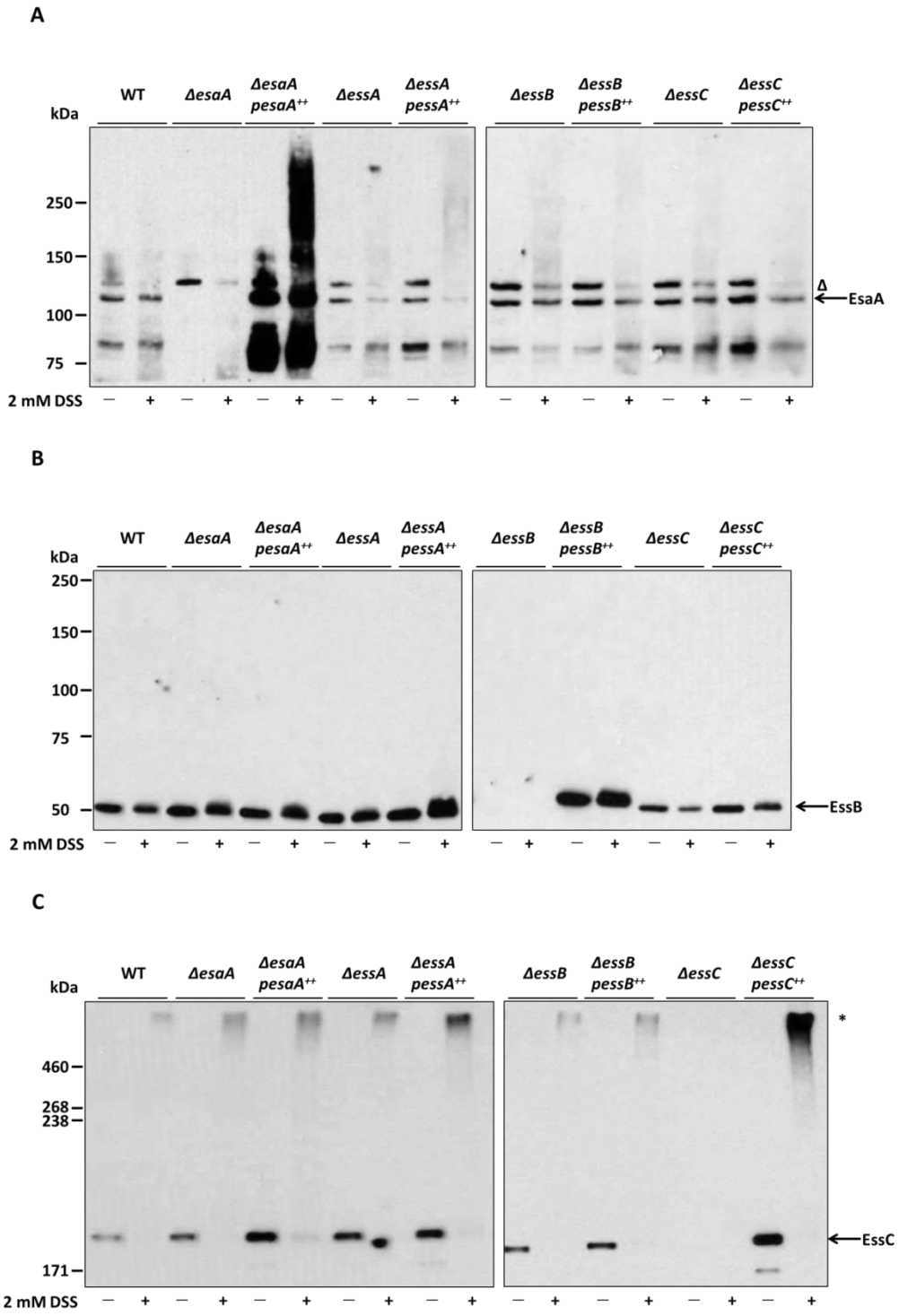

Figure 4.3: DSS crosslinking of the Ess membrane components *in vitro*. Membrane fractions of the RN6390 WT strain together with the isogenic deletion strains harbouring the empty pRMC2 vector (Δ*esaA,* Δ*essA,* Δ*essB,* Δ*essC*) or pRMC2 overproducing a His-tagged variant (Δ*esaA pesaA*$^{++}$, Δ*essA pessA*$^{++}$, Δ*essB pessB*$^{++}$, Δ*essC pessC*$^{++}$) were prepared and treated with DSS as described in Section 2.9.7.1. After incubating with 2 mM DSS crosslinker for 30 min at RT the reaction was quenched by adding Tris/HCl, pH 8.0 (final concentration of 100 mM). 1 µg of total membrane protein was loaded on a bis-Tris gel containing 8 % acrylamide when blotting against EsaA or EssB (**A** and **B**, respectively) or SDS gel containing 5 % acrylamide when blotting against EssC (**C**). For immunological detection polyclonal antibodies raised against the proteins were used. Crosslinked products are indicated with an asterisk; nonspecific bands detected with the EsaA antiserum are marked with an open triangle.

It can be seen in Fig 4.3 A that native EsaA was detected in membranes derived from the WT strain as well as each of the *essA, essB* and *essC* deletion strain backgrounds, indicating that it is stably produced in the absence of each of these Ess components. No higher molecular weight bands could be detected in the presence of the DSS crosslinker in membrane fractions from any of these strains, or when EssA, EssB or EssC was overproduced. Only a dark smear of EsaA-containing material was visible in the crosslinked sample containing overproduced EsaA (Figure 4.3 A).

Similar findings were obtained when blotting against EssB (Fig 4.3 B). Monomeric EssB could be detected in the WT strain as well as in the strains lacking either *esaA, essA* or *essC* showing that the protein is stably produced in the absence of other Ess membrane components. No higher molecular weight crosslinked products could be detected from membranes of any of these strains, or these strains overproduced plasmid-encoded variants of EsaA, EssA or EssC. Crosslinking of membranes containing overproduced EssB also did not result in any higher molecular weight crosslinked products, contrary to the dimerization observed on BN PAGE. It may be that EssB lacks suitably juxtaposed lysine residues that can crosslink with DSS. Indeed, the only notable difference for this sample is that the plasmid encoded variant of EssB migrates slightly higher on SDS PAGE than in the other samples, due to the added His-tag.

Fig 4.3 C shows that it was possible to detect EssC monomers in membranes of the RN6390 WT strain and in membranes of the isogenic deletion strains of *esaA, essA* and *essB* or the strains encoding a His-tagged variant of EsaA or EssB. Contrary to the observations with EsaA and EssB, the monomer of EssC disappeared in the DSS treated samples and a higher molecular weight band was generated that cross-reacted with the EssC antibody. The crosslinked band migrates above the 460 kDa marker in membrane fractions of the WT as well as the *esaA, essA* and *essB* deletion strains indicating that EssC forms homomeric complexes and does not appear to interact with any of the other membrane components of the Ess machinery (Figure 4.3 C).

4.4 *In vivo* crosslinking studies using PFA

The *in vitro* crosslinking analysis using DSS revealed very few detectable interactions. However, in these experiments, the proton-motive force, ATP and soluble proteins are lacking, and any of these factors may influence the behaviour of the Ess components. Therefore similar experiments were next carried out under *in vivo* conditions, in whole cells using paraformaldehyde (PFA) as a crosslinker, which also crosslinks amine residues (but with a much shorter spacer arm). Cultures of the RN6390 WT strain, the *esaA, essA, essB* and *essC* isogenic deletion strains and the isogenic deletion strains that had been complemented with a plasmid-encoded copy of the missing gene were grown to an OD_{600} = 1.0. Cells were harvested, washed in 1 x PBS and incubated with a final concentration of 0.6 % PFA for 30 min. After quenching the reaction with 100 mM Tris/HCl, pH 8.0, membrane fractions were prepared as described in Section 2.9.1.3 and immunoblotted using antibodies raised against EsaA, EssB and EssC. Once again, an untreated sample of each strain/plasmid combination sample was kept as a negative control.

Interestingly, *in vivo* crosslinking with PFA gave different results for EsaA than the *in vitro* incubation with DSS. Fig 4.4 A shows that four or five discrete EsaA-containing bands at or above the 250 kDa marker could be detected for the WT strain. Similar high molecular weight crosslinked bands could be also detected in the samples where EssA, EssB or EssC is absent, indicating that the crosslinked products are unlikely to contain any of these proteins (Figure 4.4 A).

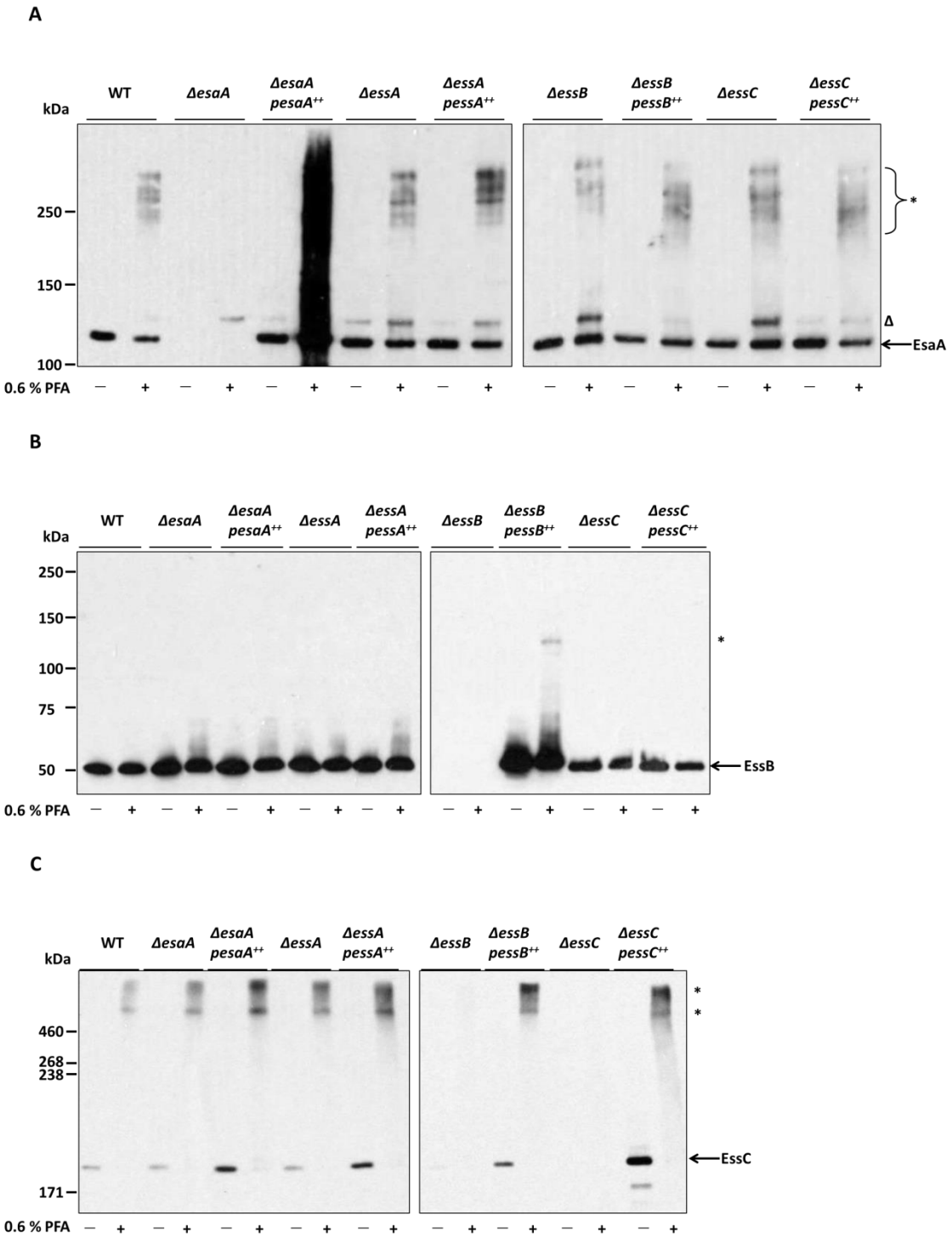

Figure 4.4: PFA crosslinking of the Ess membrane proteins *in vivo*. The RN6390 WT strain together with the isogenic deletion strains harbouring the empty pRMC2 vector (Δ*esaA,* Δ*essA,* Δ*essB,* Δ*essC*) or pRMC2 overproducing a His-tagged variant (Δ*esaA pesaA*$^{++}$, Δ*essA pessA*$^{++}$, Δ*essB pessB*$^{++}$, Δ*essC pessC*$^{++}$) were treated with PFA as described in Section 2.9.7.2. Following quenching, cells were lysed and membrane fractions prepared. 1 µg of total membrane protein was loaded on a bis-Tris gel containing 8 % acrylamide when blotting against EsaA or EssB (**A** and **B**, respectively) or 2 µg on a SDS gel containing 5 % acrylamide when blotting against EssC (**C**). For immunological detection polyclonal antibodies raised against the proteins were used. Crosslinked products are indicated with an asterisk; nonspecific bands detected with the EsaA antiserum are marked with an open triangle.

In vivo crosslinking of EssB yielded similar results to the *in vitro* crosslinking experiments, with only monomers of EssB being detected. Only the sample in which EssB is overproduced showed a very faint crosslinked product running at the approximate size of an EssB dimer, which would be in agreement with the findings from BN PAGE (Figure 4.4 B). Similar to the *in vitro* crosslinking analysis, crosslinking *in vivo* also resulted in high molecular weight products for EssC. However, while *in vitro* there was only one major crosslinked product seen, the *in vivo* crosslinking resulted in at least two distinct high molecular weight bands, both of them migrating above the 460 kDa molecular weight marker. Notably, these bands also appeared in the absence of EsaA, EssA or EssB indicating that neither of the two crosslinking products arise from interaction of EssC with any of the other core components of the Ess system, and therefore likely represent homo-multimeric forms of EssC (Figure 4.4 C).

4.4.1 Crosslinking of EssC in the absence of Ess substrates

The multimerisation of EssC seen here by crosslinking is in accordance with findings reported in the literature where hexamerisation could be shown for *S. aureus* EssC (Zoltner *et al.*, 2016) as well as for the homologue in Actinobacteria, EccC (Rosenberg *et al.*, 2015), with the latter study indicating that multimerisation occurs upon binding of a substrate. Thus, Rosenberg *et al.* (2015) showed that the interaction of purified EccC with the small substrate protein EsxB induces the formation of EccC multimers, whereas interaction of EsxA with the EccC-EsxB complex resulted in disassembly of EccC.

To determine whether the multimerisation of EssC observed in the *in vitro* and *in vivo* crosslinking experiments was also a result of the presence of EsxA and/or EsxB, the *in vivo* crosslinking reactions were repeated in whole cells of the RN6390 WT strain alongside a strain deleted for all 12 genes encoded at the *ess* locus, including *esxA* and *esxB*, either carrying the empty pRMC2 vector or the plasmid encoded His-tagged variant of EssC. As a control, the

isogenic deletion strain of *essC* and its plasmid-complemented derivative was also used. Fig 4.5 shows that, as observed previously, higher molecular weight bands of crosslinked EssC were detected in the RN6390 WT strain as well as in the *essC* deletion strain overproducing the plasmid encoded His-tagged variant. Interestingly, the same pattern of bands was also detectable when EssC was overproduced in absence of any other Ess component. These results indicate that the multimerisation of EssC is independent of any previously identified Ess components.

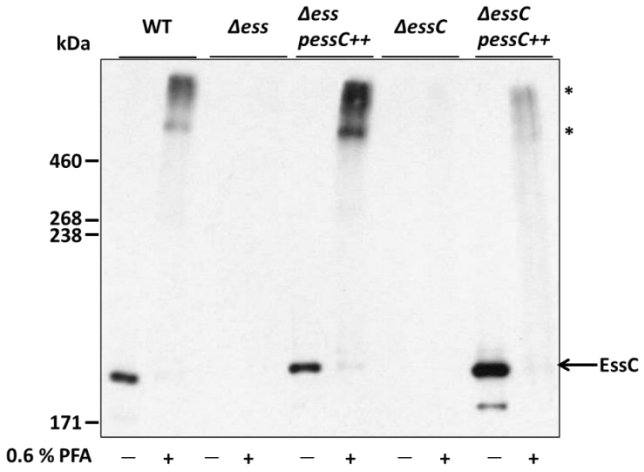

Figure 4.5: PFA-mediated crosslinking of EssC in the presence and absence of other Ess components. Whole cells of the RN6390 WT strain together with the isogenic Δ*esxA* – *esaG* deletion or the isogenic *essC* deletion variant of EssC strain harbouring the empty pRMC2 vector (Δ*ess* and Δ*essC*, respectively) or pRMC2 overproducing a His-tagged variant of EssC (Δ*ess pessC*$^{++}$ or Δ*essC pessC*$^{++}$) were treated with PFA as described under 2.9.7.2. After quenching the reaction cells were lysed and membrane fractions prepared. 2 µg of total membrane protein was loaded on a SDS gel containing 5 % acrylamide followed by immunological detection of EssC. Crosslinked products are indicated with an asterisk.

4.5 Crosslinking studies after overproduction of Ess substrates and soluble components

So far the results have shown that EsaA and EssC form homo-multimeric complexes, with no indication of interaction with one another or any other components of the Ess machinery. However, as discussed in Section 4.1, for many secretion systems, interactions between

components can be transient and may depend on the presence of a substrate protein. If complex formation between the Ess membrane components is dependent upon the translocation of a substrate it might be possible that under the conditions tested it was not possible to trap a translocating complex. In order to maximise the formation of putative assembled complexes, crosslinking experiments were repeated in the presence of overproduced substrates.

4.5.1 Probing interaction of EsxA and EsxA-YFP with membrane components of the Ess machinery

As discussed in Chapter 1, EsxA is considered a core component of the Ess machinery that is secreted in a T7SS-dependent manner, and therefore is highly likely to interact with one or more of the Ess membrane proteins. Purified EsxA crystallises as a homo-dimer (Sundaramoorthy *et al.*, 2008), and secreted homo-dimers of the *B. subtilis* EsxA homologue have been observed (Sysoeva *et al.*, 2014).

Before testing possible interaction of EsxA with the membrane components of the Ess machinery, crosslinking experiments were first undertaken to confirm the dimerization of EsxA *in vivo.* Cells of the RN6390 WT strain and strains lacking either *esxA* or all 12 genes encoded at the *ess* locus harbouring the empty pRMC2 vector or plasmid encoded EsxA were grown to an OD_{600} of 1.0. Supernatant and cells were separated and collected, with the cells being subsequently washed in 1 x PBS. Supernatant and cells were then incubated with a final concentration of 0.6 % PFA for 30 min. After quenching the reaction, cells were lysed and membrane fractions prepared as described in Section 2.9.1.3 this time retaining the cytosol. Supernatant and cytosol samples were loaded on a bis-Tris gel followed by immunological detection of EsxA.

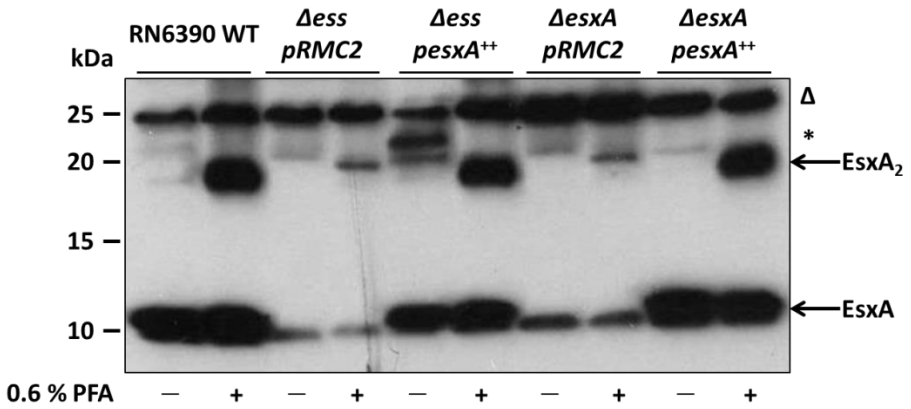

Figure 4.6: *in vivo* dimerization of EsxA detected by PFA crosslinking. Whole cells of strain RN6390 WT, the isogenic Δ*esxA – esaG* deletion strain (Δ*ess*) together with the isogenic Δ*esxA* deletion strain, either harbouring the empty pRMC2 vector or pEsxA were treated with PFA. Following quenching, cells were lysed and membrane fractions prepared. 10 µl of cytosol was loaded on a bis-Tris gel containing 15 % acrylamide. Samples were transferred to nitrocellulose membrane and proteins detected using polyclonal antibodies raised against EsxA. The apparent EsxA dimer detected in the untreated Δ*ess/pesxA* sample is marked with an asterisk; nonspecific bands detected with the EsxA antiserum are marked with an open triangle.

Unfortunately only a faint band was detectable for EsxA in the untreated supernatant samples whereas no signal could be detected in the supernatant samples treated with PFA probably due to the TCA precipitation after the crosslinking step (data not shown). In the cytosol samples strong bands of EsxA could be detected from the WT strain as well as from the strains carrying the plasmid encoded variant (Figure 4.6). Much fainter bands at a similar but slightly lower apparent mass were also detected from strains lacking *esxA*, and most likely result from cross-reaction of the antibody with an unrelated protein. Interestingly, in the Δ*ess* strain overproducing plasmid-encoded EsxA, in the absence of PFA crosslinker, a strong cross-reacting band could be detected migrating just above the 20 kDa marker, at the expected size for an EsxA dimer. It has been observed previously that some proteins are able to form non-covalent dimers that are partially resistant to SDS denaturation (e.g. the membrane-extrinsic domain of TatB (De Leeuw *et al.*, 2001)). This EsxA 'dimer' band is not detected to the same degree in the wild type or Δ*esxA* strain backgrounds suggesting that a component encoded at the *ess* locus may be involved in modulating the formation of this dimer.

Following treatment with PFA, a higher molecular weight band containing EsxA was visible in samples of the WT strain or the strains carrying the plasmid-encoded EsxA (Fig 4.6). This band migrated slightly below the 20 kDa marker. However, since the same band is detectable in the treated sample of the complete *ess* knockout strain harbouring plasmid encoded EsxA, it is unlikely to represent a crosslink of EsxA with another Ess component, and most likely represents a covalently crosslinked EsxA dimer. This crosslink migrates slightly faster than the putative EsxA dimer species seen in the non-crosslinked sample from the Δ*ess*/pEsxA strain suggesting that crosslinking results in a more compact form of the EsxA dimer.

After dimerization of EsxA in solution was confirmed, membrane fractions were tested for interaction of EsxA with one of the membrane components of the Ess machinery. Membrane fractions of the same strains and plasmid combinations used in Fig 4.6 were loaded on a bis-Tris gel followed by immunological detection of EsxA and the membrane components EsaA, EssB and EssC. When blotting against EsxA only a black smear could be detected in the crosslinked samples making it difficult to distinguish between unspecific and cross-reacting bands. Blotting against the membrane components EsaA, EssB and EssC resulted in the same crosslinking pattern as already described in Figure 4.4. Due to the small size of EsxA it was not possible to detect any changes in this crosslinking pattern when crosslinking was carried out in presence or absence of EsxA (data not shown).

Previously, Dr Holger Kneuper constructed a fusion of YFP to the C-terminus of EsxA as a high throughput tool to monitor T7 secretion activity. He found that the YFP-tag on EsxA appeared to block T7 activity by preventing the secretion of untagged EsxA (Kneuper and Palmer, unpublished). These findings imply that EsxA-YFP may negatively interact with the Ess machinery, and therefore might be a potentially useful tool to trap complexes of the Ess membrane components.

Firstly, the initial findings of Dr Kneuper were repeated and extended to examine the secretion of the T7 substrate protein EsxC. The RN6390 WT strain carrying the empty pRMC2-YFP vector, the untagged EsxA or the YFP-tagged variant of EsxA was utilised, alongside the *esxA* deletion strain carrying EsxA or EsxA-YFP constructs. The Δ*ess* strain (lacking all 12 genes of the *ess* locus) harbouring the empty vector was used as a negative control. Cultures were grown to an OD_{600} = 2.0 and separated into culture supernatant (sn) and cellular fractions (c). An equivalent of 10 µl cells adjusted to an OD_{600} of 1.0 and an equivalent of 200 µl TCA precipitated supernatant were separated on a bis-Tris gel and subsequently immunoblotted against EsxA and EsxC (Figure 4.7).

Wild type EsxA was stably produced in all strains but was absent in the negative control, as expected. However, secretion of EsxA was only detectable in the strains not producing the EsxA-YFP variant (Figure 4.7 A; lower panel), very little was found in the supernatant when cells also contained EsxA-YFP. The EsxA-YFP fusion protein also appeared to be secreted (Figure 4.7 A; upper panel, Fig 4.7 B). EsxC could also be detected in the cell samples of most of the strains, but was absent from the negative control, as expected. Very little EsxC was also seen when the cells produced EsxA-YFP as the only EsxA variant. It has been reported that EsxA and EsxC interact (Anderson *et al.*, 2013), and it is possible that the YFP tag might block such an interaction which could destabilise EsxC. Interestingly, although EsxA-YFP could be secreted, in the presence of EsxA-YFP secretion of EsxC appeared to be almost completely blocked (Figure 4.7 C). In these experiments TrxA was used as a cytosolic control protein to confirm that detection of proteins in the supernatant is due to secretion and not lysis (Figure 4.7 D).

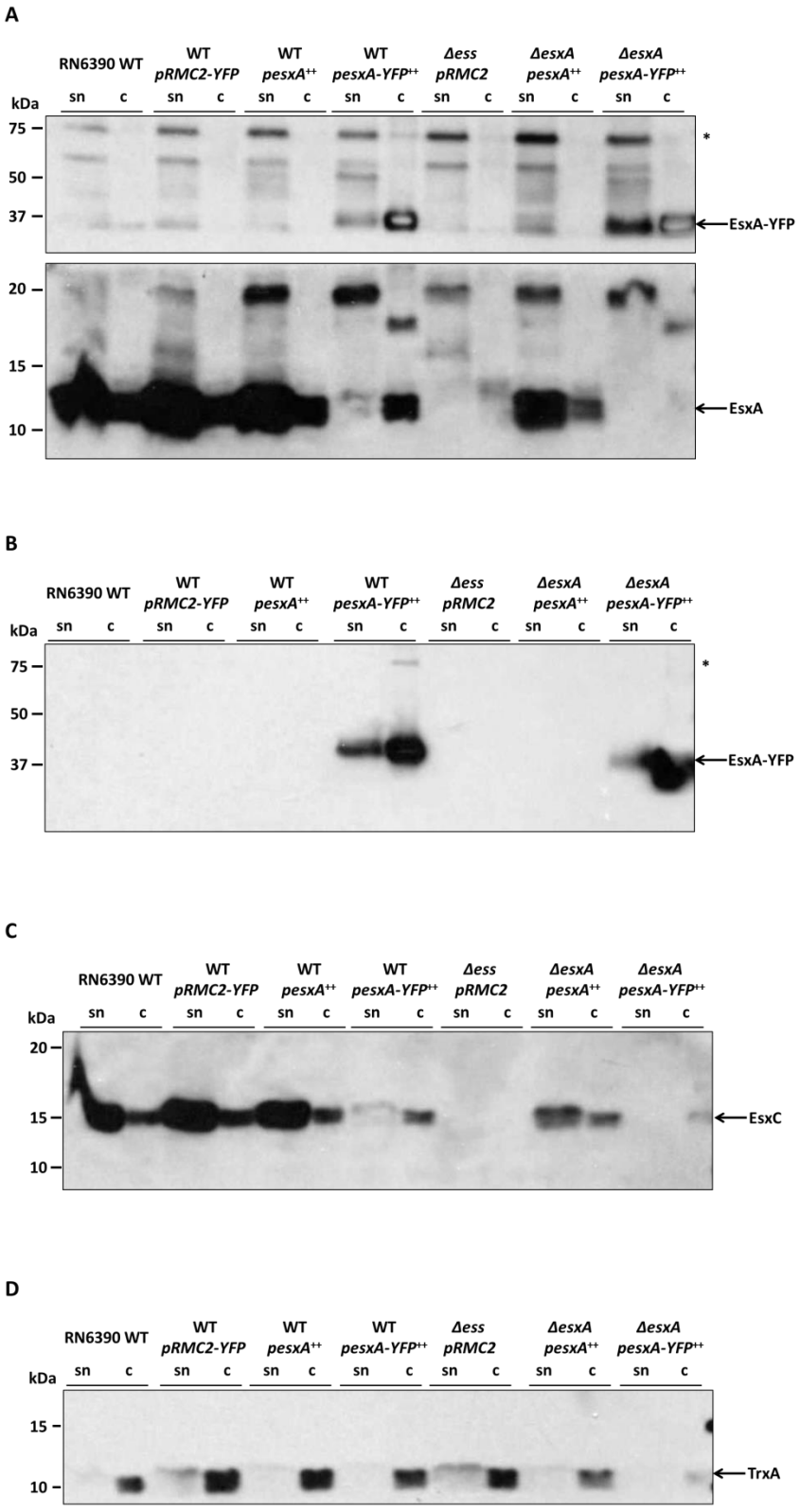

Figure 4.7: Overproduction of EsxA-YFP negatively affects T7 secretion. Whole cells of RN6390 WT or the isogenic Δ*esxA* or Δ*ess* deletion strains harbouring either the empty pRMC2 vector or pRMC2 encoding the indicated variants of EsxA were grown in TSB. Cell and supernatant samples were prepared as described earlier and separated on bis-Tris gels containing 15 % acrylamide followed by immunological detection of **(A):** EsxA; **(B):** YFP; **(C):** EsxC or **(D):** TrxA. Crosslinking products of EsxA-YFP are marked with an asterisk.

The blocking of EsxA and EsxC secretion by EsxA-YFP is consistent with this fusion protein interacting with the Ess machinery, and slowing down or impeding transport potentially by complexing with one or more of the Ess membrane components. To explore this, *in vivo* crosslinking experiments were carried out using the RN6390 WT strain and the isogenic Δ*ess* and Δ*esxA* deletion strains harbouring either the empty pRMC2 vector or the same vector producing the YFP-tagged EsxA variant. Whole cells were treated with PFA and membrane fractions prepared as described earlier. Proteins were transferred onto a nitrocellulose membrane followed by immunoblotting against antibodies to the membrane proteins EsaA, EssB and EssC (Figure 4.8). Only a black smear could be detected for EsaA in the PFA treated samples and it is difficult to identify possible higher molecular weight bands (Figure 4.8 A). Interestingly, the EssB monomer appears to be weaker in the treated samples of the *esxA* deletion strain compared to the WT but again no higher molecular weight bands could be detected in these samples (Figure 4.8 B). However, considering that the monomer is also weaker following PFA treatment of the same strain harbouring the empty pRMC2 vector, this suggests that the YFP-tagged variant of EsxA was not the cause of this. Higher molecular weight bands are detectable in the RN6390 WT sample and variants of the *esxA* deletion strain for EssC (Figure 4.8 C). The bands migrate well above the 250 kDa marker making it difficult to distinguish between bands only representing the previous observed multimerisation of EssC and bands showing a possible interaction with the YFP-tagged variant of EsxA.

To follow up this question the same samples were also blotted against EsxA and the YFP-tag to test if the same higher molecular weight bands can be picked up. As it can be seen in Figure 4.9 higher molecular weight bands running at the approximately same size as in the EssC blot are detectable when blotting against EsxA as well as GFP. However, the same band is also detectable in the strain deleted of the 12 genes encoded at the *ess* locus, indicating that this higher molecular weight band most likely represents oligomerisation of EsxA rather than an interaction with any of the membrane components (Figure 4.9 A + B).

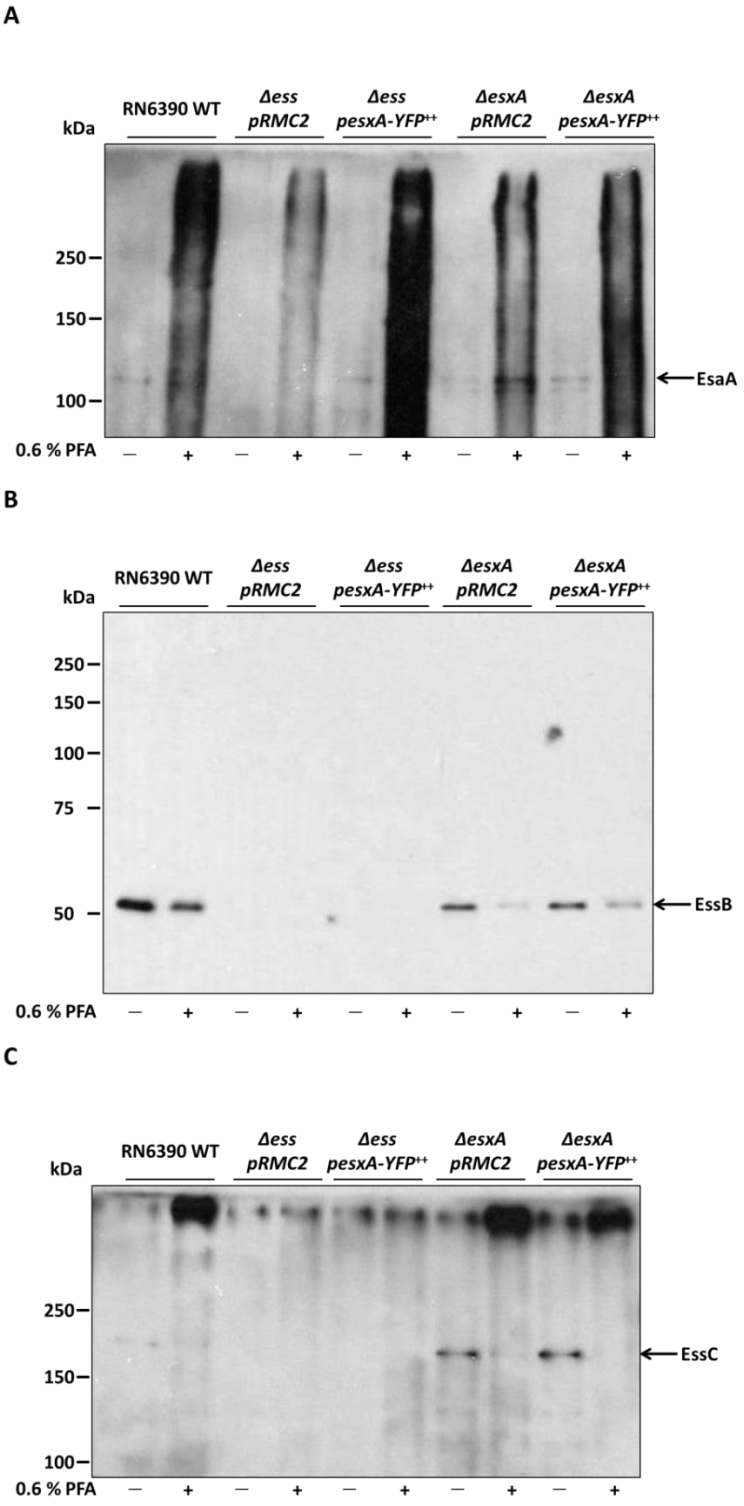

Figure 4.8: Formaldehyde mediated crosslinking of EsaA, EssB and EssC in the presence of EsxA-YFP in whole cells. Whole cells of strain RN6390 WT, the isogenic Δ*esxA – esaG* deletion strain (Δ*ess*) or the isogenic *esxA* deletion strain, either harbouring the empty pRMC2 vector or pEsxA-YFP were treated with PFA. Following quenching, cells were lysed and membrane fractions prepared. 1 µg of total membrane protein were loaded on a SDS gel containing 10 % acrylamide for the immunological detection of the membrane proteins EsaA **(A)**, EssB **(B)** or EssC **(C)**.

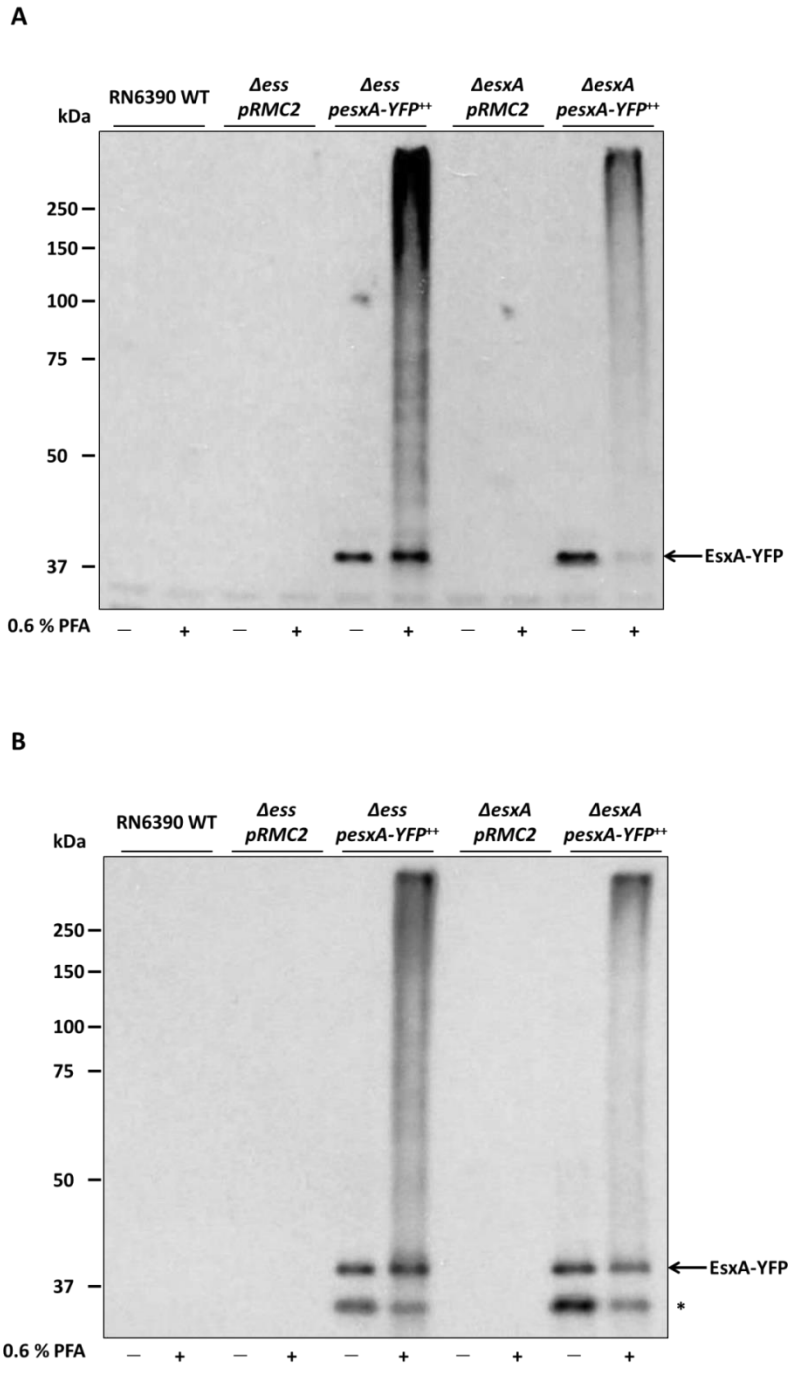

Figure 4.9: Immunological detection of EsxA-YFP. Whole cells of strain RN6390 WT, the isogenic Δ*esxA* – *esaG* deletion strain or the isogenic *esxA* deletion strain, either harbouring the empty pRMC2 vector or pesxA-YFP were treated with PFA. Following quenching, cells were lysed and membrane fractions prepared. 1 µg of total membrane protein were loaded on a SDS gel containing 12.5 % acrylamide for the immunological detection of EsxA **(A)** and YFP **(B)**.Marked with an asterisk is free YFP.

4.5.2 Probing interaction of EsaD-YFP with membrane components of the Ess machinery

Previous unpublished work in the Palmer group indicated that producing an inactive variant of the soluble T7 substrate protein EsaD (harbouring a point mutation in the nuclease active site) with YFP fused at its C-terminus caused *S. aureus* cells to die (Cao and Palmer, unpublished). This observation led to the idea that YFP-tagged EsaD may be too large for the T7 translocation channel, potentially resulting in blockage of the system and cell death by ion leakage or futile hydrolysis of ATP. If this were the case, then such a 'suicide substrate' might be an ideal tool to trap active complexes of Ess membrane components.

To explore this further, it was first necessary to ascertain the threshold of EsaD-YFP after which cell death occurs. To this end, the *S. aureus* RN6390 WT strain was cultured alongside the *esaD* deletion strain and the *esaD* strain harbouring the plasmid-encoded YFP-tagged variant. Once the cultures reached an OD_{600} = 0.5, those cultures harbouring the plasmid encoded YFP-tagged variants of EsaD were supplemented with different concentrations of ATc to induce EsaD-YFP production and growth was followed (Figure 4.10).

As shown in Fig 4.10, the *S. aureus* RN6390 strain exhibited normal grow behaviour, reaching an OD_{600} = 2.2 after 3 hours. A similar pattern of growth could be seen for both the *S. aureus* strain lacking EsaD, and for the Δ*esaD* strain harbouring a plasmid encoding *esaD-yfp* in the absence of any inducer. However, upon induction of EsaD-YFP production, a change in growth behaviour was seen. Even the lowest concentration of inducer tested (50 ng/ml ATc) caused a slowdown in cell growth, with the cells reaching an OD_{600} = 2.0 after 3.5 hours. When incubated with a higher concentration of ATc, cultures only reached an OD_{600} of 1.3 or 1.4 after 3 hours which decreased to OD_{600} = 1.1 or 1.0 within the next hour. The decline in growth after 3 hours strongly suggests that at these levels of induction EsaD-YFP causes cell death.

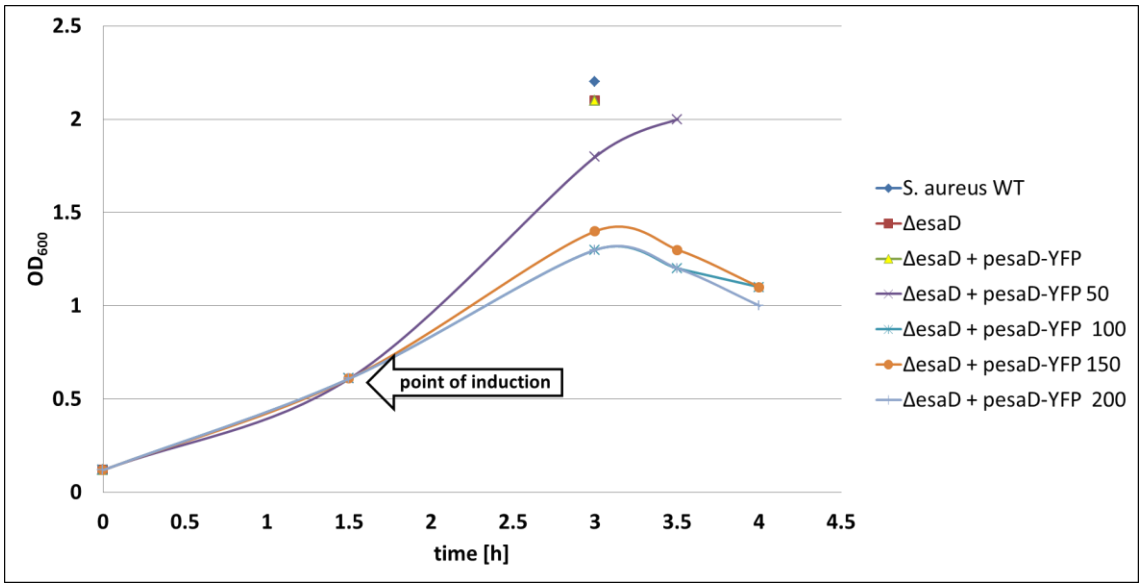

Figure 4.10: Growth of *S. aureus* producing different levels of EsaD-YFP. Cultures of the indicated strains were grown until an OD_{600} = 0.5 was reached before inducing the production of EsaD-YFP using either 50, 100, 150 or 200 nm/ml ATc as indicated. Cell growth was monitored over a time of 4 hours and cells harvested as soon as they reached an OD_{600} = 2.0.

To get an idea of the relative amounts of EsaD-YFP in the cells following the different induction levels, membrane fractions were prepared and the cytosol retained. Cytosol samples were loaded on a bis-Tris gel followed by immunological detection of the YFP-tag. However, no signal for EsaD-YFP could be obtained in the cytosol samples (data not shown). To determine whether EsaD-YFP was associated with the membranes, membrane fractions were also blotted against the YFP-tag using an anti GFP antibody (Figure 4.11). The blot revealed that in samples treated with an ATc-concentration of 100 ng/ml or higher a GFP cross-reacting band was detectable running at ~100 kDa, close to the expected size for EsaD-YFP. As the induction level was increased, additional higher bands were also detected. At the highest concentration of ATc used, only a black smear was detectable following western blotting of membranes. Therefore, for further experiments a concentration of 150 ng/ml ATc, which gave clearly detectable EsaD-YFP, was chosen.

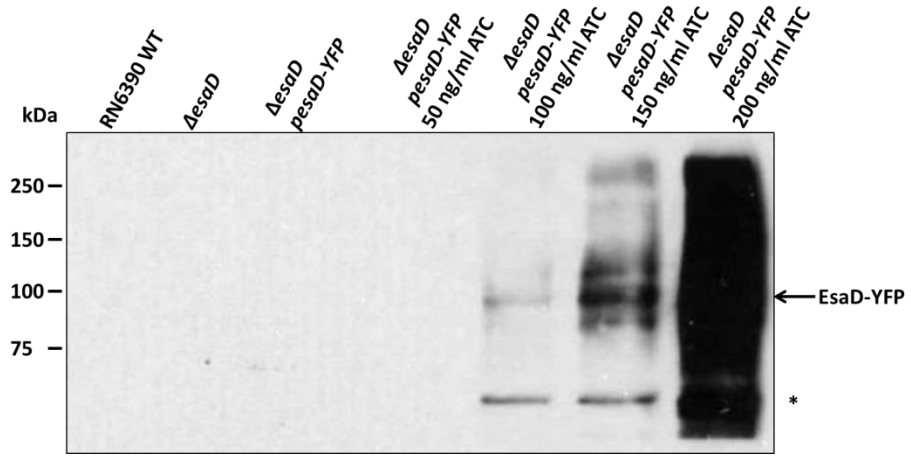

Figure 4.11: Detection of EsaD-YFP in membrane samples following different levels of induction. Cells were grown and harvested as described in figure 4.10. Membrane fractions were prepared from 5ml cultures of cells as described in Section 2.9.1.1 and 10 µg of total membrane protein run on a bis-Tris gel containing 10 % acrylamide. Proteins were subsequently transferred onto a nitrocellulose membrane and blotted using an anti GFP antibody. Degradation products are marked with an asterisk.

Since the EsaD-YFP fusion protein could be detected in membrane fractions it supported the idea that EsaD-YFP might get stuck in the transport channel, causing a blockage of the system leading cell death. To investigate this further, and to try and identify which Ess membrane protein/s EsaD-YFP might interact with, membrane fractions were prepared from strains lacking genes for each one of the membrane components EsaA, EssA, EssB or EssC. Strains deleted for chromosomal *esaD* or all 12 genes of the *ess* locus were simultaneously used as controls. In each case experiments were run in duplicate, with strains carrying either plasmid-encoded YFP alone, or pRMC2-EsaD-YFP, in the absence of any chemical crosslinker. The results are shown in Figure 4.12.

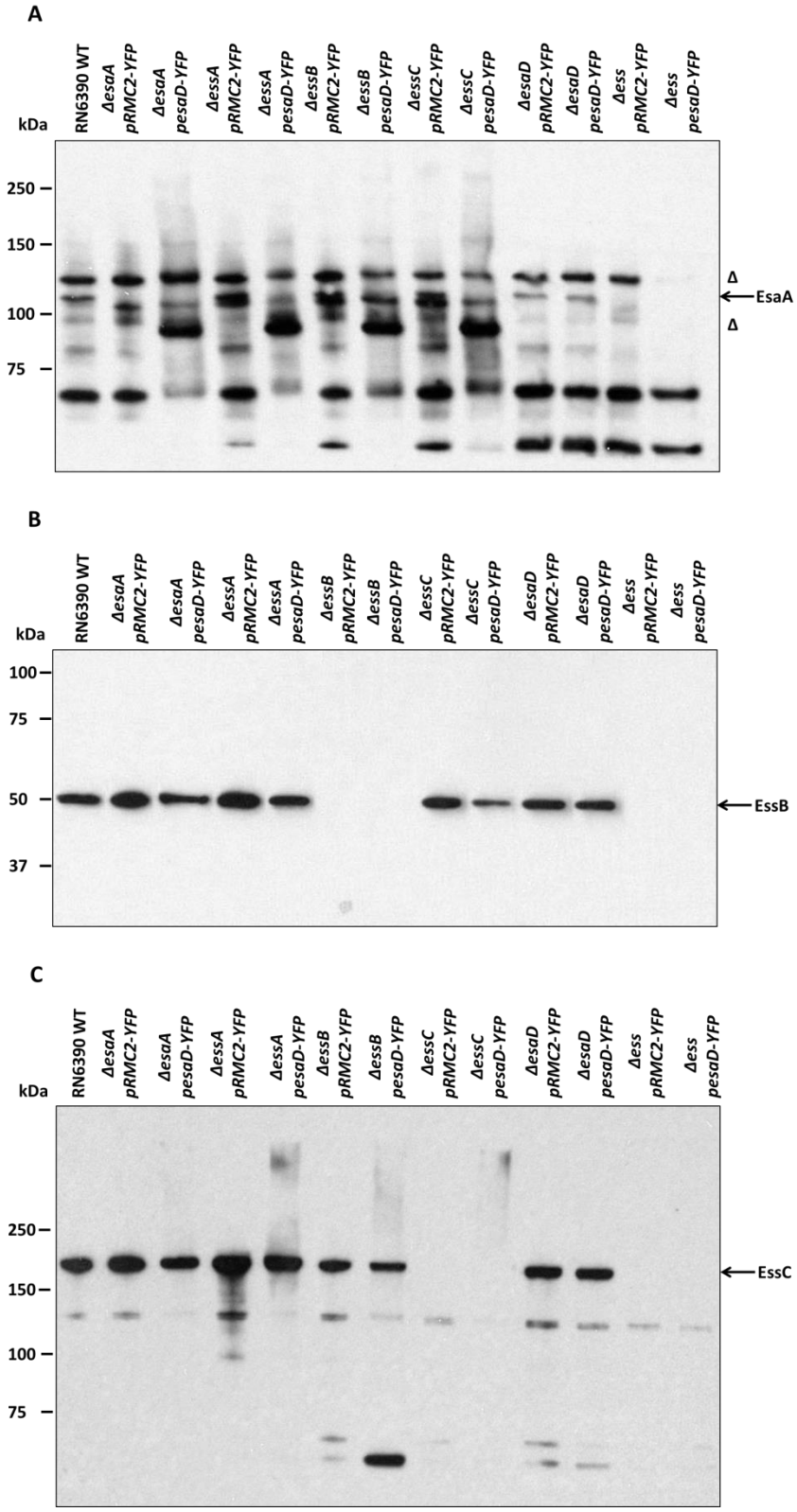

Figure 4.12: Analysis of EsaA, EssB and EssC in membranes from strains overproducing EsaD-YFP. Membrane fractions of RN6390 WT together with the Δ*esaA*, Δ*essA*, Δ*essB*, Δ*essC*, Δ*esaD* and Δ*ess* deletion strains harbouring either pRMC2-YFP or pRMC2-EsaD-YFP were prepared as described in Section 2.9.1.1 and 5 µg of total protein loaded on a bis-Tris gel containing 10 % acrylamide. Proteins were subsequently transferred onto a nitrocellulose membrane followed by immunological detection of the membrane components EsaA **(A)**, EssB **(B)** and EssC **(C)**. Nonspecific bands detected with the EsaA antiserum are marked with an open triangle.

Western blot analysis for EsaA shows that monomers of EsaA migrating just above the 100 kDa marker can be detected in all samples except for the Δ*esaA* and Δ*ess* deletion strains (Figure 4.12 A). Curiously, a strongly cross-reacting band migrating below the 100 kDa marker is detected in many of the lanes containing samples overproducing EsaD-YFP. This band is very similar in mass to that detected with the GFP antibody in Fig 4.11 and may therefore be this fusion being picked up by the polyclonal EsaA antibody for unknown reasons. A faint signal is detected running above the 250 kDa marker for samples overproducing the YFP-tagged EsaD lacking either EssB or EssC. However, the same signal can be detected in the strain overproducing EsaD-YFP lacking EsaA, indicating that this band does not correspond to a potential interaction between these two proteins (Figure 4.12 A).

Western blot analysis for EssB revealed that the EssB monomer is stably produced in all strains except for the Δ*essB* and Δ*ess* strains, but no higher molecular weight bands were generated in the presence of overproduced EsaD-YFP (Figure 4.12 B). Blotting the samples for EssC showed a similar result as that seen for EsaA, i.e. a faint signal was detected running above the 250 kDa marker in samples derived from strains overproducing EsaD-YFP while lacking either EssA or EssB. Again, however, this signal is also detectable in the Δ*essC* strain indicating that it cannot correspond to an interaction between EsaD-YFP and EssC (Figure 4.12 C).

Since testing the membrane fractions for higher molecular complexes using antibodies raised against the Ess membrane components did not give indication of EsaD-YFP interaction with any of the membrane proteins, the same samples were re-run and blotted with anti-GFP to detect EsaD-YFP. It can be seen in Figure 4.13 that there are several bands detectable in strains harbouring EsaD-YFP. The highest band runs above the 250 kDa size marker. However, as this band is detectable in all strains individually lacking EsaA, EssA, EssB or EssC, it is unlikely to represent EsaD-YFP interacting with any of the Ess membrane proteins. In samples derived from strains lacking chromosomally-encoded EsaD or deleted for all 12 genes at the *ess* locus, bands were only detected close to the 50 kDa marker, which is too small for an EsaD-YFP monomer

and may correspond to *S. aureus* protein A (which binds antibodies). No other bands could be detected in these samples, suggesting a lack of EsaD-YFP production. It should also be noted that these two strains also showed strong growth after induction of EsaD-YFP production, whereas the other strains producing plasmid-encoded EsaD-YFP variant grew poorly following ATc addition. This raised the possibility that EsaD-YFP was either not being produced or was highly unstable in these strain backgrounds.

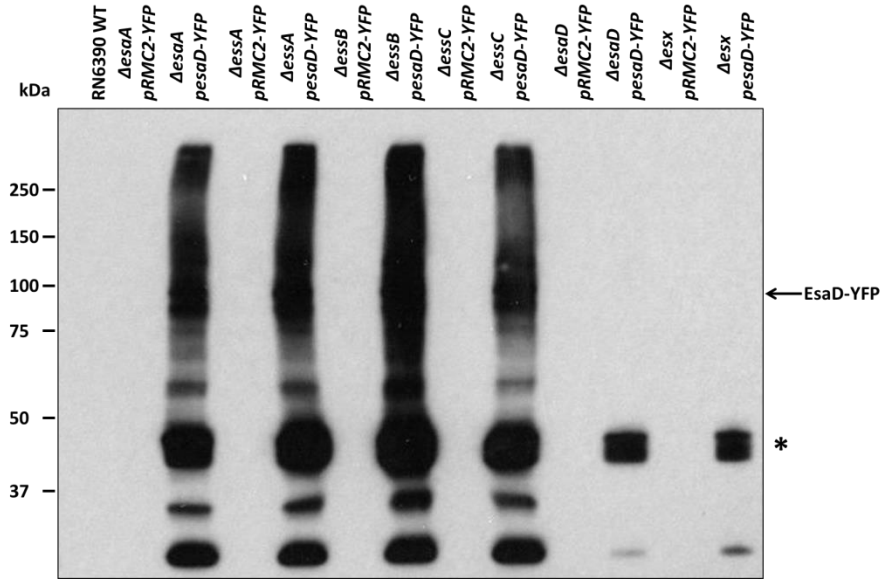

Figure 4.13: Analysis of EsaD-YFP in membranes derived from *S. aureus* T7 mutant backgrounds. Membrane fractions of RN6390 WT together with Δ*esaA*, Δ*essA*, Δ*essB*, Δ*essC*, Δ*esaD* and Δ*ess* deletion strains harbouring either pRMC2-YFP or pRMC2-EsaD-YFP were prepared as described in Section 2.9.1.1 and 5 µg of total protein loaded on a bis-Tris gel containing 10 % acrylamide. Proteins were subsequently transferred onto a nitrocellulose membrane followed by immunological detection of EsaD-YFP using an anti-GFP antibody. Cross-reaction of the GFP antibody with Protein A is marked with an asterisk.

To investigate this further, each of the strains lacking individual *ess* genes and harbouring either the plasmid-encoded EsaD-YFP variant or a control plasmid encoding YFP alone (pRMC2-YFP), were monitored for cell growth and fluorescence over a period of 18 hours. In these experiments, cells were grown in 10 ml TSB to an OD_{600} = 0.5 after which 1 ml of each sample was withdrawn. Initiation of EsaD-YFP production was induced by adding 500 ng/ml ATc,

whereas no ATc was added to strains harbouring pRMC2-YFP and 150 µl of each sample was aliquoted into a 96 well plate to allow simultaneous monitoring of OD_{600} and fluorescence.

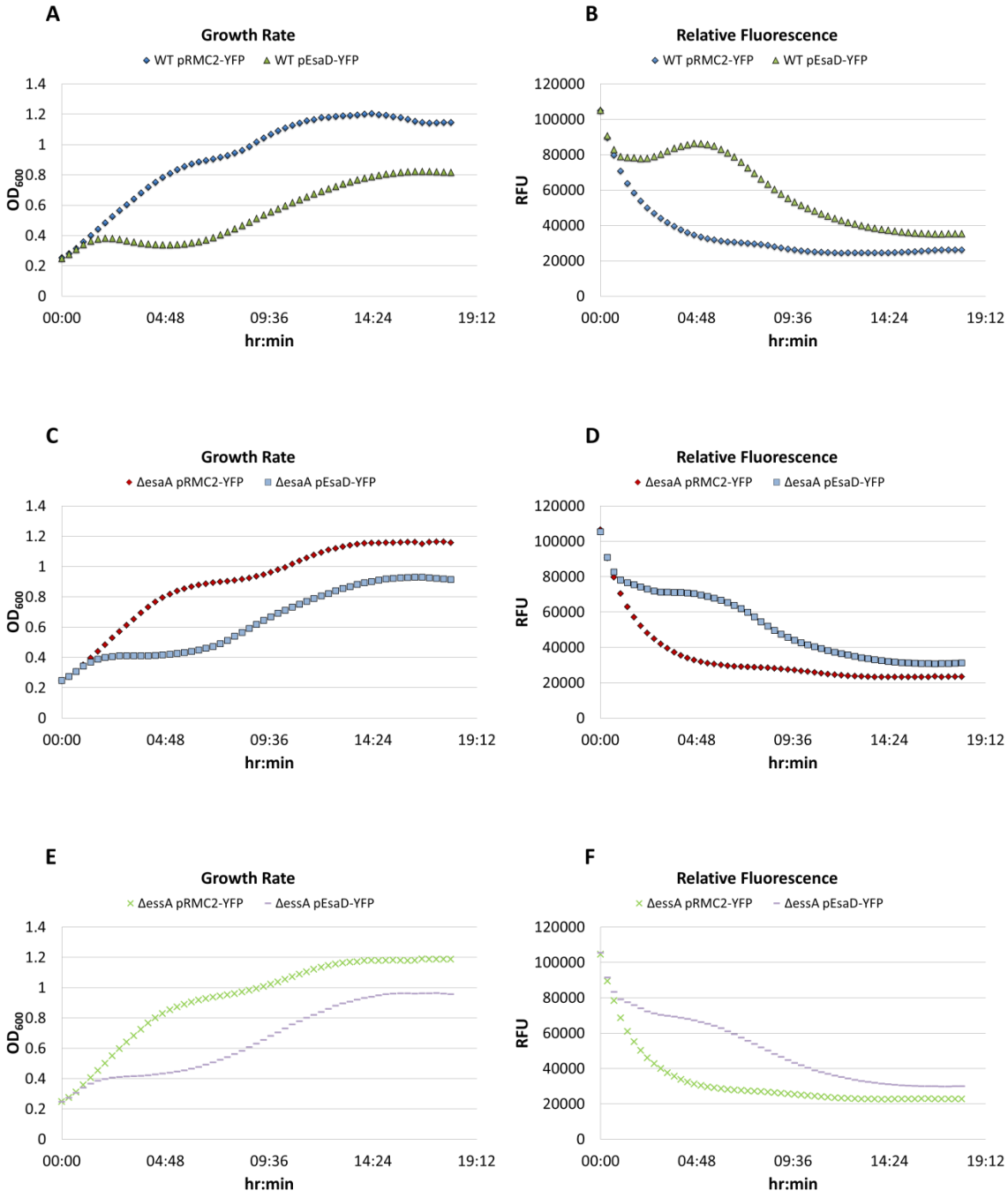

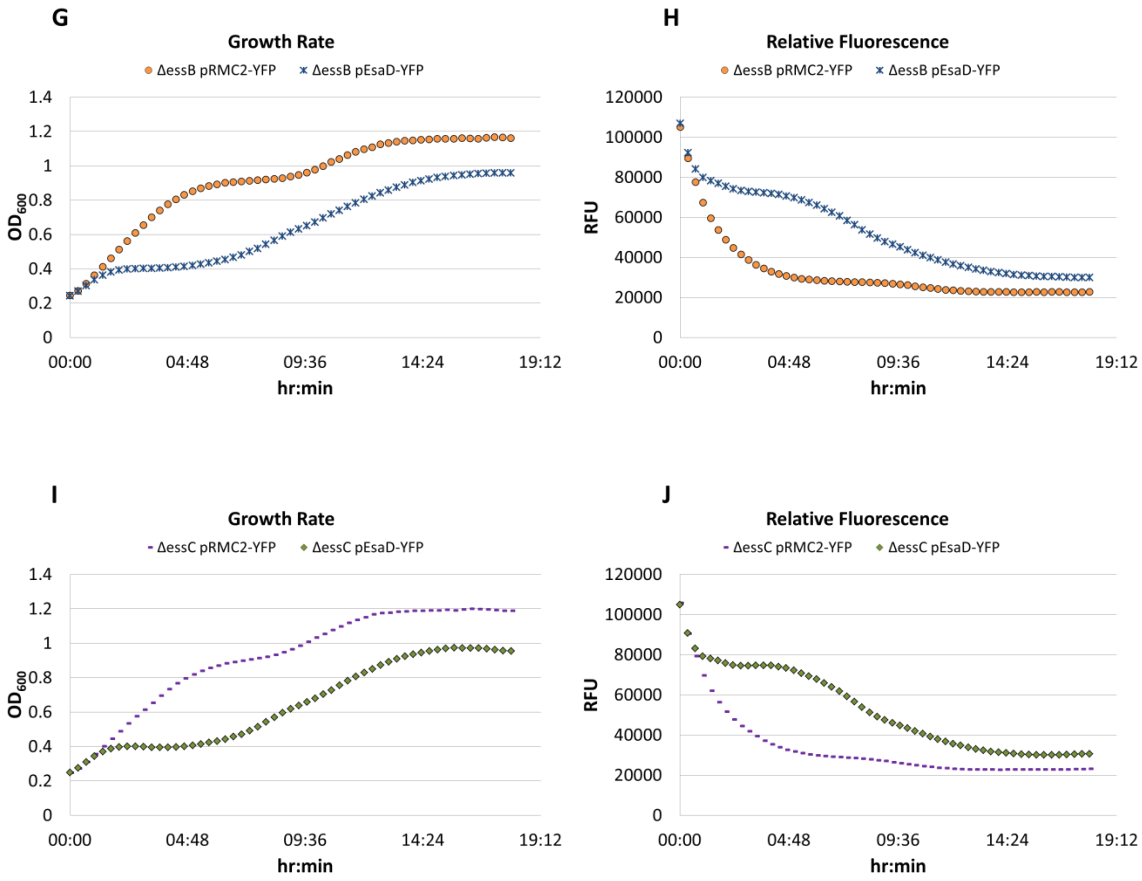

Figure 4.14: OD_{600} and YFP fluorescence measurements for the indicated *S. aureus* strains harbouring plasmids encoding YFP or EsaD-YFP. RN6390 WT and strains lacking the individual Ess membrane proteins EsaA, EssA, EssB or EssC harbouring either pRMC2-YFP or pRMC2-EsaD-YFP. Cells were grown at 37 °C for 18 h with regular measurement of OD_{600} and fluorescence (excitation at 485 nm/ emission at 528 nm) in 20 min intervals. Culture was shaken for 20 seconds before every read.

Figure 4.14 shows the growth and fluorescence measurements for cultures of the RN6390 WT strain and of strains individually lacking one of the membrane components EsaA, EssA, EssB and EssC in presence of overproduced EsaD-YFP. Strains harbouring the control pRMC2-YFP vector show an increase of cell density over a time of ~16 hours after which they start to reach the stationary phase. Strains producing EsaD-YFP showed similar growth as the control strains over the first 1.0 - 1.5 hours, after which a pronounced growth lag was seen before growth rate was restored after ~9.5 hours. Although strains producing EsaD-YFP also reached stationary phase after ~16 hours they did not reach the same final OD_{600} as strains harbouring pRMC2-YFP. Looking at the fluorescence of theses strains it can be seen that all samples tested show an initial

level of ~100 000 RFU which decreased to 40 000 RFU within the first hour for strains harbouring the vector encoding YFP alone (Figure 4.14 right panel). The WT strain producing pEsaD-YFP shows the highest fluorescence of all the strains tested, peaking at ~86 000 RFU after 4.5 to 5.0 hours (Figure 4.14 B). This strain is also the only one to show a decline in OD_{600} at that time (Figure 4.14 A).

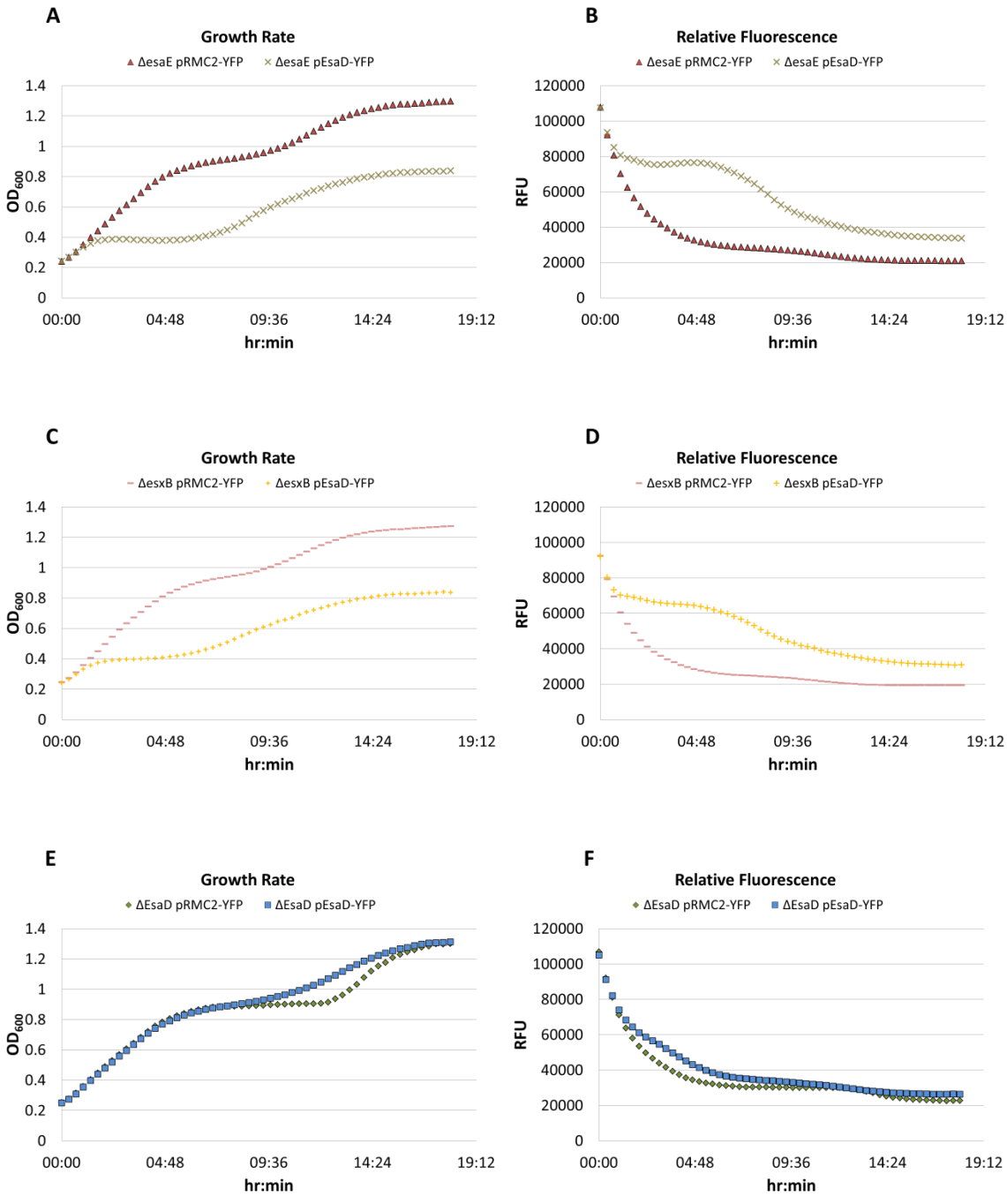

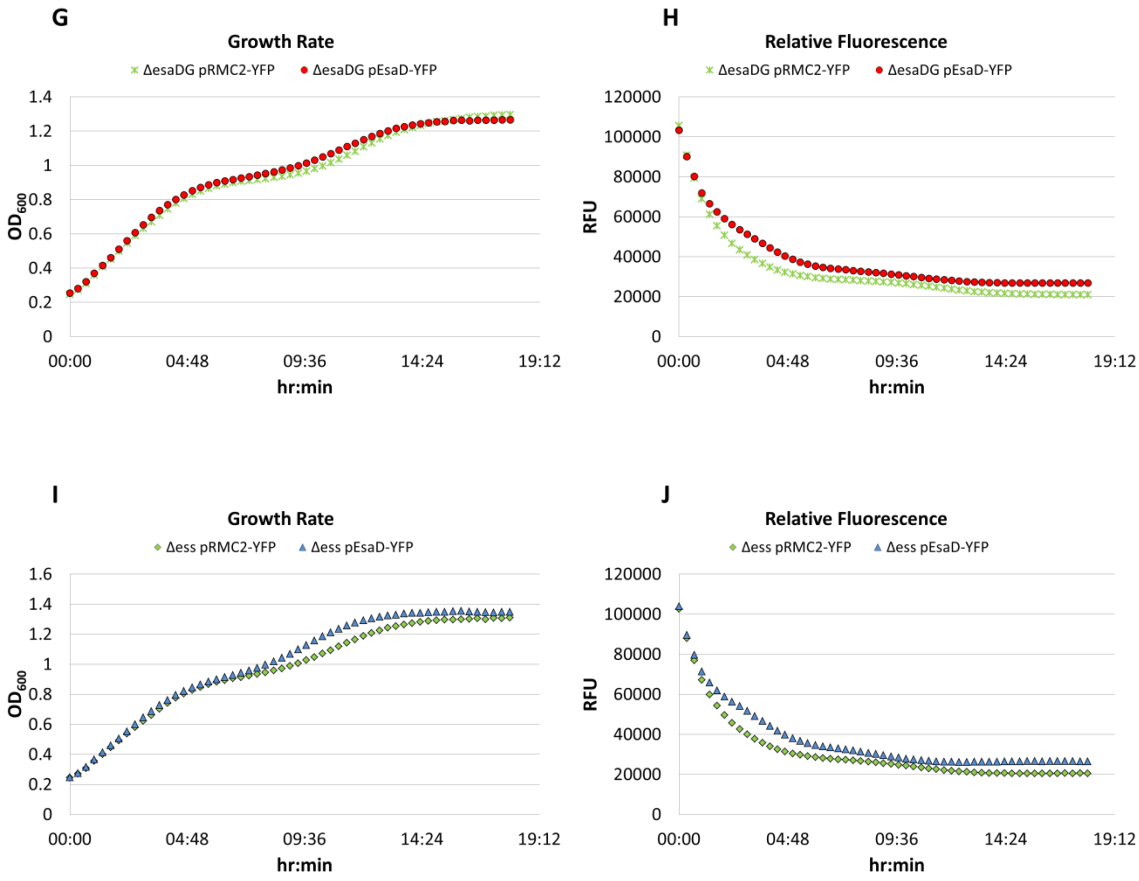

Figure 4.15: OD_{600} and YFP fluorescence measurements for the indicated *S. aureus* strains harbouring plasmids encoding YFP or EsaD-YFP. Cells lacking either of EsaE, EsaD or EsxB, both EsaD and EsaG, or all 12 genes of the *ess* locus were grown at 37 °C for 18 h with regular measurement of the relative fluorescence unit **(RFU)** in 20 min intervals. Culture was shaken for 20 seconds before every read.

Next strains lacking individual soluble components encoded at the *ess* locus were investigated in a similar way. Here the strain growth behaviour fell into two distinct patterns (Figure 4.15). Strains lacking either of EsaE or EsxB showed a similar slowing of growth upon production of EsaD-YFP as the wild type strain or the strains lacking EsaA, EssA, EssB or EssC, and also produced very similar fluorescence profiles. By contrast, strains deleted for *esaD*, *esaDG* or all 12 genes from the *ess* locus did not show the slowdown of cell growth when EsaD-YFP production was induced (Figure 4.15 E, G and I). Instead growth of these strains was very similar to the same strains harbouring the pRMC2-YFP control. Moreover, these strains showed a much lower level of fluorescence than all of the other strains analysed (Figure 4.15 F, H and J). In fact, fluorescence of these strains is more comparable with the fluorescence of the strains harbouring the empty

pRMC2-YFP vector and therefore suggests that they indeed do not carry the plasmid or are not expressing the plasmid-encoded construct.

4.6 Discussion

4.6.1 EsaA and EssC form homomeric complexes

As outlined in Chapter 3, EsaA and EssB form homomeric complexes in detergent extracts. In this chapter complex formation between the membrane components was addressed in the native membrane environment, both *in vitro* and *in vivo*, using chemical crosslinking reagents. *In vitro* experiments with isolated membrane fractions were undertaken using DSS as a crosslinker, which crosslinks amine residues of proteins with a preference for the side chain of lysine. Results obtained with this method revealed multimeric complex formation for EssC, but homo-oligomerisation of EsaA, which was observed in BN PAGE analysis, was not seen (Figure 4.3), potentially due to a lack of appropriately positioned lysine residues. No dimerization of EssB was detected in any of these crosslinking experiments, which is surprising as it was previously demonstrated that EssB crystallises as a dimer (Zoltner *et al.*, 2013a; Zoltner *et al.*, 2013b). Again, this may reflect a lack of appropriately positioned reactive side chains.

Different results for EsaA were seen when crosslinking was undertaken in whole cells using PFA as a crosslinking reagent, compared to *in vitro* crosslinking with DSS. Under *in vivo* conditions 4 - 5 EsaA-cross-reacting bands could be detected migrating around 250 kDa. Since these bands were also detected in strains lacking each of the other Ess membrane components, they cannot represent crosslinks to known membrane proteins of the T7SS. They may potentially reflect crosslinks to other unknown proteins, or more likely (given that they are approximately twice the size of an EsaA monomer) they may be different conformers of an EsaA homo-dimer. In this context it should be noted that the *Bacillus subtilis* homologue of EsaA is known to form a high elongated homo-dimer (São-José *et al.*, 2006).

Crosslinking analysis of EssC *in vivo* with PFA also revealed differences to the *in vitro* analysis with DSS. Whereas the DSS crosslinking gave only one higher molecular weight EssC-reacting band, migrating well above the 460 kDa marker, the *in vivo* crosslinking revealed two EssC-reacting bands that both migrate above the 460 kDa marker. The EssC monomer has a calculated mass of 170,930 Da, although it migrates above the 171 kDa marker on SDS PAGE analysis (e.g. Fig 4.4). Aberrant migration of membrane proteins on SDS PAGE is a common phenomenon for membrane proteins (De Leeuw *et al.*, 2001). However, both of the crosslinked products detected are too large to represent a homo-dimer (which would be expected to migrate below the 460 kDa marker), and, assuming they are homomeric EssC complexes, they must correspond to at least homo-trimers. EssC belongs to the FtsK/SpoIIIE ATPase family which is known to form hexameric complexes (Massey *et al.*, 2006; Rosenberg *et al.*, 2015; Beckham *et al.*, 2017), and purified, recombinant EssC isolated from *E. coli* membranes has an apparent molecular mass of 1 mDa, consistent with hexamer formation (which has a calculated mass of 1.026 mDa; Zoltner *et al.*, 2016)). It is highly unusual that no EssC dimers were detected here by crosslinking as the crosslinker is bifunctional, so dimeric complexes should always be an intermediate. Repeating the crosslinking at lower temperatures or for shorter times may allow dimeric intermediates of EssC to be observed.

Multimerisation of the purified C-terminal domain of the actinobacterial EccC has also been observed by crosslinking (Rosenberg *et al.*, 2015). In that study, glutaraldehyde was used as a crosslinker, and both dimeric and multimeric EccC species were detected. It was shown that multimerisation was apparently controlled by the presence of the small substrate proteins EsxA and EsxB. However, Fig 4.5 shows that *in vivo* crosslinking of a plasmid-encoded variant of EssC in a strain lacking all 12 genes at the *ess* locus can still be detected. This indicates that for the *S. aureus* Type VII secretion system multimerisation is not dependent upon any of the known substrates. In this context, a very recent study has also shown substrate-independent hexamerisation of *M. xenopi* EccC under native conditions (Beckham *et al.*, 2017).

Differences between the patterns of crosslinking seen *in vivo* and *in vitro* may have several potential explanations. As already mentioned the presence of substrates, ATP and the proton motive force in whole cells could play an important role, but the crosslinkers and the conditions in which they were used could also have an effect. DSS and PFA both belong to the NHS ester family, which preferably crosslink amine-residues of amino acids. With a spacer arm length of 11.4 Å for DSS compared to a spacer arm length of only 2.3 – 2.7 Å for PFA it might be expected that more crosslinks would be detected in the *in vitro* experiments since proteins under *in vivo* conditions using PFA would need to be in closer proximity to each other for crosslinking to happen. However, one explanation for less crosslinking seen with DSS could be that there are no suitable lysine residues exposed for an interaction with neighbouring proteins. Another reason for less interaction under *in vitro* conditions could be that NHS esters are known to be subject to rapid hydrolysis in aqueous solution giving them a half-life of only a couple of minutes under the reaction conditions used (Leitner *et al.*, 2010).

It is interesting to note that to detect complex formation for the distantly related Esx-5 secretion system in *M. marinum* DSP was used as a crosslinker under *in vitro* conditions (Houben *et al.*, 2012). DSP is a DSS homologue with the only difference that the spacer arm contains a disulphide bond allowing crosslinks to be reversibly formed. At present it is not clear why heteromeric complexes of the Ess membrane components cannot be detected, although it should be noted, that the *S. aureus* strain RN6390 used in this study is known to have a rather low T7 secretion activity under laboratory conditions (Kneuper *et al.*, 2014) which could also contribute to the fact that no interaction between the membrane components could be detected. In future it might be interesting to repeat this analysis in more actively secreting *S. aureus* strains.

4.6.2 Interaction of the membrane components is not dependent on EsxA and EsaD

For the Twin arginine transport system it is known that the membrane protein TatA only interacts with TatBC upon binding of a substrate (Gohlke *et al.*, 2005; Leake *et al.*, 2008). Therefore experiments were undertaken to determine whether substrate overproduction could allow Ess complexes to be detected by crosslinking. It was noted that adding a C-terminal YFP-tag onto the secreted protein EsxA prevented this variant from being efficiently secreted and it also showed dominant negative activity as it blocked the secretion of native EsxA and EsxC (Figure 4.7). These findings suggested that EsxA-YFP interacts with Ess machinery, blocking it at one step in the transport pathway and therefore offering a potential opportunity to catch a 'snapshot' of Ess complex formation. Unfortunately *in vivo* crosslinking studies in the presence and absence of the YFP-tagged EsxA-variant did not result in a noticeable difference in the crosslinking pattern, making it difficult to identify a potential interaction of the membrane components with each other or with EsxA-YFP. Even when samples were blotted with an anti-EsxA or anti-GFP antibody the same crosslinking products were detected in presence and absence of the membrane components indicating that EsxA-YFP oligomerises but does not appear to interact with the secretion machinery (Figure 4.9).

An even more drastic effect was observed when a YFP-tag was fused to a nuclease-inactive variant of the EsaD substrate, as overproduction of this construct caused cell death. The initial conclusion was that EsaD-YFP may become jammed in the Ess transport channel, blocking the system. In support of this, EsaD-YFP was detected in membrane fractions as both monomeric and high molecular weight forms. However, no corresponding high molecular weight bands could be detected when blotting for the membrane components EsaA, EssB and EssC (Figure 4.12) indicating that EsaD-YFP probably does not interact with the machinery.

When blotting against the YFP-tag it was noted that strains lacking chromosomally-encoded EsaD or all 12 genes of the *ess* locus did not show a YFP signal, indicating that these strains did not contain EsaD-YFP. This was also confirmed by monitoring growth curves and levels of

fluorescence of different strains in the presence and absence of the plasmid-encoded YFP-tagged EsaD-variant. Here it was discovered that strains lacking all twelve genes at the entire *ess* locus, the *esaD* gene or the *esaDG* genes displayed reduced fluorescence together with unaffected cell growth, whereas strains encoding chromosomal *esaD* showed a high fluorescence with a significant decrease in cell growth over the time.

EsaD was recently discovered to be a secreted nuclease toxin killing competitive bacteria (Cao *et al.*, 2016). EsaG, another cytosolic protein, works as an antitoxin by interacting with the predicted nuclease-domain of EsaD and therefore protecting *S. aureus*. The YFP-tagged variant of plasmid-encoded EsaD carries a codon substitution (H528A) at the predicted nuclease active site since it was not possible to clone the wild type *esaD* due to the toxic activity (Cao *et al.*, 2016). A potential explanation for the toxicity of plasmid-encoded EsaD-YFP could be that the non-toxic pEsaD-YFP variant titrates away the cellular EsaG leaving the chromosomally-produced, nuclease-active EsaD free of toxin and therefore able to kill the producing cell. This toxicity would clearly be alleviated in any cells that lack chromosomal *esaD* which would account for the almost normal growth of *esaD*$^{-}$ strains producing EsaD-YFP. It is, however, harder to explain why the EsaD-YFP fusion protein is not detected in these strain backgrounds unless the EsaD-YFP fusion protein requires interaction with native, untagged EsaD for stability.

5
EssC is a specificity determinant for T7 secretion in *S. aureus*

5.1 Introduction

As discussed in Chapter 1, EsaD is a secreted nuclease toxin which forms a heterodimer prior to secretion with its antitoxin partner EsaG (Cao *et al.*, 2016). In the same study it could be shown that this heterodimer pair additionally interacts with a further protein EsaE. Moreover, PFA crosslinking in whole cells revealed an interaction of EsaE with the T7 membrane component EssC (Cao *et al.*, 2016), suggesting that EsaE functions as a chaperone delivering EsaD to the transport channel. Similar results were also obtained by Anderson *et al.* (2017) where pull down experiments revealed that not only do EsaE, EsaD, EsaG and EssC co-purify, but that a further substrate protein EsxC also co-purifies with EsaE. EsxC has been identified as a secreted protein, playing an important role in abscess formation in a mouse infection model (Burts *et al.*, 2008; Kneuper *et al.*, 2014). EsxC, like the other known T7SS substrates EsxB, EsxD and EsaD are encoded downstream of *essC* in the *ess* loci of *S. aureus* strains such as RN6390, USA300, Newman and COL (Burts *et al.*, 2005; Kneuper *et al.*, 2014; Warne *et al.*, 2016).

The dependence of substrates on chaperones for secretion by the T7SS is also described in Mycobacteria, where EspG was shown to bind PE/PPE dimers (Daleke *et al.*, 2012b). PE and PPE proteins are secreted proteins, named after highly conserved proline-glutamic acid (PE) and proline-proline-glutamic acid (PPE) motifs that are found in these protein families (Cole *et al.*, 1998). EspG proteins are only encoded in *esx* gene clusters that also encode PE and PPE proteins indicating that EspG proteins from one cluster specifically interact with PE and PPE proteins from the same cluster. Indeed it was demonstrated that the chaperone of the Esx-3 secretion system, $EspG_3$, binds to PPE69 while $EspG_5$ of the Esx-5 secretion system binds to PPE14, PPE17 and PPE60 (Ekiert and Cox, 2014). The recognition of the PE/PPE complex by EspG takes place through binding to a specific binding domain located at the N-termini of the PPE proteins (Ekiert and Cox, 2014; Korotkova *et al.*, 2014), building a complex with the PE/PPE dimer in a ratio of 1:1:1 (Daleke *et al.*, 2012b).

Similar to EspG, genomic analysis revealed that EsaE in *S. aureus* is only present in strains also coding for *esaD* and *esxC,* supporting the idea that EsaE functions as a specific chaperone for strain-specific proteins. EsaE, as well as EsaG and EsaD are encoded downstream of *essC*, a part of the *ess* locus which is highly diverse among the different *S. aureus* strains (Warne *et al.*, 2016; Figure 5.1). Warne *et al*. (2016) divided the *S. aureus ess* loci into four modules. The first module contains the first five genes of the *ess* locus, namely *esxA, esaA, essA, esaB* and *essB*, which are known to encode core components of the secretion system (Burts *et al.*, 2005; Burts *et al.*, 2008; Kneuper *et al.*, 2014). The 5' end of the second module covers the *essC* gene coding for the ATPase protein as well as the five genes encoded immediately downstream of *essC* with which they are co-transcribed, at least in strain RN6390 (Kneuper *et al.*, 2014). Four of these five genes code for the substrate proteins EsxBCD and EsaD, while the remaining gene codes for EsaE. Within the second module it was also discovered that although the 5' portion of *essC* is highly conserved, there are four variants of the *essC* 3' region (Figure 5.1). Each *essC* variant was associated with a unique set of downstream genes encoded within Module 2 suggesting that the C-terminus of EssC is linked with a distinct repertoire of secreted and accessory proteins. The first EssC variant, EssC1, is encoded in *S. aureus* strains such as Newman, COL, USA300 and RN6390 while variant two (EssC2) is encoded in the ST398 strain. Variant *essC3* was found in strains including MRSA252 and ST239 while the final variant, *essC4*, was found in the *S. aureus* strain EMRSA15. Modules 3 and 4 of the *ess* loci contained a variable number of hypothetical membrane proteins and genes coding for DUF600–domain proteins, which are EsaG-like anti-toxins (Cao *et al.*, 2016).

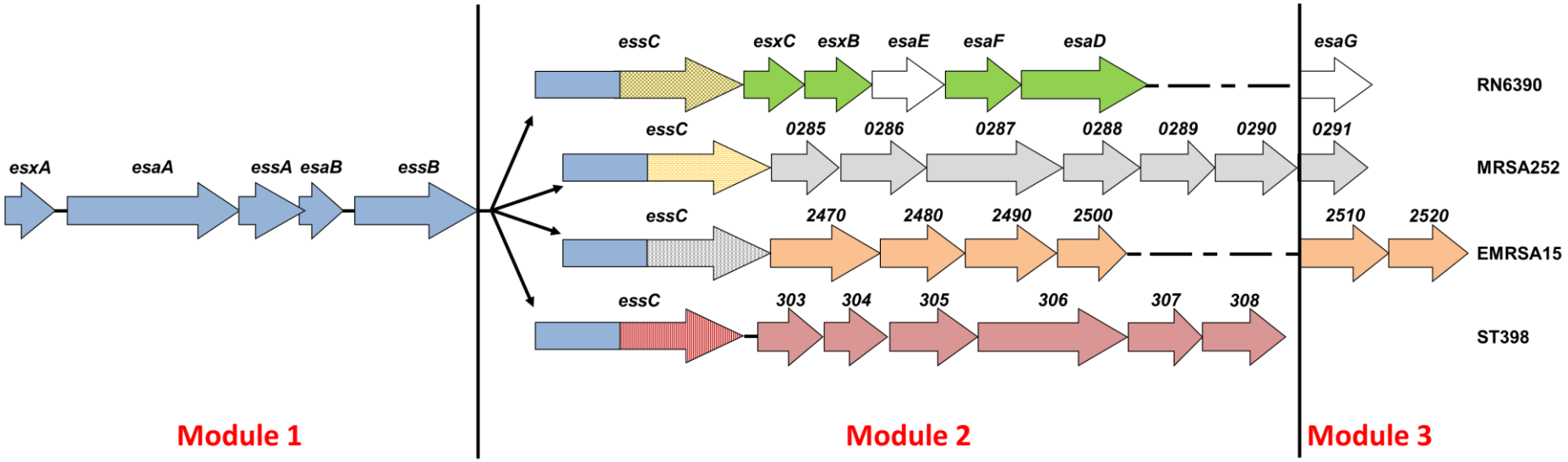

Figure 5.1: Schematic representation of the four genetic variants of the *ess* locus found across *S. aureus* strains. Adapted from Warne et al. (2016).

5.2 Aim

The genetic diversity in the 3' region of the different *essC* variants together with the genes encoded immediately downstream suggest that these genes code for strain specific substrates only recognised and secreted by the specific EssC. The aim of this chapter was to specifically test this hypothesis.

Results

5.3 Strain specific T7 substrate secretion

A sequence alignment of the three C-terminal ATPase domains of the different EssC variants shows that the first ATPase domain (residues 626 - 931) is highly conserved. (Figure 5.2) Towards the second half of ATPase Domain 2 (residues 932 - 1219) it can be seen that EssC from RN6390 begins to exhibit sequence variation relative to the EssC proteins from the other strains. The EssC variants from MRSA252 and ST398 are the most similar to each other, and only start to diverge in sequence towards the middle of ATPase Domain 3 (Figure 5.2). This variability is also shown on the crystal structure of the C-terminal ATPase domains of EssC from *G. thermodenitrificans* (Figure 5.3).

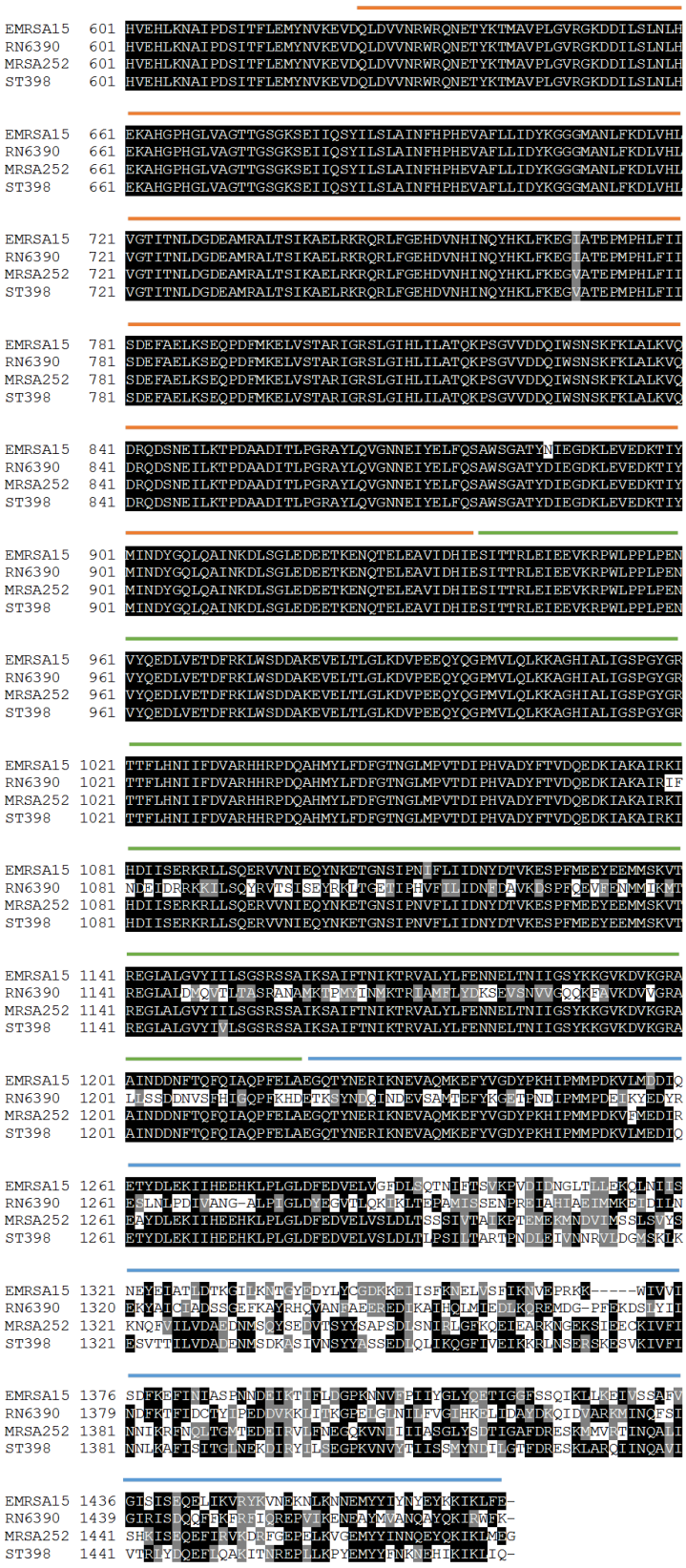

Figure 5.2: Sequence alignment of EssC sequences encoded by RN6390, EMRSA15, MRSA252 and ST398. Only the sequences of the last three ATPase domains are shown which are indicated with colour coding **red** for ATP1, **green** for ATP2 and **blue** for ATP3. The alignment was generated using the programme Clustal W and shaded with Boxshade.

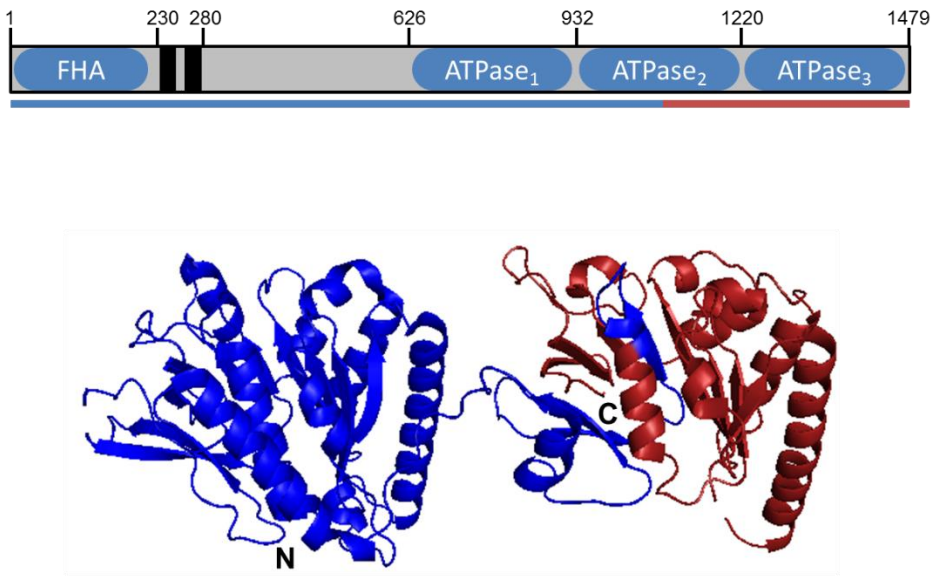

Figure 5.3: Crystal structure of the C-terminal region of EssC. Shown in blue is the extent of the conserved and in red the variable regions identified between *essC1* and *essC2* on the x-ray structure of the ATPase domains of *G. thermodenitrificans* EssC. Taken from Warne *et al.* (2016), with permission.

In order to test the hypothesis that the C-terminal, variable domain of EssC is involved in strain specific substrate recognition, firstly the four *essC* variants needed to be cloned. The laboratory strain RN6390 was chosen as representative of variant EssC1, ST398 for EssC2, MRSA252 for EssC3 and EMRSA15 for EssC4. A construct encoding RN6390 and MRSA252 *essC* in pRAB11 had already been made by Dr Holger Kneuper (Chapters 3 and 4), and constructs of the other two variants in the same vector were also generated, using the oligonucleotides listed in Table 2.6. Dr Holger Kneuper had previously constructed in frame deletions of *essC* in each of these four strain backgrounds (Kneuper *et al.*, 2014; Kneuper and Palmer, unpublished). The plasmid-encoded EssC-variants of each group were then introduced into each of these *essC* deletion strains.

5.3.1 Testing production of EssC-variants in the different strain backgrounds

Before undertaking any secretion assays, it was first necessary to confirm stable production of each of the EssC variants in the four different strain backgrounds. To this end, the wild type strains RN6390, ST398, MRSA252 and EMRSA15, the four *essC* deletion strains harbouring empty pRAB11 vector and the four *essC* deletion strains harbouring each of pRAB11-EssCV1, -EssCV2, -EssCV3 and -EssCV4 were grown to an OD_{600} of 2.0 in the presence of ATc. Whole cell samples were then immunoblotted using an antibody raised against purified RN6390 EssC (Figure 5.4).

For *S. aureus* RN6390 it can be seen that native EssC is stably produced from the chromosome and it is also stably produced in the Δ*essC* strain carrying the plasmid-encoded RN6390 variant of EssC (Figure 5.4 A). The plasmid-encoded EssC variants derived from MRSA252, EMRSA15 and ST398 can also be detected when produced in the RN6390 *essC* deletion strain, although the signals for these proteins are weaker than for the cognate EssC1 variant. This is because the antibody used in this study is raised against C-terminal 60kDa portion of EssC from RN6390, covering the conserved second P-loop ATPase domain and the sequence variable third P-loop domain. Immunological detection of EssC2, EssC3 and EssC4 is therefore weaker because there are fewer epitopes recognised by the antiserum. Each of the plasmid-encoded EssC variants were also stably produced in the *essC* mutants derived from strains MRSA252, EMRSA15 and ST398 (Figure 5.4 B – D).

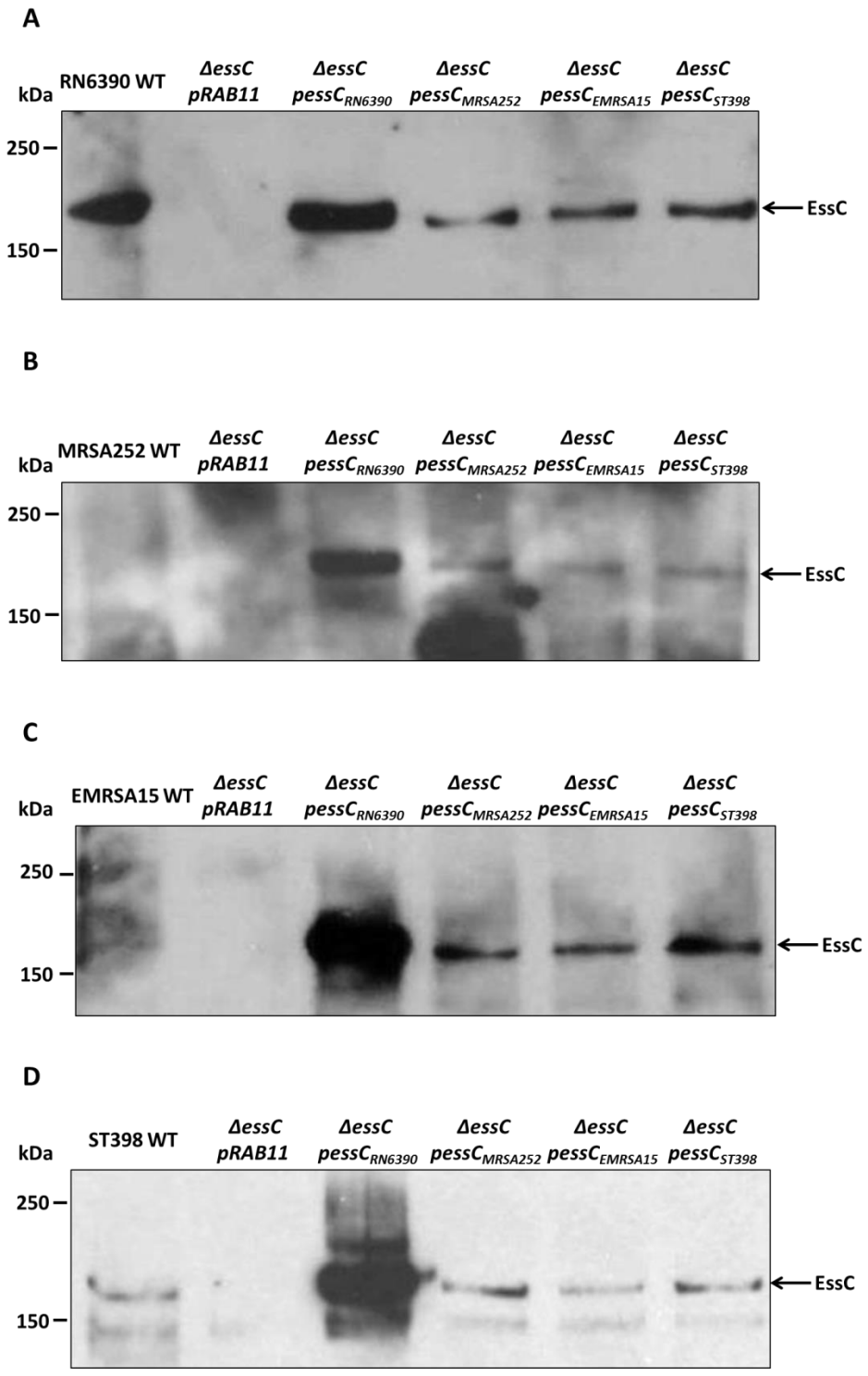

Figure 5.4: Immunological detection of EssC in different strain backgrounds WT strains of **(A)** RN6390, **(B)** MRSA252, **(C)** EMRSA15 and **(D)** ST398 were grown together with the individual *essC* deletion strains either harbouring the empty pRAB11 vector or pRAB11 encoding the indicated EssC variants and harvested once they reached an OD_{600} of 2.0. 10 µl of whole cell samples adjusted to an OD_{600} = 1.0 were loaded on a bis-Tris gel containing 8 % acrylamide and subsequently transferred onto a PVDF membrane for immunological detection of EssC.

5.3.2 Testing T7 secretion after complementation of *S. aureus* strains with non-cognate *essC* genes

Once stable production of all four plasmid-encoded EssC-variants was confirmed in each strain background, it was next tested whether they were able to functionally complement and restore T7 secretion. As discussed in Chapter 1, the secreted protein EsxA is a core component of the Ess machinery and Figure 5.5 shows that the EsxA proteins from the four *S. aureus* strains are almost 100% identical. It was therefore hypothesized that secretion of this protein was likely to be independent of the EssC subtype. Cells of each of the RN6390, MRSA252, EMRSA15 and ST398 *essC* mutant strains carrying the plasmid-encoded EssC variant of groups 1 – 4 were grown to an OD_{600} = 2.0. Samples were then separated into culture supernatant and cellular fractions, transferred onto nitrocellulose membrane and immunoblotted using anti-EsxA antibodies. Blotted samples were also probed with antibodies to the cytosolic protein TrxA as a negative control.

```
RN6390      1 MAMIKMSPEEIRAKSQSYGQGSDQIRQILSDLTRAQGEIAANWEGQAFSRFEEQFQQLSP
MRSA252     1 MAMIKMSPEEIRAKSQSYGQGSDQIRQILSDLTRAQGEIAANWEGQAFSRFEEQFQQLSP
ST398       1 MAMIKMSPEEIRAKSQSYGQGSDQIRQILSDLTRAQGEIAANWEGQAFSRFEEQFQQLSP
EMSRA15     1 MAMIKMSPEEIRAKSQSYGQGSDQIRQILSDLTRAQGEISANWEGQAFSRFEEQFQQLSP

RN6390     61 KVEKFAQLLEEIKQQLNSTADAVQEQDQQLSNNFGLQ
MRSA252    61 KVEKFAQLLEEIKQQLNSTADAVQEQDQQLSNNFGLQ
ST398      61 KVEKFAQLLEEIKQQLNSTADAVQEQDQQLSNNFGLQ
EMSRA15    61 KVEKFAQLLEEIKQQLNSTADAVQEQDQQLSNNFGLQ
```

Figure 5.5: Sequence alignment of EsxA from RN6390, EMRSA15, MRSA252 and ST398. The alignment was generated using the programme Clustal W and shaded with Boxshade.

Figure 5.6 A shows that EsxA is detectable in the supernatant of the RN6390 WT strain but not in the *essC* deletion strain, as expected. Re-introducing plasmid-encoded RN6390 EssC protein restored secretion activity. Moreover, plasmid-encoded variants of EssC2, EssC3 and EssC4 each

restored EsxA secretion to the *essC* mutant of RN6390 indicating that they retained function when produced in the heterologous background.

Slightly different results were obtained with the MRSA252 strains (Figure 5.6. B). EsxA was not detectable in the supernatant of either the WT or the *essC* deletion strain. Even re-introducing and overproducing MRSA252 EssC from a plasmid did not lead to EsxA secretion. These observations indicate that the T7SS of strain MRSA252 is not active under laboratory conditions. As expected, introduction of any of the other EssC variants into the MRSA252 Δ*essC* strain did not lead to EsxA secretion.

EsxA could be clearly detected in the supernatants of the EMRSA15 and ST398 strains but not in the *essC* derivatives (Figure 5.6 C and D). Re-introducing the cognate plasmid-encoded EssC variant restored EsxA secretion to both strains as did all other plasmid-encoded EssC variants tested. However, it should be noted that TrxA can be detected in the supernatant sample of the EMRSA15 WT strain, indicating that the strong signal detected for EsxA in the supernatant of this strains might not solely be due to secretion, but may also be attributable to cell lysis (Figure 5.6 C).

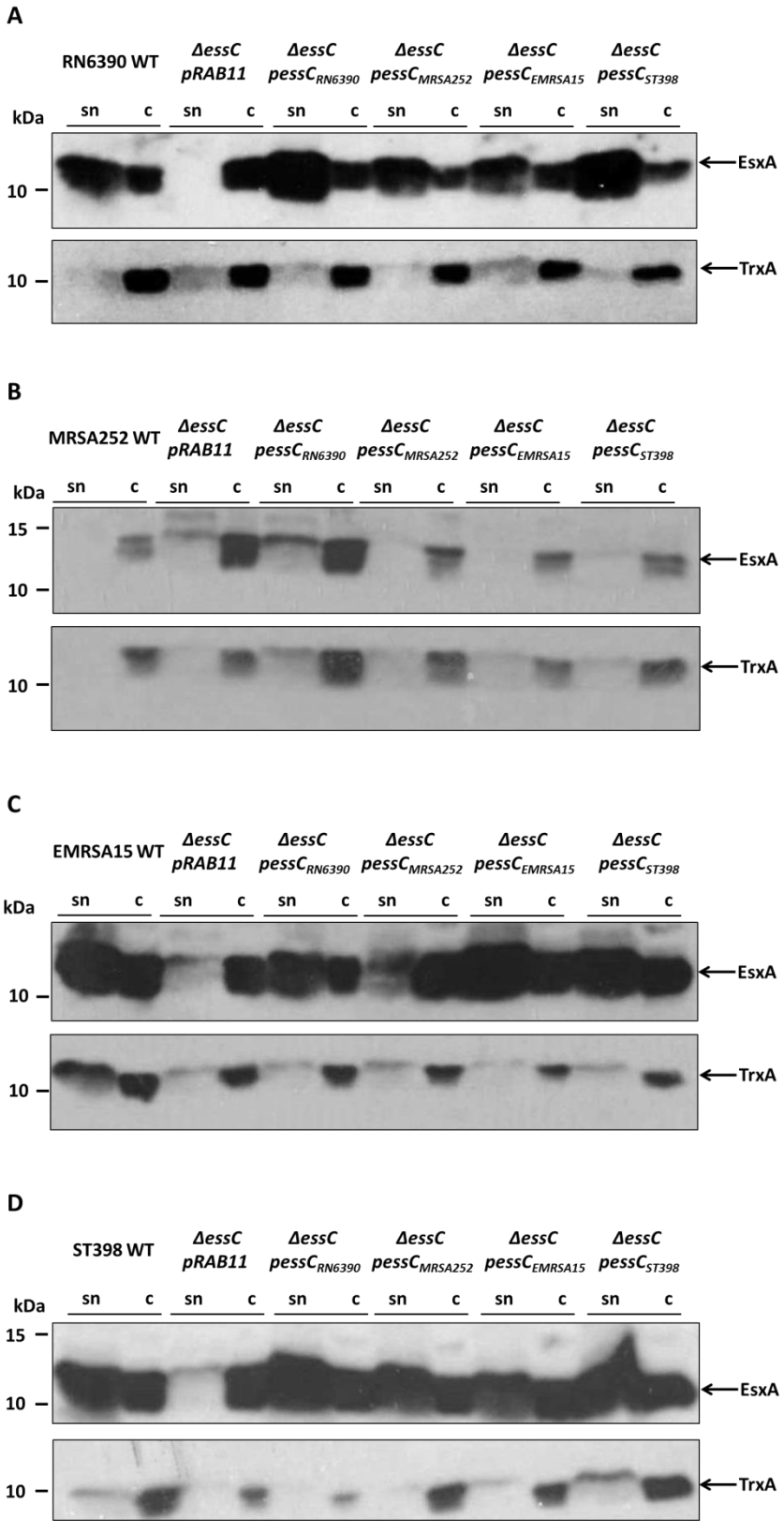

Figure 5.6: EsxA secretion is not dependent on the origin of EssC. WT strains of **(A)** RN6390, **(B)** MRSA252, **(C)** EMRSA15 and **(D)** ST398 were grown together with the individual *essC* deletion strains either harbouring the empty pRAB11 vector or pRAB11 encoding the indicated EssC variants and harvested once they reached an OD_{600} of 2.0. An equivalent of 200 µl of culture supernatant (sn) and 10 µl of resuspended cell sample (c) adjusted to an OD_{600} = 1.0 were separated on a bis-Tris-gel containing 15 % acrylamide and immunoblotted using the antiserum raised against EsxA or the control TrxA.

5.3.3 Secretion of EsxC is dependent on the EssC variant

Since variant EssC proteins from different *S. aureus* strains all supported the secretion of the core component EsxA in different strain backgrounds the next step was to test whether they could also mediate secretion of strain-specific substrates. EsxC is a small substrate protein encoded downstream of *essC* in RN6390 but is not found in MRSA252, ST398 or EMRSA15. The RN6390 WT strain together with the isogenic *essC* deletion strain either harbouring the empty pRAB11 vector or pRAB11 encoding for each of the EssC variants was grown to an OD_{600} = 2.0, samples separated into culture supernatant and whole cells followed by immunoblotting against EsxC or the cytosolic control TrxA.

It can be seen (Figure 5.7) that native EsxC was detected in the supernatant of the WT but remained in the cells of the *essC* deletion strain harbouring the empty vector. Re-introducing the cognate plasmid-encoded EssC protein restored EsxC secretion. However, plasmid-encoded variants of EssC2, EssC3 or EssC4 did not support secretion of EsxC and the protein was only detectable in the cell samples of the strains harbouring EssC from MRSA252, EMRSA15 or ST398 (Figure 5.7). These findings are in accordance with the hypothesis that genes located downstream of *essC* encode for strain-specific substrates and that these substrates are recognised by the C-terminal domain of EssC. However, since all four EssC proteins can recognise 'non-cognate' EsxA proteins it strongly suggests that EsxA interacts elsewhere on EssC.

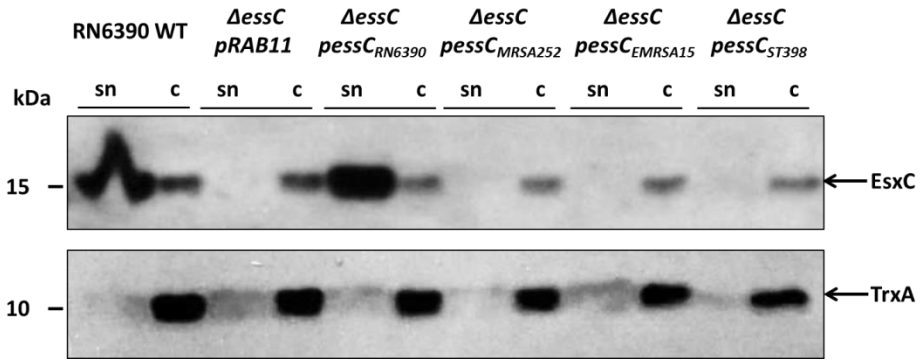

Figure 5.7: EsxC secretion is supported only by the EssC variant from RN6390. RN6390 or the *essC* mutant derivative harbouring either empty pRAB11 or pRAB11 encoding the indicated EssC variant were cultured and harvested once they reached an OD_{600} of 2.0. An equivalent of 200 µl of culture supernatant (sn) and 10 µl of resuspended cell sample (c) adjusted to an OD_{600} = 1.0 were separated on a bis-Tris-gel containing 15 % acrylamide and immunoblotted using the antiserum raised against EsxC or the control TrxA.

5.4 Crosslinking studies using purified proteins.

The results obtained above support the idea that genes downstream of *essC* code for strain-specific substrates that are recognised by the most C-terminal domain of the ATPase protein. As discussed previously, Cao *et al.* (2016) showed that the nuclease toxin EsaD binds to the soluble protein EsaE which then interacts with EssC upon secretion. Both EsaD and EsaE proteins are encoded downstream of *essC* at the *ess* locus of RN6390 and therefore EsaE might also interact with the C-terminal domain of EssC. To test this hypothesis, the proteins of interest were overproduced and purified for interaction studies. To this end, a His-tagged variant of the last two ATPase domains of EssC was purified, as well as His-tagged versions of the soluble proteins EsaE and EsxC. EsxA was shown to be secreted by all EssC-variants and is therefore thought to bind to a conserved region of the EssC protein, either the first ATPase-domain or the N-terminus of the protein. EsxA was therefore also purified for use in interaction studies as a potential negative control.

5.4.1 Purification of EsxA, EsxC, EsaE and $EssC_{ATP2}$

To facilitate purification it was first necessary to generate plasmid-encoded His-tagged variants of the proteins to allow for heterologous production and purification from *E. coli.* To achieve this, the backbone vector pET15bTEV was chosen which codes for an N-terminal His-tag followed by a Tobacco etch virus (TEV) cleavage site. Plasmid-encoded His-tagged variants of the soluble proteins EsxA and EsxC as well as EsaE were already generated by Dr Martin Zoltner and Dr Zhenping Cao, respectively. The gene coding for $essC_{ATP2}$ was introduced into this vector using the restriction sites *Xho*I and *Bam*HI.

Proteins were overproduced in *E. coli* BL21 DE3 and purified using a His-trap column. Following purification, elution fractions were analysed by SDS PAGE to check purity of the protein, after which fractions containing the protein of interest were pooled, concentrated and the imidazole removed. Figure 5.8 shows the concentrated protein fractions together with the mass spectrometry analyses for each of the purified proteins.

Figure 5.8 A shows that EsxA could be purified in very large amounts. Low levels of a dimeric form were also detected on SDS PAGE. Several EsxC-containing bands could be detected following coomassie staining, with the highest one running at 25 kDa followed by two strong bands between 10 and 15 kDa. Mass spectrometry analyses revealed that all three bands contained EsxC with the lowest molecular weight band probably containing one or more degradation products of the protein. The faint band at 25 kDa probably corresponds to a dimeric form of EsxC (Figure 5.8 B). Similar to EsxA and EsxC it was possible to purify EsaE to almost complete homogeneity (Figure 5.8 C). Two bands were detectable with a size of ~25 kDa, of which both corresponded to EsaE by mass spectrometry analyses. Purification of $EssC_{ATP2}$ was not as successful as purification of the other proteins. As it can be seen in Figure 5.8 D there were still many bands detectable on SDS PAGE after purification of the protein. Four strong bands could be detected between 25 and 75 kDa. Mass spectrometry analyses revealed the

lower three bands containing $EssC_{ATP2}$ while the highest band contained solely proteins of *E. coli* origin.

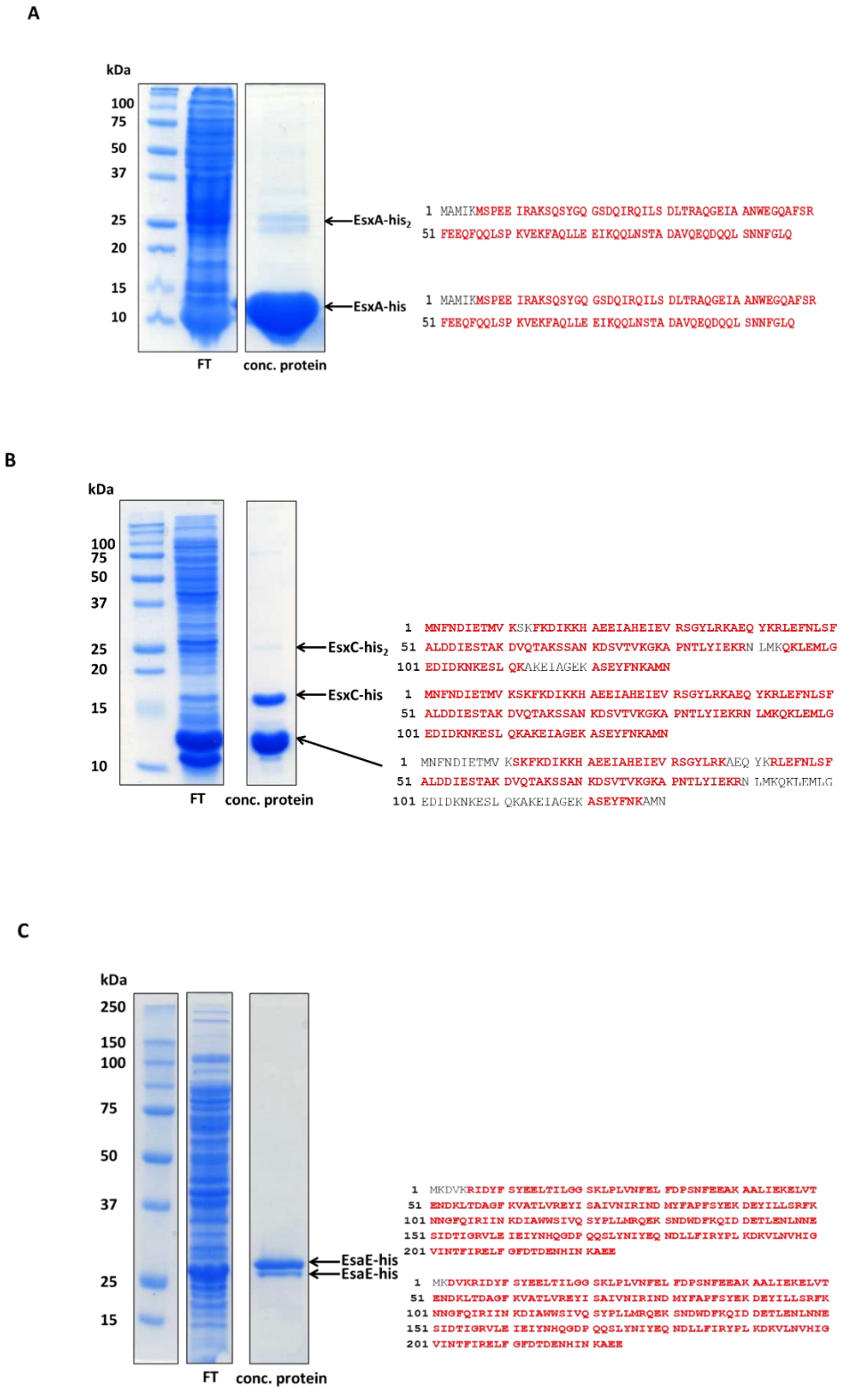

D

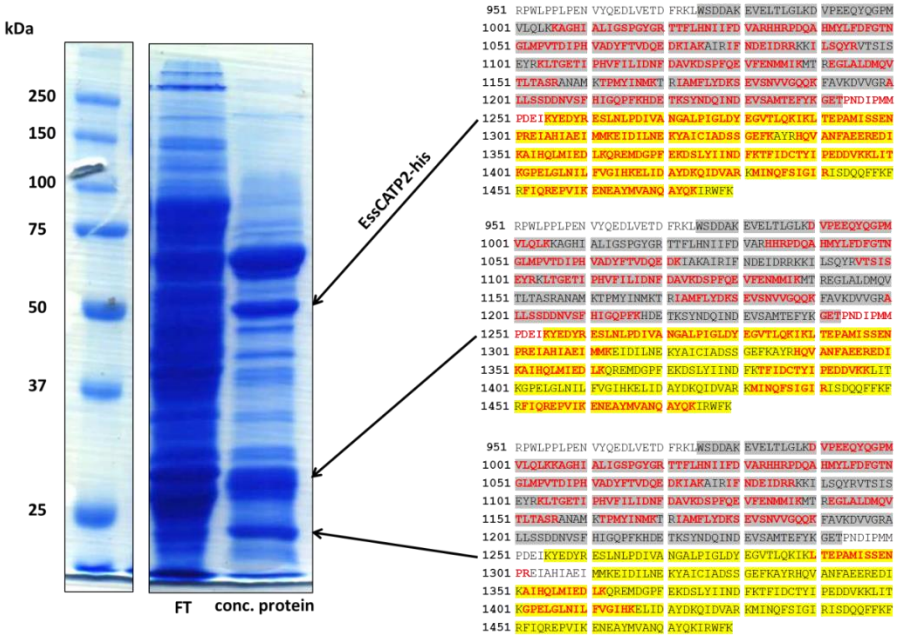

Figure 5.8: Purification of EsxA, EsxC, EsaE and EssCATP2. Proteins were purified using a His-Trap column. Following purification eluted fractions were pooled and concentrated using a vivaspin concentrator. Concentrated proteins and flow through (FT) were loaded onto an SDS gel containing 15 % acrylamide for EsxA and EsxC, 12 % acrylamide for EsaE and 10 % acrylamide for EssCATP$_2$. The left panel shows the peptide coverage for the indicated bands generated by mass spectrometry with matching peptides in bold red. For EssC$_{ATP2}$ the second and third ATPase domains are highlighted in grey and yellow, respectively.

To obtain cleaner protein, the His-Trap purified and concentrated sample of EssC$_{ATP2}$ was subsequently run over size exclusion chromatography in an attempt to remove unspecific bands. During this step it was possible to remove some of the contaminating *E. coli* proteins that migrate around 75 kDa although a small amount was still co-purified with EssC$_{ATP2}$ (Figure 5.9). Elution fractions B12 – C2 were subsequently pooled, concentrated and used for crosslinking experiments.

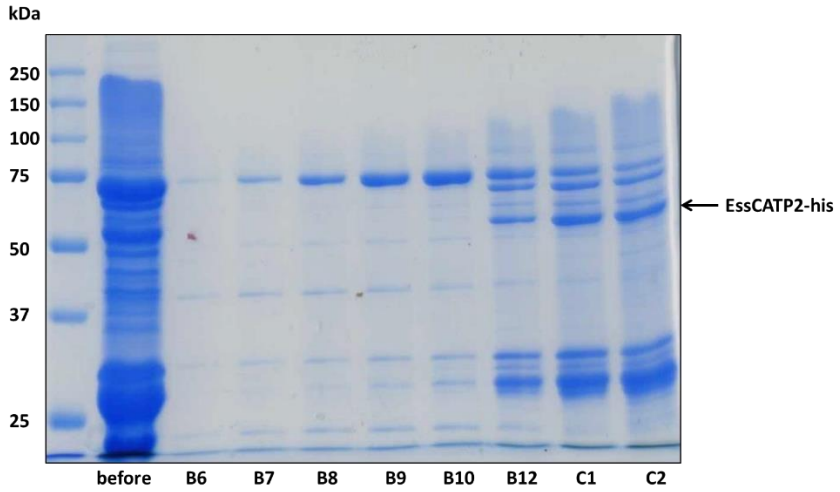

Figure 5.9: Size exclusion chromatography of $EssC_{ATP2}$. $EssC_{ATP2}$-containing fractions from three separate His-Trap purification experiments were pooled and concentrated to 500 µl before being loaded onto a Superdex 200 300/10 GL column. 10 µl was retained as the input sample ('before') and was loaded onto an SDS gel containing 10 % acrylamide together with 10 µl of each indicated elution fraction.

Before starting crosslinking analyses it was next confirmed that the His-tag was still present in each of the purified proteins. Western Blot analysis using an anti-His-tag antibody was in agreement with the SDS PAGE and mass spectrometry results, revealing the dimer and monomer bands for EsxA and EsxC (Figure 5.10 left panel). It could also be shown that the degradation product obtained following EsxC purification contained a His-tag since the signal for this smaller band is as strong as for the monomeric form of the protein. An additional faint band could also be detected for EsxC-His which was not seen in the coomassie-stained gel. Considering that the size of EsxC is ~17 kDa this band could correspond to a protein-trimer. The purification of His-tagged $EssC_{ATP2}$ and EsaE could also be verified with the His-tag antibody.

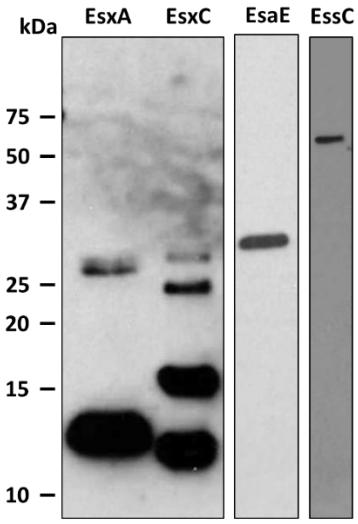

Figure 5.10: Immunological detection of the purified His-tagged proteins. Purified and concentrated protein were loaded onto an SDS gel containing 15 %, 12 % and 10 % acrylamide for the detection of EsxA and EsxC, EsaE and $EssC_{ATP2}$, respectively. Proteins were detected using a monoclonal anti His-Tag antibody (Abcam).

5.4.2 Probing interaction of EsaE with the last two ATPase domains of EssC

Since it is already known from PFA crosslinking analysis that EsaE interacts with EssC *in vivo* (Cao *et al.*, 2016) the first experiments aimed to test whether an interaction between purified EsaE and the last two ATPase domains of EssC could be detected after PFA treatment. Following crosslinking, samples were subsequently immunoblotted using anti-EssC and anti-His antibodies (Figure 5.11).

$EssC_{ATP2}$ could be detected in the treated and untreated samples when blotting against EssC, running at an approximate size of 50 kDa (Figure 5.11 A). Following PFA-treatment, higher molecular weight bands containing EssC could be detected in samples containing $EssC_{ATP2}$ alone. In total four different crosslinking products could be identified with the lowest one running just below the 100 kDa marker and the biggest product detectable well above 250 kDa. The same bands were detectable when $EssC_{ATP2}$ was crosslinked in the presence of EsaE, indicating that these bands probably represent different oligomerisation stages of EssC. Unfortunately no additional bands were detected when $EssC_{ATP2}$ was mixed with purified EsaE

which leads to the conclusion that these two proteins do not detectably interact in these experiments.

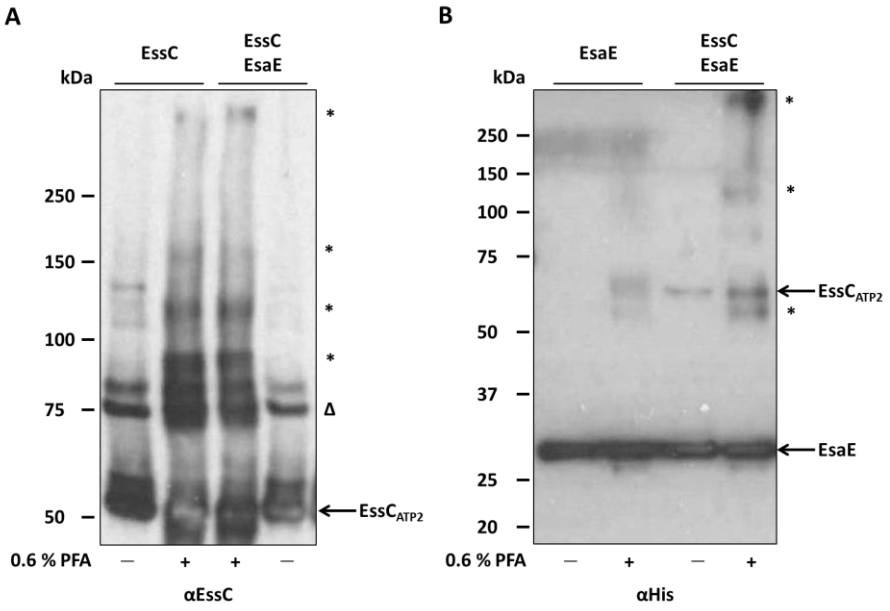

Figure 5.11: PFA crosslinking of EsaE with the last two ATPase domains of EssC. Purified EssC and EsaE were mixed in a 1:1 molar ratio of in the presence of 0.6 % PFA for 30 min after which the reaction was quenched with 100 mM Tris/HCl, pH 8.0. A 5 µl aliquot of sample was loaded on a bis-Tris gel containing 8 % acrylamide when blotting against EssC **(A)** and 10 % acrylamide when blotting against the His-tag **(B)**. Homomeric rrosslinking products are marked with an asterisk; nonspecific bands detected with the EssC antiserum are marked with an open triangle.

Since there is currently no antibody available against EsaE, detection of this protein was only possible by blotting against the His-tag. Unfortunately, as all of the proteins used in this study contain a His-tag it was difficult to unequivocally identify samples containing EsaE. However, monomeric EsaE could be recognized running just above 25 kDa in the treated and untreated samples (Figure 5.11 B). A higher molecular weight band, running between 50 and 75 kDa was detectable in the treated sample of EsaE alone which could be a possible multimer of this protein. Bands of a similar size were also detectable in the treated and untreated sample of EsaE when mixed with $EssC_{ATP2}$, and at least one of these should be the monomeric form of His-tagged $EssC_{ATP2}$. Two cross-reacting bands running between 100 and 150 kDa and well above the 250

kDa marker were also detectable when EsaE was incubated $EssC_{ATP2}$. These bands likely correspond to the oligomerisation of $EssC_{ATP2}$ observed in Figure 5.11 A. It is not possible to deduce whether this crosslink also contains EsaE.

5.4.3 Probing interaction of EsxC with EssC and EsaE

As already mentioned in the introduction Anderson *et al.* (2017) were able to co-purify EsxC together with EsaE and EssC. Given that EsaE also interacts with EsaD (Cao *et al.*, 2016) it is possible that EsaE is a chaperone for EssC1-secreted T7 substrate proteins. Initially, therefore, it was tested whether EsaE and EsxC interact under purified conditions following PFA treatment. Samples were crosslinked, followed by immunoblotting using anti-EsxC and anti-His antibodies (Figure 5.12).

When testing for EsxC the monomer as well as the degradation product can be detected in the treated and untreated samples for EsxC alone and when mixed with EsaE (Figure 5.12 A). Faint bands for the homo-dimer and homo-trimer of EsxC could also be detected in the untreated samples, which showed a stronger signal after incubation with the crosslinker. Two additional bands were detected in the treated sample of EsxC when mixed with EsaE running just below 25 and 37 kDa (Figure 5.12 A right panel). However, the same bands were detected when EsxC was treated alone and therefore probably represent homo-oligomeric states of EsxC.

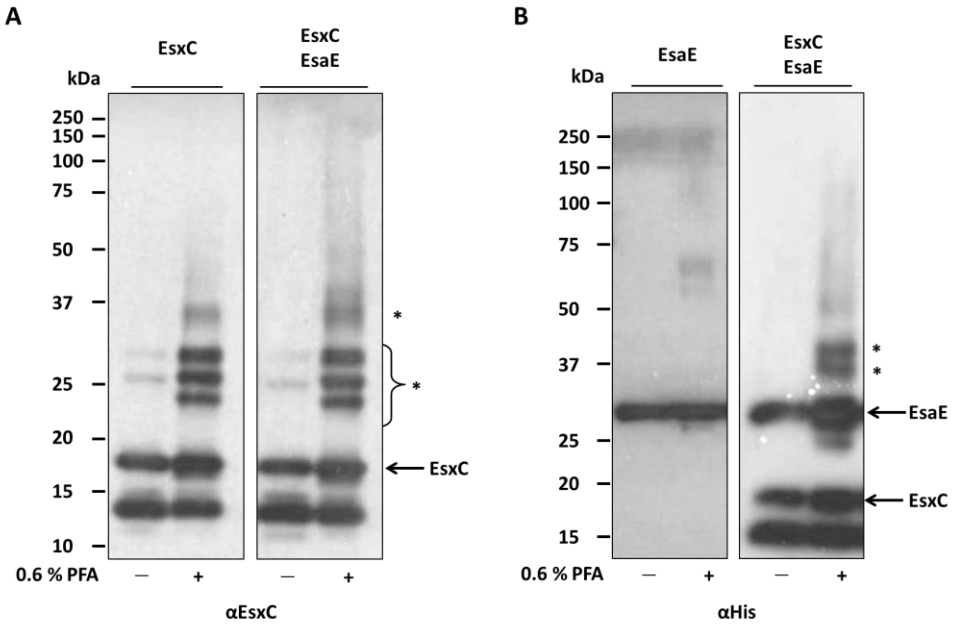

Figure 5.12: Probing interaction of EsxC with the chaperone EsaE. Purified EsaE and EsxC were mixed together in a molar ratio of 1:1 and incubated with a final concentration of 0.6 % PFA for 30 min after which the reaction was quenched with a final concentration of 100 mM Tris/HCl, pH 8.0. 5 µl of sample was loaded on a bis-Tris gel containing 13 % acrylamide when blotting against EsxC **(A)** and 10 % acrylamide when blotting against the His-tag **(B)**. Homomeric crosslinking products are marked with an asterisk.

Blotting against the His-tag showed the monomeric forms of EsaE (Figure 5.12 B) as well as the EsxC monomer and degradation product (Figure 5.12 B right panel). When incubated with the crosslinking reagent no additional bands could be detected when EsaE was treated alone. However, two higher molecular weight bands could be seen in the crosslinked sample when EsaE and EsxC were mixed in a molar ratio of 1:1. The lower of these two bands was migrating just below the 37 kDa marker, most likely corresponding to EsxC since the same band could be detected when blotting directly against the substrate (Figure 5.12 A+B). However, the second band, running just above the 37 kDa marker, could neither be detected in the treated sample of EsaE alone nor when EsxC was crosslinked in presence or absence of the chaperone.

Since no interaction of the substrate EsxC with the chaperone EsaE could be identified under purified conditions it was questioned whether EsxC might interact directly with domains of the membrane component, EssC. To test this hypothesis EsxC and $EssC_{ATP2}$ were mixed in a molar

ratio of 1:1 and treated with PFA as a crosslinker. Samples were subsequently immunoblotted using anti-EsxC and anti-EssC antibodies.

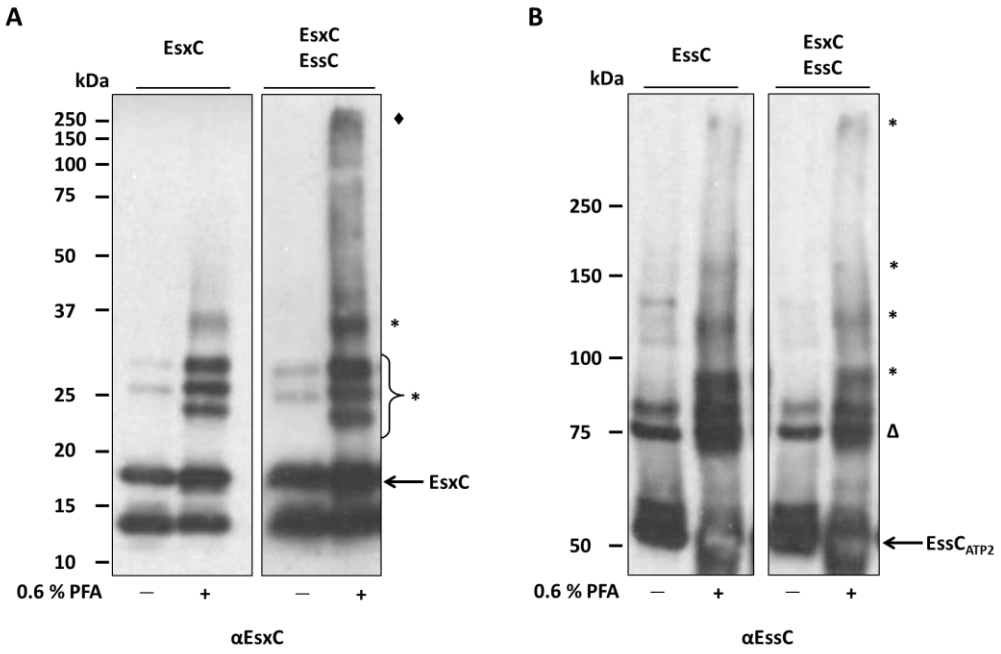

Figure 5.13: Probing interaction of EsxC with the C-terminal ATPase domains of EssC. Purified $EssC_{ATP2}$ and EsxC were mixed in a molar ratio of 1:1 and incubated with a final concentration of 0.6 % PFA for 30 min after which the reaction was quenched with a final concentration of 100 mM Tris/HCl, pH 8.0. 5 µl of sample was loaded on a bis-Tris gel containing 13 % acrylamide when blotting against EsxC **(A)** and 8 % acrylamide when blotting against EssC **(B)**. Homomeric crosslinking products are marked with an asterisk; Potential heteromeric crosslinking products are marked with a diamond; nonspecific bands detected with the EssC antiserum are marked with an open triangle.

In these experiments, a higher molecular weight band was detected in the treated sample of EsxC when incubated together with $EssC_{ATP2}$ running at 250 kDa. There is no band this size detectable when EsxC is treated alone and therefore it may correspond to an EssC-EsxC-hetero-multimer (Figure 5.13 A). However, when blotting against EssC there was no difference detectable between crosslinking the protein in presence or absence of the substrate EsxC and the same higher molecular weight bands were detectable in the treated samples of EssC alone or when incubated together with EsxC (Figure 5.13 B). It should be borne in mind, however, that EsxC is a small protein, and the level of resolution in the high molecular weight area of the gel is

poor, so a complex of hexameric EssC crosslinked to EsxC may not differ in migration to the EssC multimer alone. It is tentatively concluded that EsxC may directly interact with EssC.

As already discussed in Chapter 4, interaction of the membrane components of the T7SS may require binding of a substrate and energisation (for example by the pmf or ATP hydrolysis). Since no convincing interaction between purified EssC and EsaE could be observed, it may be that EsaE needs to interact with a client protein before binding to EssC. To investigate this further, purified $EssC_{ATP2}$ and EsaE were also mixed with EsxC in a molar ratio of 1:1:1 followed by immunological detection of EssC and EsxC using polyclonal antisera raised to the purified proteins, and by detection of all three proteins using an anti-His-tag antibody (Figure 5.14).

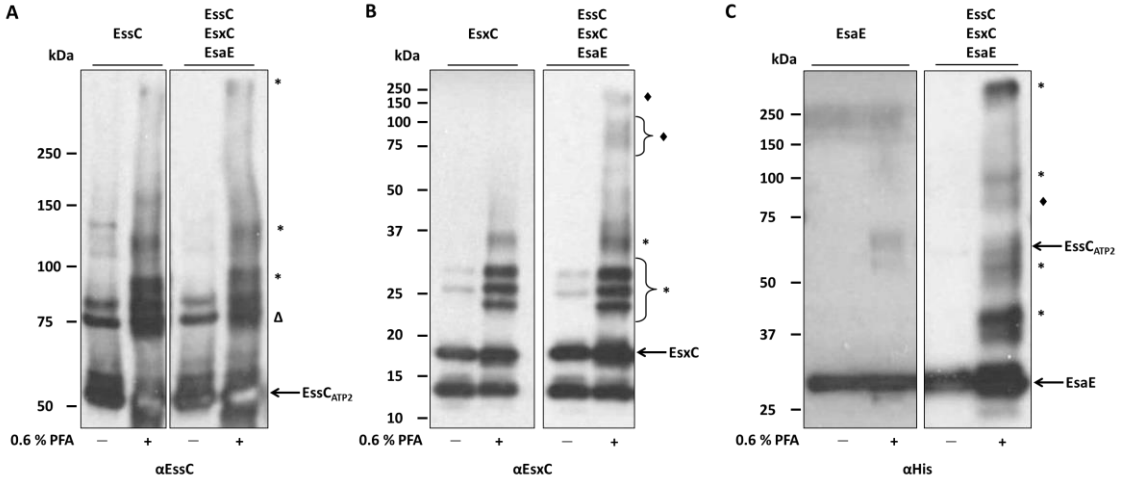

Figure 5.14: Immunological detection of EsxC following PFA crosslinking in the presence and absence of EssC and EsaE. Purified EsxC was mixed with either EsaE or EssC in a molar ratio of 1:1:1 and incubated with a final concentration of 0.6 % PFA for 30 min after which the reaction was quenched with a final concentration of 100 mM Tris/HCl, pH 8.0. 5 µl of sample were loaded on a bis-Tris gel containing 8 % acrylamide when blotting against EssC **(A)**, 13 % acrylamide when blotting against EsxC **(B)** and 10 % acrylamide when blotting against the His-tag **(C)**. Homomeric crosslinking products are marked with an asterisk; Potential heteromeric crosslinking products are marked with a diamond; nonspecific bands detected with the EssC antiserum are marked with an open triangle.

As it can be seen in Figure 5.14 A there is no change in the crosslinking pattern for $EssC_{ATP2}$ when the protein is crosslinked in the presence or absence of proteins EsaE and EsxC. When blotting

against the substrate EsxC, additional to the higher molecular weight bands already detected in the previous experiments a further crosslinking product could be identified migrating between 75 and 100 kDa (Figure 5.14 B right panel). According to the size and the fact that this band was not detected when the substrate was crosslinked with either $EssC_{ATP2}$ or EsaE alone it may be a hetero-multimeric state of all three proteins in a ratio of 1:1:1. Bands of similar size could also be detected when blotting against EssC and with the anti His-tag antiserum (Figure 5.14 C), supporting this idea.

5.4.4 Interaction of EsxA with the membrane component EssC

EsxA is a core component of the Ess machinery and was seen to be secreted by almost all *S. aureus* strains tested in this study, independent of the origin of EssC. These results suggested that EsxA may bind to a conserved region of the ATPase protein, either the first ATPase domain or the N-terminus, rather than to the last two ATPase domains of EssC. To test this, purified EsxA was incubated with $EssC_{ATP2}$ in the presence of PFA. The results are shown in Figure 5.15.

Incubation of EssC with PFA with or without EsxA gives an identical crosslinking pattern (Figure 5.15 A). When analysing EsxA, monomeric EsxA is detectable in the treated and untreated sample of EsxA alone running at a size of ~15 kDa (Figure 5.15 B). Five higher molecular weight bands are detectable in the treated sample, four with a size of ~20 to 50 kDa and one with a molecular weight of 250 kDa. These bands most likely represent oligomeric states of EsxA. Incubating EsxA and EssC resulted in an additional band detectable at the size of 75 kDa cross-reacting with the EsxA antiserum. However this band was also detected in the untreated sample and therefore represents some unspecific cross-reaction with the EsxA antibody rather than an interaction between EsxA and $EssC_{ATP2}$.

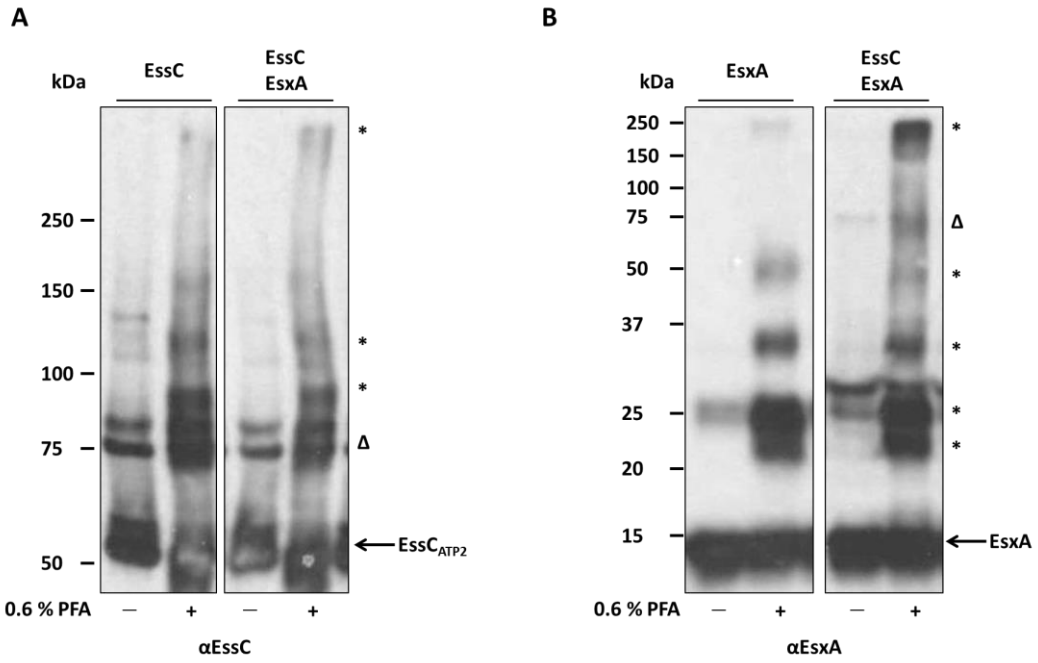

Figure 5.15: PFA crosslinking of EsxA in presence and absence of the membrane component EssC. Purified EssC and EsxA were mixed in a molar ratio of 1:1 and incubated with a final concentration of 0.6 % PFA for 30 min after which the reaction was quenched with a final concentration of 100 mM Tris/HCl, pH 8.0. 5 µl of sample was loaded on a bis-Tris gel containing 8 % acrylamide when blotting against EssC **(A)** and 13 % acrylamide when blotting against EsxA **(B)**. Homomeric crosslinking products are marked with an asterisk; nonspecific bands detected with the EssC and EsxA antiserum are marked with an open triangle.

5.5 Discussion

5.5.1 Genes immediately downstream of *essC* code for strain specific substrates

S. aureus strains can be grouped according to unique clusters of downstream genes associated with different variants of the gene coding for the ATPase protein EssC (Warne *et al.*, 2016). In this Chapter the hypothesis was tested whether the C-terminal variation in the different *S. aureus* EssC proteins can be linked to substrate specificity. It was shown that the four different EssC variants were stably produced in strain backgrounds of *S. aureus* representing the different groups described by Warne *et al.* (2016). Moreover, secretion of the core component EsxA could be confirmed for strains RN6390, EMRSA15 and ST398 after *essC* mutants of each strain were successfully complemented for EsxA secretion with plasmid-encoded EssC-variants of each group (Figure 5.6). This finding indicates that all four EssC variants must retain the ability to

interact with the other core components of the T7SS and strongly suggests that the C-terminal variable region of EssC is not involved in any of these core interactions.

Interestingly, of all of the plasmid-encoded EssC-variants only the cognate RN6390 EssC protein was able to support secretion of EsxC in the RN6390 strain background (Figure 5.7), and none of the other EssC proteins facilitated secretion of EsxC. These findings support the hypothesis that the C-terminal variable domain is a specificity determinant for T7 substrate secretion in *S. aureus.* It has been reported in the literature that the mycobacterial EsxB protein binds to a pocket located at the final ATPase domain of EccC and that this facilitates assembly of the EccC hexamer (Rosenberg *et al.*, 2015). It is interesting to note that within module 2, downstream of each *essC* variant, is a variant-specific gene coding for a protein of the WXG100 superfamily in group 1 represented by EsxB (Warne *et al.*, 2016). This raises the possibility that each of these specific WXG100 proteins may be involved in modulating assembly and/or activity of their cognate EssCs.

5.5.2 Interaction of EsxC with the membrane component EssC is not dependent on EsaE under purified conditions.

According to literature some of the strain specific substrates of the T7SS rely on the chaperones for their secretion (Cao *et al.*, 2016; Anderson *et al.*, 2017). Indeed, pulldown experiments revealed that EsxC was co-purified not only with EsaE but also with the membrane component EssC (Anderson *et al.*, 2017). Crosslinking experiments using purified proteins were undertaken to investigate the interaction of the secretion substrate EsxC, the chaperone EsaE, and the final two ATPase domains of the membrane component EssC. Although the work here was somewhat hampered by the lack of a specific anti-EsaE antibody it did not appear that there were any detectable interactions of EsaE with ATPase domains of EssC (Figure 5.11).

As already discussed in Chapter four it is known for the Twin arginine transport system that the membrane protein TatA only interacts with the TatBC complex upon binding of a substrate (Alcock *et al.*, 2013). It was therefore tested whether further addition of purified EsxC to the crosslinking mixture would result in crosslinks between EsaE and EssC. Surprisingly, under these conditions, an additional signal running just above the 37 kDa could be detected when blotting against the His-tag antibody which could not be confirmed when blotting against either EssC or EsxC (Figure 5.12). When testing interaction of EsxC separately with EsaE and EssC it was found that EsxC does not interact with the chaperone but directly with the membrane component EssC under purified conditions (Figure 5.13). These findings have some support from the mycobacterial T7SS, where EsxB was shown to directly interact with the membrane component EccC (Rosenberg *et al.*, 2015). It should also be noted that in the mycobacterial T7SS, large secreted substrates such as the PE/PPE proteins require the participation of EspG chaperones, whereas small substrates do not (Daleke *et al.*, 2012b). This is somewhat analogous to the situation in *S. aureus* as EsaD is much larger than EsxC and was shown to absolutely require EsaE for secretion whereas some EsxC could be secreted in the absence of EsaE (Cao *et al.*, 2016).

In these experiments, crosslinking between EsxA and the EssC ATPase domains was tested as a negative control since it was anticipated that this highly-conserved component should interact with a highly conserved region of EssC, either the first ATPase domain or the N-terminal domain, both of which were missing from the purified protein. No crosslinks were detected between the two purified proteins, as expected, although there could be other explanations for a negative result. Intriguingly, however, it was noted that homomeric crosslinks for EsxA could be detected, including at least one of very high molecular weight. This raises the possibility that EsxA could potentially exist in a higher order oligomer. There is no published evidence to support the suggestion that EsxA forms a polymer, but unpublished results from the Palmer and Hunter groups have shown that EsxA from *Geobacillus thermodentrificans* crystallises as an octamer

(Ng, Zoltner, Palmer and Hunter, unpublished). Whether multimeric forms of EsxA are essential for T7 secretion might be an interesting avenue for future study.

6
Conclusions and future prospects

6.1 Homo-oligomeric complexes of Ess membrane components

The main objective of this project was to probe the organisation of the *S. aureus* Ess machinery by examining complexes of the Ess membrane-bound proteins using crosslinking and BN PAGE analysis. One of the key findings from this study is that EsaA, EssB and EssC proteins were shown to form homomeric complexes, but under the conditions tested there was no evidence that these components interact with one another.

For extraction of the proteins from *S. aureus* membranes, six different detergents were tested. Contrary to previous findings where DDM was successfully used to isolate a complex of the distantly related ESX-5 secretion system of *M. marinum* (Houben *et al.*, 2012) only the zwitterionic detergent Fos-Choline-12 was able to extract reasonable quantities of all three of the EsaA, EssB and EssC membrane proteins. The subsequent use of this detergent might be a potential reason why interaction between the different membrane components could not be observed in BN PAGE analyses since zwitterionic detergents are known to have a more deactivating effect than the non-ionic detergent DDM. Subsequent analysis of the detergent-extracted material by BN PAGE revealed self-interaction of EsaA and EssB. These findings are supported by other literature reports where the dimerization of the *B. subtilis* homologue of EsaA, YueB (São-José *et al.*, 2006) and EssB (Zoltner *et al.*, 2013a; Zoltner *et al.*, 2013b;) were described. As a future prospective it would be interesting to further investigate the role of the detergent on the complex formation of the membrane component. With 2 % the final concentration of detergent used in this study is high above the critical micelle concentration of each detergent used which could have an effect on the interaction of the membrane proteins. Testing lower detergent concentrations might be gentler, ensuring the solubilisation of the proteins without breaking possible complex formations.

Complex formation between the Ess membrane components was further addressed in the native membrane environment, both *in vitro* and *in vivo*, using chemical crosslinking reagents. Results obtained from experiments using isolated membranes under *in vitro* conditions revealed

multimeric complex formation for EssC. Since the same pattern of multimerisation was seen in the absence of the other Ess membrane proteins, it most likely represents an EssC homo-multimer. This is in accordance with the literature where hexamerisation of the ATPase protein EssC as well as its mycobacterial homologue EccC could be shown (Rosenberg *et al.*, 2015; Zoltner *et al.*, 2016). Structural and functional analysis of EccC has shown that stable multimerisation occurs upon interaction with the EsxB substrate protein (Rosenberg *et al.*, 2015). However, the same multimeric crosslinking pattern for EssC was observed in a strain background where *esxB* and all known substrate protein-encoding genes were deleted indicating that the multimerisation of EssC may be independent of substrate binding.

In this study, no evidence was obtained for heteromeric complex formation between any of the Ess membrane components, even in whole cells where T7 substrates, ATP and the protonmotive force should all be present. The reason for this is not clear, but it should be noted that the *S. aureus* strain RN6390 used in this study has low T7 secretion activity under laboratory conditions. As a future prospective it would be interesting to repeat these experiments in a more actively secreting *S. aureus* strain. It is not clear how T7 secretion activity is regulated. Study of other bacterial secretion systems has shown that they are often regulated at a post-translational level. For example the Type III secretion system of *Shigella* interacts with bile salts to drive formation of an active tip complex, and secretion by the *Yersinia* T3SS is activated by low calcium ion concentration (which mimics the eukaryotic cytosol) (Torruellas *et al.*, 2005; Olive *et al.*, 2007). The T6SS is also controlled at a posttranslational level by protein phosphorylation. A threonine kinase, PpkA, phosphorylates the FHA component of the T6SS and/or TssL component, regulating activity of the baseplate complex (Mougous *et al.*, 2007; Lin *et al.*, 2014).

It is possible that a posttranslational modification of one of the T7SS components, for example EssC, controls secretion activity and complex formation at least in *S. aureus*. Intriguingly, *S. aureus* and *M. tuberculosis* are known to harbour a membrane bound proline-directed serine/threonine kinase, PknB, with which the N-terminal domain of EssB shares structural

homology (Young *et al.*, 2003; Zoltner *et al.*, 2013a). Analysis of firmicute EssC sequences reveals a conserved sequence where a serine (or threonine in *B. subtilis* EssC) directly precedes a proline residue (Figure 6.1).

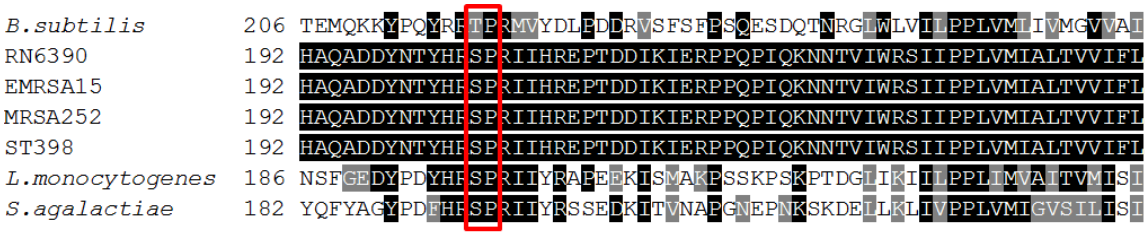

Figure 6.1: Sequence alignment of EssC sequences encoded by RN6390, MRSA252, EMRSA15, ST398, *B. subtilis, L. monocytogenes* and *S. agalactiae.* Only the sequence covering the conserved candidate phosphorylation motif is shown. The alignment was generated with Clustal Omega and shaded with Boxshade.

The serine is located at position 204 of the *S. aureus* EssC proteins, in a potential hinge region between the second FHA domain and the first transmembrane helix. A potential hypothesis is that PknB phosphorylates this position of EssC altering its conformation and modulating interaction with EssB and subsequently the formation of an active membrane complex. As part of the work in this thesis, attempts were made to test this hypothesis through the use of Phosphate Affinity SDS PAGE using an acrylamide-pendant Phos-tag, as well as through mass spec analysis of trypsin-treated samples enriched for EssC. Unfortunately the results obtained were inconclusive, and therefore further work will be required to determine whether and how T7 secretion activity is regulated in *S. aureus*.

6.2 *S. aureus* shows substrate specificity among different strains

Bioinformatic analyses identified a unique set of genes located immediately downstream of *essC* among different *S. aureus* strains. This variation was linked with sequence diversity of the C-

terminal domain of EssC (Warne *et al.*, 2016). A further aim of this thesis was to identify a link between this diversity and the unique set of genes encoded downstream of the ATPase protein. It could be shown that plasmid-encoded EssC variants of different *S. aureus* strains were cross-functional and that all four variants could support secretion of the core component EsxA, which is highly conserved across all strains. However, secretion of EsxC, a substrate specific for *S. aureus* RN6390, was only supported by its cognate EssC variant. These findings strongly suggest that strain-specific substrates are only recognised by their cognate T7SSs, and more precisely by the C-terminal domain of EssC.

Further crosslinking experiments using purified proteins revealed that EsxC directly interacts with the ATPase domain of EssC and does not require a chaperone, in contrast to findings for the much larger substrate protein EsaD, that is probably targeted for secretion by EsaE (Cao *et al.*, 2016). These findings have some support from the mycobacterial T7SS where large secreted substrates such as PE/PPE proteins need the participation of EspG chaperones to be secreted whereas small substrates do not (Daleke *et al.*, 2012b). Interestingly, previous work has shown that secretion of EsxC is abolished in an *esaE* background and it has been suggested that EsaE acts as an assembly platform for T7 substrates in EssC1 strain variants (Cao *et al.*, 2016; Anderson *et al.*, 2017). However it should be noted that the total cellular level of EsxC was greatly decreased in the *esaE* mutant background and that overproduction of EsxC in this strain resulted in secretion (Cao *et al.*, 2016). Further work will be required to determine whether EsaE is a chaperone specific for the EsaD substrate or for all substrates in EssC1 strains.

Crosslinking between purified EsxA and the last two ATPase domains of EssC was also tested as a negative control since it was thought that EsxA interacts elsewhere on the ATPase protein at the much more highly conserved N-terminus or the first ATPase domain. As expected the results showed no interaction of the secreted core component with this region of EssC, but did reveal oligomerisation of EsxA. These findings are in conformity with *in vivo* crosslinking experiments in this thesis where oligomerisation could be observed for YFP-tagged EsxA (see chapter 4).

Moreover, it was previously seen that EsxA crystallises as an octamer (Ng, Zoltner, Palmer and Hunter, unpublished) and is significantly overexpressed compared to other *ess* genes (Cao and Palmer, unpublished). An interesting future prospective could therefore be the investigation whether multimeric forms of EsxA are essential for T7 secretion.

On a final note the bioinformatic analysis undertaken by Warne *et al.* (2016) suggested that although there was variability in the genes downstream of *essC*, each variant encoded a protein of the WXG100 family, EsxB in RN6390. An interesting path for future studies could lie in investigating whether these proteins are involved in modulating activity of their cognate EssCs.

References

Abdallah, A.M., Gey van Pittius, N.C., DiGiuseppe Champion, P.A., Cox, J., Luirink, J., Vandenbroucke-Grauls, C.M.J.E., *et al.* (2007) Type VII secretion — mycobacteria show the way. *Nat Rev Microbiol* **5**: 883–891.

Abdallah, A.M., Verboom, T., Hannes, F., Safi, M., Strong, M., Eisenberg, D., *et al.* (2006) A specific secretion system mediates PPE41 transport in pathogenic mycobacteria. *Mol Microbiol* **62**: 667–679.

Abdallah, A.M., Verboom, T., Weerdenburg, E.M., Gey van Pittius, N.C., Mahasha, P.W., Jiménez, C., *et al.* (2009) PPE and PE_PGRS proteins of Mycobacterium marinum are transported via the type VII secretion system ESX-5. *Mol Microbiol* **73**: 329–340.

Abrusci, P., McDowell, M.A., Lea, S.M., and Johnson, S. (2014) Building a secreting nanomachine: A structural overview of the T3SS. *Curr Opin Struct Biol* **25**: 111–117.

Aguilo, J.I., Alonso, H., Uranga, S., Marinova, D., Arbués, A., Martino, A. de, *et al.* (2013) ESX-1-induced apoptosis is involved in cell-to-cell spread of Mycobacterium tuberculosis. *Cell Microbiol* **15**: 1994–2005.

Aguiló, N., Marinova, D., Martín, C., and Pardo, J. (2013) ESX-1-induced apoptosis during mycobacterial infection: to be or not to be, that is the question. *Front Cell Infect Microbiol* **3**: 88.

Alami, M., Lüke, I., Deitermann, S., Eisner, G., Koch, H.G., Brunner, J., and Müller, M. (2003) Differential interactions between a twin-arginine signal peptide and its translocase in Escherichia coli. *Mol Cell* **12**: 937–946.

Alami, M., Trescher, D., Wu, L.-F., and Muller, M. (2002) Separate Analysis of Twin-arginine Translocation (Tat)-specific Membrane Binding and Translocation in Escherichia coli. *J Biol Chem* **277**: 20499–20503.

Alcock, F., Baker, M.A.B., Greene, N.P., Palmer, T., Wallace, M.I., and Berks, B.C. (2013) Live cell imaging shows reversible assembly of the TatA component of the twin-arginine protein transport system. *Proc Natl Acad Sci U S A* **110**: E3650-9.

Anderson, M., Aly, K. a, Chen, Y.-H., and Missiakas, D. (2013) Secretion of atypical protein substrates by the ESAT-6 Secretion System of S taphylococcus aureus. *Mol Microbiol* **90**: 734–743.

Anderson, M., Chen, Y.-H., Butler, E.K., and Missiakas, D.M. (2011) EsaD, a Secretion Factor for the Ess Pathway in Staphylococcus aureus. *J Bacteriol* **193**: 1583–1589.

Anderson, M., Ohr, R.J., Aly, K.A., Nocadello, S., Kim, H.K., Schneewind, C.E., *et al.* (2017) EssE Promotes Staphylococcus aureus ESS-Dependent Protein Secretion To Modify Host Immune Responses during Infection. *J Bacteriol* **199**: 1–15.

Ates, L.S., Houben, E.N.G., and Bitter, W. (2016) Type VII Secretion: A Highly Versatile Secretion System. *Microbiol Spectr* **4**: 1–21.

Ates, L.S., Ummels, R., Commandeur, S., Weerd, R. van der, Sparrius, M., Weerdenburg, E., *et al.* (2015) Essential Role of the ESX-5 Secretion System in Outer Membrane Permeability of Pathogenic Mycobacteria. *PLoS Genet* **11**: 1–30.

Ates, L.S., Woude, A.D. van der, Bestebroer, J., Stempvoort, G. van, Musters, R.J.P., Garcia-Vallejo, J.J., *et al.* (2016) The ESX-5 System of Pathogenic Mycobacteria Is Involved In Capsule Integrity and Virulence through Its Substrate PPE10. *PLoS Pathog* **12**: e1005696.

Back, J.W., Jong, L. De, Muijsers, A.O., and Koster, C.G. De (2003) Chemical cross-linking and mass spectrometry for protein structural modeling. *J Mol Biol* **331**: 303–313.

Backert, S., and Meyer, T.F. (2006) Type IV secretion systems and their effectors in bacterial pathogenesis. *Curr Opin Microbiol* **9**: 207–217.

Baptista, C., Barreto, H.C., and São-José, C. (2013) High Levels of DegU-P Activate an Esat-6-Like Secretion System in Bacillus subtilis. *PLoS One* **8**.

Barber, M. (1961) Methicillin-resistant staphylococci. *J Clin Pathol* **14**: 385 LP-393.

Bartlett, A.H., Foster, T.J., Hayashida, A., and Park, P.W. (2008) α-Toxin Facilitates the Generation of CXC Chemokine Gradients and Stimulates Neutrophil Homing in Staphylococcus aureus Pneumonia. *J Infect Dis* **198**: 1529–1535.

Basu, S., Pathak, S.K., Banerjee, A., Pathak, S., Bhattacharyya, A., Yang, Z., *et al.* (2007) Execution of macrophage apoptosis by PE_PGRS33 of Mycobacterium tuberculosis is mediated by toll-like receptor 2-dependent release of tumor necrosis factor-α. *J Biol Chem* **282**: 1039–1050.

Beckham, K.S.H., Ciccarelli, L., Bunduc, C.M., Mertens, H.D.T., Ummels, R., Lugmayr, W., *et al.* (2017) Structure of the mycobacterial ESX-5 type VII secretion system membrane complex by single-particle analysis. *Nat Microbiol* **2**: 17047.

Bensing, B.A., and Sullam, P.M. (2002) An accessory sec locus of Streptococcus gordonii is required for export of the surface protein GspB and for normal levels of binding to human platelets. *Mol Microbiol* **44**: 1081–1094.

Bernstein, H.D. (2015) Looks can be deceiving: Recent insights into the mechanism of protein secretion by the autotransporter pathway. *Mol Microbiol* **97**: 205–215.

Bitter, W., Houben, E.N.G., Bottai, D., Brodin, P., Brown, E.J., Cox, J.S., *et al.* (2009) Systematic genetic nomenclature for type VII secretion systems. *PLoS Pathog* **5**: e1000507.

Bogsch, E.G., Sargent, F., Stanley, N.R., Berks, B.C., Robinson, C., and Palmer, T. (1998) An Essential Component of a System with Homologues in Plastids and Mitochondria. *J Biol Chem* **273**: 18003–18006.

Bottai, D., Luca, M. di, Majlessi, L., Frigui, W., Simeone, R., Sayes, F., *et al.* (2012) Disruption of the ESX-5 system of Mycobacterium tuberculosis causes loss of PPE protein secretion, reduction of cell wall integrity and strong attenuation. *Mol Microbiol* **83**: 1195–1209.

Bradshaw, W.J., Davies, A.H., Chambers, C.J., Roberts, A.K., Shone, C.C., and Acharya, K.R. (2015) Molecular features of the sortase enzyme family. *FEBS J* **282**: 2097–2114.

Braunstein, M., Espinosa, B.J., Chan, J., Belisle, J.T., and Jacobs, W.R. (2003) SecA2 functions in the secretion of superoxide dismutase A and in the virulence of Mycobacterium tuberculosis. *Mol Microbiol* **48**: 453–464.

Brodin, P., Eiglmeier, K., Marmiesse, M., Billault, A., Garnier, T., Niemann, S., *et al.* (2002) Bacterial Artificial Chromosome-Based Comparative Genomic Analysis Identifies Mycobacterium microti as a Natural ESAT-6 Deletion Mutant. *Infect Immun* **70**: 5568–5578.

Brodin, P., Majlessi, L., Marsollier, L., Jonge, M.I. de, Bottai, D., Demangel, C., *et al.* (2006) Dissection of ESAT-6 system 1 of Mycobacterium tuberculosis and impact on immunogenicity and virulence. *Infect Immun* **74**: 88–98.

Brown, G.D., Dave, J.A., Gey van Pittius, N.C., Stevens, L., Ehlers, M.R., and Beyers, A.D. (2000) The mycosins of Mycobacterium tuberculosis H37Rv: a family of subtilisin-like serine proteases. *Gene* **254**: 147–55.

Burts, M.L., DeDent, A.C., and Missiakas, D.M. (2008) EsaC substrate for the ESAT-6 secretion pathway and its role in persistent infections of Staphylococcus aureus. *Mol Microbiol* **69**: 736–46.

Burts, M.L., Williams, W.A., DeBord, K., and Missiakas, D.M. (2005) EsxA and EsxB are secreted by an ESAT-6-like system that is required for the pathogenesis of Staphylococcus aureus infections. *Proc Natl Acad Sci U S A* **102**: 1169–74.

Büttner, D. (2012) Protein export according to schedule: architecture, assembly, and regulation of type III secretion systems from plant- and animal-pathogenic bacteria. *Microbiol Mol Biol Rev* **76**: 262–310.

Cao, Z., Casabona, M.G., Kneuper, H., Chalmers, J.D., and Palmer, T. (2016) The type VII secretion system of Staphylococcus aureus secretes a nuclease toxin that targets competitor bacteria. *Nat Microbiol* **2**: 16183.

Casabona, M.G., Buchanan, G., Zoltner, M., Harkins, C.P., Holden, T.G., Palmer, T., and Andrews, S. (2017) EsaB is a core component of the Staphylococcus aureus Type VII secretion system. *BioRxiv* .

Casabona, M.G., Kneuper, H., Alferes de Lima, D., Harkins, C.P., Zoltner, M., Hjerde, E., *et al.* (2017) Heme-Iron Plays A Key Role In The Regulation Of The Ess/Type VII Secretion System Of Staphylococcus aureus RN6390. *bioRxiv* .

Cascales, E., and Christie, P.J. (2003) The versatile bacterial type IV secretion systems. *Nat Rev Microbiol* **1**: 137–49.

Champion, P.A.D., Stanley, S.A., Champion, M.M., Brown, E.J., and Cox, J.S. (2006) C-terminal signal sequence promotes virulence factor secretion in Mycobacterium tuberculosis. *Science* **313**: 1632–6.

Champion, P. a D., Champion, M.M., Manzanillo, P., and Cox, J.S. (2009) ESX-1 secreted virulence factors are recognized by multiple cytosolic AAA ATPases in pathogenic mycobacteria. *Mol Microbiol* **73**: 950–62.

Chen, Y.-H., Anderson, M., Hendrickx, A.P. a, and Missiakas, D. (2012) Characterization of EssB, a protein required for secretion of ESAT-6 like proteins in Staphylococcus aureus. *BMC Microbiol* **12**: 219.

Chen, Y.Y., Peng, B., Yang, Q., Glew, M.D., Veith, P.D., Cross, K.J., *et al.* (2011) The outer membrane protein LptO is essential for the O-deacylation of LPS and the co-ordinated secretion and attachment of A-LPS and CTD proteins in Porphyromonas gingivalis. *Mol Microbiol* **79**: 1380–1401.

Cianfanelli, F.R., Monlezun, L., and Coulthurst, S.J. (2016) Aim, Load, Fire: The Type VI Secretion System, a Bacterial Nanoweapon. *Trends Microbiol* **24**: 51–62.

Cléon, F., Habersetzer, J., Alcock, F., Kneuper, H., Stansfeld, P.J., Basit, H., *et al.* (2015) The TatC component of the twin-arginine protein translocase functions as an obligate oligomer. *Mol Microbiol* **98**: 111–129.

Cole, S.T., Brosch, R., Parkhill, J., Garnier, T., Churcher, C., Harris, D., *et al.* (1998) Deciphering the biology of Mycobacterium tuberculosis from the complete genome sequence. *Nature* **393**: 537–544.

Cole, S.T., Brosch, R., Parkhill, J., Garnier, T., Churcher, C., Harris, D., *et al.* (1998) Deciphering the biology of Mycobacterium tuberculosis from the complete genome sequence. *Nature* **393**: 537–544.

Coros, A., Callahan, B., Battaglioli, E., and Derbyshire, K.M. (2008) The specialized secretory apparatus ESX-1 is essential for DNA transfer in Mycobacterium smegmatis. *Mol Microbiol* **69**: 794–808.

Corrigan, R.M., and Foster, T.J. (2009) An improved tetracycline-inducible expression vector for Staphylococcus aureus. *Plasmid* **61**: 126–9.

Costa, T.R.D., Felisberto-Rodrigues, C., Meir, A., Prevost, M.S., Redzej, A., Trokter, M., and Waksman, G. (2015) Secretion systems in Gram-negative bacteria: structural and mechanistic insights. *Nat Rev Microbiol* **13**: 343–359.

Dabney-Smith, C., and Cline, K. (2009) Clustering of C-Terminal Stromal Domains of Tha4 Homo-oligomers during Translocation by the Tat Protein Transport System. *Mol Biol Cell* **20**: 2060–2069.

Daleke, M.H., Cascioferro, A., Punder, K. de, Ummels, R., Abdallah, A.M., Wel, N. van der, *et al.* (2011) Conserved Pro-Glu (PE) and Pro-Pro-Glu (PPE) protein domains target LipY lipases of pathogenic mycobacteria to the cell surface via the ESX-5 pathway. *J Biol Chem* **286**: 19024–34.

Daleke, M.H., Ummels, R., Bawono, P., Heringa, J., Vandenbroucke-Grauls, C.M.J.E., Luirink, J., and Bitter, W. (2012) General secretion signal for the mycobacterial type VII secretion pathway. *Proc Natl Acad Sci U S A* **109**: 11342–7.

Daleke, M.H., Woude, A.D. Van Der, Parret, A.H.A., Ummels, R., Groot, A.M. De, Watson, D., *et al.* (2012) Specific chaperones for the type VII protein secretion pathway. *J Biol Chem* **287**: 31939–31947.

Dave, J.A., Gey van Pittius, N.C., Beyers, A.D., Ehlers, M.R.W., and Brown, G.D. (2002) Mycosin-1, a subtilisin-like serine protease of Mycobacterium tuberculosis, is cell wall-associated and expressed during infection of macrophages. *BMC Microbiol* **2**: 30.

Delepelaire, P. (2004) Type I secretion in gram-negative bacteria. *Biochim Biophys Acta - Mol Cell Res* **1694**: 149–161.

Dinges, M.M., Orwin, P.M., Schlievert, P.M., Dinges, M.M., and Orwin, P.M. (2000) Exotoxins of Staphylococcus aureus Exotoxins of Staphylococcus aureus. **13**: 16–34.

Dreisbach, A., Hempel, K., Buist, G., Hecker, M., Becher, D., and Dijl, J.M. van (2010) Profiling the surfacome of Staphylococcus aureus. *Proteomics* **10**: 3082–96.

Ekiert, D.C., and Cox, J.S. (2014) Structure of a PE-PPE-EspG complex from Mycobacterium tuberculosis reveals molecular specificity of ESX protein secretion. *Proc Natl Acad Sci* **111**: 14758–14763.

Elliott, S.R., and Tischler, A.D. (2016) Phosphate starvation: A novel signal that triggers ESX-5 secretion in Mycobacterium tuberculosis. *Mol Microbiol* **100**: 510–526.

Ent, F. Van Den, and Löwe, J. (2005) Crystal structure of the ubiquitin-like protein YukD from Bacillus subtilis. *FEBS Lett* **579**: 3837–3841.

Fagan, R.P., and Fairweather, N.F. (2011) Clostridium difficile has two parallel and essential sec secretion systems. *J Biol Chem* **286**: 27483–27493.

Foster, T.J. (2005) Immune evasion by staphylococci. *Nat Rev Microbiol* **3**: 948–958.

Foster, T.J., Geoghegan, J. a, Ganesh, V.K., and Höök, M. (2014) Adhesion, invasion and evasion: the many functions of the surface proteins of Staphylococcus aureus. *Nat Rev Microbiol* **12**: 49–62.

Gey van Pittius, N.C., Sampson, S.L., Lee, H., Kim, Y., Helden, P.D. van, and Warren, R.M. (2006) *Evolution and expansion of the Mycobacterium tuberculosis PE and PPE multigene families and their association with the duplication of the ESAT-6 (esx) gene cluster regions.* .

Gohlke, U., Pullan, L., McDevitt, C.A., Porcelli, I., Leeuw, E. de, Palmer, T., *et al.* (2005) The TatA component of the twin-arginine protein transport system forms channel complexes of variable diameter. *Proc Natl Acad Sci U S A* **102**: 10482–6.

Gomez, M.I., Lee, A., Reddy, B., Muir, A., Soong, G., Pitt, A., *et al.* (2004) Staphylococcus aureus protein A induces airway epithelial inflammatory responses by activating TNFR1. *Nat Med* **10**: 842–848.

Gould, R.M., and Lennarz, W.J. (1967) Biosynthesis of aminoacyl derivatives of phosphatidylglycerol. *Biochem Biophys Res Commun* **26**: 510–515.

Gröschel, M.I., Sayes, F., Simeone, R., Majlessi, L., and Brosch, R. (2016) ESX secretion systems: mycobacterial evolution to counter host immunity. *Nat Publ Gr* **14**: 677–691.

Grundmann, H., Tami, A., Hori, S., Halwani, M., and Slack, R. (2002) Nottingham Staphylococcus aureus population study: prevalence of MRSA among elderly people in the community. *BMJ* **324**: 1365–6.

Harbarth, S., François, P., Shrenzel, J., Fankhauser-Rodriguez, C., Hugonnet, S., Koessler, T., *et al.* (2005) Community-associated methicillin-resistant Staphylococcus aureus, Switzerland. *Emerg Infect Dis* **11**: 962–5.

Harkins, C.P., Pichon, B., Doumith, M., Parkhill, J., Westh, H., Tomasz, A., *et al.* (2017) Methicillin-resistant Staphylococcus aureus emerged long before the introduction of methicillin into clinical practice. *Genome Biol* **18**: 130.

Hayami, M., Okabe, A., Kariyama, R., Abe, M., and Kanemasa, Y. (1979) Lipid Composition of Staphylococcus aureus and Its Derived L-forms. *Microbiol Immunol* **23**: 435–442.

Hayashida, A., Bartlett, A.H., Foster, T.J., and Park, P.W. (2009) Staphylococcus aureus Beta-Toxin Induces Lung Injury through Syndecan-1. *Am J Pathol* **174**: 509–518.

Heath, J.E., Seers, C.A., Veith, P.D., Butler, C.A., Nor Muhammad, N.A., Chen, Y.Y., *et al.* (2016) PG1058 is a novel multidomain protein component of the bacterial type IX secretion system. *PLoS One* **11**: 1–29.

Henderson, I.R., Navarro-Garcia, F., Desvaux, M., Fernandez, R.C., and Ala'Aldeen, D. (2004) Type V Protein Secretion Pathway : the Autotransporter Story Type V Protein Secretion Pathway : the Autotransporter Story. *Microbiol Mol Biol Rev* **68**: 692–744.

Hiramatsu, K., Hanaki, H., Ino, T., Yabuta, K., Oguri, T., and Tenover, F.C. (1997) Methicillin-resistant Staphylococcus aureus clinical strain with reduced vancomycin susceptibility. *J Antimicrob Chemother* **40**: 135–6.

Hiraoka, S., Matsuzaki, H., and Shibuya, I. (1993) Active increase in cardiolipin synthesis in the stationary growth phase and its physiological significance in Escherichia coli. *FEBS Lett* **336**: 221–224.

Hoffman, E.A., Frey, B.L., Smith, L.M., and Auble, D.T. (2015) Formaldehyde crosslinking: A tool for the study of chromatin complexes. *J Biol Chem* **290**: 26404–26411.

Houben, E.N.G., Bestebroer, J., Ummels, R., Wilson, L., Piersma, S.R., Jiménez, C.R., *et al.* (2012) Composition of the type VII secretion system membrane complex. *Mol Microbiol* **86**: 472–84.

Hsu, T., Hingley-Wilson, S.M., Chen, B., Chen, M., Dai, A.Z., Morin, P.M., *et al.* (2003) The primary mechanism of attenuation of bacillus Calmette-Guerin is a loss of secreted lytic function required for invasion of lung interstitial tissue. *Proc Natl Acad Sci U S A* **100**: 12420–12425.

Huang, Q., Alcock, F., Kneuper, H., Deme, J.C., Rollauer, S.E., Lea, S.M., *et al.* (2017) A signal sequence suppressor mutant that stabilizes an assembled state of the twin arginine translocase. *Proc Natl Acad Sci* 201615056.

Huppert, L. a, Ramsdell, T.L., Chase, M.R., Sarracino, D. a, Fortune, S.M., and Burton, B.M. (2014) The ESX system in Bacillus subtilis mediates protein secretion. *PLoS One* **9**: e96267.

Jäger, F., Zoltner, M., Kneuper, H., Hunter, W.N., and Palmer, T. (2016) Membrane interactions and self-association of components of the Ess/Type VII secretion system of Staphylococcus aureus. *FEBS Lett* **590**: 349–357.

Jankute, M., Cox, J.A.G., Harrison, J., and Besra, G.S. (2015) Assembly of the Mycobacterial Cell Wall. *Annu Rev Microbiol* **69**: 405–23.

Jevons, M.P.; R.G.N. and K.R. (1961) "Celbenin"-resistant staphylococci. *BMJ* **1**: 124–26.

Kirby, W.M.M. (1944) Extraction of a highly potent Penicillin inactivator from Penicillin resistant Staphylococci. *Science (80-)* **99**: 452–453.

Kline, K.A., Kau, A.L., Chen, S.L., Lim, A., Pinkner, J.S., Rosch, J., *et al.* (2009) Mechanism for sortase localization and the role of sortase localization in efficient pilus assembly in Enterococcus faecalis. *J Bacteriol* **191**: 3237–3247.

Kluytmans, J., Belkum, A. van, and Verbrugh, H. (1997) Nasal carriage of Staphylococcus aureus: epidemiology, underlying mechanisms, and associated risks. *Clin Microbiol Rev* **10**: 505–20.

Kneuper, H., Cao, Z.P., Twomey, K.B., Zoltner, M., Jäger, F., Cargill, J.S., *et al.* (2014) Heterogeneity in ess transcriptional organization and variable contribution of the Ess/Type VII protein secretion system to virulence across closely related Staphylocccus aureus strains. *Mol Microbiol* **93**: 928–43.

Kneuper, H., Maldonado, B., Jäger, F., Krehenbrink, M., Buchanan, G., Keller, R., *et al.* (2012) Molecular dissection of TatC defines critical regions essential for protein transport and a TatB-TatC contact site. *Mol Microbiol* **85**: 945–61.

Kong, C., Neoh, H.M., and Nathan, S. (2016) Targeting Staphylococcus aureus toxins: A potential form of anti-virulence therapy. *Toxins (Basel)* **8**: 1–21.

Korea, C.G., Balsamo, G., Pezzicoli, A., Merakou, C., Tavarini, S., Bagnoli, F., *et al.* (2014) Staphylococcal Esx proteins modulate apoptosis and release of intracellular Staphylococcus aureus during infection in epithelial cells. *Infect Immun* **82**: 4144–53.

Korotkov, K. V., Sandkvist, M., and Hol, W.G.J. (2012) The type II secretion system: biogenesis, molecular architecture and mechanism. *Nat Rev Microbiol* **10**: 336–351.

Korotkov, K. V, Gonen, T., and Hol, W.G.J. (2011) Secretins: dynamic channels for protein transport across membranes. *Trends Biochem Sci* **36**: 433–43.

Korotkova, N., Freire, D., Phan, T.H., Ummels, R., Creekmore, C.C., Evans, T.J., *et al.* (2014) Structure of the Mycobacterium tuberculosis type VII secretion system chaperone EspG5 in complex with PE25-PPE41 dimer. *Mol Microbiol* **94**: 367–382.

Kubori, T., Matsushima, Y., Nakamura, D., Uralil, J., Lara-Tejero, M., Sukhan, a, *et al.* (1998) Supramolecular structure of the Salmonella typhimurium type III protein secretion system. *Science* **280**: 602–605.

Leake, M.C., Greene, N.P., Godun, R.M., Granjon, T., Buchanan, G., Chen, S., *et al.* (2008) Variable stoichiometry of the TatA component of the twin-arginine protein transport system observed by in vivo single-molecule imaging. *Proc Natl Acad Sci U S A* **105**: 15376–81.

Leavell, M.D., Novak, P., Behrens, C.R., Schoeniger, J.S., and Kruppa, G.H. (2004) Strategy for selective chemical cross-linking of tyrosine and lysine residues. *J Am Soc Mass Spectrom* **15**: 1604–1611.

Lee, P.A., Tullman-Ercek, D., and Georgiou, G. (2006) The bacterial twin-arginine translocation pathway. *Annu Rev Microbiol* **60**: 373–95.

Leeuw, E. De, Porcelli, I., Sargent, F., Palmer, T., and Berks, B.C. (2001) Membrane interactions and self-association of the TatA and TatB components of the twin-arginine translocation pathway. *FEBS Lett* **506**: 143–148.

Leitner, A., Walzthoeni, T., Kahraman, A., Herzog, F., Rinner, O., Beck, M., and Aebersold, R. (2010) Probing Native Protein Structures by Chemical Cross-linking, Mass Spectrometry, and Bioinformatics. *Mol Cell Proteomics* **9**: 1634–1649.

Lenz, L.L., Mohammadi, S., Geissler, A., and Portnoy, D.A. (2003) SecA2-dependent secretion of autolytic enzymes promotes Listeria monocytogenes pathogenesis. *Proc Natl Acad Sci U S A* **100**: 12432–12437.

Leo, J.C., Grin, I., and Linke, D. (2012) Type V secretion: mechanism(s) of autotransport through the bacterial outer membrane. *Philos Trans R Soc Lond B Biol Sci* **367**: 1088–101.

Li, M., Lu, L.Y., Yang, C.Y., Wang, S., and Yu, X. (2013) The FHA and BRCT domains recognize ADP-ribosylation during DNA damage response. *Genes Dev* **27**: 1752–1768.

Liang, J., Suhandynata, R.T., and Zhou, H. (2015) Phosphorylation of Sae2 mediates Forkhead-associated (FHA) domain-specific interaction and regulates its DNA repair function. *J Biol Chem* **290**: 10751–10763.

Lin, J.S., Wu, H.H., Hsu, P.H., Ma, L.S., Pang, Y.Y., Tsai, M.D., and Lai, E.M. (2014) Fha Interaction with Phosphothreonine of TssL Activates Type VI Secretion in Agrobacterium tumefaciens. *PLoS Pathog* **10**.

Lou, Y., Rybniker, J., Sala, C., and Cole, S.T. (2017) EspC forms a filamentous structure in the cell envelope of Mycobacterium tuberculosis and impacts ESX-1 secretion. *Mol Microbiol* **103**: 26–38.

Lowy, F.D. (1998) Staphylococcus aureus Infections. *N Engl J Med* **339**: 520–532.

Luca, M. Di, Bottai, D., Batoni, G., Orgeur, M., Aulicino, A., Counoupas, C., *et al.* (2012) The ESX-5 Associated eccB5-eccC5 Locus Is Essential for Mycobacterium tuberculosis Viability. *PLoS One* **7**.

Maciag, A., Dainese, E., Rodriguez, G.M., Milano, A., Provvedi, R., Pasca, M.R., *et al.* (2007) Global analysis of the Mycobacterium tuberculosis Zur (FurB) regulon. *J Bacteriol* **189**: 730–40.

Mahairas, G.G., Sabo, P.J., Hickey, M.J., Singh, D.C., and Stover, C.K. (1996) Molecular analysis of genetic differences between Mycobacterium bovis BCG and virulent M . bovis . Molecular Analysis of Genetic Differences between Mycobacterium bovis BCG and Virulent M . bovis. *J Bacteriol* **178**: 1274–1282.

Målen, H., Berven, F.S., Fladmark, K.E., and Wiker, H.G. (2007) Comprehensive analysis of exported proteins from Mycobacterium tuberculosis H37Rv. *Proteomics* **7**: 1702–1718.

Massey, T.H., Mercogliano, C.P., Yates, J., Sherratt, D.J., and Löwe, J. (2006) Double-stranded DNA translocation: structure and mechanism of hexameric FtsK. *Mol Cell* **23**: 457–69.

Miller, M., Donat, S., Rakette, S., Stehle, T., Kouwen, T.R.H.M., Diks, S.H., *et al.* (2010) Staphylococcal PknB as the first prokaryotic representative of the proline-directed kinases. *PLoS One* **5**: e9057.

Monk, I.R., Shah, I.M., Xu, M., Tan, M.-W., and Foster, T.J. (2012) Transforming the untransformable: application of direct transformation to manipulate genetically Staphylococcus aureus and Staphylococcus epidermidis. *MBio* **3**.

Mori, H., and Cline, K. (2002) A twin arginine signal peptide and the pH gradient trigger reversible assembly of the thylakoid ΔpH/Tat translocase. *J Cell Biol* **157**: 205–210.

Mougous, J.D., Gifford, C.A., Ramsdell, T.L., and Mekalanos, J.J. (2007) Threonine phosphorylation post-translationally regulates protein secretion in Pseudomonas aeruginosa. *Nat Cell Biol* **9**: 797–803.

Natale, P., Brüser, T., and Driessen, A.J.M. (2008) Sec- and Tat-mediated protein secretion across the bacterial cytoplasmic membrane-Distinct translocases and mechanisms. *Biochim Biophys Acta - Biomembr* **1778**: 1735–1756.

Navarre, W.W., and Schneewind, O. (1999) Surface proteins of gram-positive bacteria and mechanisms of their targeting to the cell wall envelope. *Microbiol Mol Biol Rev* **63**: 174–229.

Novick, R.P., Ross, H.F., Projan, S.J., Kornblum, J., Kreiswirth, B., and Moghazeh, S. (1993) Synthesis of staphylococcal virulence factors is controlled by a regulatory RNA molecule. *EMBO J* **12**: 3967–75.

Ochsner, U.A., Snyder, A., Vasil, A.I., and Vasil, M.L. (2002) Effects of the twin-arginine translocase on secretion of virulence factors, stress response, and pathogenesis. *Proc Natl Acad Sci* **99**: 8312–8317.

Ohol, Y.M., Goetz, D.H., Chan, K., Shiloh, M.U., Craik, C.S., and Cox, J.S. (2010) Mycobacterium tuberculosis MycP1 Protease Plays a Dual Role in Regulation of ESX-1 Secretion and Virulence. *Cell Host Microbe* **7**: 210–220.

Ohr, R.J., Anderson, M., Shi, M., Schneewind, O., and Missiakas, D. (2017) EssD, a nuclease effector of the Staphylococcus aureus ESS pathway. *J Bacteriol* **199**.

Olive, A.J., Kenjale, R., Espina, M., Moore, D.S., Picking, W.L., and Picking, W.D. (2007) Bile salts stimulate recruitment of IpaB to the Shigella flexneri surface, where it colocalizes with IpaD at the tip of the type III secretion needle. *Infect Immun* **75**: 2626–2629.

Pallen, M.J. (2002) The ESAT-6/WXG100 superfamily -- and a new Gram-positive secretion system? *Trends Microbiol* **10**: 209–12.

Palmer, T. (2017) Structural biology: Mycobacterial ESX secrets revealed. *Nat Microbiol* **2**: 17074.

Palmer, T., and Berks, B.C. (2012) The twin-arginine translocation (Tat) protein export pathway. *Nat Rev Microbiol* **10**: 483–496.

Palmer, T., Sargent, F., and Berks, B.C. (2010) The Tat Protein Export Pathway. *EcoSal Plus* **4**: 260–274.

Papanikou, E., Karamanou, S., and Economou, A. (2007) Bacterial protein secretion through the translocase nanomachine. *Nat Rev Microbiol* **5**: 839–851.

Peschel, A., Jack, R.W., Otto, M., Collins, L.V., Staubitz, P., Nicholson, G., *et al.* (2001) Staphylococcus aureus Resistance to Human Defensins and Evasion of Neutrophil Killing via the Novel Virulence Factor Mprf Is Based on Modification of Membrane Lipids with l-Lysine. *J Exp Med* **193**: 1067–1076.

Phan, T.H., Ummels, R., Bitter, W., and Houben, E.N.G. (2017) Identification of a substrate domain that determines system specificity in mycobacterial type VII secretion systems. *Sci Rep* **7**: 42704.

Portal-Celhay, C., Tufariello, J.M., Srivastava, S., Zahra, A., Klevorn, T., Grace, P.S., *et al.* (2016) Mycobacterium tuberculosis EsxH inhibits ESCRT-dependent CD4(+) T-cell activation. *Nat Microbiol* **2**: 16232.

Pugsley, A.P. (1993) The complete general secretory pathway in gram-negative bacteria. *Microbiol Rev* **57**: 50–108.

Pym, A.S., Brodin, P., Brosch, R., Huerre, M., and Cole, S.T. (2002) Loss of RD1 contributed to the attenuation of the live tuberculosis vaccines Mycobacterium bovis BCG and Mycobacterium microti. *Mol Microbiol* **46**: 709–717.

Pym, A.S., Brodin, P., Majlessi, L., Brosch, R., Demangel, C., Williams, A., *et al.* (2003) Recombinant BCG exporting ESAT-6 confers enhanced protection against tuberculosis. *Nat Med* **9**: 533–9.

Ramakrishnan, L. (2000) Granuloma-Specific Expression of Mycobacterium Virulence Proteins from the Glycine-Rich PE-PGRS Family. *Science (80-)* **288**: 1436–1439.

Ramsdell, T.L., Huppert, L.A., Sysoeva, T.A., Fortune, S.M., and Burton, B.M. (2015) Linked domain architectures allow for specialization of function in the FtsK/SpoIIIE ATPases of ESX secretion systems. *J Mol Biol* **427**: 1119–1132.

Renshaw, P.S., Lightbody, K.L., Veverka, V., Muskett, F.W., Kelly, G., Frenkiel, T. a, *et al.* (2005) Structure and function of the complex formed by the tuberculosis virulence factors CFP-10 and ESAT-6. *EMBO J* **24**: 2491–8.

Rigel, N.W., Gibbons, H.S., McCann, J.R., McDonough, J.A., Kurtz, S., and Braunstein, M. (2009) The accessory SecA2 system of Mycobacteria requires ATP binding and the canonical SecA1. *J Biol Chem* **284**: 9927–9936.

Robinson, C., and Bolhuis, A. (2004) Tat-dependent protein targeting in prokaryotes and chloroplasts. *Biochim Biophys Acta - Mol Cell Res* **1694**: 135–147.

Rodriguez, G.M., Voskuil, M.I., Gold, B., Schoolnik, G.K., and Smith, I. (2002) ideR , an Essential Gene in Mycobacterium tuberculosis : Role of IdeR in Iron-Dependent Gene Expression , Iron Metabolism , and Oxidative Stress Response. *Infect Immun* **70**: 3371–3381.

Rollauer, S.E., Tarry, M.J., Graham, J.E., Jääskeläinen, M., Jäger, F., Johnson, S., *et al.* (2012) Structure of the TatC core of the twin-arginine protein transport system. *Nature* **492**: 210–4.

Rösch, T.C., Golman, W., Hucklesby, L., Gonzalez-Pastor, J.E., and Graumann, P.L. (2014) The presence of conjugative plasmid pLS20 affects global transcription of its Bacillus subtilis host and confers beneficial stress resistance to cells. *Appl Environ Microbiol* **80**: 1349–1358.

Rosenberg, O.S., Dovala, D., Li, X., Connolly, L., Bendebury, A., Finer-Moore, J., *et al.* (2015) Substrates Control Multimerization and Activation of the Multi-Domain ATPase Motor of Type VII Secretion. *Cell* 1–12.

Russell, A.B., Peterson, S.B., and Mougous, J.D. (2014) Type VI secretion system effectors: poisons with a purpose. *Nat Rev Microbiol* **12**: 137–48.

Sandkvist, M. (2001) Type II secretion and pathogenesis. *Infect Immun* **69**: 3523–35.

Sandkvist, M., Michel, L.O., Hough, L.P., Morales, V.M., Bagdasarian, M., Koomey, M., *et al.* (1997) General secretion pathway (eps) genes required for toxin secretion and outer membrane biogenesis in Vibrio cholerae. *J Bacteriol* **179**: 6994–7003.

Sani, M., Houben, E.N.G., Geurtsen, J., Pierson, J., Punder, K. De, Zon, M. Van, *et al.* (2010) Direct visualization by Cryo-EM of the mycobacterial capsular layer: A labile structure containing ESX-1-secreted proteins. *PLoS Pathog* **6**.

São-José, C., Baptista, C., and Santos, M.A. (2004) Bacillus subtilis operon encoding a membrane receptor for bacteriophage SPP1. *J Bacteriol* **186**: 8337–46.

São-José, C., Lhuillier, S., Lurz, R., Melki, R., Lepault, J., Santos, M.A., and Tavares, P. (2006) The ectodomain of the viral receptor YueB forms a fiber that triggers ejection of bacteriophage SPP1 DNA. *J Biol Chem* **281**: 11464–70.

Sardis, M.F., and Economou, A. (2010) SecA: A tale of two protomers: MicroReview. *Mol Microbiol* **76**: 1070–1081.

Sargent, F., Bogsch, E.G., Stanley, N.R., Wexler, M., Robinson, C., Berks, B.C., and Palmer, T. (1998) Overlapping functions of components of a bacterial Sec-independent protein export pathway. *EMBO J* **17**: 3640–3650.

Sargent, F., Stanley, N.R., Berks, B.C., and Palmer, T. (1999) Sec-independent Protein Translocation in Escherichia coli. *J Biol Chem* **274**: 36073–36082.

Sassetti, C.M., Boyd, D.H., and Rubin, E.J. (2003) Genes required for mycobacterial growth defined by high density mutagenesis. *Mol Microbiol* **48**: 77—84.

Sassetti, C.M., and Rubin, E.J. (2003) Genetic requirements for mycobacterial survival during infection. *Proc Natl Acad Sci U S A* **100**: 12989–94.

Sato, K., Naito, M., Yukitake, H., Hirakawa, H., Shoji, M., McBride, M.J., *et al.* (2010) A protein secretion system linked to bacteroidete gliding motility and pathogenesis. *Proc Natl Acad Sci U S A* **107**: 276–281.

Schneewind, O., and Missiakas, D.M. (2012) Protein secretion and surface display in Gram-positive bacteria. *Philos Trans R Soc Lond B Biol Sci* **367**: 1123–39.

Seddon, A.M., Curnow, P., and Booth, P.J. (2004) Membrane proteins, lipids and detergents: Not just a soap opera. *Biochim Biophys Acta - Biomembr* **1666**: 105–117.

Seers, C.A., Slakeski, N., Veith, P.D., Nikolof, T., Chen, Y.Y., Dashper, S.G., and Reynolds, E.C. (2006) The RgpB C-terminal domain has a role in attachment of RgpB to the outer membrane and belongs to a novel C-terminal-domain family found in Porphyromonas gingivalis. *J Bacteriol* **188**: 6376–6386.

Serafini, A., Boldrin, F., Palù, G., and Manganelli, R. (2009) Characterization of a Mycobacterium tuberculosis ESX-3 conditional mutant: Essentiality and rescue by iron and zinc. *J Bacteriol* **191**: 6340–6344.

Sharma, V., Arockiasamy, A., Ronning, D.R., Savva, C.G., Holzenburg, A., Braunstein, M., *et al.* (2003) Crystal structure of Mycobacterium tuberculosis SecA, a preprotein translocating ATPase. *Proc Natl Acad Sci U S A* **100**: 2243–8.

Short, S.A., and White, D.C. (1971) Metabolism of phosphatidylglycerol, lysylphosphatidylglycerol, and cardiolipin of Staphylococcus aureus. *J Bacteriol* **108**: 219–226.

Shrivastava, A., Johnston, J.J., Baaren, J.M. Van, and McBride, M.J. (2013) Flavobacterium johnsoniae GldK, GldL, GldM, and SprA are required for secretion of the cell surface gliding motility adhesins sprb and remA. *J Bacteriol* **195**: 3201–3212.

Sibbald, M.J.J.B., Ziebandt, a K., Engelmann, S., Hecker, M., Jong, a de, Harmsen, H.J.M., *et al.* (2006) Mapping the pathways to staphylococcal pathogenesis by comparative secretomics. *Microbiol Mol Biol Rev* **70**: 755–788.

Siegrist, M.S., Unnikrishnan, M., McConnell, M.J., Borowsky, M., Cheng, T., Siddiqi, N., *et al.* (2009) Mycobacterial Esx-3 is required for mycobactin-mediated iron acquisition. *Proc Natl Acad Sci U S A* **106**: 18792–7.

Sievers, S., Ernst, C.M., Geiger, T., Hecker, M., Wolz, C., Becher, D., and Peschel, A. (2010) Changing the phospholipid composition of Staphylococcus aureus causes distinct changes in membrane proteome and membrane-sensory regulators. *Proteomics* **10**: 1685–1693.

Singh, P., Benjak, A., Schuenemann, V.J., Herbig, A., Avanzi, C., Busso, P., *et al.* (2015) Insight into the evolution and origin of leprosy bacilli from the genome sequence of Mycobacterium lepromatosis. *Proc Natl Acad Sci* **112**: 4459–4464.

Smith, J., Manoranjan, J., Pan, M., Bohsali, A., Xu, J., Liu, J., *et al.* (2008) Evidence for pore formation in host cell membranes by ESX-1-secreted ESAT-6 and its role in Mycobacterium marinum escape from the vacuole. *Infect Immun* **76**: 5478–5487.

Solomonson, M., Setiaputra, D., Makepeace, K.A.T., Lameignere, E., Petrotchenko, E. V., Conrady, D.G., *et al.* (2015) Structure of EspB from the ESX-1 type VII secretion system and insights into its export mechanism. *Structure* **23**: 571–583.

Sørensen, A.L., Nagai, S., Houen, G., Andersen, P., Andersen, A.B., Sørensen, A.L., *et al.* (1995) Purification and characterization of a low-molecular-mass T-cell antigen secreted by Mycobacterium tuberculosis . Purification and Characterization of a Low-Molecular-Mass T-Cell Antigen Secreted by Mycobacterium tuberculosis. *Infect Immun* **63**: 1710–1717.

Spirig, T., Weiner, E.M., and Clubb, R.T. (2011) Sortase enzymes in Gram-positive bacteria. *Mol Microbiol* **82**: 1044–1059.

Stanley, S.A., Raghavan, S., Hwang, W.W., and Cox, J.S. (2003) Acute infection and macrophage subversion by Mycobacterium tuberculosis require a specialized secretion system. *Proc Natl Acad Sci U S A* **100**: 13001–6.

Staubitz, P., Neumann, H., Schneider, T., Wiedemann, I., and Peschel, A. (2004) MprF-mediated biosynthesis of lysylphosphatidylglycerol, an important determinant in staphylococcal defensin resistance. *FEMS Microbiol Lett* **231**: 67–71.

Stoop, E.J.M., Bitter, W., and Sar, A.M. van der (2012) Tubercle bacilli rely on a type VII army for pathogenicity. *Trends Microbiol* **20**: 477–84.

Strong, M., Sawaya, M.R., Wang, S., Phillips, M., Cascio, D., and Eisenberg, D. (2006) Toward the structural genomics of complexes: crystal structure of a PE/PPE protein complex from Mycobacterium tuberculosis. *Proc Natl Acad Sci U S A* **103**: 8060–8065.

Sundaramoorthy, R., Fyfe, P.K., and Hunter, W.N. (2008) Structure of Staphylococcus aureus EsxA suggests a contribution to virulence by action as a transport chaperone and/or adaptor protein. *J Mol Biol* **383**: 603–14.

Sutherland, B.W., Toews, J., and Kast, J. (2008) Utility of formaldehyde cross-linking and mass spectrometry in the study of protein-protein interactions. *J Mass Spectrom* **43**: 699–715.

Sysoeva, T.A., Zepeda-Rivera, M.A., Huppert, L.A., and Burton, B.M. (2014) Dimer recognition and secretion by the ESX secretion system in Bacillus subtilis. *Proc Natl Acad Sci* **111**: 7653–7658.

Tanaka, Y., Kuroda, M., Yasutake, Y., Yao, M., Tsumoto, K., Watanabe, N., *et al.* (2007) Crystal structure analysis reveals a novel forkhead-associated domain of ESAT-6 secretion system C protein in Staphylococcus aureus. *Proteins Struct Funct Bioinforma* **69**: 659–664.

Thomas, S., Holland, I.B., and Schmitt, L. (2014) The Type 1 secretion pathway - The hemolysin system and beyond. *Biochim Biophys Acta - Mol Cell Res* **1843**: 1629–1641.

Tinaztepe, E., Wei, J.R., Raynowska, J., Portal-Celhay, C., Thompson, V., and Philipsa, J.A. (2016) Role of metal-dependent regulation of ESX-3 secretion in intracellular survival of Mycobacterium tuberculosis. *Infect Immun* **84**: 2255–2263.

Torruellas, J., Jackson, M.W., Pennock, J.W., and Plano, G. V. (2005) The Yersinia pestis type III secretion needle plays a role in the regulation of Yop secretion. *Mol Microbiol* **57**: 1719–1733.

Tsai, M., Ohniwa, R.L., Kato, Y., Takeshita, S.L., Ohta, T., Saito, S., *et al.* (2011) Staphylococcus aureus requires cardiolipin for survival under conditions of high salinity. *BMC Microbiol* **11**: 13.

Tseng, T.-T., Tyler, B.M., and Setubal, J.C. (2009) Protein secretion systems in bacterial-host associations, and their description in the Gene Ontology. *BMC Microbiol* **9 Suppl 1**: S2.

Tufariello, J.M., Chapman, J.R., Kerantzas, C.A., Wong, K.-W., Vilchèze, C., Jones, C.M., *et al.* (2016) Separable roles for Mycobacterium tuberculosis ESX-3 effectors in iron acquisition and virulence. *Proc Natl Acad Sci* **113**: E348-357.

Ulsen, P. Van, Rahman, S. ur, Jong, W.S.P., Daleke-Schermerhorn, M.H., and Luirink, J. (2014) Type V secretion: From biogenesis to biotechnology. *Biochim Biophys Acta - Mol Cell Res* **1843**: 1592–1611.

Vandenesch, F., Naimi, T., Enright, M.C., Lina, G., Nimmo, G.R., Heffernan, H., *et al.* (2003) Community-acquired methicillin-resistant Staphylococcus aureus carrying Panton-Valentine leukocidin genes: worldwide emergence. *Emerg Infect Dis* **9**: 978–84.

Vasilescu, J., Guo, X., and Kast, J. (2004) Identification of protein-protein interactions using in vivo cross-linking and mass spectrometry. *Proteomics* **4**: 3845–3854.

Veith, P.D., Glew, M.D., Gorasia, D.G., and Reynolds, E.C. (2017) Type IX secretion: the generation of bacterial cell surface coatings involved in virulence, gliding motility and the degradation of complex biopolymers. *Mol Microbiol* **106**: 35–53.

Wagner, J.M., Chan, S., Evans, T.J., Kahng, S., Kim, J., Arbing, M.A., *et al.* (2016) Structures of EccB1 and EccD1 from the core complex of the mycobacterial ESX-1 type VII secretion system. *BMC Struct Biol* **16**: 5.

Wang, Y., Hu, M., Liu, Q., Qin, J., Dai, Y., He, L., *et al.* (2016) Role of the ESAT-6 secretion system in virulence of the emerging community-associated Staphylococcus aureus lineage ST398. *Sci Rep* **6**: 25163.

Warne, B., Harkins, C.P., Harris, S.R., Vatsiou, A., Stanley-Wall, N., Parkhill, J., *et al.* (2016) The Ess/Type VII secretion system of Staphylococcus aureus shows unexpected genetic diversity. *BMC Genomics* **17**: 222.

Way, S.S., and Wilson, C.B. (2005) The Mycobacterium tuberculosis ESAT-6 homologue in Listeria monocytogenes is dispensable for growth in vitro and in vivo. *Infect Immun* **73**: 6151–6153.

Weigel, L.M., Clewell, D.B., Gill, S.R., Clark, N.C., McDougal, L.K., Flannagan, S.E., *et al.* (2003) Genetic analysis of a high-level vancomycin-resistant isolate of Staphylococcus aureus. *Science* **302**: 1569–71.

Weiner, J.H., Bilous, P.T., Shaw, G.M., Lubitz, S.P., Frost, L., Thomas, G.H., *et al.* (1998) A novel and ubiquitous system for membrane targeting and secretion of cofactor-containing proteins. *Cell* **93**: 93–101.

Whitney, J.C., Peterson, S.B., Kim, J., Pazos, M., Verster, A.J., Radey, M.C., *et al.* (2017) *A broadly distributed toxin family mediates contact-dependent antagonism between gram-positive bacteria*. .

Winden, V.J.C. Van, Ummels, R., Piersma, S.R., Jiménez, C.R., Korotkov, K. V., Bitter, W., and Houben, E.N.G. (2016) Mycosins are required for the stabilization of the ESX-1 and ESX-5 type VII secretion membrane complexes. *MBio* **7**: 1–11.

Wittig, I., Braun, H.-P., and Schägger, H. (2006) Blue native PAGE. *Nat Protoc* **1**: 418–28.

Worrall, L.J., Hong, C., Vuckovic, M., Deng, W., Bergeron, J.R.C., Majewski, D.D., *et al.* (2016) Near-atomic-resolution cryo-EM analysis of the Salmonella T3S injectisome basal body. *Nature* **540**: 597–601.

Xu, Q., Deller, M.C., Nielsen, T.K., Grant, J.C., Lesley, S.A., Elsliger, M.A., *et al.* (2014) Structural insights into the recognition of phosphopeptide by the FHA domain of Kanadaptin. *PLoS One* **9**.

Young, T. a, Delagoutte, B., Endrizzi, J. a, Falick, A.M., and Alber, T. (2003) Structure of Mycobacterium tuberculosis PknB supports a universal activation mechanism for Ser/Thr protein kinases. *Nat Struct Biol* **10**: 168–174.

Zhang, Y.-M., and Rock, C.O. (2008) Membrane lipid homeostasis in bacteria. *Nat Rev Micro* **6**: 222–233.

Zoltner, M., Fyfe, P.K., Palmer, T., and Hunter, W.N. (2013) Characterization of Staphylococcus aureus EssB, an integral membrane component of the Type VII secretion system: atomic resolution crystal structure of the cytoplasmic segment. *Biochem J* **449**: 469–77.

Zoltner, M., Ng, W.M.A. V, Money, J.J., Fyfe, P.K., Kneuper, H., Palmer, T., and Hunter, W.N. (2016) EssC: domain structures inform on the elusive translocation channel in the Type VII secretion system. *Biochem J* **0**: BCJ20160257.

Zoltner, M., Norman, D.G., Fyfe, P.K., Mkami, H. El, Palmer, T., and Hunter, W.N. (2013) The architecture of EssB, an integral membrane component of the type VII secretion system. *Structure* **21**: 595–603.

Appendix

FEBS Letters

FEBS PRESS science publishing by scientists

Membrane interactions and self-association of components of the Ess/Type VII secretion system of *Staphylococcus aureus*

Franziska Jäger[1], Martin Zoltner[2], Holger Kneuper[1], William N. Hunter[2] and Tracy Palmer[1]

1 Divisions of Molecular Microbiology, School of Life Sciences, University of Dundee, Dundee, UK
2 Biological Chemistry and Drug Discovery, School of Life Sciences, University of Dundee, Dundee,, UK

Correspondence
T. Palmer, Divisions of Molecular Microbiology, School of Life Sciences, University of Dundee, Dow Street, Dundee DD1 5EH, UK
Fax: +44 (0)1382 388216
Tel: +44 (0)1382 386464
E-mail: tracy.palmer@dundee.ac.uk

(Received 3 December 2015, revised 8 January 2016, accepted 12 January 2016)

doi:10.1002/1873-3468.12065

Edited by Renee Tsolis

The Ess/Type VII protein secretion system, essential for virulence of pathogenic *Staphylococcus aureus*, is dependent upon the four core membrane proteins EssA, EssB, EssC and EsaA. Here, we use crosslinking and blue native PAGE analysis to show that the EssB, EssC and EsaA proteins individually form homomeric complexes. Surprisingly, these components appear unable to interact with each other, or with the EssA protein. We further show that two high molecular weight multimers of EssC detected in whole cells are not dependent upon the presence of EsxA, EsxB or any other Ess component for their assembly.

Keywords: membrane protein complex; protein secretion; *Staphylococcus aureus*; Type VII secretion

Protein secretion systems allow bacteria to interact with and manipulate their environments, and in pathogens, they play critical roles in host colonisation and disease [1]. The Gram-positive bacterium *Staphylococcus aureus* produces a Type VII protein secretion system, also known as Ess (ESAT-6 secretion system), that is required for pathogenesis in murine models of infection [2,3]. Substrates of the *S. aureus* Ess machinery include two small proteins, EsxA and EsxB, of the WXG100 superfamily, and two additional proteins, EsxC and EsxD, which lack the W-X-G motif [2,4,5]. Mutational and bioinformatic analyses have revealed six core components of the *S. aureus* Ess machinery, of which four (EsaA, EssA, EssB and EssC) are predicted to be membrane-bound proteins, one (EsaB) to be cytoplasmic and one (EsxA) extracellular [2,3,6; Fig 1]. Little is known about how the core Ess machinery is organised or how protein secretion is mediated.

The *S. aureus* Ess system is distantly related to the ESX/type VII secretion system of actinobacteria, sharing EsxA/B-like and EssC-like components. EssC proteins (termed EccC in actinobacteria) are membrane-bound ATPases of the FtsK/SpoIIIE family that form hexameric membrane-spanning pores which traffic macromolecules [7]. Very recently, the structure of EccC from the thermophilic actinobacterium *Thermomonospora curvata* was reported. The protein has three interlocking ATPase domains at its C terminus and its multimerisation was unexpectedly shown to depend upon the binding of EsxB to a pocket on the most C-terminal ATPase domain [8]. In the same study, the structure of the two C-terminal domains of EssC from *Geobacillus thermodenitrificans*, a thermophilic relative of *S. aureus* was also described, although it is not clear whether multimerisation of this protein is also controlled by interaction with EsxB (or EsxA) [8]. Analysis of more than 150 *S. aureus*

Abbreviations
ATC, anhydrotetracycline; DDM, *n*dodecyl-β-D-maltoside; DSS, disuccinimidyl suberate.

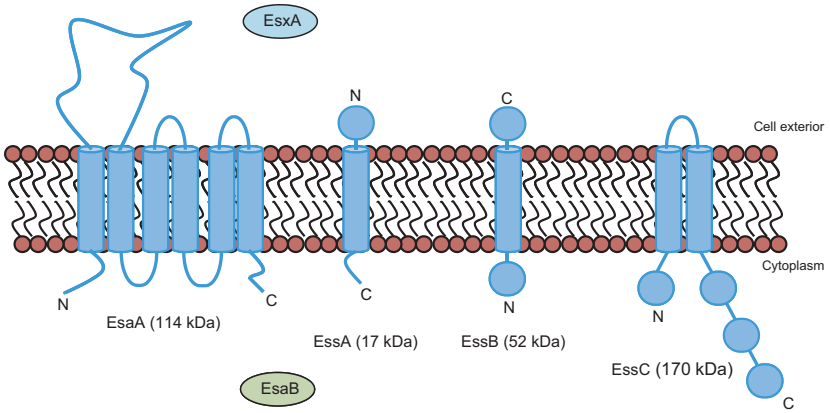

Fig. 1. The membrane components of the *Staphylococcus aureus* Ess/Type VII protein secretion system. The sizes and predicted topologies of EsaA, EssA, EssB and EssC are shown. The other two essential components, EsxA and EsaB, are also shown, along with their known or predicted subcellular location.

genome sequences has shown that the C-terminal ATPase domain of EssC falls into one of four different sequence variants that cluster with genes coding cognate suites of candidate substrate proteins, implicating this domain in substrate recognition [6].

The EccC protein of pathogenic *Mycobacteria* has been shown to form a large (1.5 MDa) complex with three additional membrane proteins, EccB, EccD and EccE [9]. However, these accessory proteins are found only in actinobacteria and it is not known whether *S. aureus* EssC forms part of a larger membrane-bound complex containing additional components. To investigate this question, we probed the organisation of the essential membrane components of the *S. aureus* Ess system. Our results are consistent with three of the proteins, EsaA, EssB and EssC forming homo-oligomeric complexes; however, we find no evidence for hetero-oligomeric assemblies between any of these proteins or even with a fourth membrane-bound protein, EssA, under the conditions we examined.

Methods

Plasmids and strains

Staphylococcus aureus strain RN6390 (WT; *ess*$^{+}$) [10] along with a series of isogenic strains lacking individual genes coded at the *ess* locus, or a deletion of all 12 of the coexpressed *ess* genes [3] were used for all experiments in this study. A plasmid construct producing N-terminally hexahistidine-tagged EsaA has been described previously [3]. Plasmid pEssB-nhis encodes N-terminally hexahistidine-tagged EssB was constructed as follows: the *essB* coding region was amplified from RN6390 genomic DNA using primers: 5′-GATAGATCTGTTAAAAATCATAACCCTA AAAATG-3′ and 5′-CGAGAATTCACTATTTTTTT. CT TTCAGCTTCTTGGCGT-3′, digested with *Bgl*II–*Eco*RI and cloned into the expression vector pRMC2h [3]. A variant of plasmid pRMC2 [11] coding for a C-terminal hexahistidine tag (pRMC2ch) was generated by amplification across the multiple cloning site of pRMC2 using primers pRMC2seq1 (5′-ATTTGGATCCCCTCGAGTTCATG-3′) and Chisins (5′-TTGAATTCATTAATGATGATGATGAT GATGGAGCTCAGATCTGTTACC-3′), digestion of the product with *Xho*I and *Eco*RI and cloning into similarly digested pRMC2. Plasmid pEssA-chis encodes C-terminally hexahistidine-tagged EssA and was constructed following amplification of the *essA* coding region from RN6390 genomic DNA using primers: 5′-CTAGATCTAATGT-TACTTTTACGTGCTGATTCA-3′ was digested with *Kpn*I and *Bgl*II and cloned into pRMC2ch. Plasmid pEssC-chis encodes C-terminally hexahistidine-tagged EssC and was constructed by amplification of the *essC* coding region from RN6390 genomic DNA primers: 5′-AAATAGATC-TAGGACTGAGGCAAAG-3 and 5′-TGAATTCATTAAT GATGATGATGATGAT. GACTACCAGATTTAAACCA TCTAATCTTTTG-3′ was digested with *Bgl*II and *Eco*RI and cloned into vector pRMC2.

Biochemical methods

For *in vitro* crosslinking experiments with disuccinimidyl suberate (DSS), 50 mL of TSB medium was inoculated from an overnight culture of the strain of interest to give an OD_{600} of 0.1. For induction of expression of plasmid-encoded proteins, the indicated concentration of anhydrotetracycline (ATC) was added when the OD_{600} of the culture reached 0.5, and the culture was incubated at 37 °C with vigorous shaking until an OD_{600} of 2.0 was reached. Cells were pelleted by centrifugation for 10 min at 2770 × ***g***, washed once with 1 mL 20 mM MOPS/NaOH, pH 7.2, 200 mM NaCl (M1 buffer), and resuspended in 1 mL M1 buffer containing 2.5 mM EDTA. The resuspended sample was supplemented with 200 μg lysostaphin and incubated for 30 min at 37 °C to digest the cell wall, after which sphaeroplasts were lysed by sonication and centrifuged for 5 min at 17 000 × ***g*** to remove unbroken cells. The clari-

fied supernatant (containing the cytoplasm and membranes) was centrifuged again for 30 min at 227 000 × ***g*** at 4 °C to pellet the membranes. The membrane fraction was resuspended in 100 μL M1 buffer. For DSS crosslinking, membranes (30 μg of protein) were supplemented with either DSS (to a final concentration of 2 mM) or an equivalent volume of DMSO (control sample) and made up to 50 μL final volume with 20 mM HEPES/NaOH, pH 7.4, 20 mM KCl, 250 mM sucrose, 1 mM EDTA. After incubation for 30 min at room temperature, the reaction was quenched by addition of Tris/HCl, pH 8.0 to a final concentration of 100 mM. For analysis of EsaA or EssB crosslinks, samples were made up to 73 μL with 4 × NuPAGE loading buffer prior to separation on Bis-Tris gels. For analysis of EssC crosslinks, samples were made up to 66 μL with 6 × SDS sample buffer prior to separation by SDS PAGE.

Formaldehyde (PFA) crosslinking experiments were carried out using whole cell samples. About 50 mL of TSB medium was inoculated from an overnight culture of the strain of interest to give an OD_{600} of 0.1. For induction of expression of plasmid-encoded proteins, anhydrotetracycline (ATC; 50 ng·mL^{-1} for EsaA production, 100 ng·mL^{-1} for EssA production and 25 ng·mL^{-1} for EssB and EssC production) was added when the OD_{600} of the culture reached 0.5. Once an OD_{600} of 1.0 was reached, cells were pelleted by centrifugation for 10 min at 2770 × ***g*** and resuspended in 1 mL 1 × PBS. Paraformaldehyde was added to the cell suspension to a final concentration of 0.6% and samples incubated for 30 min at room temperature before the reaction was quenched by addition of Tris/HCl, pH 8.0 to a final concentration of 100 mM. Cells were pelleted by centrifugation for 10 min at 2770 × ***g***, resuspended in 1 mL 50 mM Tris/HCl, pH 7.5, 200 mM NaCl, 2.5 mM EDTA and treated as described above to obtain the isolated membrane fraction. Membranes were resuspended in 100 μL 50 mM Tris/HCl, pH 7.5, 200 mM NaCl prior to separation on Bis-Tris gels (for analysis of EsaA or EssB crosslinks) or SDS gels (for analysis of EssC crosslinks).

Growth of cells and preparation of cell and supernatant samples for secretion experiments were performed as described previously [3]. The same cell samples were also used to analyse the level of production of EsaA. To analyse the level of EssB and EssC, membrane fractions were prepared from whole cell samples as described above.

For detergent solubilisation tests, cells were harvested at OD_{600} of 2.0, following supplementation with ATC when the OD_{600} of the culture reached 0.5, conditions where the T7SS is active (Fig. S1). Membrane fractions were prepared as described above, and samples containing 400 μg of total protein were used for solubilisation. Membrane fractions were pelleted by centrifugation for 30 min at 227 000 × ***g*** at 4 °C and resuspended in solubilisation buffer (50 mM sodium phosphate, pH 8.0, 300 mM NaCl, 10% glycerol) to a final protein concentration of 10 μg·μL^{-1}. Samples were supplemented with the appropriate detergent to a final concentration of 2%, and incubated at 25 °C for 2 h with shaking. To separate the solubilised protein from the insoluble material, samples were centrifuged for 20 min at 89 000 × ***g*** at 4 °C. The supernatant was taken as the solubilised membrane protein and the pellet as the insoluble material. For blue native polyacrylamide gel electrophoresis (BN PAGE), solubilised membrane protein samples were supplemented with 5% glycerol and 0.2% Coomassie Blue (final concentration) and BN PAGE was performed as described by Wittig *et al.* [12] using precast 4–16% gradient gels (Novex).

SDS PAGE was carried out using Bis-Tris gels as described previously [3], and western blotting was performed following standard protocols with the following antibody dilutions: α-EsxA [3] 1 : 2500, α-EsxC [3] 1 : 2000, α-EsaA [3] 1 : 10 000, α-EssB [3] 1 : 10 000, α-EssC [3] 1 : 10 000 and α-TrxA [13] 1 : 10 000.

Results

Currently little is known about the organisation of the membrane components of the *S. aureus* Ess machinery. A previous study has reported a membrane location for EssB in *S. aureus* [14] and when heterologously expressed in *E. coli* EssB behaves as a dimer [15,16], but interactions with other components of the Ess machinery have not yet been described. We firstly used chemical crosslinking on isolated membrane fractions to probe the organisation of the essential membrane components EsaA, EssB and EssC, using the bifunctional crosslinker disuccinimidyl suberate (DSS), which crosslinks exposed primary amine-containing residues. To maximise the possibility of detecting interactions, we also undertook these experiments with the overproduction or absence of individual Ess membrane components. Figure S1 confirms the lack of EsxA and EsxC secretion in each of the *esaA*, *essA*, *essB* and *essC* deletion strains and the complementation by the missing gene expressed *in trans* and Fig. S2 shows the level of plasmid-encoded EsaA, EssB and EssC production.

As shown in Fig. 2(A), native EsaA could be detected in membranes derived from the wild-type strain and each of the *essA*, *essB* and *essC* deletion strain backgrounds, indicating that it is stably produced in the absence of each of these Ess components. No additional EsaA-specific bands were generated in the presence of the DSS crosslinker in membrane fractions from any of these strains, or when any of EssA, EssB or EssC was overproduced, although a dark smear of EsaA-containing material was visible when crosslinking was carried out in the presence of over-

produced EsaA. Figure 2(B) shows that likewise, EssB was stably produced and found in the membrane fraction in the absence of any of EsaA, EssA or EssC, but did not yield any crosslinked products, even when it was overproduced.

By contrast, crosslinked products were detected for EssC following incubation with DSS (Fig. 2C). A very similar high molecular weight band migrating well above the 460 kDa molecular weight marker was detected in membrane fractions of the wild-type and the *esaA*, *essA* and *essB* deletion strains. It is likely that this represents a homo-multimer of EssC, an observation consistent with previous reports [8]. The mass of crosslinked product appears to be too large for a homo-dimeric species (which would be expected to migrate below the 460 kDa marker) and therefore it is likely to represent at least a homo-trimer. Note that we were unable to directly assess crosslinking of EssA as we do not have a functional antibody.

These initial crosslinking experiments, which revealed few detectable interactions, were carried out *in vitro*, where factors such as the proton-motive force, ATP and soluble proteins are absent. Therefore, we next undertook similar crosslinking experiments in whole cells, using formaldehyde as a cell-permeable crosslinker that also crosslinks amino groups. As shown in Fig. 3A, incubation with formaldehyde resulted in EsaA-specific crosslinks in whole cells of the wild-type strain. A series of 4–5 discrete bands could be detected, migrating around 250 kDa. Interestingly, essentially the same pattern of EsaA crosslinks was seen whether EssA, EssB or EssC were absent, suggesting that the crosslinked products did not contain any of these proteins. It has been reported that the long extracellular domain of YueB, the *Bacillus subtilis* homologue of EsaA, forms a highly elongated homo-dimer [17] and it is therefore likely that the crosslinks seen here correspond to different conformers of a crosslinked EsaA dimer.

In vivo crosslinking analysis of EssB resulted in no detectable EssB crosslinks unless the protein was overproduced, in which case a very faint crosslinked product running at the approximate size of an EssB homo-dimer could be detected (Fig 3B). As homo-dimerisation of EssB has been reported previously, [15,16] it is likely that this crosslink is a homo-dimeric form of EssB.

Crosslinking of EssC *in vivo* also yielded high molecular weight products, as was observed *in vitro* (Fig 3C). However, in contrast to the *in vitro* analysis, where one major crosslinked product was seen, in this instance at least two distinct high molecular weight species were detected, both of which migrated above the 460 kDa molecular weight marker. The differences between the pattern of crosslinks seen *in vivo* and *in vitro* may reflect the difference in size between DSS which was used as a crosslinker *in vitro* and formaldehyde which was used *in vivo*. Alternatively they may arise due to the presence of ATP, proton-motive force or other factors that are present in whole cells. It should be noted that as similar crosslinks were seen in the absence of any of EsaA, EssA or EssB, neither of the two crosslinks arise from interactions of EssC with any of the other core membrane components of the Ess system, and probably represent homo-multimeric forms of EssC.

It has been reported that multimerisation of EccC, the homologue of EssC found in actinobacteria, is controlled by interaction with the two small WXG100 proteins, EsxA and EsxB. Rosenberg *et al*. [8] showed that the interaction of purified EccC with EsxB drives the formation of high-order multimers, whereas interaction of EsxA with the EccC–EsxB complex resulted in cooperative disassembly of EccC and the accumulation of dimeric and monomeric species. To determine whether the high molecular weight EssC crosslinks were detected *in vivo* as a result of the presence of EsxA or EsxB, we repeated the formaldehyde crosslinking in whole cells of a strain deleted for all 12 genes encoded at the *ess* locus, including *esxA* and *esxB* [3]. Figure 3D shows that the pattern of EssC crosslinks was not affected by the absence of EsxA, EsxB or any other protein encoded at this locus. We conclude that oligomerisation of EssC is independent of any previously identified Ess component.

The results presented to date suggest that there is likely homo-oligomeric interactions for three of the membrane components of the Ess machinery, but provide no evidence for interactions between the components. One possible explanation for this is that there are no suitably juxtaposed lysine residues in neighbouring proteins to allow crosslinking to occur. Therefore, we next attempted to extract the Ess membrane proteins to examine interactions in detergent solution. We conducted solubilisation tests using the nonionic detergents Triton X-100, *n*dodecyl-β-D-maltoside (DDM) and digitonin, and the zwitterionic detergent Fos-choline-12, on membranes isolated from the *S. aureus* wild-type strain. As shown in Figure 4, the EsaA, EssB and EssC proteins differed in their behaviour with the four detergents tested. DDM was able to successfully extract all of the EsaA and EssB from the membrane, but did not solubilise full length EssC. EsaA and EssB were also partially extracted with Triton X-100 and digitonin, whereas only a very small fraction of EssC was extracted with digitonin

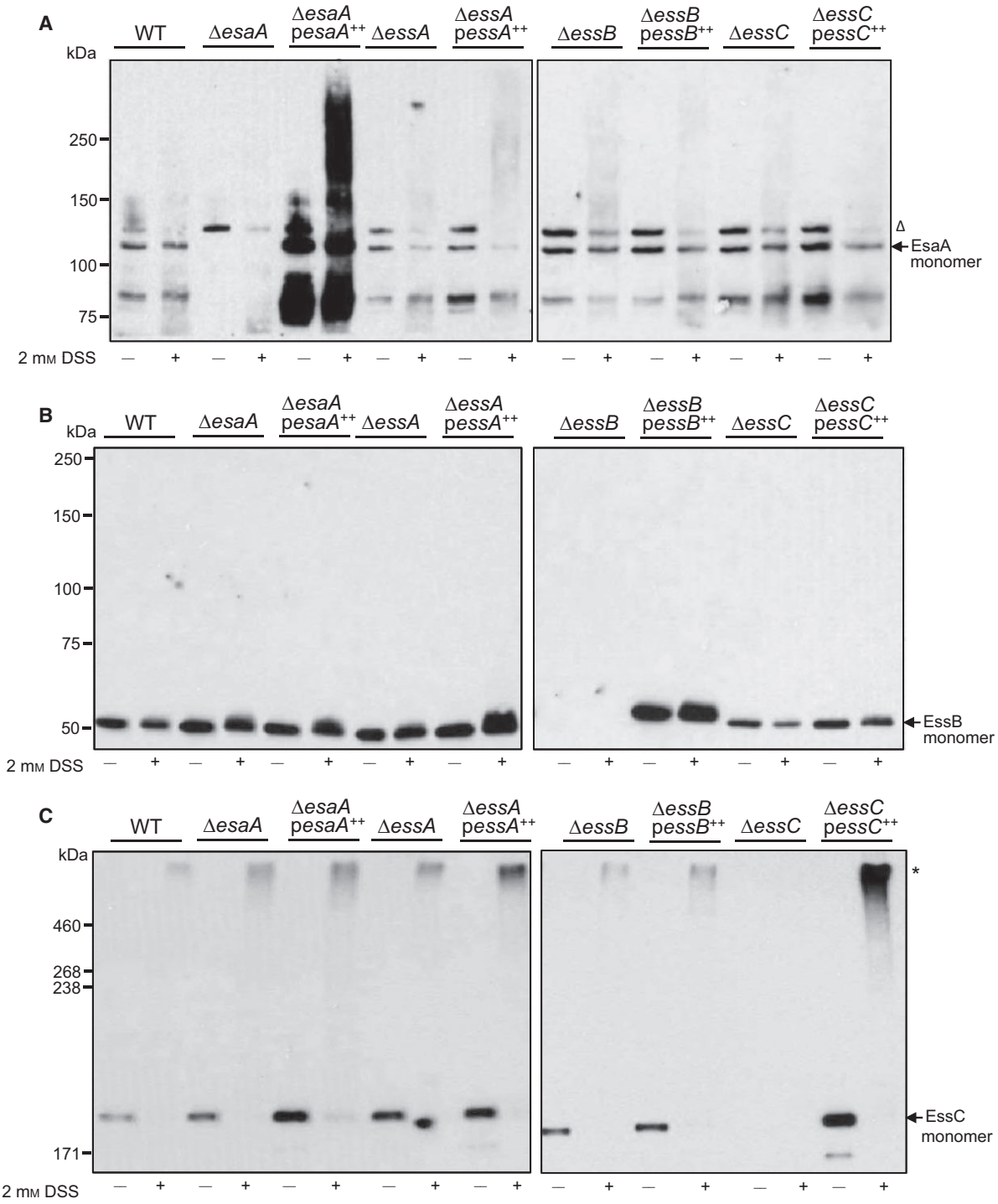

Fig. 2. DSS-mediated crosslinking of EsaA, EssB and EssC in isolated membrane fractions. Membrane fractions were prepared from strain RN6390 (WT) or the isogenic *esaA*, *essA*, *essB* or *essC* deletion strains, either harbouring the empty pRMC2 vector (lanes labelled Δ*esaA,* Δ*essA,* Δ*essB,* Δ*essC* respectively) or pRMC2 overproducing a his-tagged variant of the indicated gene (Δ*esaA pesaA*$^{++}$, Δ*essA pessA*$^{++}$, Δ*essB pessB*$^{++}$, Δ*essC pessC*$^{++}$) and treated with DSS as described under Experimental Procedures. After the reaction was quenched, aliquots (1 μg of total membrane protein for EsaA, EssB; or 2 μg of total membrane protein for EssC) were loaded on a Bis-Tris gel containing 8% acrylamide (A and B) or SDS gel containing 5% acrylamide (C), samples were transferred to nitrocellulose membrane and proteins detected using polyclonal antibodies raised against A. EsaA, B. EssB or C. EssC, as indicated. Crosslinked products are indicated to the right with an asterisk; the open triangle indicates a nonspecific band that is detected with the EsaA antiserum.

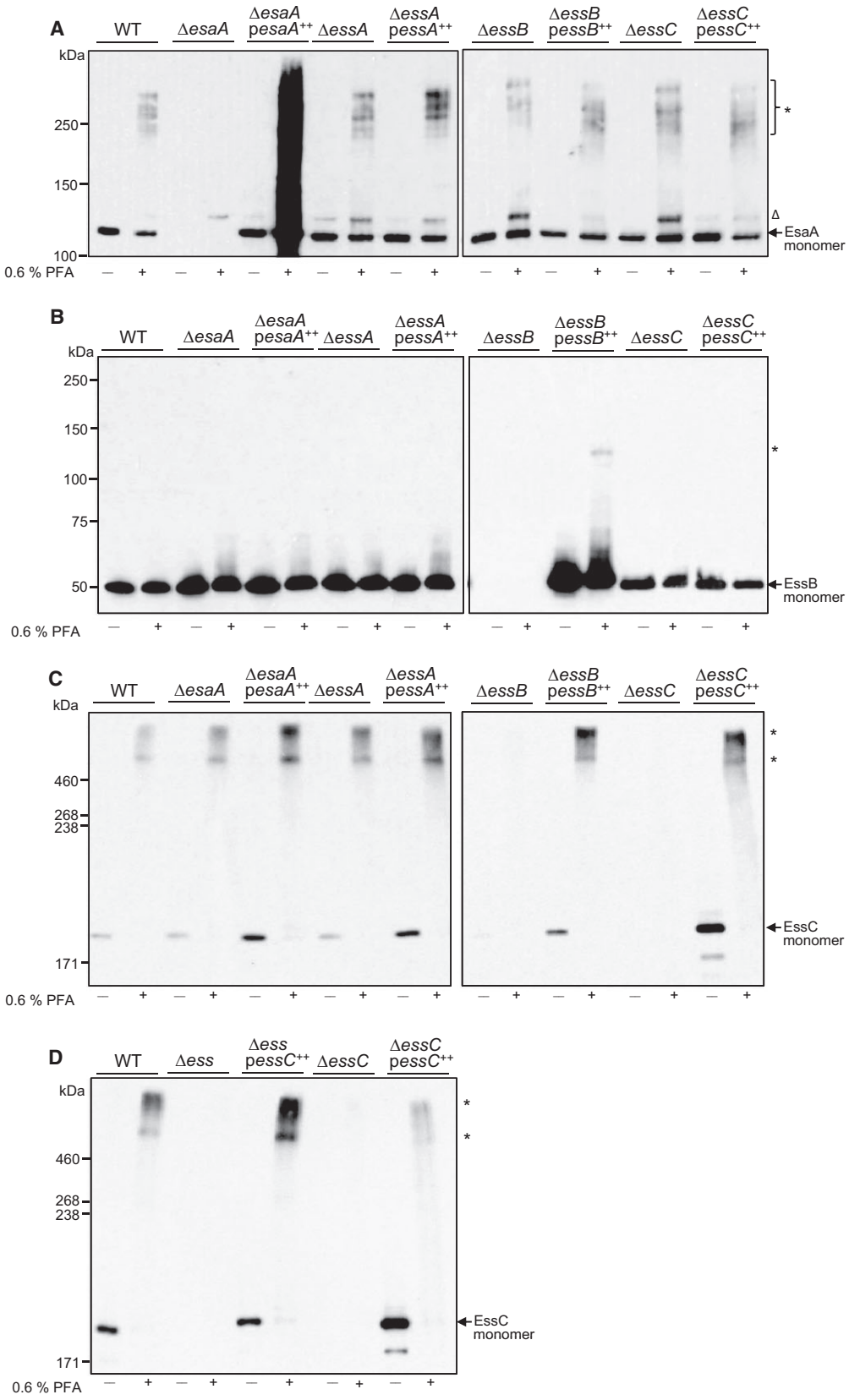
A
WT
ΔesaA
ΔesaA pesaA++
ΔessA
ΔessA pessA++
ΔessB
ΔessB pessB++
ΔessC
ΔessC pessC++
kDa
250
150
100
0.6 % PFA
*
Δ
EsaA monomer
B
WT
ΔesaA
ΔesaA pesaA++
ΔessA
ΔessA pessA++
ΔessB
ΔessB pessB++
ΔessC
ΔessC pessC++
kDa
250
150
100
75
50
0.6 % PFA
*
EssB monomer
C
WT
ΔesaA
ΔesaA pesaA++
ΔessA
ΔessA pessA++
ΔessB
ΔessB pessB++
ΔessC
ΔessC pessC++
kDa
460
268
238
171
0.6 % PFA
*
*
EssC monomer
D
WT
Δess
Δess pessC++
ΔessC
ΔessC pessC++
kDa
460
268
238
171
0.6 % PFA
*
*
EssC monomer

Fig. 3. Formaldehyde-mediated crosslinking of EsaA, EssB and EssC in whole cells. (A–C) Whole cells of strain RN6390 (WT) or the isogenic *esaA*, *essA*, *essB* or *essC* deletion strains, either harbouring the empty pRMC2 vector (lanes labelled Δ*esaA*, Δ*essA*, Δ*essB*, Δ*essC* respectively) or pRMC2 overproducing a his-tagged variant of the indicated gene (Δ*esaA pesaA*$^{++}$, Δ*essA pessA*$^{++}$, Δ*essB pessB*$^{++}$, Δ*essC pessC*$^{++}$) or (D) Whole cells of strain RN6390 (WT), the isogenic Δ*esaA* – *SAOUHSC_00269* deletion strain or the isogenic *essC* deletion strain, either harbouring the empty pRMC2 vector (lanes labelled Δ*ess* and Δ*essC* respectively) or pRMC2 overproducing a his-tagged variant of EssC (Δ*ess pessC*$^{++}$ or Δ*essC pessC*$^{++}$) were treated with paraformaldehyde (PFA) as described under Experimental Procedures. Following quenching, cells were lysed and membrane fractions prepared, and 1 μg of total membrane protein loaded on a Bis-Tris gel containing 8% acrylamide (A and B) or 2 μg of total membrane protein loaded on a SDS gel containing 5% acrylamide (C and D), samples were transferred to nitrocellulose membrane and proteins detected using polyclonal antibodies raised against A. EsaA, B. EssB or C and D. EssC, as indicated. Crosslinked products are indicated to the right with an asterisk; the open triangle indicates a nonspecific band that is detected with the EsaA antiserum.

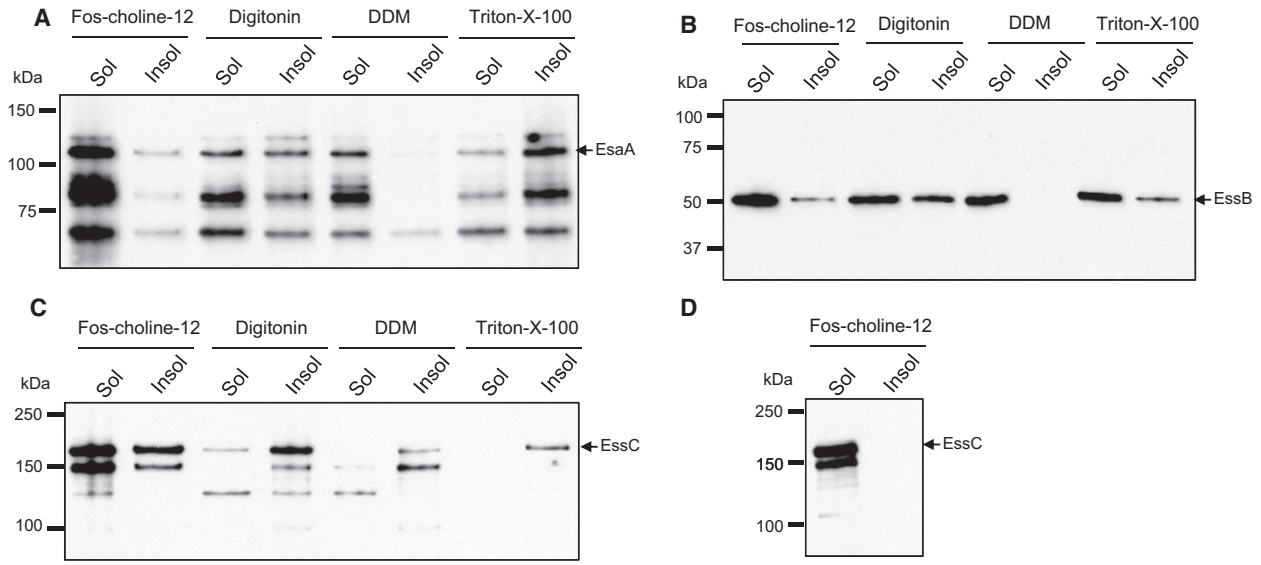

Fig. 4. Detergent extraction of EsaA, EssB and EssC. Membrane fractions were treated with 2% of the indicated detergent, as described under Experimental Procedures. About 5 μg of solubilised (sol) and insoluble material (insol) following centrifugation for 20 min at 89 000 × ***g*** were loaded on a Bis-Tris gel containing 8% acrylamide for (EsaA and EssC analysis) and 10% acrylamide (for EssB analysis). Subsequently the proteins were transferred on a nitrocellulose membrane followed by immunological detection of A. EsaA, B. EssB, C. and D. EssC.

and none when Triton X-100 was used. The most effective detergent at extracting EssC was Fos-choline-12 which extracted between 50 and 100% of the EssC present in the membrane. This detergent was also able to extract most of the EssB and EsaA.

As Fos-choline-12 was able to extract all three proteins from the membrane, we next tested whether they were part of the same complex by undertaking blue native polyacrylamide gel electrophoresis (BN PAGE), a technique that is commonly used for the analysis of membrane protein complexes [12]. After solubilisation of membranes with Fos-choline-12, the sample was separated on gels containing a gradient of 4–16% acrylamide and blotted with anti-EsaA, anti-EssB and anti-EssC antibodies. Unfortunately, the anti-EssC antibody was unable to detect any EssC-specific bands following BN PAGE (data not shown). However, bands containing EsaA and EssB were observed. As shown in Fig. 5(A), two complexes containing EsaA could be detected, one of which close to the 150 kDa marker and the second just above the 200 kDa marker, which could conceivably correspond to monomers and dimers of EsaA. In contrast, a single EssB-containing band was detected, migrating between the 66 kDa and 150 kDa marker, close to the expected size for an EssB dimer (Fig. 5B). Thus, given the differences in the masses of these bands these two proteins are highly unlikely to be part of the same complex. We confirmed this by repeating the BN PAGE on Fos-choline-12 membrane extracts from strains deleted for *esaA* or *essB*, and detected the same two EsaA complexes in the absence of EssB, and the same EssB complex in the absence of EsaA. We conclude that these two proteins do not interact with each other in isolated membranes.

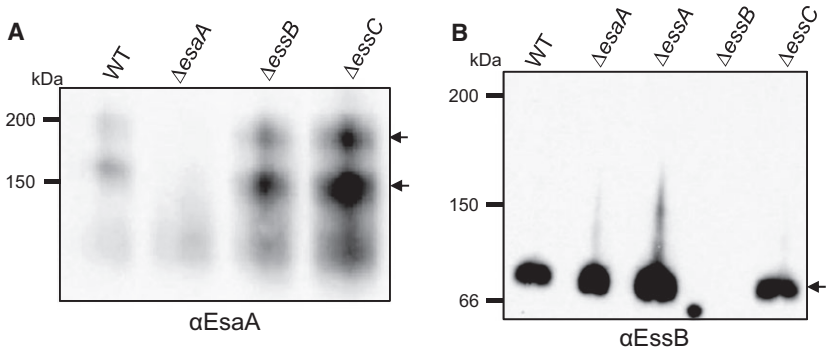

Fig. 5. Blue native PAGE analysis of EsaA- and EssB-containing complexes. Membrane fractions were prepared from strain RN6390 (WT) or the indicated deletion mutant, and samples (5 μg protein) were solubilised using 2% Fos-choline-12, as described under Experimental Procedures. The solubilised material was loaded onto a BN gel containing a gradient of 4–16% acrylamide. Subsequently, the proteins were transferred to PVDF membrane followed by immunological detection of A. EsaA or B. EssB. The arrows to the right indicate complexes containing EsaA (panel A) or EssB (panel B).

Further analysis using membranes isolated from an *essC* strain background showed that the same two EsaA complexes could be detected in the absence of EssC (Fig. 5A). Likewise, an identically migrating EssB band was seen in membrane fractions derived from the *essC* and *essA* mutant strains (Fig. 5B). Taken together with the results of the crosslinking analysis and supported by prior observations of EssB behaviour by Zoltner *et al.* [15,16], we conclude that the EsaA, EssB and EssC components of the Type VII secretion machinery show homotypic interaction but that there is no evidence that they are able to form complexes with one another, or with the fourth essential Ess membrane component, EssA, under the conditions we have examined.

Discussion

In this study, we have probed the organisation of the *S. aureus* Ess machinery by examining complexes of the Ess membrane-bound proteins using crosslinking and BN PAGE analysis. Our results are consistent with the EsaA, EssB and EssC proteins forming homomeric complexes, but under the conditions we examined, we found no evidence that these components interact with one another. Thus, we detected no heteromeric crosslinks between any of the proteins or with the fourth essential Ess membrane protein, EssA. Likewise the proteins displayed different solubility with a range of detergents, and only Fos-choline-12 of the detergents we tested was able to extract reasonable levels of EssC. BN PAGE analysis of membrane proteins extracted with Fos-choline-12 revealed EsaA and EssB to reside in separate complexes, neither of which appeared to contain any EssA or EssC. These findings contrast with a study of the distantly related ESX secretion system from *Mycobacterium marinum*, where extraction of membranes with DDM led to the isolation of a 1.5 MDa complex containing four conserved ESX membrane proteins, including the EssC homologue, EccC [9]. However, there is no detectable homology between EccB, EccD and EccE, which along with EccC localise to the *M. marinum* ESX membrane complex, and EsaA, EssA or EssB, and it is possible that they may have unrelated functions in the two different secretion systems.

Structural and functional analysis of EccC has shown that multimerisation is driven by interaction with EsxB and conversely that EsxA promotes disassembly of the EccC multimer, most likely by binding to EsxB and forming an EccC–EsxB–EsxA ternary complex. A pocket within the most C-terminal ATP-binding domain of EccC binds the C-terminal signal sequence of EsxB [8], providing structural clues about how multimerisation is controlled. However, it is not apparent whether this signal sequence binding pocket feature is conserved in EssC, and moreover we detected similar high-order EssC multimers in a strain lacking EsxB and EsxA suggesting that oligomerisation is not dependent upon binding of any of the known *S. aureus* WXG100 proteins.

In conclusion, we see no evidence for the existence of a heteromeric Ess membrane complex. It remains possible that interactions between the membrane components are transient and depend upon the presence of a translocating substrate. An alternative explanation is that, under the conditions we have examined, the secretion machinery is not fully active, as it has been noted previously that Ess secretion is only poorly active under laboratory growth conditions [3]. Further work will be required to distinguish between these possibilities.

Acknowledgements

This study was supported by UK Biotechnology and Biological Sciences Research Council EASTBIO Doctoral Training Partnership (award number BB/J01446X/1) which provided a PhD studentship (to FJ) and the UK Medical Research Council (Grant number MR/M011224/1 to TP and WNH). TP is a Royal Society/Wolfson merit award holder.

Author contributions

TP and WNH conceived and supervised the study; FJ designed and performed experiments; MZ and HK provided new tools and reagents; FJ, MZ, HK, WNH and TP analysed data; FJ and TP wrote the manuscript.

References

1 Costa TR, Felisberto-Rodrigues C, Meir A, Prevost MS, Redzej A, Trokter M and Waksman G (2015) Secretion systems in Gram-negative bacteria: structural and mechanistic insights. *Nat Rev Microbiol* **13**, 343–359.

2 Burts ML, Williams WA, DeBord K and Missiakas DM (2005) EsxA and EsxB are secreted by an ESAT-6-like system that is required for the pathogenesis of *Staphylococcus aureus* infections. *Proc Natl Acad Sci USA* **102**, 1169–1174.

3 Kneuper H , Cao ZP, Twomey KB, Zoltner M, Jäger F, Cargill JS, Chalmers J, van der Kooi-Pol MM, van Dijl JM, Ryan RP *et al.* (2014) Heterogeneity in *ess* transcriptional organization and variable contribution of the Ess/Type VII protein secretion system to virulence across closely related *Staphylocccus aureus* strains. *Mol Microbiol* **93**, 928–943.

4 Burts ML, DeDent AC and Missiakas DM (2008) EsaC substrate for the ESAT-6 secretion pathway and its role in persistent infections of *Staphylococcus aureus*. *Mol Microbiol* **69**, 736–746.

5 Anderson M, Aly KA, Chen YH and Missiakas D (2013) Secretion of atypical protein substrates by the ESAT-6 secretion system of *Staphylococcus aureus*. *Mol Microbiol* **90**, 734–743.

6 Warne B, Harkins CP, Harris SR, Vatsiou A, Stanley-Wall N, Parkhill J, Peacock SJ, Palmer T and Holden MTG (2016) The Ess/Type VII secretion system of *Staphylococcus aureus* shows unexpected genetic diversity. *BMC Genom*.

7 Gomis-Ruth FX, Moncalian G, Perez-Luque R, Gonzalez A, Cabezon E, de la Cruz F and Coll M (2001) The bacterial conjugation protein TrwB resembles ring helicases and F1-ATPase. *Nature* **409**, 637–641.

8 Rosenberg OS, , Dovala D, Li X, Connolly L, Bendebury A, Finer-Moore J, Holton J, Cheng Y, Stroud RM and Cox JS (2015) Substrates Control Multimerization and Activation of the Multi-Domain ATPase Motor of Type VII Secretion. *Cell* **161**, 501–512.

9 Houben EN, Bestebroer J, Ummels R, Wilson L, Piersma SR, Jiménez CR, Ottenhoff TH, Luirink J and Bitter W (2012) Composition of the type VII secretion system membrane complex. *Mol Microbiol* **86**, 472–484.

10 Novick RP, Ross HF, Projan SJ, Kornblum J, Kreiswirth B and Moghazeh S (1993) Synthesis of staphylococcal virulence factors is controlled by a regulatory RNA molecule. *EMBO J* **12**, 3967–3975.

11 Corrigan RM and Foster TJ (2009) An improved tetracycline-inducible expression vector for *Staphylococcus aureus*. *Plasmid* **61**, 126–129.

12 Wittig I, Braun HP and Schagger H (2006) Blue native PAGE. *Nat Protoc* **1**, 418–428.

13 Miller M, Donat S, Rakette S, Stehle T, Kouwen TR, Diks SH, Dreisbach A, Reilman E, Gronau K, Becher D *et al.* (2010) Staphylococcal PknB as the first prokaryotic representative of the proline-directed kinases. *PLoS One* **5**, e9057.

14 Chen YH, Anderson M, Hendrickx AP and Missiakas D (2012) Characterization of EssB, a protein required for secretion of ESAT-6 like proteins in *Staphylococcus aureus*. *BMC Microbiol* **12**, 219.

15 Zoltner M, Norman DG, Fyfe PK, El Mkami H, Palmer T and Hunter WN (2013) The architecture of EssB, an integral membrane component of the type VII secretion system. *Structure* **21**, 595–603.

16 Zoltner M, Fyfe PK, Palmer T and Hunter WN (2013) Characterization of *Staphylococcus aureus* EssB, an integral membrane component of the Type VII secretion system: atomic resolution crystal structure of the cytoplasmic segment. *Biochem J* **449**, 469–477.

17 Sao-Jose C, Lhuillier S, Lurz R, Melki R, Lepault J, Santos MA and Tavares P (2006) The ectodomain of the viral receptor YueB forms a fiber that triggers ejection of bacteriophage SPP1 DNA. *J Biol Chem* **281**, 11464–11470.

Supporting information

Additional supporting information may be found in the online version of this article at the publisher's web site:

Fig. S1. Complementation of *esaA*, *essA*, *essB* and *essC* deletion strains by provision of the missing gene *in trans*.

Fig. S2. Immunological detection of plasmid-encoded EsaA-his, EssB-his and EssC-his.

Molecular Microbiology (2014) 93(5), 928–943 ■
doi:10.1111/mmi.12707
First published online 30 July 2014

Heterogeneity in *ess* transcriptional organization and variable contribution of the Ess/Type VII protein secretion system to virulence across closely related *Staphylocccus aureus* strains

Holger Kneuper,[1] Zhen Ping Cao,[1] Kate B. Twomey,[2] Martin Zoltner,[3] Franziska Jäger,[1] James S. Cargill,[1] James Chalmers,[1] Magdalena M. van der Kooi-Pol,[4] Jan Maarten van Dijl,[4] Robert P. Ryan,[1,2] William N. Hunter[3] and Tracy Palmer[1]*

Divisions of [1]Molecular Microbiology and [3]Biological Chemistry and Drug Discovery, College of Life Sciences, University of Dundee, Dundee, UK.
[2]School of Microbiology, Biosciences Institute, University College Cork, Cork, Ireland.
[4]Department of Medical Microbiology, University of Groningen, University Medical Center Groningen, Hanzeplein 1, P.O. Box 30001, 9700 RB Groningen, The Netherlands.

Summary

The Type VII protein secretion system, found in Gram-positive bacteria, secretes small proteins, containing a conserved W-x-G amino acid sequence motif, to the growth medium. *Staphylococcus aureus* has a conserved Type VII secretion system, termed Ess, which is dispensable for laboratory growth but required for virulence. In this study we show that there are unexpected differences in the organization of the *ess* gene cluster between closely related strains of *S. aureus*. We further show that in laboratory growth medium different strains of *S. aureus* secrete the EsxA and EsxC substrate proteins at different growth points, and that the Ess system in strain Newman is inactive under these conditions. Systematic deletion analysis in *S. aureus* RN6390 is consistent with the EsaA, EsaB, EssA, EssB, EssC and EsxA proteins comprising core components of the secretion machinery in this strain. Finally we demonstrate that the Ess secretion machinery of two *S. aureus* strains, RN6390 and COL, is important for nasal colonization and virulence in the murine lung pneumonia model. Surprisingly, however, the secretion system plays no role in the virulence of strain SA113 under the same conditions.

Accepted 3 July, 2014. *For correspondence. E-mail t.palmer@dundee.ac.uk; Tel. (+44) 1382 386464; Fax (+44) 1382 385893.

Introduction

Most bacteria secrete proteins into their external environments, where they play essential roles in nutrient acquisition, colonization and host interactions. Gram-negative bacteria may elaborate any of six different protein secretion systems (named Type I through Type VI) to move proteins across their double-membrane cell envelopes, in either a single step, or by a two-step mechanism (Desvaux *et al.*, 2009). Protein secretion systems that operate by a two-step mechanism first rely on the translocation of proteins across the inner membrane by either the general secretory (Sec) or twin arginine translocase (Tat) machineries, before they mediate the secretion of substrates across the outer membrane (e.g. Pugsley, 1993; Voulhoux *et al.*, 2001).

Protein secretion in Gram-positive bacteria is, in most cases, a simpler process because these organisms (with the exception of the didermic Mycobacterial and Corynebacterial species) are bounded by a single membrane. The Sec and Tat pathways, to which proteins are targeted by the presence of cleavable signal peptides at their N-termini, directly secrete extracellular proteins in these bacteria (e.g. Sibbald *et al.*, 2006; Widdick *et al.*, 2006; Goosens *et al.*, 2014). In addition, a secretion system that has, to date, only been experimentally described in Gram-positive bacteria, variously termed the ESX, Ess or Type VII protein secretion system, also serves to translocate proteins to the extracellular environment. This secretion system was first described in pathogenic mycobacteria where it secretes two T cell antigens, ESAT-6 (early secreted antigenic target, 6 kDa) and CFP-10 (culture filtrate protein 10 kDa), now renamed EsxA and EsxB, respectively, and was shown to be essential for virulence (Hsu *et al.*, 2003; Pym *et al.*, 2003; Stanley *et al.*, 2003). This secretion system has variously been shown to function in other actinobacterial species,

© 2014 The Authors. *Molecular Microbiology* published by John Wiley & Sons Ltd.
This is an open access article under the terms of the Creative Commons Attribution License, which permits use, distribution and reproduction in any medium, provided the original work is properly cited.

including non-pathogenic members (Abdallah *et al*., 2006; Akpe San Roman *et al*., 2010; Fyans *et al*., 2013).

A related secretion system is found in bacteria of the low-GC *Firmicutes* phylum. It has been best characterized in the opportunistic human and animal pathogen *Staphylococcus aureus*. The relationship between the *S. aureus* secretion system and the Mycobacterial ESX machineries is limited, with only two types of conserved components. The first is an ATPase of the FtsK/SpoIIIE protein family, while the second is the presence of one or more of the secreted EsxA/EsxB proteins (Pallen, 2002). EsxA and EsxB are small acidic proteins of the WXG100 superfamily that are structurally organized as a helical hairpin with a conserved Trp–Xaa–Gly (WXG) motif that localizes in a loop between the two α-helices (e.g. (Renshaw *et al*., 2005; Sundaramoorthy *et al*., 2008). In *Mycobacteria*, EsxA and EsxB form tight heterodimers that are co-dependent on each other for secretion by the Type VII system (Renshaw *et al*., 2002; Stanley *et al*., 2003; Champion *et al*., 2006), whereas in *S. aureus* and related bacteria EsxA forms homodimers (Sundaramoorthy *et al*., 2008; Shukla *et al*., 2010; Anderson *et al*., 2013). Other essential secretion components are non-conserved (at least at the amino acid sequence level) between actinobacterial and *Firmicutes* systems, leading to them being designated as ESX (actinobacteria) and Ess (*Firmicutes*) secretion systems respectively (Burts *et al*., 2005; 2008; Bitter *et al*., 2009).

In *S. aureus* the Ess system has been shown to contribute to virulence in a mouse model of abscess formation. Mutations in the *S. aureus* Newman strain where any of *esxA*, *esxB* or *essC* (which encodes the FtsK/SpoIIIE family ATPase) were inactivated resulted in a significant reduction in cfu recovered from the livers and kidneys of mice that had been retro-orbitally injected with these strains (Burts *et al*., 2005). It was later shown that EsxC (formerly EsaC), a conserved *S. aureus* protein, is a substrate of the Ess machinery that has a small role in abscess formation but a more significant role during long-term persistence of abscesses (Burts *et al*., 2008). Recently EsxD was identified as a further secreted substrate (Anderson *et al*., 2013). The precise function of any of the *S. aureus* Ess substrate proteins remains to be elucidated.

The *S. aureus* Ess secretion system is encoded within the *ess* gene cluster and transcription of *esxA*, the first gene of the cluster, has been shown to be subject to complex regulation by the alternative sigma factor σ^B (Schulthess *et al*., 2012). In the *S. aureus* strain Newman background, *esxA* appears to be monocistronic and is not co-transcribed with the downstream *ess* genes (Schulthess *et al*., 2012). However, transposon mutagenesis has confirmed that each of EssA, EssB, EssC, which are encoded downstream of *esxA* in the *ess* cluster (Fig. 1A) are essential for the secretion of EsxA or EsxB (Burts *et al*., 2005). The EssA, EssB and EssC proteins are membrane-bound (Burts *et al*., 2005; Chen *et al*., 2012; Zoltner *et al*., 2013b) and probably form the membrane-embedded secretion apparatus. Two further membrane proteins are also encoded at the *ess* locus. Of these EsaA is reported to have no role in EsxA secretion (Burts *et al*., 2005), while loss of EsaD (recently re-named EssD) reduces, but does not abolish, the export of EsxA (Anderson *et al*., 2011).

In this study we have examined the organization of the *ess* gene cluster in a range of *S. aureus* strain backgrounds. Our results indicate that there are unexpected differences in the organization of the cluster, with the *esxA* gene being clearly co-transcribed with downstream *ess* genes in the COL, USA300 and SA113 strains, but transcribed as a monocistronic gene in the RN6390 and Newman strains. In the RN6390 and COL strains, EsxA and EsxC secretion could be detected throughout the growth phase, with substantial levels of extracellular protein accumulating from mid-logarithmic growth onwards. Systematic deletion analysis in the RN6390 strain background confirmed prior observations that *essA*, *essB* and *essC* were required for the secretion of EsxA, but surprisingly we also show that *esaA* and *esaB* are essential for secretion of EsxA and EsxC. Finally we show that the Ess secretion machinery of two *S. aureus* strains (RN6390 and COL) but not a third (SA113) is important for murine nasal colonization and virulence in the murine lung pneumonia model.

Results

The esxA gene is co-transcribed with downstream genes in S. aureus *COL, USA300 and SA113 strains, but not in RN6390 or Newman*

The *ess* gene cluster (Fig. 1A) has been reported to comprise at least 11 genes, several of which have essential or accessory roles in the secretion of Ess substrate proteins (Burts *et al*., 2005; 2008; Anderson *et al*., 2011). Previous work using the *S. aureus* Newman strain showed that *esxA* was a monocistronic gene, but the arrangement of the downstream genes was not examined (Schulthess *et al*., 2012). We therefore decided to examine whether any of these genes were co-transcribed.

To this end, mRNA was isolated from each of five different *S. aureus* strains during exponential growth in TSB medium (OD_{600} of 2.0). The strains we selected, RN6390, Newman, USA300, SA113 and COL are all relatively closely related strains of *S. aureus* from clonal complex 8 (CC8). Strains RN6390, Newman, USA300 and SA113 are of the same sequence type, ST8, whereas COL is of sequence type 250 within CC8 (Herbert *et al*., 2010). Oligonucleotide primer pairs were designed that either

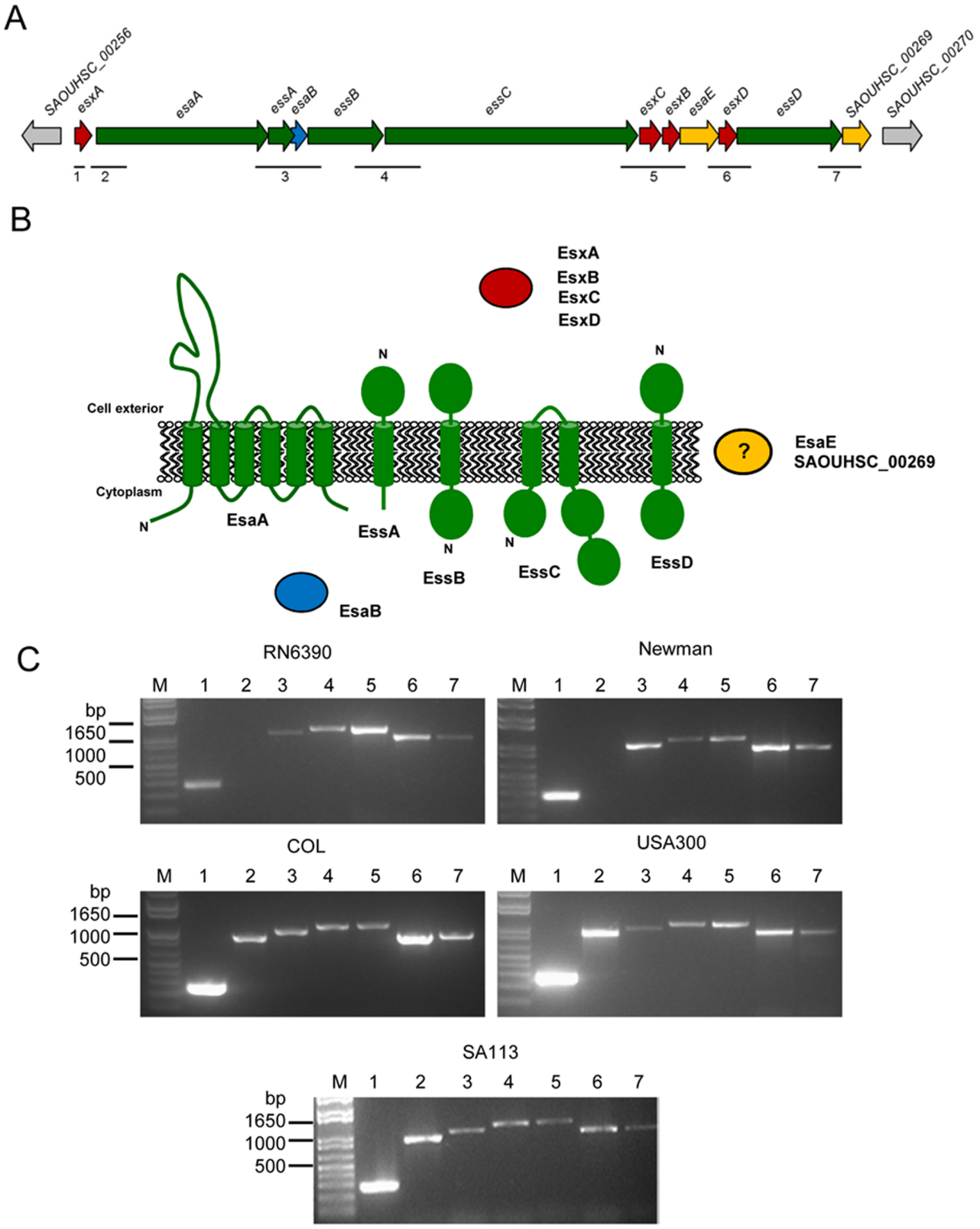
A
SAOUHSC_00256
esxA
esaA
essA
esaB
essB
essC
esxC
esxB
esaE
esxD
essD
SAOUHSC_00269
SAOUHSC_00270
1
2
3
4
5
6
7
B
EsxA
EsxB
EsxC
EsxD
Cell exterior
Cytoplasm
N
EsaA
EssA
EssB
EssC
EssD
EsaB
?
EsaE
SAOUHSC_00269
C
RN6390
Newman
COL
USA300
SA113
M 1 2 3 4 5 6 7
bp
1650
1000
500

Fig. 1. Organization of the *ess* locus in different strains of *S. aureus*.
A. Schematic representation of the *S. aureus ess* locus derived from the NCTC8325 genome sequence. The region from the start of *esxA* to the end of *SAOUHSC_00269* covers approximately 14 kb and is almost 100% identical between the RN6390, Newman, COL and USA300 strains (only two nucleotide differences over this region). Genes encoding secreted substrates are coloured in red, membrane components in green, cytoplasmic components in blue and unknown components in orange. Putative unrelated genes are shaded in grey. Note that the sizes of the intergenic regions are as follows: *SAOUHSC_00256-esxA*, 247 bp; *esxA-esaA*, 83 bp; *esaA-essA*, –1 bp; *essA-esaB*, –68 bp; *esaB-essB*, 12 bp; *essB-essC*, 21 bp; *essC-esxC*, 29 bp; *esxC-esxB*, 15 bp; *esxB-esaE*, –1 bp; *esaE-esxD*, –1 bp; *esxD-essD*, 9 bp; *essD-SAOUHSC_00269*, 10 bp; *SAOUHSC_00269-SAOUHSC_00270*, 207 bp.
B. Schematic representation of subcellular location and predicted topologies of the proteins encoded at the *ess* locus (not to scale). Shading as in part A.
C. RT-PCR analysis of mRNA isolated from each of the five different strains, using primer pairs listed in Table S1. The expected sizes for PCR products 1–7 are 272, 953, 1023, 1153, 1168, 959 and 946 bp respectively.

primed within the *esxA* gene (primer pair 1), that spanned the 83 bp intergenic region between *esxA* and *esaA*, or that spanned intergenic regions between the additional downstream genes (primer pairs 3 – 7; Fig. 1A, Table S1). For strains Newman and RN6390, primers amplifying within *esxA* gave a product of the expected size; however, no product was obtained using primers that spanned between *esxA* and *esaA* (Fig. 1C), confirming previous findings with Newman that *esxA* is a monocistronic gene (Schulthess *et al.*, 2012). Unexpectedly, however, the same primer pairs amplified a clear product of the expected size from the mRNA of strains COL, USA300 and SA113. Thus it can be concluded that the *esxA* and *esaA* genes are part of the same transcriptional unit in these three strains, and that there is heterogeneity in the transcriptional organization of the *ess* gene cluster between different strains of *S. aureus*.

Primer pairs 3–7 gave products of the expected sizes for mRNA isolated from all five *S. aureus* strains, strongly indicating the presence of a single transcript spanning from *esaA* to *SAOUHSC_00269*, for strains Newman and RN6390, and from *esxA* to *SAOUHSC_00269*, for strains COL, USA300 and SA113. These findings suggest that the uncharacterized gene *SAOUHSC_00269* is associated with Ess secretion.

A promoter is present in the esxA-esaA intergenic region in strain RN6390

To confirm the findings from the RT PCR experiments, 5′-RACE was used to identify transcription start sites within the *esxA-esaA* intergenic region and upstream of *esxA*, using an oligonucleotide that primes within *esaA*, or within *esxA* respectively. We focused on strains RN6390 and USA300, representing the two different transcriptional organizations of the *ess* operon, and sampled at two time points during exponential growth in TSB medium (OD_{600} of 1.0 and 2.0 respectively). When mRNA from RN6390 was used as template, a transcriptional start site within the *esxA-esaA* intergenic region was identified (labelled TSP2 in Fig. 2). This start site is downstream of a likely promoter sequence showing a reasonable match to the –35 and –10 consensus sequences. This transcriptional start site was not identified when mRNA from USA300 was used, instead the sequence read continued into the upstream *esxA* gene. Using a primer that primes within *esxA*, the

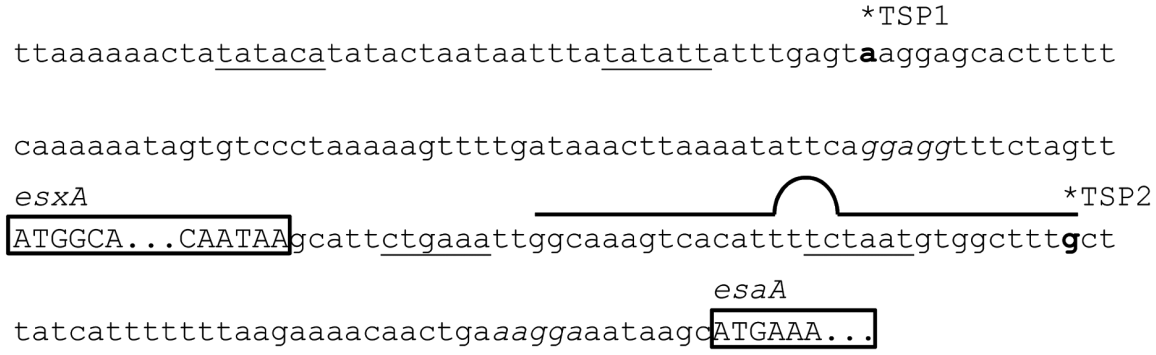

Fig. 2. A transcription start site in the *esxA-esaA* intergenic region of strain RN6390. DNA sequence covering the promoter region and transcriptional start site of the *esxA* gene through to the start of *esaA*. Note that the sequence of this region is identical between all strains used in this study. Transcriptional start points (indicated TSP1 and TSP2), mapped by 5′-RACE, are indicated in bold. TSP1 was identified from strains RN6390 and USA300, whereas TSP2 was identified from RN6390 only. Putative –35/–10 regions are underlined, the coding regions for *esxA* and *esaA* are shown in upper case letters and boxed (*esxA* is truncated to save space), and putative Shine–Dalgarno sequences are given in italics. A predicted rho-independent terminator for the *esxA* gene is indicated above the sequence.

© 2014 The Authors. *Molecular Microbiology* published by John Wiley & Sons Ltd.,

same transcriptional start site (TSP1 in Fig. 2) was identified from both of the mRNA samples. This is the same start site for *esxA* transcription identified by Schulthess *et al.* (2012).

It is interesting to note that there is a potential rho-independent terminator sequence in the *esxA-esaA* intergenic region, overlapping with the transcriptional start site and putative promoter for *esaA*. The same sequence is found in all five strains, and although it presumably acts as an effective terminator in strains Newman and RN6390, it must allow at least partial readthrough in the other strains examined here.

The esxA gene is overexpressed compared to other genes in the ess cluster

We next examined whether the two different transcriptional organizations of the *ess* clusters affected the ratio between *esxA* transcript level and the levels of downstream transcripts. For these experiments, mRNA was isolated from strains RN6390, USA300 and COL when the culture optical density at 600 nm (OD_{600}) reached 1.0 and 2.0 respectively. Reverse transcription of the mRNA followed by quantitative PCR, using the relative standard curve method, was undertaken to determine the relative levels of the *ess* genes *esxA*, *esaA*, *essC* and *esxB*, using the 16s rRNA gene as the endogenous control in these experiments. The relative expression levels were subsequently normalized, against *essC*, which was set to a relative expression level of 1 in each case.

As shown in Fig. 3, *esxA* is by far the most highly expressed of the *ess* genes tested, at an expression level approximately 100 times higher than that of *essC* for all three strains. The *esaA* gene is also more highly expressed than *essC*, being up to around 10 times more highly expressed, while *esxB* is expressed to similar levels as *essC* in all three strains. We conclude that despite the different mechanisms for transcriptional control of the *ess* genes in different *S. aureus* strains they ultimately give similar transcript level ratios among the encoded genes.

The Ess secretion system is active in different S. aureus *strains*

The experiments described above show that mRNA encoding Ess secretion system components is expressed in *S. aureus* strains cultured in the laboratory growth medium Trypticase Soy Broth (TSB). To determine whether the secretion system is active under these growth conditions, each strain was cultured under similar growth conditions and samples were withdrawn when the culture OD_{600} reached 1.0, 2.0, 3.0 or 5.0. The withdrawn samples were centrifuged to separate the cells from the culture supernatant, and each fraction was analysed by Western blotting with antibodies to each of the two Ess-secreted proteins EsxA and EsxC, and the cytoplasmic marker protein TrxA.

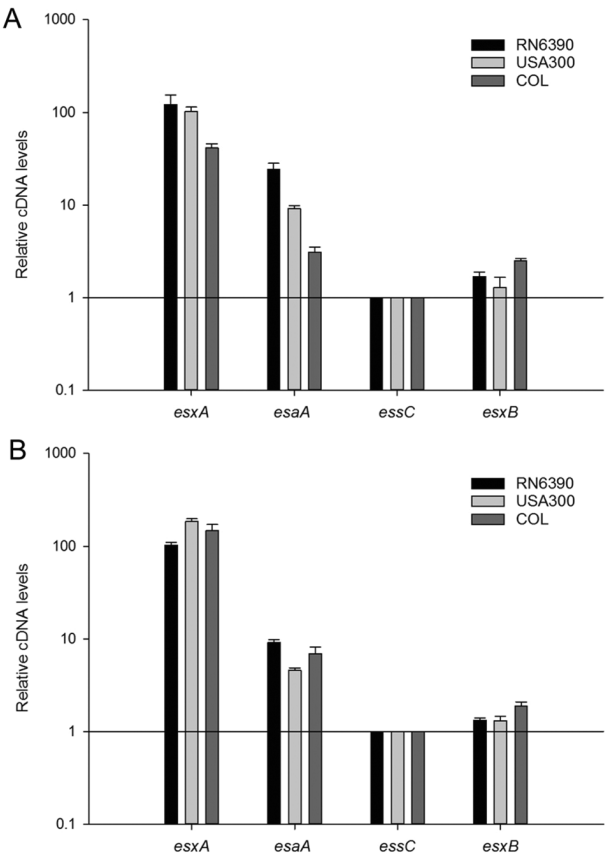

Fig. 3. The *esxA* gene is overexpressed compared to *esaA*, *essC* and *esxB*. mRNA isolated from the indicated strains that had been grown aerobically in TSB medium to an OD_{600} of 1 (A) or 2 (B) was reverse transcribed into cDNA for use in quantitative RT-qPCR experiments. Relative cDNA of *esxA*, *esaA* and *esxB*, calibrated in relation to *essC* levels, were calculated by the relative standard curve method (Larionov *et al.*, 2005), using 16S cDNA as endogenous control.

As shown in Fig. 4, secretion of both of the Ess substrates tested could be detected for strains RN6390, USA300, COL and SA113. Ess secretion activity of USA300 grown in TSB medium has also been reported previously (Anderson *et al.*, 2013). For strains COL and RN6390 secretion of EsxA and EsxC could be detected at the earliest growth point tested, whereas secretion of these proteins was not detected for USA300 until the cells had reached an OD_{600} of 2, and for SA113 secretion was only clearly detectable when cells reached an OD_{600} of 3 or above. It should be noted that the presence of EsxA was detected on the surface of cells in shaving experiments of COL harvested in early exponential phase (Dreisbach *et al.*, 2010; Solis *et al.*, 2010). At the latest growth point tested, EsxA (but not EsxC) had disappeared from the culture supernatant of RN6390, although it was still present

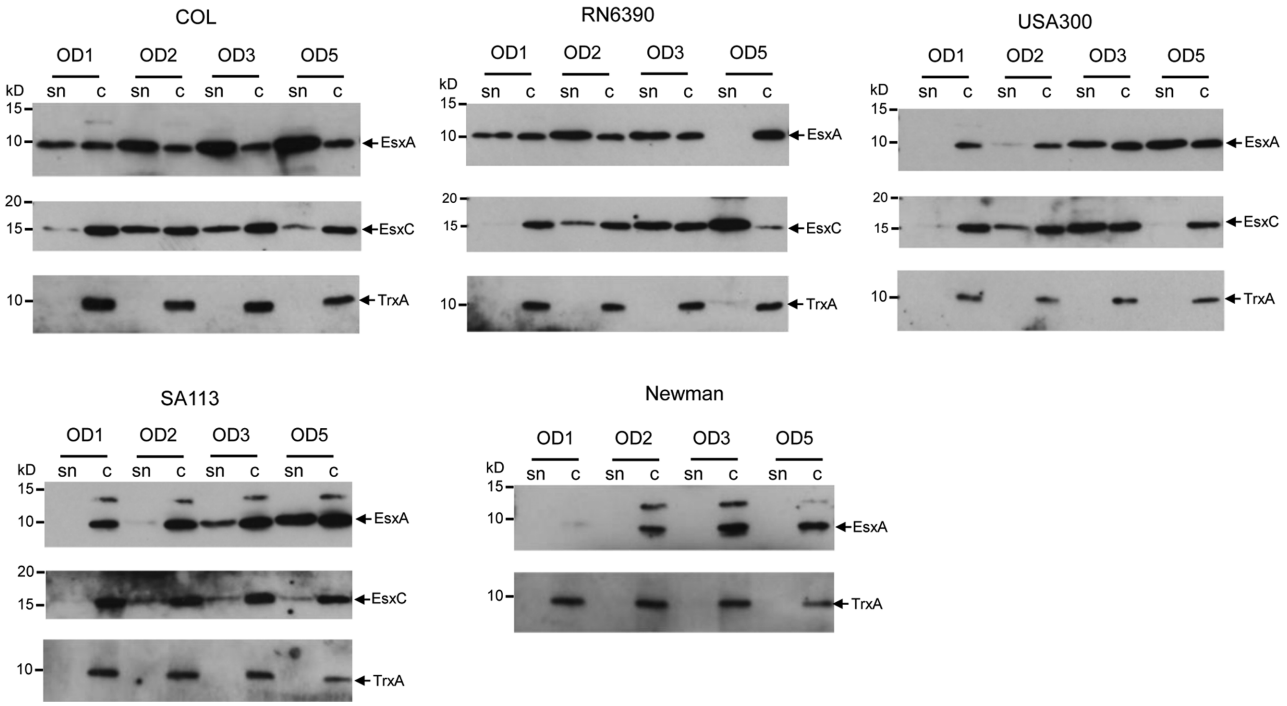

Fig. 4. The Ess secretion system is active in different *S. aureus* strains. The indicated *S. aureus* strains were cultured in TSB medium, and once the OD_{600} of the culture reached each of 1, 2, 3 or 5 an aliquot was removed and centrifuged to give the culture supernatant (sn) and cellular (c) fractions. Samples were separated on 15% bis-Tris gels and immunoblotted using anti-EsxA, EsxC or TrxA antisera. For the EsxA blots, 7.5 μl of culture supernatant and 5 μl of cells adjusted to an OD_{600} of 0.25 were loaded (5 μl of OD_{600} 1 cells for Newman and SA113). For the TrxA blots, twice the amount of supernatant and cells samples as described for the EsxA blots were used. For the EsxC blots, TCA precipitated supernatant equivalent to 100 μl culture supernatant and 10 μl of cells adjusted to an OD_{600} of 1 were loaded.

in the supernatants of the other three strains. It has been reported that RN6390 is deregulated for the production of extracellular protease which may account for the loss of EsxA from the supernatant at high cell density (Karlsson and Arvidson, 2002; Rigoulay *et al*., 2005). Indeed, we did note the presence of an additional smaller form of EsxA in the supernatant fractions of RN6390 (but not of other strains) with some batches of our polyclonal EsxA antiserum (not shown).

By contrast with the other four strains, no secretion of EsxA was detectable for strain Newman at any of the growth points examined. Some EsxA antigen was detected at OD_{600} of 2 and above, but this was found exclusively in the cellular fraction. We were unable to detect any clear signal for EsxC in either the supernatant or cellular fractions (not shown) – this is consistent with a previous study which showed that EsxC was repressed when Newman was grown in broth (Burts *et al*., 2008).

Deletion analysis confirms that EssA, EssB and EssC are essential to support Ess-dependent secretion in strain RN6390

To identify genes encoded at the *ess* locus that are essential for Ess secretion system activity, we constructed in-frame deletions of each of *esaA*, *esaB*, *essA*, *essB*, *essC*, *esxA*, *esxB* and *esxC* in *S. aureus* strain RN6390. We first confirmed that each of the individual deletion strains did not have a polar effect on downstream genes by blotting for the presence of the secretion substrate EsxC (Fig. 5) and/or the membrane components EsaA, EssB and EssC (Fig. S2). We then tested the effect of each individual deletion on the presence of Ess substrates EsxA and EsxC in the culture supernatant.

EssA and EssB are monotopic membrane proteins (Fig. 1B) that are conserved components encoded at *ess* loci in Firmicutes (e.g. Burts *et al*., 2005; Baptista *et al*., 2013). Previous studies in the Newman strain background reported that transposon insertions in either *essA* or *essB* abolished secretion of EsxA (Burts *et al*., 2005). In agreement with this, it can be seen (Fig. 5) that in-frame deletion of either *essA* or *essB* resulted in a complete absence of EsxA from the culture supernatant. However, in the Newman background insertional inactivation of either of these genes resulted in a destabilization of EsxA and EsxB (Burts *et al*., 2005), whereas in RN6390 (Fig. 5), as in USA300 (Anderson *et al*., 2013), EsxA protein is clearly detectable in the cellular fraction, even when the Ess system is inactivated. Analysis of EsxC localization showed a similar pattern, i.e. that deletion of *essB*

© 2014 The Authors. *Molecular Microbiology* published by John Wiley & Sons Ltd.,

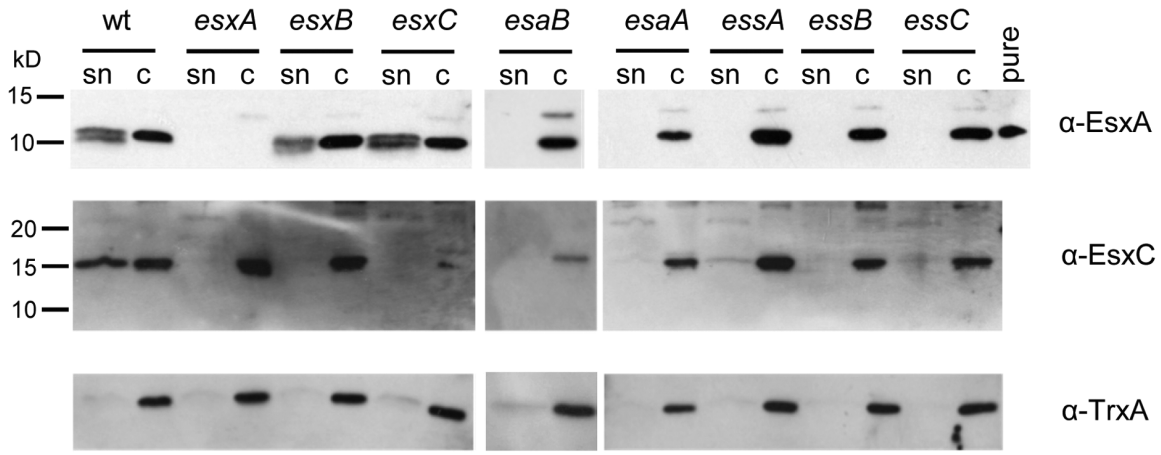

Fig. 5. EsxA and EsxC are not detected in culture supernatants if *esaA*, *esaB*, *essA*, *essB*, or *essC* are deleted in the RN6390 strain background. The RN6390 wild-type (wt) or isogenic deletion strains, as indicated, were cultured in TSB medium until an OD_{600} of 2 was reached. Samples were withdrawn and separated into culture supernatant (sn) and cellular (c) fractions. An equivalent of 200 μl of culture supernatant and 10 μl of resuspended cell sample adjusted to a calculated cell density of OD 1 was loaded in each lane, samples were separated on 15% bis-Tris gels and immunoblotted with anti-EsxA, anti-EsxC or anti-TrxA antibodies. For the EsxA immunoblot, 1 ng of purified EsxA protein (pure) was loaded as control. Molecular weight markers are indicated to the left of the blot.

resulted in no detectable secretion of EsxC, and that deletion of *essA* also resulted in a very severe EsxC secretion defect, although we routinely always detect a very low level of EsxC in the supernatant fraction of this strain. Again it should be noted that, similar to EsxA, cellular EsxC appeared stable even when the Ess system was inactivated.

EssC is a bitopic membrane protein that is conserved among the Ess and ESX secretion systems. Sequence and structural analysis indicates that the *Firmicutes* proteins have an N-terminal cytoplasmic region that adopts a tandem forkhead-associated domain fold and two iterations of the FtsK/SpoIIIE family domain in the C-terminal region that contain putative ATP binding P-loop motifs (Tanaka *et al*., 2007). Wherever examined, the EssC-like proteins have been shown to be essential for Ess secretion (e.g. Burts *et al*., 2005; Garufi *et al*., 2008; Baptista *et al*., 2013), and indeed in-frame deletion of *essC* in *S. aureus* RN6390 leads to total absence of EsxA and EsxC from the culture supernatant (Fig. 5).

To determine where the EsxA and EsxC proteins were localized when the secretion system was inactivated, we fractionated cells of the *essA* and *essC* mutant strains, along with the wild-type into the cell wall, membrane and cytoplasmic fractions. These samples were then probed with anti-EsxA and anti-EsxC antisera, along with antisera to the control proteins thioredoxin A (TrxA), protein A (Spa) or sortase A (SrtA). In the wild-type strain, EsxA and EsxC were detected largely in the cytoplasmic and supernatant samples, although some antigen was detected in the cell wall and traces of EsxC were also present in the membrane fraction. By contrast, in the *essC* mutant strain EsxA and EsxC were detected exclusively in the cytoplasmic fraction, confirming that EssC is essential for secretion of these proteins across the cytoplasmic membrane. Fractionation of the *essA* strain gave a slightly different result. Although EsxA was found exclusively in the cytoplasmic fraction in the absence of EssA, some EsxC protein could be detected in the cell wall and membrane fraction in the *essA* mutant. This is consistent with the results presented in Fig. 4, where low levels of EsxC were detected in the supernatant of the *essA* strain. We conclude that although clearly important, EssA is not absolutely essential for secretion of EsxC.

Deletion analysis reveals an essential role for EsaA and EsaB in the export or extracellular stability of Ess substrates in strain RN6390

EsaA is a polytopic membrane protein with a long extracellular loop that has been shown through protease shaving experiments to extend to the surface of *S. aureus* (Dreisbach *et al*., 2010). The homologous protein in *Bacillus subtilis*, YueB, is also surface-exposed and serves as a receptor for phage SPP1 infection (Sao-Jose *et al*., 2004; 2006). It has previously been reported in the Newman strain background that a transposon insertion in *esaA* had no effect on EsxA and EsxB secretion (Burts *et al*., 2005). Interestingly, however, we noted that deletion of *esaA* completely abolished secretion of EsxA and EsxC in strain RN6390. It is unlikely that the secretion defect seen with the RN6390 *esaA*$^{-}$ strain arose due to polar downstream effects because (i) the EssB and EssC proteins that are encoded immediately downstream of *esaA* are clearly

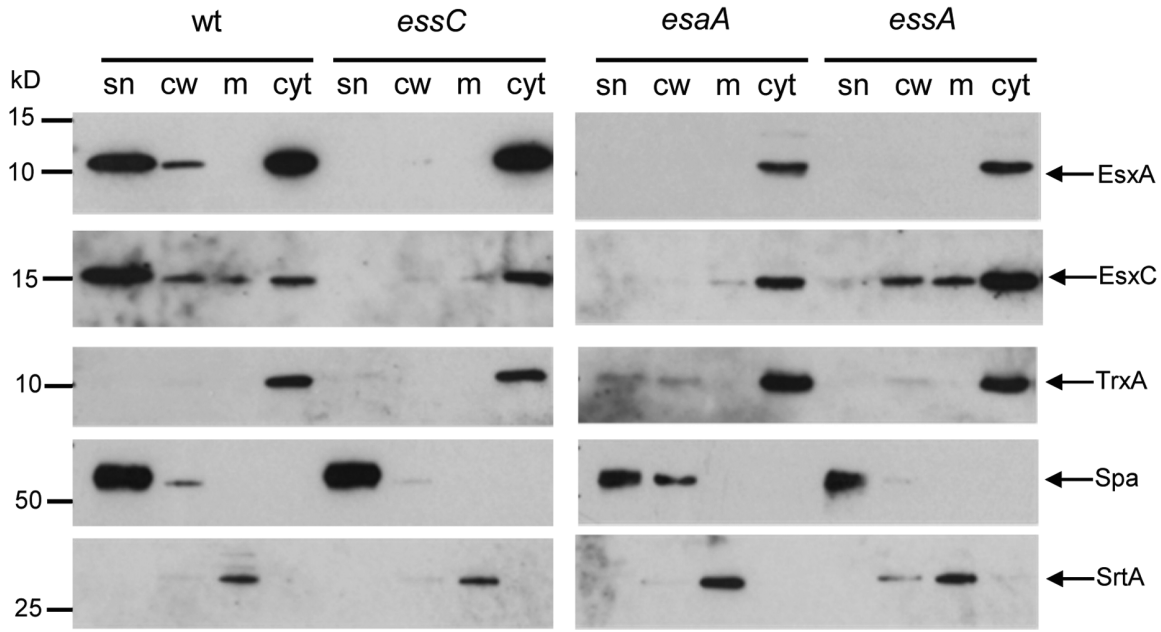

Fig. 6. Subcellular location of EsxA and EsxC in RN6390 and isogenic *esaA*, *essA* and *essC* mutant strains. The RN6390 wild-type (wt) or isogenic deletion strains, as indicated, were cultured in TSB medium until an OD_{600} of 2 was reached. The cells were spun down and the supernatant (sn) was retained as the secreted protein fraction. The cell pellets were subsequently fractionated into cell wall (cw), membrane (m) and cytoplasmic (cyt) fractions as described in *Experimental procedures*. An equivalent of 100 μl of culture supernatant and cell wall, membrane and cytoplasmic samples corresponding to the respective fractions from 10 μl of cells adjusted to an OD_{600} of 1 were separated on bis-Tris gels and immunoblotted using the anti-EsxA or EsxC antisera, or control antisera raised to TrxA (cytoplasmic protein), protein A (Spa, cell wall) or sortase A (SrtA, membrane).

detectable in the *esaA* mutant strain (Fig. S2), and (ii) re-introduction of plasmid-encoded his-tagged EsaA into the *esaA* mutant background restored EsxA secretion (Fig. S3). We therefore conclude that in RN6390, EsaA is an essential component of the Ess secretion machinery. It should be noted that the *B. subtilis* EsaA homologue, YueB, which is encoded within the *B. subtilis ess* gene cluster, is similarly also essential for the secretion of *B. subtilis* EsxA (YukE) (Baptista *et al.*, 2013). Subcellular fractionation of the *esaA* strain showed that EsxA and EsxC were located almost exclusively in the cytoplasm (Fig. 6).

We also examined the roles of soluble Ess-encoded components on secretion of EsxA and EsxC. EsaB is a small (93 aa) protein that is structurally closely related to ubiquitin, although it lacks the conserved C-terminal double glycine motif (van den Ent and Lowe, 2005). It has been reported to act as a negative regulator for EsxC in *S. aureus* Newman and EsxC could only be detected when *esaB* was deleted. EsxC antigen could be detected in other strains of *S. aureus*, but again in the USA300 background deletion of *esaB* resulted in upregulation of EsxC levels. In each case loss of *esaB* did not affect secretion of EsxC to the growth medium (Burts *et al.*, 2008). Deletion of *esaB* in strain RN6390 resulted in an unexpected phenotype, because it abolished detectable secretion of EsxA and EsxC, indicating that it is essential for Ess secretion system activity in this strain background. It should be noted that a homologue of *S. aureus* EsaB (YukD) is also encoded within the *B. subtilis ess* gene cluster and is likewise essential for the secretion of EsxA (Baptista *et al.*, 2013). Thus, an essential role for EsaB in Ess secretion appears to be at least partially conserved.

Previous reports have indicated that in strain Newman the presence of EsxB is essential for the stability of EsxA (Burts *et al.*, 2005). However in RN6390, loss of *esxB* does not affect the stability or secretion of EsxA (Fig. 5). This is also in contrast to reports of the interdependence of EsxA and EsxB for secretion by the ESX machinery in *Mycobacteria* (Champion *et al.*, 2006), although it should be noted that Mycobacterial EsxA and EsxB interact strongly (Renshaw *et al.*, 2002; 2005) whereas there is no detectable interaction between *S. aureus* EsxA and EsxB (Sundaramoorthy *et al.*, 2008; Anderson *et al.*, 2013). Loss of *esxB* does, however, abolish secretion of EsxC (Fig. 5).

Similar to the *esxB* deletion, the deletion of *esxA* severely affected the secretion of EsxC (Fig. 5). In contrast, deletion of the *esxC* gene did not affect the secretion of EsxA. Thus EsxC depends upon EsxA for secretion but this is not a reciprocal requirement.

From the results presented here we conclude that in *S. aureus* strain RN6390 the Ess secretion system com-

© 2014 The Authors. *Molecular Microbiology* published by John Wiley & Sons Ltd.,

prises the membrane proteins EsaA, EssA, EssB and EssC, along with the secreted protein EsxA and the cytoplasmic protein EsaB.

The Ess system in two strains of S. aureus *contributes significantly to virulence in a murine pneumonia model*

It has previously been demonstrated that components and secreted substrates of the Ess system in the *S. aureus* Newman strain contribute to virulence in a mouse model of abscess formation (Burts *et al*., 2008). We therefore first sought to test whether Ess secretion was required for virulence in additional models of infection, and second whether there might be any strain-specific differences in Ess requirement for virulence.

To this end, we constructed complete deletions of the entire 12 gene *ess* loci in each of the RN6390, COL and SA113 strains. Deletion of this locus had no effect on growth rate of the strains in different laboratory growth media (Fig. S4 and data not shown). Loss of *ess* also had no detectable effect on virulence of RN6390 or COL in the insect infection model, *Galleria mellonella* (Fig. S5). We conclude that loss of Ess secretion does not have a phenotypic effect on growth of these *S. aureus* strains.

Staphylocccus aureus frequently colonizes the anterior nares of humans, and is an important cause of ventilator-associated pneumonia in hospital settings (e.g. Rocha *et al*., 2013). It is also one of the earliest bacterial pathogens to colonize the airways of cystic fibrosis patients, where it often persists for many years (e.g. Kahl *et al*., 1998; Kahl *et al*., 2003; The United States Cystic Fibrosis Foundation, 2011, Patient Registry Annual Data Report). We therefore sought to assess whether the Ess secretion system was required first for nasal colonization and second for the development of pneumonia in the cystic fibrosis mouse infection model (McCarthy *et al*., 2010; Twomey *et al*., 2012).

To test the ability of RN6390, COL and SA113 or the cognate *ess* deletion strains to colonize the mouse nasal passages, C57BL/6 mice were inoculated with 10^8 colony-forming units (cfu) of each of the strains, and the number of cfu colonizing the nares were assessed after 3 days. Significantly lower cfu ml^{-1} were recovered from the nares for the Δ*ess* strains of RN6390 ($P = 0.003$) and COL ($P = 0.02$) compared to the cognate wild-type, demonstrating that the Ess system is required to support nasal colonization in these strain backgrounds (Fig. 7D). Surprisingly, no difference in colonizing ability was observed between SA113 and its corresponding Δ*ess* mutant ($P = 1.0$). It should be noted that SA113, which carries a mutation in *agr,* forms more robust biofilms than RN6390 and COL (e.g. Beenken *et al*., 2003; Herbert *et al*., 2010), and that SA113 also reportedly produces larger amounts of certain MSCRAMM adhesins, for example Spa, than COL (Herbert *et al*., 2010). It is possible that these features of SA113 may over-ride for any role of the Ess system in colonization by this strain.

To determine whether the Ess system was required for virulence in the murine pneumonia model, we infected cystic fibrosis transmembrane conductance regulator (CFTR) knockout mice intra-nasally with either of RN6390, COL and SA113 or the cognate *ess* deletion strains (Fig. 7A–C). Again, it can clearly be seen that there were strain-specific differences in the contribution of the Ess secretion system to virulence in the pneumonia model. Thus, mortality was significantly reduced following infection with the Δ*ess* mutants at 48 h in the RN6390 strain background ($P = 0.03$ by log-rank test), and in the COL background ($P = 0.008$). Strain SA113 was less virulent than the other strains we tested in our particular virulence model, which may arise due to the *agr* mutation that is known to lead to a downregulation of virulence factor production (e.g. Abdelnour *et al*., 1993; Novick *et al*., 1993). However, again we noted that there no difference in survival was observed between SA113 the cognate Δ*ess* strains ($P = 1.0$).

Discussion

In this study we have investigated the genetic organization of loci encoding the Type VII/Ess protein secretion system in closely related strains of *S. aureus* and assessed whether the secretion systems are active in these organisms and contribute to virulence. We chose to focus on five strains from clonal complex 8, RN6390, Newman, USA300, SA113 and COL. While the *ess* gene cluster is almost identical in nucleotide sequence between these strains (two nucleotide differences over the approximately 14 kb region), the genetic organization surprisingly differed between RN6390 and Newman on the one hand and USA300, SA113 and COL on the other. In the latter three strains the first gene of the cluster, *esxA*, was coexpressed with *esaA*, which is positioned 83 nucleotides downstream. By contrast, in RN6390, *esxA* was monocistronic and *esaA* was expressed exclusively from a promoter located in the *esxA*-*esaA* intergenic region. Despite the 100% sequence conservation between the five strains over this region, no promoter activity in this intergenic region was detected for USA300.

A putative rho-independent terminator sequence is located in the *esxA*-*esaA* intergenic region. Ostensibly, this must function as a highly effective terminator in RN6390 and Newman, while allowing readthrough in USA300, SA113 and COL. However, despite the surprising differences in transcriptional organization of *esxA* and *esaA* between strains, comparison of transcript levels of these two genes indicate that the ratio of *esxA* and *esaA* transcripts remain remarkably similar. The molecular basis for

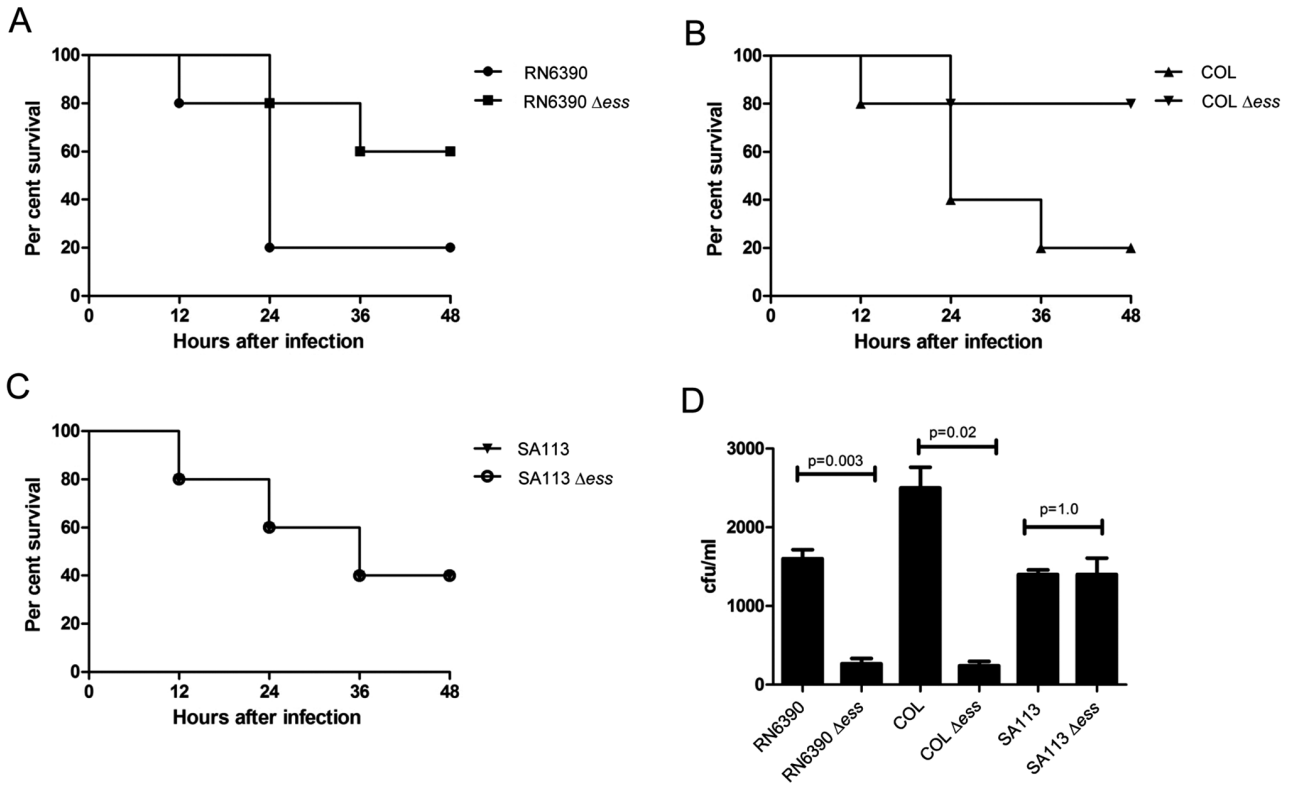

Fig. 7. The Ess secretion system of strains RN6390 and COL contributes to nasal colonization and virulence in the murine pneumonia model. For the murine pneumonia model mice ($n = 10$ mice per experiment) were infected at time zero with 2×10^8 cfu of *S. aureus* strains RN6390 (A), COL (B) or SA113 (C) or the cognate Δ*ess* mutant strains as indicated. Survival was assessed for up to 48 h. (B) For the murine nasal colonization model, mice ($n = 10$ mice per experiment) were infected with 2×10^8 cfu per nostril of the indicated strains and colonization status determined following nasal excision at 48 h.

these unexpected transcriptional differences is not known, but presumably it results from strain-specific variation in the function of *trans*-acting factors. Our additional RT-PCR analyses, coupled with the short intergenic regions between the remaining genes, make it highly likely that *esaA* through *SAOUHSC_00269* are all coexpressed.

In addition to the heterogeneity of *ess* transcriptional organization, we also saw that there were notable differences between strains in the activity of the Ess secretion system. During growth in TSB medium strains RN6390 and COL secreted EsxA and EsxC at relatively early growth points, whereas for USA300 and SA113, secretion appeared to be delayed and was only observed at later growth points. We were unable to observe any secretion of EsxA in strain Newman at any of the growth points we tested, and could not detect EsxC antigen. It has been noted previously that Newman produces and secretes EsxA at a low level relative to USA300 (Burts *et al.*, 2008). Recently, it was shown that the *ess* cluster in Newman and USA300 is negatively regulated by the SaeRS two-component system, but that this system is constitutively active in the Newman strain due to a point mutation in the SaeS kinase, accounting for the low Ess activity (Anderson *et al.*, 2013).

Selecting one of the early secreting strains, RN6390, we made a series of in-frame deletions in the first eight *ess*-encoded genes to determine whether they were essential to support Ess secretion system activity. Our results were in partial agreement with prior observations in strain Newman (Burts *et al.*, 2005; 2008) – thus we confirmed in the RN6390 background that the EssA, EssB and EssC membrane components are required for secretion of EsxA and EsxC. However, we also demonstrated an essential role for a further membrane protein, EsaA, in secretion system activity. This contrasts with Burts *et al.* (2005) who reported that a transposon insertion in *esaA* did not abolish secretion of EsxA or EsxB. However in that study the transposon was inserted after codon 370 of *esaA*, raising the possibility that a truncated protein product was produced that may retain some function. It should be noted that EsaA homologues are conserved in *Firmicutes* and the *B. subtilis* EsaA homologue, YueB, is essential for Ess secretion activity in this organism (Baptista *et al.*, 2013). Taken together, these results strongly suggest that EsaA

proteins are essential components of the Ess secretion machinery.

A striking finding was that for all strains examined, secretion appeared to be relatively inefficient, with significant amounts of EsxA and EsxC detected in the cellular fraction, and subcellular fractionation of RN6390 showed that they were primarily located in the cytoplasm. We also noted that for USA300 and SA113, cellular EsxA was detected at early growth points, but did not appear in the growth medium until later. These findings raise the possibility that the system may be subject to post-translational regulation. Other protein secretion systems are also regulated at the post-translational level, for example the Type VI secretion system in Gram-negative bacteria. In *Pseudomonas aeruginosa* it has been shown that a serine-threonine kinase, PpkA, phosphorylates a FHA domain-containing protein, regulating the activity of the Type VI secretion system (Mougous *et al*., 2007). It is interesting to note that in *Firmicutes*, the EssC component has tandem FHA domains at its N-terminus (Tanaka *et al*., 2007) that may be involved in controlling secretion activity. The small ubiquitin-related protein, EsaB, could also play a role in post-translational regulation of the secretion system. Here we found that *esaB* is essential for secretion of EsxA and EsxC, and Baptista *et al*. (2013) similarly reported that the *B. subtilis* EsaB homologue, YukD, was required for activity. By contrast, in the *S. aureus* Newman strain EsaB is dispensable for secretion of EsxA or EsxB but has a negative regulatory effect on the expression of *esxC* at the post-transcriptional level (Burts *et al*., 2008). Given that EsaB is not universally essential for Ess secretion it is unlikely to be a structural component of the machinery. Instead we favour the idea that it plays a regulatory role albeit one that may differ between strains.

Our qRT-PCR analysis has shown that *esxA* is very highly expressed relative to the other genes at the *ess* locus, approximately 100 times more than *essC* or *esxB*. The role of EsxA in Type VII secretion systems is not completely clear. It is evident that it is secreted by the Type VII machinery, but deletion or insertional activation of *esxA* always results in a complete absence of all other secreted substrate proteins in the growth medium (Burts *et al*., 2005; Anderson *et al*., 2013; this study). In this respect it behaves like one of the core components of the secretion machinery (potentially an extracellular structural component or chaperone) rather than a secreted substrate. By contrast, deletion of genes coding for two further secreted substrates, *esxB* and *esxC*, did not affect secretion of EsxA in RN6390, placing EsxA at the top of the hierarchy of Ess-secreted proteins. It should be noted that complex effects have been observed in other strain backgrounds, for example EsxA was destabilized in the *esxB* mutant of Newman (Burts *et al*., 2005) but not USA300, although EsxA was not secreted in this case (Anderson *et al*., 2013). Likewise, absence of EsxC, with which EsxA was demonstrated to interact, appeared to destabilize EsxA in USA300 (Anderson *et al*., 2013), but this was not evidenced here for RN6390. Such complex, strain-specific effects make it difficult to tease out the roles of individual secreted proteins in secretion system function and to pin-point what contribution, if any, each secreted protein has to *S. aureus* virulence.

Prior reports have defined a role for the Ess system of strain Newman in virulence in a murine abscess infection model. Here we asked whether the Ess system was required for *S. aureus* to colonize the murine nasal passage, which is usually asymptomatic and benign, and to cause pneumonia following intra-nasal inoculation. Surprisingly we found for two of the three strains tested, RN6390 and COL, that the Ess system was important for both of these processes. Currently it is not clear how the Ess system could contribute to nasal colonization, although it has been observed that other secretion systems also play a major role in this bacterial behaviour (e.g. Skinner *et al*., 2004). Very recently it was reported that the *essC* gene in strain Newman was upregulated in the presence of pulmonary surfactant and that deletion of *essC* was accompanied by a similar attenuation in virulence in the murine pneumonia model as we report here (Ishii *et al*., 2014). By contrast, the third strain we tested, SA113, showed no significant contribution of the Ess system to either colonization or disease. The underlying reasons for these strain-specific differences are not known, and do not entirely correlate with the activity of the Ess secretion systems in laboratory growth media. Taken together with previous findings, the results presented here demonstrate that there are notable differences between the transcriptional organization of the *ess* locus, the absolute requirement of individual *ess*-encoded genes for secretion system function, secretion activity in laboratory broth and requirement for virulence between relatively closely related strains of *S. aureus* and that findings cannot necessarily be extrapolated between strains. Therefore, the precise role of individual machinery components and contribution of specific secreted substrates to disease requires further study.

Experimental procedures

Bacterial strains and growth conditions

Strains and plasmids used in this study are listed in Table 1. *S. aureus* strains were grown in TSB at 37°C under vigorous agitation. Chloramphenicol (Cm) at a final concentration of 10 μg ml^{-1} or erythromycin (Erm, 5 μg ml^{-1}) was added for plasmid selection. Anhydrotetracycline (ATc) was used at various concentrations as a selection during allelic gene replacement using the pIMAY system [1 μg ml^{-1} (Monk *et al*., 2012)] or for induction of target gene expression from the

Table 1. Strains and plasmids used in this study.

Strain or plasmid	Description	Reference
Strains		
S. aureus		
RN6390	NCTC8325 derivative, *rbsU*, *tcaR*, cured of φ11, φ12, φ13	Novick *et al.* (1993)
COL	MRSA, *agr*	Dyke *et al.* (1966), Gill *et al.* (2005)
USA300	Community-acquired MRSA	McDougal *et al.* (2003)
Newman	ATCC 25904	Duthie and Lorenz (1952), Baba *et al.* (2008)
SA113	NCTC8325 derivative, *agr*, *rbsU*, *tcaR, hsdR*	Iordanescu and Surdeanu (1976)
RN6390 ess	Complete deletion from *esxA* – *SAOUHSC_00269*	This work
RN6390 esxA	*esxA* deletion	This work
RN6390 esaA	*esaA* deletion	This work
RN6390 essA	*essA* deletion	This work
RN6390 esaB	*esaB* deletion	This work
RN6390 essB	*essB* deletion	This work
RN6390 essC	*essC* deletion	This work
RN6390 esxC	*esxC* deletion	This work
RN6390 esxB	*esxB* deletion	This work
COL ess	Complete deletion from *Sacol0271* (*esxA*) -*Sacol0282*	This work
SA113 ess	Complete deletion from *esxA* – *SAOUHSC_00269*	This work
E. coli		
JM110	*rpsL thr leu thi lacY galK galT ara tonA tsx dam dcm glnV44* Δ(*lac-proAB*) e14- [F' *traD36 proAB*$^+$ *lacI*^{q} *lacZ*ΔM15] *hsdR17*($r_K^-m_K^+$)	Stratagene
MC1061	F^- Δ(*ara-leu*)7697 [*araD139*]$_{B/r}$ Δ(*codB-lacI*)3 *galK16 galE15* λ^- *e14*$^-$ *mcrA0 relA1 rpsL150*(strR) *spoT1 mcrB1 hsdR2*(r^-m^+)	Casadaban and Cohen (1980)
DC10B	*dam*$^+$ *dcm*$^-$ *hsdRMS endA1 recA1*	Monk *et al.* (2012)
Plasmids		
pBluescript KS$^+$	General purpose *E. coli* cloning vector, amp^r	Stratagene
pMAD	*E. coli/S. aureus* shuttle vector, temperature sensitive, amp^r, ery^r	Arnaud *et al.* (2004)
pIMAY	*E. coli/S. aureus* shuttle vector, temperature sensitive, cml^r	Monk *et al.* (2012)
pRMC2	*E. coli/S. aureus* shuttle vector, inducible protein expression, amp^r, cml^r	Corrigan and Foster (2009)
pRMC2h	pRMC2 variant coding for N-terminal hexahistidine tag	This work
pEsaA-nhis	pRMC2h expressing His_6-EsaA	This work

pRMC2 plasmid (Corrigan and Foster, 2009). *Escherichia coli* was grown aerobically in Luria–Bertani (LB) medium at 37°C. If required, cultures were supplemented with ampicillin (Amp, 100 μg ml^{-1}) or chloramphenicol (15 μg ml^{-1}) for plasmid selection.

Strain and plasmid construction

In-frame deletions of individual *ess* genes or a 12-gene *ess* deletion (encompassing *esxA* through *SAOUHSC_00269*) were performed by allelic exchange using either plasmid pMAD (for *essA*, *esaB*, *essB*, *esxC*, *esxB*) or pIMAY (for *esxA*, *esaA*, *essC*, and the 12 gene *ess* deletion) as described (Arnaud *et al.*, 2004; Monk *et al.*, 2012). For each gene, the upstream and downstream regions including at least the first three and last three codons were amplified from RN6390 genomic DNA using primers listed in Table S1. In the case of overlapping genes within the *ess* cluster (*esaA-essA*, *essA-esaB*, *esxB-esxD*), the amplified flanking regions were designed to leave the putative ribosome binding site and start codon or stop codon of the overlapping gene intact. Clones containing the amplified flanking regions in vectors pMAD or pIMAY were selected in *E. coli* and plasmids were subsequently electroporated into *S. aureus* strains using published methods (Monk *et al.*, 2012). Chromosomal deletions were verified by amplification of the genomic region from isolated genomic DNA (GeneElute Bacterial Genomic DNA Kit, Sigma Aldrich) and DNA sequencing of the amplified products. To ensure that no unwanted secondary mutations arose in virulence regulators such as *agr* or *sae*, each mutant was also tested for haemolytic activity on sheep blood agar plates. In each case no detectable difference in haemolytic activity between the wild-type and any of the mutant strains was observed.

A variant of plasmid pRMC2 coding for an N-terminal hexahistidine tag (pRMC2h) was generated by insertion of the additional coding sequence into the multiple cloning site (MCS). Briefly, the region between the XhoI site and the MCS of pRMC2 was amplified with primers pRMC2seq1 and Nhisins, adding an 18 bp stretch corresponding to the short sequence of DNA from the ribosome binding site to the ATG start codon of the *esxA* gene followed by the hexahistidine coding sequence (6× CAT repeats) between the KpnI and BglII restriction sites of the MCS. pEsaA-nhis was constructed by amplification of the *esaA* coding region from RN6390 genomic DNA using primers esaA nhis fw and esaA nhis rev (see Table S1) and cloning between the BglII and SacI sites of pRMC2h.

RT-PCR and 5′-RACE experiments

mRNA extraction from *S. aureus* strains grown aerobically in TSB to an OD_{600} of 1 or 2 was performed using the SV

© 2014 The Authors. *Molecular Microbiology* published by John Wiley & Sons Ltd.,

Total RNA Isolation Kit (Promega) with some minor modifications. Briefly, cell samples were stabilized in 5% phenol/95% ethanol and centrifuged at 2770 *g* for 10 min. Cells were resuspended in 100 µl TE buffer containing 500 µg ml^{-1} lysostaphin and 50 µg ml^{-1} lysozyme and incubated at 37°C for 30 min followed by isolation of the RNA according to the manufacturer's instructions. Isolated RNA was further purified using the DNA-free kit (Ambion) to remove DNA and salt.

RT-PCR to probe co-transcription of *ess* genes was carried out using the Superscript III Reverse Transcriptase kit (Invitrogen) using region-specific primers (region-x-f and region-x-r) listed in Table S1, followed by incubation with 2 units of *E. coli* RNaseH (Invitrogen) to remove template RNA. PCR products were purified using the PCR purification kit (Qiagen) and visualized on 1% agarose gels.

First-strand cDNA synthesis for 5′-RACE was performed following the protocol for the Roche second-generation 5′/3′-RACE kit using 500 ng of template RNA prepared as described above, gene-specific primers for *esxA* or *esaA* GSP1-3 and anchor primers listed in Table S1. Single PCR products were purified using the PCR purification kit (Qiagen), digested with ClaI/XhoI (esxA) or ClaI/EcoRI (*esaA*) and cloned into pBluescript KS^+. Transcriptional start points were determined by sequencing with primer M13-F.

RT-qPCR

RNA was extracted as described above and 600 ng of total RNA was used to generate 20 µl of cDNA using the QuantiTect Reverse Transcription Kit (Qiagen), following the manufacturer's instructions. For each sample, a negative control was prepared replacing the enzyme mixture with additional water. Quantitative PCR was performed using a Stratagene Mx3005P thermal cycler. Triplicate reactions for each culture condition were set using 7.5 µl Brilliant II SYBR Green Low Rox SuperMix (Agilent), 0.6 µl 10 mM primers (see Table S1) and 3.0 µl of cDNA diluted 1:20, and made up to 15 µl with sterile water. PCR was performed using an initial 10 min 95°C denaturing step followed by 40 repeated cycles of 30 s 95°C denaturing, 30 s 55°C annealing, and 30 s 72°C extension steps. A final 10 min denaturing curve analysis was performed. Standard curves were generated from serial 10-fold dilutions of genomic DNA (see Fig. S1). Amplification results were analysed with MxPro QPCR software to give the levels of mRNA normalized to the level of 16S rRNA amplification in each sample. Results were further analysed in Microsoft Excel to calculate relative expression levels using *essC* mRNA as the comparator.

Antibody production

Coding sequences for *S. aureus* EsxA, EsaC (Uniprot: Q99WU4 and Q99WT8), predicted cytoplasmic fragments of EssB (Uniprot: Q99WU0, residues: 12–226) and EssC (Uniprot: Q932J9, residues: 964–1479) and predicted extracellular fragment of EsaA (Uniprot: Q99WU3, residues: 313–749) were PCR amplified from synthetic genes [codon optimized for *E. coli* K12 (Genscript)] and individually cloned between the SalI/XhoI sites of a modified pET27b vector (Novagen). All primers are listed in Table S1. The plasmids produce proteins with an N-terminal hexahistidine tag separated by a tobacco etch virus (TEV) protease cleavage site. Proteins were expressed and purified as reported previously (Zoltner *et al.*, 2013a), except in the final size exclusion chromatography step a HR 30/100 GL Superdex75 column (CV = 24 ml, GE healthcare) equilibrated with 20 mM Tris pH 7.8, 100 mM NaCl was used.

The purified proteins (retaining a Gly–Ala–Ser–Thr sequence at the N-terminus after the cleavage step) were utilized as antigens to immunize rabbits for polyclonal antibody production in a standard three injections protocol (Seqlab, Goettingen, Germany).

The anti-TrxA antibody was described earlier (Miller *et al.*, 2010) and commercially available antibodies against Spa (HRP-conjugate, LifeSpan Biotechnologies) and SrtA (Abcam) were used according to the manufacturers' recommendations.

S. aureus *sample preparation and Western blotting*

Staphylococcus aureus strains were grown overnight in TSB at 37°C. Cells were diluted 1/100 into fresh TSB medium and growth was monitored by measuring the optical density of the cultures at 600 nm. At indicated time points, samples were withdrawn and cells pelleted by centrifugation at 2770 *g*. Supernatant samples were further filtered through a 0.45 µm filter and proteins precipitated with trichloroacetic acid (TCA, 10% final concentration) in the presence of 50 µg ml^{-1} deoxycholate, which has been reported to improve recovery of precipitated proteins (Bensadoun and Weinstein, 1976). Precipitates were centrifuged (10 000 *g*, 4°C, 15 min), washed with 80% ice-cold ethanol and resulting pellets resuspended in 50 mM Tris-HCl pH 8, 4% SDS. Samples were mixed with NuPage LDS loading buffer (life Technologies) and boiled for 10 min.

Cells for whole cell fractions were pelleted by centrifugation, washed with 1× PBS buffer and normalized to an OD_{600} of 2 in 1× PBS. Cells were lysed by addition of 50 µg ml^{-1} lysostaphin (Ambi) and incubation at 37°C for 30 min. Samples were mixed with an equal volume of LDS buffer and boiled for 10 min.

Samples for further subcellular fractionation were pelleted and washed as above and resuspended in fractionation buffer (50 mM Tris-HCl pH 7.6, 0.5 M sucrose, 10 mM $MgCl_2$). Lysostaphin was added as above and the cell wall was digested at 37°C for 30 min. Protoplasts were sedimented (10 000 *g*, 10 min) and the supernatant kept as the cell wall fraction. Protoplasts were resuspended in 1× PBS and broken by sonication (2 × 15s, 20% amplitude, Branson Digital Sonifier). Samples were subjected to ultracentrifugation (227 000 *g*, 30 min, 4°C), the supernatant was removed as the cytoplasmic fraction and the membrane pellet resuspended in 1× PBS, 0.5% Triton X-100.

Samples were mixed with LDS loading buffer and boiled for 10 min prior to separation on bis-Tris gels. Western blotting was performed according to standard protocols with the following antibody dilutions: α-EsxA 1:2500, α-EsxC 1:2000, α-EsaA 1:10 000, α-EssB 1:10 000, α-EssC 1:10 000, α-TrxA 1:25 000, α-Hla 1:2000, α-Spa 1:10 000, α-SrtA 1:3000.

Virulence assays

For the *G. mellonella* virulence assay, overnight cultures of *S. aureus* and the isogenic Δ*ess* mutant were used to prepare a 10-fold dilution series in phosphate-buffered saline (PBS). The infecting dose of wild-type RN6390 and COL strains required to cause 80% mortality (LD_{80}) in the model was determined (1×10^7 cfu ml^{-1} for RN6390 and 1×10^8 cfu ml^{-1} for COL) and used in subsequent experiments. Larvae were removed from storage at 4°C and allowed to warm to room temperature. Prior to inoculation, larvae were briefly placed on ice; then a Hamilton syringe was used to inject larvae with 10 μl of culture in PBS via the hind left proleg ($n = 10$ larvae per experiment; repeated three times). Ten control larvae were injected with PBS only. Following injection, larvae were incubated in the dark at 25°C. After 24 h, larvae were scored as dead or alive, with larvae considered dead if they did not respond to touch and were usually visibly black. Infection models were continued for 7 days and differences in survival assessed using the Kaplan-Meier method.

The murine pneumonia model was performed using CFTR –/– mice, a relevant model of pulmonary *S. aureus* infection (Bragonzi, 2010) as *S. aureus* is the most common organism colonizing children with cystic fibrosis. Briefly, *S. aureus* strains were grown in TSB medium at 37°C overnight with shaking, after which bacteria were collected by centrifugation and resuspended in PBS. The exact number of bacteria was determined by plating serial dilutions of each inoculum on Luria broth agar plates. Female C57BL/6 mice CF transmembrane conductance regulator (CFTR) knockout (CF) mice (approximately 10 weeks old) were anaesthetized and infected by the intranasal route with 10 μl of culture of RN6390, RN6390 Δ*ess*, COL, COL Δ*ess*, SA113 and SA113 Δ*ess* strains to have a final inoculum of 2×10^8 colony-forming units (cfu) per mouse. Survival was assessed up to 48 h after induction of pneumonia and compared using the Kaplan-Meier method.

Murine nasal colonization assays were carried out as previously reported (Kiser *et al*., 1999). Briefly, an inoculum of each of the *S. aureus* strains, 10^8 cfu in 10 μl of PBS, was pipetted slowly onto the nares of wild-type female C57BL/6 mice. After inoculation, mice were killed 3 days post-infection by intraperitoneal injection of 0.3 ml of 30% pentobarbital. Nares were harvested aseptically and homogenized in sterile PBS. A 10-fold serial dilution and plating was carried out to assess cfu. All animal experiments were approved by the Animal Ethics Committees of University College Cork.

Acknowledgements

This study was supported by the UK Biotechnology and Biological Sciences Research Council (through Grant BB/H007571/1 to W.N.H. and T.P. and an EASTBIO Doctoral Training Partnership PhD studentship to F.J.), the UK Medical Research Council (through a Senior Non Clinical Fellowship award to T.P. and a Clinical Research Training Fellowship to J.S.C.), the Wellcome Trust (via an Early Postdoctoral Training Fellowship for Clinician Scientists to J.C. and through their Institutional Strategic Support Fund), a China Scholarship Council PhD studentship (to Z.P.C.). The work by K.B.T. and R.P.R. is supported in part by grants awarded by the Wellcome Trust (Senior Fellowship WT100204AIA to R.P.R.); the Science Foundation of Ireland (SFI 09/SIRG/B1654 to R.P.R.). M.M.v.d.K.-P. and J.M.v.D. were supported by the Top Institute Pharma (through Grants T4-213 and T4-502). We thank Professor Timothy Foster and Dr Ian Monk (Trinity College, Dublin) for providing plasmids (pRMC2 and pIMAY) and for their technical advice.

References

Abdallah, A.M., Verboom, T., Hannes, F., Safi, M., Strong, M., Eisenberg, D., *et al*. (2006) A specific secretion system mediates PPE41 transport in pathogenic mycobacteria. *Mol Microbiol* **62:** 667–679.

Abdelnour, A., Arvidson, S., Bremell, T., Rydén, C., and Tarkowski, A. (1993) The accessory gene regulator (*agr*) controls *Staphylococcus aureus* virulence in a murine arthritis model. *Infect Immun* **61:** 3879–3885.

Akpe San Roman, S., Facey, P.D., Fernandez-Martinez, L., Rodriguez, C., Vallin, C., Del Sol, R., and Dyson, P. (2010) A heterodimer of EsxA and EsxB is involved in sporulation and is secreted by a type VII secretion system in *Streptomyces coelicolor*. *Microbiology* **156:** 1719–1729.

Anderson, M., Chen, Y.H., Butler, E.K., and Missiakas, D.M. (2011) EsaD, a secretion factor for the Ess pathway in *Staphylococcus aureus*. *J Bacteriol* **193:** 1583–1589.

Anderson, M., Aly, K.A., Chen, Y.H., and Missiakas, D. (2013) Secretion of atypical protein substrates by the ESAT-6 secretion system of *Staphylococcus aureus*. *Mol Microbiol* **90:** 734–743.

Arnaud, M., Chastanet, A., and Debarbouille, M. (2004) New vector for efficient allelic replacement in naturally nontransformable, low-GC-content, gram-positive bacteria. *Appl Environ Microbiol* **70:** 6887–6891.

Baba, T., Bae, T., Schneewind, O., Takeuchi, F., and Hiramatsu, K. (2008) Genome sequence of *Staphylococcus aureus* strain Newman and comparative analysis of staphylococcal genomes: polymorphism and evolution of two major pathogenicity islands. *J Bacteriol* **190:** 300–310.

Baptista, C., Barreto, H.C., and Sao-Jose, C. (2013) High levels of DegU-P activate an Esat-6-like secretion system in *Bacillus subtilis*. *PLoS ONE* **8:** e67840.

Beenken, K.E., Blevins, J.S., and Smeltzer, M.S. (2003) Mutation of *sarA* in *Staphyloccus aureus* limits biofilm formation. *Infect Immun* **71:** 4206–4211.

Bensadoun, A., and Weinstein, D. (1976) Assay of proteins in the presence of interfering materials. *Anal Biochem* **70:** 241–250.

Bitter, W., Houben, E.N., Bottai, D., Brodin, P., Brown, E.J., Cox, J.S., *et al*. (2009) Systematic genetic nomenclature for type VII secretion systems. *PLoS Pathog* **5:** e1000507.

Bragonzi, A. (2010) Murine models of acute and chronic lung infection with cystic fibrosis pathogens. *Int J Med Microbiol* **300:** 584–593.

Burts, M.L., Williams, W.A., DeBord, K., and Missiakas, D.M. (2005) EsxA and EsxB are secreted by an ESAT-6-like system that is required for the pathogenesis of *Staphylococcus aureus* infections. *Proc Natl Acad Sci USA* **102:** 1169–1174.

Burts, M.L., DeDent, A.C., and Missiakas, D.M. (2008) EsaC substrate for the ESAT-6 secretion pathway and its role in

persistent infections of *Staphylococcus aureus*. *Mol Microbiol* **69:** 736–746.
Casadaban, M.J., and Cohen, S.N. (1980) Analysis of gene control signals by DNA fusion and cloning in *Escherichia coli*. *J Mol Biol* **138:** 179–207.
Champion, P.A., Stanley, S.A., Champion, M.M., Brown, E.J., and Cox, J.S. (2006) C-terminal signal sequence promotes virulence factor secretion in *Mycobacterium tuberculosis*. *Science* **313:** 1632–1636.
Chen, Y.H., Anderson, M., Hendrickx, A.P., and Missiakas, D. (2012) Characterization of EssB, a protein required for secretion of ESAT-6 like proteins in *Staphylococcus aureus*. *BMC Microbiol* **12:** 219.
Corrigan, R.M., and Foster, T.J. (2009) An improved tetracycline-inducible expression vector for *Staphylococcus aureus*. *Plasmid* **61:** 126–129.
Desvaux, M., Hebraud, M., Talon, R., and Henderson, I.R. (2009) Secretion and subcellular localizations of bacterial proteins: a semantic awareness issue. *Trends Microbiol* **17:** 139–145.
Dreisbach, A., Hempel, K., Buist, G., Hecker, M., Becher, D., and van Dijl, J.M. (2010) Profiling the surfacome of *Staphylococcus aureus*. *Proteomics* **10:** 3082–3096.
Duthie, E.S., and Lorenz, L.L. (1952) *Staphylococcal* coagulase; mode of action and antigenicity. *J Gen Microbiol* **6:** 95–107.
Dyke, K.G., Jevons, M.P., and Parker, M.T. (1966) Penicillinase production and intrinsic resistance to penicillins in *Staphylococcus aureus*. *Lancet* **1:** 835–838.
van den Ent, F., and Lowe, J. (2005) Crystal structure of the ubiquitin-like protein YukD from *Bacillus subtilis*. *FEBS Lett* **579:** 3837–3841.
Fyans, J.K., Bignell, D., Loria, R., Toth, I., and Palmer, T. (2013) The ESX/type VII secretion system modulates development, but not virulence, of the plant pathogen *Streptomyces scabies*. *Mol Plant Pathol* **14:** 119–130.
Garufi, G., Butler, E., and Missiakas, D. (2008) ESAT-6-like protein secretion in *Bacillus anthracis*. *J Bacteriol* **190:** 7004–7011.
Gill, S.R., Fouts, D.E., Archer, G.L., Mongodin, E.F., Deboy, R.T., Ravel, J., *et al*. (2005) Insights on evolution of virulence and resistance from the complete genome analysis of an early methicillin-resistant *Staphylococcus aureus* strain and a biofilm-producing methicillin-resistant *Staphylococcus epidermidis* strain. *J Bacteriol* **187:** 2426–2438.
Goosens, V.J., Monteferrante, C.G., and van Dijl, J.M. (2014) The Tat system of Gram-positive bacteria. *Biochim Biophys Acta* **1843:** 1698–1706.
Herbert, S., Ziebandt, A.K., Ohlsen, K., Schafer, T., Hecker, M., Albrecht, D., *et al*. (2010) Repair of global regulators in *Staphylococcus aureus* 8325 and comparative analysis with other clinical isolates. *Infect Immun* **78:** 2877–2889.
Hsu, T., Hingley-Wilson, S.M., Chen, B., Chen, M., Dai, A.Z., Morin, P.M., *et al*. (2003) The primary mechanism of attenuation of bacillus Calmette-Guerin is a loss of secreted lytic function required for invasion of lung interstitial tissue. *Proc Natl Acad Sci USA* **100:** 12420–12425.
Iordanescu, S., and Surdeanu, M. (1976) Two restriction and modification systems in *Staphylococcus aureus* NCTC8325. *J Gen Microbiol* **96:** 277–281.
Ishii, K., Adachi, T., Yasukawa, J., Suzuki, Y., Hamamoto, H., and Sekimizu, K. (2014) Induction of virulence gene expression in *Staphylococcus aureus* by pulmonary surfactant. *Infect Immun* **82:** 1500–1510.
Kahl, B., Herrmann, M., Everding, A.S., Koch, H.G., Becker, K., Harms, E., *et al*. (1998) Persistent infection with small colony variant strains of *Staphylococcus aureus* in patients with cystic fibrosis. *J Infect Dis* **177:** 1023–1029.
Kahl, B.C., Duebbers, A., Lubritz, G., Haeberle, J., Koch, H.G., Ritzerfeld, B., *et al*. (2003) Population dynamics of persistent *Staphylococcus aureus* isolated from the airways of cystic fibrosis patients during a 6-year prospective study. *J Clin Microbiol* **41:** 4424–4427.
Karlsson, A., and Arvidson, S. (2002) Variation in extracellular protease production among clinical isolates of *Staphylococcus aureus* due to different levels of expression of the protease repressor sarA. *Infect Immun* **70:** 4239–4246.
Kiser, K.B., Cantey-Kiser, J.M., and Lee, J.C. (1999) Development and characterisation of a *Staphylococcus aureus* nasal colonization model in mice. *Infect Immun* **67:** 5001–5006.
Larionov, A., Krause, A., and Miller, W. (2005) A standard curve based method for relative real time PCR data processing. *BMC Bioinformatics* **6:** 62.
McCarthy, Y., Yang, L., Twomey, K.B., Sass, A., Tolker-Nielsen, T., Mahenthiralingam, E., *et al*. (2010) A sensor kinase recognizing the cell–cell signal BDSF (cis-2-dodecenoic acid) regulates virulence in *Burkholderia cenocepacia*. *Mol Microbiol* **77:** 1220–1236.
McDougal, L.K., Steward, C.D., Killgore, G.E., Chaitram, J.M., McAllister, S.K., and Tenover, F.C. (2003) Pulsed-field gel electrophoresis typing of oxacillin-resistant *Staphylococcus aureus i*solates from the United States: establishing a national database. *J Clin Microbiol* **41:** 5113–5120.
Miller, M., Donat, S., Rakette, S., Stehle, T., Kouwen, T.R., Diks, S.H., *et al*. (2010) *Staphylococcal* PknB as the first prokaryotic representative of the proline-directed kinases. *PLoS ONE* **5:** e9057.
Monk, I.R., Shah, I.M., Xu, M., Tan, M.W., and Foster, T.J. (2012) Transforming the untransformable: application of direct transformation to manipulate genetically *Staphylococcus aureus* and *Staphylococcus epidermidis*. *MBio* **3:** pii: e00277-11.
Mougous, J.D., Gifford, C.A., Ramsdell, T.L., and Mekalanos, J.J. (2007) Threonine phosphorylation post-translationally regulates protein secretion in *Pseudomonas aeruginosa*. *Nat Cell Biol* **9:** 797–803.
Novick, R.P., Ross, H.F., Projan, S.J., Kornblum, J., Kreiswirth, B., and Moghazeh, S. (1993) Synthesis of *staphylococcal* virulence factors is controlled by a regulatory RNA molecule. *EMBO J* **12:** 3967–3975.
Pallen, M.J. (2002) The ESAT-6/WXG100 superfamily – and a new Gram-positive secretion system? *Trends Microbiol* **10:** 209–212.
Pugsley, A.P. (1993) The complete general secretory pathway in gram-negative bacteria. *Microbiol Rev* **57:** 50–108.
Pym, A.S., Brodin, P., Majlessi, L., Brosch, R., Demangel, C., Williams, A., *et al*. (2003) Recombinant BCG exporting ESAT-6 confers enhanced protection against tuberculosis. *Nat Med* **9:** 533–539.

Renshaw, P.S., Panagiotidou, P., Whelan, A., Gordon, S.V., Hewinson, R.G., Williamson, R.A., and Carr, M.D. (2002) Conclusive evidence that the major T-cell antigens of the *Mycobacterium tuberculosis* complex ESAT-6 and CFP-10 form a tight, 1:1 complex and characterization of the structural properties of ESAT-6, CFP-10, and the ESAT-6*CFP-10 complex. Implications for pathogenesis and virulence. *J Biol Chem* **277:** 21598–21603.

Renshaw, P.S., Lightbody, K.L., Veverka, V., Muskett, F.W., Kelly, G., Frenkiel, T.A., *et al*. (2005) Structure and function of the complex formed by the tuberculosis virulence factors CFP-10 and ESAT-6. *EMBO J* **24:** 2491–2498.

Rigoulay, C., Entenza, J.M., Halpern, D., Widmer, E., Moreillon, P., Poquet, I., and Gruss, A. (2005) Comparative analysis of the roles of HtrA-like surface proteases in two virulent *Staphylococcus aureus* strains. *Infect Immun* **73:** 563–572.

Rocha, L.A., Ribas, R.M., Darini, A.L., and Filho, P.P. (2013) Relationship between nasal colonization and ventilator-associated pneumonia and the role of the environment in transmission of *Staphylococcus aureus* in intensive care units. *Am J Infect Control* **41:** 1236–1240.

Sao-Jose, C., Baptista, C., and Santos, M.A. (2004) *Bacillus subtilis* operon encoding a membrane receptor for bacteriophage SPP1. *J Bacteriol* **186:** 8337–8346.

Sao-Jose, C., Lhuillier, S., Lurz, R., Melki, R., Lepault, J., Santos, M.A., and Tavares, P. (2006) The ectodomain of the viral receptor YueB forms a fiber that triggers ejection of bacteriophage SPP1 DNA. *J Biol Chem* **281:** 11464–11470.

Schulthess, B., Bloes, D.A., and Berger-Bachi, B. (2012) Opposing roles of sigmaB and sigmaB-controlled SpoVG in the global regulation of *esxA* in *Staphylococcus aureus*. *BMC Microbiol* **12:** 17.

Shukla, A., Pallen, M., Anthony, M., and White, S.A. (2010) The homodimeric GBS1074 from *Streptococcus agalactiae*. *Acta Crystallograph Sect F Struct Biol Cryst Commun* **66:** 1421–1425.

Sibbald, M.J., Ziebandt, A.K., Engelmann, S., Hecker, M., de Jong, A., Harmsen, H.J., *et al*. (2006) Mapping the pathways to staphylococcal pathogenesis by comparative secretomics. *Microbiol Mol Biol Rev* **70:** 755–788.

Skinner, J.A., Reissinger, A., Shen, H., and Yuk, M.H. (2004) *Bordetella* type III secretion and adenylate cyclase toxin synergize to drive dendritic cells into a semimature state. *J Immunol* **173:** 1934–1940.

Solis, N., Larsen, M.R., and Cordwell, S.J. (2010) Improved accuracy of cell surface shaving proteomics in *Staphylococcus aureus* using a false-positive control. *Proteomics* **10:** 2037–2049.

Stanley, S.A., Raghavan, S., Hwang, W.W., and Cox, J.S. (2003) Acute infection and macrophage subversion by *Mycobacterium tuberculosis* require a specialized secretion system. *Proc Natl Acad Sci USA* **100:** 13001–13006.

Sundaramoorthy, R., Fyfe, P.K., and Hunter, W.N. (2008) Structure of *Staphylococcus aureus* EsxA suggests a contribution to virulence by action as a transport chaperone and/or adaptor protein. *J Mol Biol* **383:** 603–614.

Tanaka, Y., Kuroda, M., Yasutake, Y., Yao, M., Tsumoto, K., Watanabe, N., *et al*. (2007) Crystal structure analysis reveals a novel forkhead-associated domain of ESAT-6 secretion system C protein in *Staphylococcus aureus*. *Proteins* **69:** 659–664.

The United States Cystic Fibrosis Foundation (2011) Patient Registry Annual Data Report [WWW document]. URL: http://www.cff.org/UploadedFiles/research/ClinicalResearch/2011-Patient-Registry.pdf

Twomey, K.B., O'Connell, O.J., McCarthy, Y., Dow, J.M., O'Toole, G.A., Plant, B.J., and Ryan, R.P. (2012) Bacterial cis-2-unsaturated fatty acids found in the cystic fibrosis airway modulate virulence and persistence of *Pseudomonas aeruginosa*. *ISME J* **6:** 939–950.

Voulhoux, R., Ball, G., Ize, B., Vasil, M.L., Lazdunski, A., Wu, L.F., and Filloux, A. (2001) Involvement of the twin-arginine translocation system in protein secretion via the type II pathway. *EMBO J* **20:** 6735–6741.

Widdick, D.A., Dilks, K., Chandra, G., Bottrill, A., Naldrett, M., Pohlschroder, M., and Palmer, T. (2006) The twin-arginine translocation pathway is a major route of protein export in *Streptomyces coelicolor*. *Proc Natl Acad Sci USA* **103:** 17927–17932.

Zoltner, M., Fyfe, P.K., Palmer, T., and Hunter, W.N. (2013a) Characterization of *Staphylococcus aureus* EssB, an integral membrane component of the Type VII secretion system: atomic resolution crystal structure of the cytoplasmic segment. *Biochem J* **449:** 469–477.

Zoltner, M., Norman, D.G., Fyfe, P.K., El Mkami, H., Palmer, T., and Hunter, W.N. (2013b) The architecture of EssB, an integral membrane component of the type VII secretion system. *Structure* **21:** 595–603.

Supporting information

Additional supporting information may be found in the online version of this article at the publisher's web-site.